

SINTEF Building and Infrastructure

Rolands Cepuritis and Stefan Jacobsen (NTNU), Bård Pedersen and Hedda Vikan (NPRA) and Klaartje De Weerd (SINTEF)

Rheology of matrix and SCC with different mineral fillers and admixtures

COIN Project report 41 – 2012



SINTEF Building and Infrastructure

Rolands Cepuritis and Stefan Jacobsen (NTNU), Bård Pedersen and Hedda Vikan (NPRA)
and Klaartje De Weerd (SINTEF)

Rheology of matrix and SCC with different mineral fillers and admixtures

FA 2 Competitive constructions

SP 2.1 High quality manufactured sand for concrete

COIN Project report 41 – 2012

COIN Project report no 41

Rolands Cepuritis and Stefan Jacobsen (NTNU), Bård Pedersen and Hedda Vikan (NPRA) and Klaartje De Weerd (SINTEF)

Rheology of matrix and SCC with different mineral fillers and admixtures

FA 2 Competitive constructions

SP 2.1 High quality manufactured sand for concrete

Keywords:

Manufactured sand; filler; admixture; matrix; rheology

Project no.: 3D005940

Photo, cover: «Gallery» iStock

ISSN 1891-1978 (online)

ISBN: 978-82-536-1288-1 (pdf)

ISBN 978-82-536-1289-8 (printed)

13 copies printed by AIT AS e-dit

Content: 100 g Scandia

Cover: 240 g Trucard

© Copyright SINTEF Building and Infrastructure 2012

The material in this publication is covered by the provisions of the Norwegian Copyright Act. Without any special agreement with SINTEF Building and Infrastructure, any copying and making available of the material is only allowed to the extent that this is permitted by law or allowed through an agreement with Kopinor, the Reproduction Rights Organisation for Norway. Any use contrary to legislation or an agreement may lead to a liability for damages and confiscation, and may be punished by fines or imprisonment.

Address: Forskningsveien 3 B
POBox 124 Blindern
N-0314 OSLO

Tel: +47 22 96 55 55

Fax: +47 22 69 94 38 and 22 96 55 08

www.sintef.no/byggforsk

www.coinweb.no

Cooperation partners / Consortium Concrete Innovation Centre (COIN)

Aker Solutions

Contact: Jan-Diederik Advocaat
Email: jan-diederik.advocaat@akersolutions.com
Tel: +47 67595050

Mapei AS

Contact: Trond Hagerud
Email: trond.hagerud@mapei.no
Tel: +47 69972000

Norwegian Public Roads Administration

Contact: Kjersti K. Dunham
Email: kjersti.kvalheim.dunham@vegvesen.no
Tel: +47 22073940

Saint Gobain Weber

Contact: Geir Norden
Email: geir.norden@saint-gobain.com
Tel: +47 22887700

SINTEF Building and Infrastructure

Contact: Tor Arne Hammer
Email: tor.hammer@sintef.no
Tel: +47 73596856

Unicon AS

Contact: Stein Tosterud
Email: stto@unicon.no
Tel: +47 22309035

Norcem AS

Contact: Terje Rønning
Email: terje.ronning@norcem.no
Tel: +47 35572000

Skanska Norge AS

Contact: Sverre Smeplass
Email: sverre.smeplass@skanska.no
Tel: +47 40013660

Veidekke Entreprenør ASA

Contact: Christine Hauck
Email: christine.hauck@veidekke.no
Tel: +47 21055000

NTNU

Contact: Terje Kanstad
Email: terje.kanstad@ntnu.no
Tel: +47 73594700

Preface

This study has been carried out within COIN - Concrete Innovation Centre - one of presently 14 Centres for Research based Innovation (CRI), which is an initiative by the Research Council of Norway. The main objective for the CRIs is to enhance the capability of the business sector to innovate by focusing on long-term research based on forging close alliances between research-intensive enterprises and prominent research groups.

The vision of COIN is creation of more attractive concrete buildings and constructions. Attractiveness implies aesthetics, functionality, sustainability, energy efficiency, indoor climate, industrialized construction, improved work environment, and cost efficiency during the whole service life. The primary goal is to fulfil this vision by bringing the development a major leap forward by more fundamental understanding of the mechanisms in order to develop advanced materials, efficient construction techniques and new design concepts combined with more environmentally friendly material production.

The corporate partners are leading multinational companies in the cement and building industry and the aim of COIN is to increase their value creation and strengthen their research activities in Norway. Our over-all ambition is to establish COIN as the display window for concrete innovation in Europe.

About 25 researchers from SINTEF (host), the Norwegian University of Science and Technology – NTNU (research partner) and industry partners, 15 – 20 PhD-students, 5 – 10 MSc-students every year and a number of international guest researchers, work on presently 5 projects:

- Advanced cementing materials and admixtures
- Improved construction techniques
- Innovative construction concepts
- Operational service life design
- Energy efficiency and comfort of concrete structures

COIN has presently a budget of NOK 200 mill over 8 years (from 2007), and is financed by the Research Council of Norway (approx. 40 %), industrial partners (approx 45 %) and by SINTEF Building and Infrastructure and NTNU (in all approx 15 %).

For more information, see www.coinweb.no

Tor Arne Hammer
Centre Manager

Summary

The main objective of this study has been to obtain a clearer knowledge about the effect of different crushed and natural mineral fillers on rheological parameters of matrix and concrete, in order to answer one of the most important questions when using manufactured sand – the question about the very high filler content.

The effect of 7 widely different fillers on rheology of filler modified paste (= matrix) and SCC was investigated at different w/b ratios (0.4, 0.5, 0.6 and 0.77). The fraction of solids Φ was kept constant for most of the mixes. A total of 38 matrices were tested which were later “up-scaled” to 22 SCC mixes. Two replacement levels of $V_{\text{filler}}/V_{\text{powder}} = 0.20$ and 0.33 were used in all matrix mixes (equal to the fly ash cement volume fraction in the reference with w/b = 0.4 without filler). Two different types of co-polymeric superplasticizers were used for the studies keeping the dosage constant at the level of 0.4% for the matrix mixes and adjusting the dosage according to the w/b ratio for the SCC mixes.

A Physica MCR300 Rheometer was used for the matrix flow tests (yield stress, plastic viscosity), static tests (yield stress, shear modulus) as well as for oscillatory tests (viscoelastic properties). Fresh concrete properties such as slump-flow, density and air-void content were measured for the SCC mixes along with the rheological measurements being performed on a coaxial cylinder viscometer Viscometer 5 by ConTec.

Within the project filler particle size distribution and specific surface area has been determined using four different characterization methods – sedimentation (Stoke’s law), laser diffraction, Blaine and BET.

The research carried out within this study is a strong foundation in order to fully understand the interaction between different types of mineral fillers and admixtures one hand and rheological properties of cement based particle suspensions such as matrix and concrete on the other. However, based on the results so far it’s still more new questions than answers.

First, it is rather clear that most of the available mineral particle characterization methods give very different results and it is still a challenge to get more understanding on this topic. Mineral composition of the fillers has been suggested as one of the possible reasons and further research directions have been proposed. The obtained results confirmed that it is possible to some extent relate the rheological differences of matrices to the specific surfaces of the fillers used to mix them. This seems to also be true for the structural regeneration and decomposition of the filler modified paste. However, the relation was rather limited and other relevant parameters for further studies have been proposed. No relation between the specific surface of the fillers and rheological properties of fresh SCC was found. The flowability of both matrix and concrete mixes was considerably improved when the mineral fillers replaced parts of the finer fly ash cement on volume basis. The natural filler gave the best flowability for both matrix and concrete as expected.

Table of contents

1. INTRODUCTION.....	7
1.1 PRINCIPAL OBJECTIVES AND SCOPE	7
1.2 BACKGROUND – RESEARCH NEEDS	7
1.3 PROPORTIONS, RHEOLOGY AND STABILITY – SCOPE	9
2. MATERIALS – INVESTIGATIONS – EXPERIMENTAL METHODS	13
2.1 MATRIX RHEOLOGY TESTS	13
2.1.1 <i>Materials</i>	13
2.1.2 <i>Mix composition</i>	16
2.1.3 <i>Rheometer</i>	17
2.1.4 <i>Mixing and measurement sequence</i>	18
2.1.5 <i>Oscillatory tests to determine complex shear modulus and critical strain</i>	21
2.1.6 <i>Rheological model functions for the flow curves</i>	22
2.1.7 <i>Gel strength, static yield stress and shear modulus</i>	23
2.2 SCC RHEOLOGY TESTS	24
2.2.1 <i>Materials and mix composition</i>	24
2.2.2 <i>Rheometer</i>	25
2.2.3 <i>Mixing, determination of fresh concrete properties and rheological parameters</i>	26
3. RESULTS	28
3.1 OVERVIEW OF THE MATRIX TEST RESULTS	28
3.1.1 <i>Repeatability of the matrix rheology test method</i>	38
3.1.2 <i>Overview of the test results</i>	38
3.1.3 <i>Repeatability of the SCC rheology test method</i>	41
4. DISCUSSION	42
4.1 FILLER CHARACTERIZATION	42
4.2 MATRIX RHEOLOGY TESTS	47
4.2.1 <i>Influence of the rheological test sequence</i>	47
4.2.2 <i>Influence of different fillers and superplasticizers</i>	48
4.2.3 <i>Structural decomposition and regeneration</i>	50
4.2.4 <i>Stability</i>	57
4.2.5 <i>Correlation to specific surface area of the fillers</i>	58
4.3 CONCRETE	68
4.3.1 <i>Influence of different fillers</i>	68
4.3.2 <i>Correlation to specific surface area of the fillers</i>	69
4.4 CORRELATION BETWEEN CONCRETE AND MATRIX RHEOLOGY	72
4.5 SUMMARY AND CONCLUDING DISCUSSION	76
5. CONCLUSIONS	78
6. FURTHER RESEARCH NEEDS.....	79
7. REFERENCES.....	80

APPENDIX A – EXAMPLE CALCULATION FOR SURFACE AREA OF FILLER	83
APPENDIX B – MATERIAL DATA SHEETS	84
APPENDIX C – COMPOSITION OF THE TESTED MATRICES	89
APPENDIX D – PLOTS OF OSCILLATORY TEST RESULTS AND UP-DOWN FLOW CURVES FOR THE TESTED MATRICES.....	91
APPENDIX E – MIX DESIGN OF THE TESTED SCC.....	127
APPENDIX F – SCC DOWN FLOW CURVES.....	128
APPENDIX G – CORRELATION ANALYSIS BETWEEN MEDIAN PARTICLE SIZE D_{50} OF THE FILLERS AND RHEOLOGICAL PARAMETERS OF SCC	140

1. Introduction

This test report is written within Sub-project No 2.3 High quality manufactured sand for concrete, as part of COIN (Concrete Innovation Centre) at SINTEF. It is based on the research carried out at NTNU, SINTEF and industrial partners Rescon Mapei AS and NorStone AS from May to June 2010.

1.1 Principal objectives and scope

The principal objectives and scope of this study have been to obtain a clearer knowledge about the effect of different crushed and natural mineral fillers on rheological parameters of matrix and concrete, in order to answer one of the most important questions when using manufactured sand – the question about the very high filler content.

To answer the question we would need to decide how much of the filler do we need to remove from the sand (by using new technology such as air classification we can even modify the filler itself, for example by removing basically only particles below a certain size), in which way do we have to change the concrete mix design compared to concrete with natural aggregate and to what extent can we use admixtures to modify "unwanted" properties caused by the crushed fillers. We cannot give an answer including it all based on this work, but we can draw some essential conclusions that will help us for the further research. For example, that the type of admixture is maybe even more important than the type of filler – which has major industrial implications.

The overall objective is to develop a technology platform for the shift from natural to manufactured aggregates based on hard rock. This includes knowledge of resource management, cost effective production, use of manufactured aggregates in concrete and mix design concepts for concrete.

1.2 Background – research needs

Mineral concrete aggregates can only be extracted where these resources are provided by the nature, but the aggregates have to be used in the places according to the needs of the construction industry and society. Recently it has been realized that the natural sand resources, which previously were taken for granted, now are depleted in many populated areas in Norway and several other parts of the world (Danielsen 2009). This is resulting in a traffic pollution and excess use of energy. Therefore renewed interest focusing on the production of manufactured sand (crushed aggregate with a grain size ≤ 4 mm) for use in concrete has arisen.

At certain conditions, with the availability of the necessary knowledge and equipment, it has been proved to be possible to produce manufactured sand allowing to make concrete that can be utilized in the same way as natural sand concrete (Hotvedt 2009).

Naturally weathered sand differs from most fine crushed aggregates by grading, particle shape and texture. The difference is more severe if the crushed fine aggregate is a by-product (also known as “waste sand” or leftover rocks from quarrying) of coarse aggregate production and no special processing techniques are utilized to improve the characteristics for the finest part of the crusher products. Typically crushed fine aggregate would incorporate a lot more fines along with having different particle size distribution (PSD) than natural sand while the particles would be more angular with rougher surface.

In the original work of Fuller and Thompson (1907) they described their particle size distributions with parabolas, ellipses and straight lines since they plotted all their curves with a linear particle diameter scale. Of their main conclusions, which were based on sieve curves and density measurements on fresh concrete for a large number of aggregates, we here quote a few:

“In ordinary proportioning with a given sand and stone and a given percentage of cement, the densest and strongest mixture is attained when the volume of the mixture of sand, cement and water is so small as just to fill the voids in the stone...” Furthermore: “The best mixture of cement and aggregate has a mechanical analysis curve (= includes cement) resembling a parabola, which is a combination of a curve approaching an ellipse for the sand portion and a tangent straight line for the stone portion. The ellipse runs to a diameter of one-tenth of the diameter of the maximum size of stone, and the stone from this point is uniformly graded...” Final quote: “The form of the best analysis curve for any given material is nearly the same for all sizes of stone, that is, the curve for ½-in., 1-in. and 2 ¼-in. maximum stone may be described by an equation with the maximum diameter as the only variable...”

This means that according to Fuller and Thomson (1907) there exists a particular gradation that, for a given maximum aggregate size, will produce the maximum packing density. Today this curve (also referred to as “classical Fuller curve” or just “Fuller curve”) is expressed as Equation 1-1 in order to describe the maximum packing density gradation for a given maximum aggregate size:

$$Y = \left(\frac{d}{D} \right)^n \cdot 100 \quad (1-1)$$

where

Y = percentage of material finer than the considered aggregate size;

d = aggregate size being considered;

D = maximum aggregate size;

n = parameter which adjusts curve for fineness or coarseness and thus defines the shape of the curve (for maximum particle density $n \approx 0.5$ was proposed by Fuller and Thompson (1907)).

The PSD curve, for manufactured sand normally resembles a curve that can be approximately described with Equation 1-1, i.e., is hanging or dense with high proportions of fines content, opposite to what is normal for natural sand (Wigum and Danielsen 2009).

In the “State-of-the-art” report regarding “Production and Utilisation of Manufactured Sand” published as part of the COIN Project at SINTEF (Wigum and Danielsen 2009) the excess amounts of fines is outlined as one of the most pressing issues when using the manufactured sand in concrete.

The particle size definition of fines is diverse. According to the EN-product standard EN 12620 (2008) for concrete aggregates, fines are all material less than 63 µm. ASTM standard C33 / C33M – 11 (2011) has a similar limit of 75 µm. For practical concrete purposes (see the Particle-Matrix proportioning method in chapter 1.3) in Norway it is quite common that all material less than or 125 µm is referred to as fines.

As reported by Wigum and Danielsen (2009) fines is a part of the sand aggregate, either the lower part of the grading curve, or sometimes also as a contamination; the well-defined, added fine size fraction is commonly referred to as filler. Commercially fillers are supplied mostly from limestone, sometimes from quartz. But even the bottom size of the actual aggregate can be produced as well defined filler.

In order to improve manufactured sand for use in concrete, it is important to know how the fines are influencing the end product. The effects of different fillers on rheological parameters and the quality of fresh concrete, is only partly known. This needs to be examined further. It is also in

particular important to examine the interaction of properties of fines and the effects of the new generation of concrete admixtures.

To solve the fines issue we would need to decide how much of the fines do we need to remove from the sand (the latest generation of dry screening equipment combined with the latest development of air classification have, enabled to govern the grading curve very precisely, including the finest part), in which way do we have to change the concrete mix design compared to concrete with natural aggregate and to what extent can we use admixtures to modify "unwanted" properties caused by the crushed fillers.

1.3 Proportions, rheology and stability – scope

The aggregate is important for most concrete properties. For fresh concrete, the main factors affecting rheology and stability can be simplified into quality and volume fraction of cement paste ($1-\Phi$) and aggregate (Φ). The effect on rheology of the filler depends largely on its specific surface (Nehdi, Mindess and Aitcin 1997, Zhang and Han 2000, Ferraris, Obla and Hill 2001, Bigas and Gillias 2002, Pedersen 2004, Esping 2004, Esping 2004, Westerholm 2006, Esping 2008, Cepuritis 2011) and mineral composition. In concrete the effect of filler becomes more important the larger is its volume fraction. Furthermore, the correlation between the rheology of filler modified paste (= matrix) and concrete is probably closer the higher the volume fraction of matrix (Mørtzell 1996). On the other hand, the maximum packing, Φ_{\max} , which is also an important parameter, becomes more difficult to measure the finer the particles. Thus it could be useful to investigate the rheology of matrix as a first step in the assessment of filler – and admixture effects on properties of fresh concrete.

The Particle-Matrix method for proportioning regards all particles > 0.125 mm as a particle phase dispersed in a lubricating matrix made up of all fluids and particles (binder, filler etc.) < 0.125 mm (Mørtzell 1996, Smeplass and Mørtzell 2001). The method has been used in Norway by many practitioners for more than a decade and has proven very useful. However, the size limit between lubrication – and particle phase when dividing between particles at 0.125 mm is somewhat arbitrary. It has been observed that cement paste and matrix may work equally well as lubricating phase (Jacobsen and Arntsen 2008). Approximately constant values for both of the parameters – (paste volume/ void volume) = paste/ aggregate void saturation ratio $k = (1-\Phi)/V_{\text{tot}}(1-\Phi_{\max})$, and matrix/ particle void saturation ratio $(1-\Phi_{<0.125\text{mm}})/V_{\text{tot}}(1-\Phi_{\max >0.125\text{mm}})$ were observed. The observations were made with constant mortar consistency and w/b for 11 widely different natural and crushed aggregates (Jacobsen and Arntsen 2008).

The maximum packing fraction or crowding factor, Φ/Φ_{\max} , is important for the rheology of particle suspensions and concrete (Barnes, Hutton and Walters 1989, de Larrard 1999) at least at not too high values of Φ/Φ_{\max} , i.e. not too crowded particles (Bager, Geiker and Jensen 2001). Here Φ_{\max} depends mainly on grading, particle shape and compaction (de Larrard 1999, Powers 1968, Glavind, Olsen and Munch-Petersen 1993). The reason why we use the particle void saturation ratio k is simply that it is physically very easy to relate k to the void volume in aggregate and that it can be used directly for proportioning. The relation k versus Φ/Φ_{\max} is shown in the plot below (Figure 1-1).

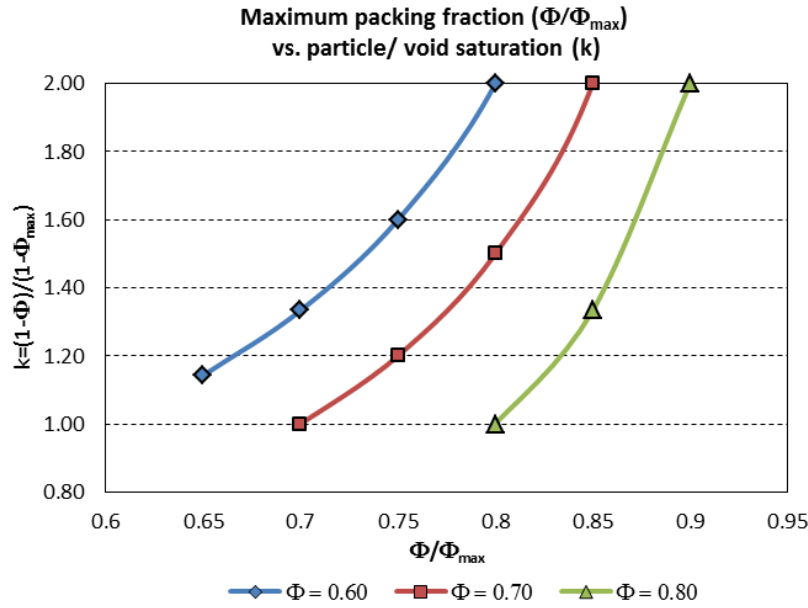


Fig. 1-1: Maximum packing fraction vs. void saturation

Figure 1-1 only shows values of $k > 1$, even though concrete can be made without saturating the void space with paste, such as in pervious concrete (ACI Committee 552 2010) (earlier called “no-fines concrete”) and light weight concrete blocks (“Leca – blocks”). For ordinary plastic- or flow-able concrete qualities k should be in the order 1.1 – 1.2 whereas ultra-high performance concrete and/ or fibre concrete require k in the order of 1.7 to be workable (Jacobsen, Haugan and Arntsen 2005, Berg and Jacobsen 2010), due to low workability of the paste or high void content between the particles, or a combination. In basic proportioning one can thus simply measure (or calculate) Φ_{\max} of the final particle mix and then the proportioning is simplified from the basic volume balance (Feret 1892, Smeplass and Mørtzell 2001):

$$V_{\text{cement}} + V_{\text{water}} + V_{\text{air}} + V_{\text{aggregate}} = V_{\text{tot}} = 1 \text{ m}^3; \quad (1-2)$$

$$V_{\text{matrix}} + V_{\text{aggregate} > 0.125\text{mm}} = V_{\text{tot}} = 1 \text{ m}^3.$$

Introducing k (Jacobsen and Arntsen 2008):

$$k = V_{\text{paste}}/(1-\Phi_{\max})V_{\text{tot}} \text{ with } V_{\text{paste}} = (V_{\text{cement}} + V_{\text{water}} + V_{\text{air}}), \quad (1-3)$$

the cement content m_c can be calculated from maximum particle packing, free w/c, assumed air-void content and density of cement and water as:

$$m_c = \frac{k(1-\Phi_{\max})V_{\text{tot}} - V_{\text{air}}}{\frac{1}{\rho_c} + \frac{w/c}{\rho_{\text{water}}}}. \quad (1-4)$$

Given that the aggregate – or particle phase can be sufficiently described by packing, what kind of lubricating phase should be used to proportion for a desired consistency? Above we used paste but also discussed that this is probably arbitrary since the Particle-Matrix method has shown its efficiency when actively using filler in controlling workability (Mortzell 1996).

Water which represents the “minimum sized” lubricating phase, has been used with success in the time before admixtures. Lyses law (Lyse 1932) predicts constant consistency at constant water content. Lyses proportioning method gave a fairly constant composition of all particles (cement+aggregate) and consequently also a fairly constant maximum packing of all solid particles ($\Phi_{\max, \text{cement+aggregate}}$). So $(1-\Phi_{\text{cement+aggregate}})/V_{\text{tot}}(1-\Phi_{\max, \text{cement+aggregate}})$ becomes the water/

total particle void saturation ratio, which in Lyses law simply means a constant concrete water requirement at constant consistency. Today, water requirement must be exchanged for a (water+admixture) requirement.

Why should Φ_{\max} , which is obtained on particles alone, be of relevance to rheology, consistency or workability of concrete where the particles with volume fraction Φ are arranged very differently?

Powers (1968) used excess paste thickness, which relates to the specific surface of the aggregate, to explain workability. The specific surface, which is needed to determine excess paste thickness, is, however, difficult to obtain since assumptions are needed to calculate it from particle distribution curves, adsorption measurements, optical measurements etc. In addition we cannot measure the excess paste thickness in the fresh mix. So clearly there are limitations to the use of specific surface as well. The answer is that we need both packing and specific surface but that Φ_{\max} is most easy to measure. The aggregate particle spacing, and thus excess paste thickness, will increase as function of $k = (1-\Phi)/V_{\text{tot}}(1-\Phi_{\max})$. At constant particle size the average Thickness T of paste around equally sized spherical particles with radius r is:

$$T = (1-\Phi)/n4\pi r^2 \quad (1-5)$$

where $n4\pi r^2 =$ total surface area. So

$$T = r(1-\Phi)/3\Phi = rk(1-\Phi_{\max})/3\Phi. \quad (1-6)$$

Also for polydispersed particles relations between T , packing and surface area can be deduced, though more cumbersome ones (de Larrard 1999; Roussel 2006). Thus, measuring Φ_{\max} gives at least equally fundamental information as the surface area.

In the question of how to obtain stable and robust SCC there are mainly two means; powders and admixtures. In the time before admixtures, stability in terms of bleeding could be approximated to a fair degree by Cozeny-Karmans equation (Carman 1938) assuming viscous flow of water through a bed of particles. Flocks and tight adsorption of water to the surface could be accounted for in terms of hydraulic radius that would be somewhat larger than the particle radius, though quite predictable (Powers 1968). The bleeding would then depend on the parameters: density, difference particle-liquid, particle volume fraction, particle specific surface and liquid viscosity. Today, due to admixture effects on liquid viscosity and on attractive and repulsive forces between particles (cement, filler), the quantification of viscous flow due to particle settlement is less straight forward as the particle size becomes smaller. The question how different minerals and admixtures affect the thickness of liquid- and admixture layers that remain adsorbed to a particle during stirring and flow is determined by the zeta-potential. The liquid- and admixture molecules carried by or attached to each particle may not only affect but control the viscous behaviour. The importance of these forces compared to mixing energy depends strongly on particle size. The order of 1 micron has been indicated as a point above which stirring and mixing energy will break up particles from both van der Waals attraction (weaker) and electrostatic repulsive barriers and coagulation (stronger) (Billberg 2006). Accordingly, we should investigate combinations of varying admixtures and particles smaller than 1 micron to see combined particle-admixture effects on rheology and stability.

The stability of a particle in terms of sinking in a yield stress fluid was determined from Stoke's law combined with a Bingham fluid giving sinking velocity as function of yield stress and plastic viscosity. Also the critical size of a particle for sinking as function of yield stress was deduced (Roussel 2006). The results showed that theoretically yield stress is the main rheological parameter controlling particle sinking. Also the particle size distribution is

important for stability with possible support of larger particles by smaller ones, see discussion on stability and maximum packing fraction (de Larrard 1999).

In practice we should probably investigate admixture-particle interaction at a bit bigger size than 1 micron. The time range is probably too short to make accurate bleeding and segregation measurements within the fresh period of less than, say, two hours. Furthermore, the critical particle size for a pure Stokes law's stability criterion, with Newtonian liquid viscosity η of water and typical aggregate density (i.e a reference case) is around 1 micron with a sinking velocity v in the order of 1 mm/ hour for a sphere, Equation 1-7:

$$F_{\text{drag}} = 6\pi r v \eta \Rightarrow d_c = 6 \sqrt{\frac{v \eta}{2g(\rho_s - \rho_f)}} \quad (1-7)$$

where

F_{drag} = frictional force acting on the interface between the fluid and the particle;

η = Newtonian liquid viscosity;

r = radius of the spherical particle;

v = particle's sinking velocity;

g = gravitational acceleration;

ρ_s = mass density of the particle;

ρ_f = mass density of the fluid.

Note that Equation 1-7 is quite a simplification compared to the sinking velocity v_s of a particle in a yield stress fluid by Roussel (2006) that includes both plastic viscosity, μ_p , and yield stress τ_0 :

$$v_s = \frac{d_c}{\mu_p} \left(\frac{d_c}{18} |\rho_s - \rho_p| g - \tau_0 \right). \quad (1-8)$$

The simple yield stress stability criterion by (Roussel 2006) obtained at $v_s = 0$ gives critical size in the order of 1 mm even for very low yield stress values in the order of 1 Pa, Equation 1-9:

$$d_c = \frac{18\tau_0}{|\rho_s - \rho_f| g}. \quad (1-9)$$

The large span in particle size effect on stability indicated above makes the exact effect of a specific combination of powder and admixture on stability (and rheology) difficult to determine theoretically. Experiment therefore plays a key role to understand stability and rheology. Considering gravity (density differences) and flow as loads, the counteracting controlling factors include yield stress, liquid viscosity, particle proximity (packing), inter-particle forces and liquid/ admixture interaction/ adsorption.

In this report we present parts of a study on the effect of different types of filler and admixtures on the rheology of matrix, always keeping the fraction of solids, Φ , constant. The work was intended as an initial study to quantify the magnitude of powder- and admixture effects on rheology to proceed in the development of sustainable proportioning and use of crushed rock filler.

2. Materials – investigations – experimental methods

2.1 Matrix rheology tests

2.1.1 Materials

A total of 7 fillers (≤ 0.125 mm) from 5 different quarries in Norway were used for the matrix rheology tests (see Table 2-1). Six of the samples were produced by crushing (or grinding in case of limestone) of different types of rocks in various processes while one was produced originally from natural deposits.

Table 2-1: Fillers used for the matrix rheology tests

No	Quarry (type)	Deposit	Source material*	Producer
1.	Årdal (natural)	Natural glaciofluvial deposit	0/8 mm	NorStone AS
2.	Årdal (crushed/ unwashed)			
3.	Årdal (crushed/ washed)			
4.	Tau	Mylonite rock	0/2 mm washed manufactured sand	Norsk Stein AS
5.	Jelsa	Gneissgranite rock		
6.	Hokksund	Gneiss rock	0/4 mm unwashed manufactured sand	Hokksund Pukkverk AS
7.	Brevik	Limestone deposit	Initial product	Norcem AS

* The source material that the fine aggregate (≤ 0.125 mm) was obtained from by dry sieving at laboratory conditions.

Concrete and matrix fresh state properties depending on the filler type used for the mix were examined extensively within the research presented. The ultimate aim of the study was to find how the fine particle (filler) properties (shape, surface area, particles size distribution etc.) affect the rheological properties of cement based systems. This clearly indicated a need to carry out particle characterization for the fillers used.

Within this project filler particle size distribution was determined using Backman Coulter LS 230 laser diffraction device and Micrometrics SediGraph 5100, specific weight was measured by Micrometrics AccuPyc 1330 Pycnometer and specific surface tests were performed with a Micrometrics FlowSorb II 2300 nitrogen adsorption device by utilizing BET approach and a Blaine apparatus for the Blaine method.

Below a short description of the test methods used is given. Most of it has been adopted from Wigum (2010) where a broader explanation and comparison of different fine particles classification methods can be found. In his work Wigum (2010) also concludes that it is still a challenge to find which test method would mirror in a best way the effects of the properties of fines as concrete aggregate.

The particle size distribution was first measured with the Coulter LS 230 and then the sample was sieved through a 63 μm sieve in order to analyse the fine particle grading again with the aid of the SediGraph.

The Coulter LS 230 measures particle sizes from 40 nm to 2000 μm (0.04 – 2000 μm) by laser diffraction. It is based on the principle that particles scatter and diffract light at certain angles based on their size, shape, and optical properties. A 750 nm diode laser is used for analysis in the size range from 400 nm to 2 mm. The beam passes through filters as well as projection and Fourier lenses and is spatially recorded onto 126 photodiode detectors. The particle size, shape, and optical properties of the particles control the spatial variation of the diffracted beam. The

calculations assume the scattering pattern is due to single scattering events by spherical particles. The advantages of this technique include ease of operation, large range of detectable particle sizes, and accuracy in the micron and submicron range. The Polarization Intensity Differential Scattering (PIDS) assembly sizes particles from 40 nm to 400 nm and improves resolution in the 400 nm to 800 nm range. PIDS uses a tungsten-halogen lamp and three sets of vertically and horizontally polarized colour filters at 450, 600, and 900 nm as the light source. PIDS is based on the principle that at high scattering angles (≈ 90 degrees) the difference in scattering intensity of the two polarizations is a sensitive function of the ratio of particle size to wavelength.

The SediGraph 5100 particle size analyser measures the sedimentation rates of particles in suspension and automatically presents these data as a cumulative mass % distribution in terms of the Stokesian or equivalent spherical diameter in micrometres (μm). The instrument determines, by means of a finely collimated beam of X-rays, the concentration of particles remaining at decreasing sedimentation depth as a function of time. The instrument typically yields a particle diameter distribution over the range 50 to 0.18 μm .

The AccuPyc 1330 Pycnometer works by measuring the amount of displaced gas (helium). The pressures observed upon filling the sample chamber and then discharging it into a second empty chamber allow computation of the sample solid phase volume. Gas molecules rapidly fill the tiniest pores of the sample; only the truly solid phase of the sample displaces the gas. This leads to that the AccuPyc 1330 Pycnometer determines density and volume by measuring the pressure change of helium in a calibrated volume.

When determining surface area of fines, e.g. in the cement industry, the usual method is the so-called Blaine method. This simple method measures the time for a specific volume of air to flow through a known volume of compacted powder and together with the density of the substance, this is used to calculate the specific surface area of the sample. The main advantages of this technique are that it is simple and rapid. However, it is not very accurate and suffers from a number of weaknesses, e.g. variable particle shape and become extremely unreliable at surface areas greater than 500 m^2/kg (Potgieter and Strydom 1996 cited in Wigum 2010).

In situation where accurate measurements are required, one of the most common method to measure surface area is the BET method (Brunauer, Emmett and Teller 1938 cited in Wigum 2010). This method relies on a mathematical formula that describes the adsorption of a particular gas on the finely divided material to calculate its surface area and measures both the internal and the external surface area of a material.

Results of the filler particle size distribution analysis are illustrated on Figures 2-1 and 2-2.

From the grading test results specific surface area has been calculated. Specific surface area was calculated following the suggestions by Erdem, Khayat and Yahia (2009). They proposed a way of calculating surface area of aggregate particles using sieve analysis and assuming that the particles are spherical in shape. An example calculation is presented in Appendix A.

Determined specific weight and surface of the particles is presented in Table 2-2.

Table 2-2: Specific weight and surface area of the fillers

No	Quarry/ type	Specific weight	Specific surface area			
			Blaine	BET	LS Particle Size Analyzer*	Micrometrics SediGraph 5100*
		[g/cm ³]	[m ² /kg]			
1	Årdal (natural)	2.71	131.1	2140	144	357
2	Årdal (crushed/ unwashed)	2.72	165.8	1600	153	364
3	Årdal (crushed/ washed)	2.73	64.5	870	93	209
4	Tau	2.79	229.5	1750	225	283
5	Jelsa	2.81	309.8	1520	192	302
6	Hokksund	2.86	225.5	3760	361	421
7	Limestone	2.74	413.3	1170	470	584

* The surface area of the aggregate was calculated according to Erdem, Khayat and Yahia (2009) using sieve curves and assuming that particles are spherical in shape.

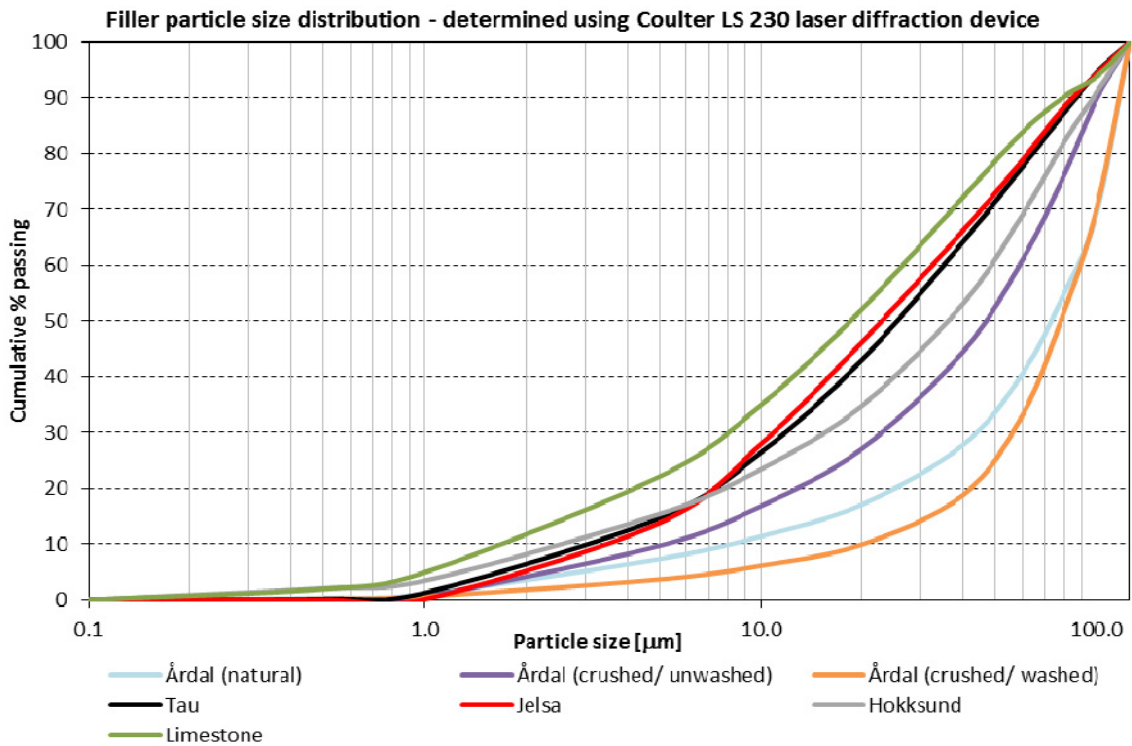


Fig. 2-1: Particle size distribution of the fillers used for the study measured with Coulter LS 230 laser diffraction device

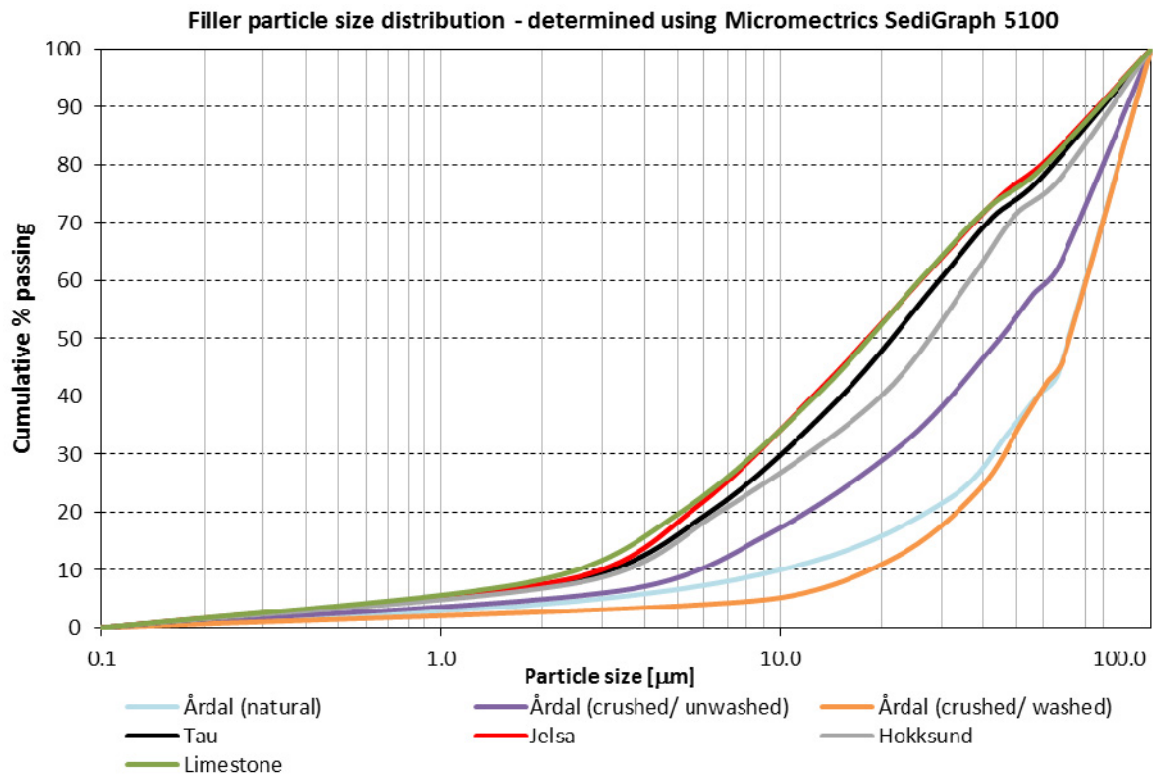


Fig. 2-2: Particle size distribution of the fillers used for the study measured with Micromeritics SediGraph 5100

The following other materials (see Appendix B for material data sheets and test results) were used for the matrix rheology experiments:

- Portland cement of type CEM II/A-V 42.5R from Norcem AS (containing 20% of low lime fly ash);
- Co-polymeric superplasticizers Dynamon SP-130 (longer side-chains dry solids content 30%), Dynamon SR-N (shorter side chains, dry solids content 19.5%) from Rescon Mapei AS and Glenium 151 (dry solids content 15%) from BASF Construction Chemicals GmbH.

2.1.2 Mix composition

A total of 38 mixes have been tested. 6 of the mixes are reference matrices where 5 of them were tested in order to see the correlation of the results with some previous research (Vikan and Jacobsen 2010, Vikan 2000) and to eliminate the time and shear history dependence phenomena of cement-based systems. The other 27 matrices form the main part of the test program.

The design of the main test program for matrices tested in Physica rheometer was based on two considerations:

- To assess the effect of different fillers on rheological parameters of the matrix phase;
- To give a possibility to study the relationship between the rheological properties of the matrix phase and the corresponding cost-efficient SCC (usable for real life concrete production).

An outline of the main testing program is given in Table 2-3 (see Appendix C for complete composition of all the matrices). As there was a need to up-scale the tested matrices to real SCC mixes, natural filler from Årdal was introduced to the compositions in the necessary amount (as a filler part from 0/8 mm low-filer sand used for the SCC mix design). Mixes with a w/c of 0.40 without filler (cement paste) were taken as a reference. Then matrices with w/c ratios of 0.50

and 0.60 had a filler fraction of 20 and 30% (in volume % from the total volume of all the powder) what made it possible for all (except the reference matrices with only natural filler) of the mixes to have an **equal water/powder ratio** $V_w/V_{\text{powder}} = (\text{voids ratio } e) = \mathbf{1.18}$ or **equal solid volume fraction** $\Phi = V_{\text{powder}}/(1.18V_{\text{powder}}+V_{\text{powder}}) = \mathbf{0.459}$. The reason for this choice is the dominating effect on rheology of a particle suspension of solid volume fraction (Barnes, Hutton and Walters 1989).

This gives the possibility to directly compare the effect of exchanging cement by filler on a volume basis. It's also possible to assess how much the matrix rheology is affected at constant water/ powder ratio by volume. Such a matrix classification parameter could hopefully be used for concrete proportioning to describe the rheological properties of the fresh SCC for different powder/ admixture combinations.

The superplasticizer dosage was set at 0.4% of cement mass for all the mixes. The dosage aimed at making very stables mixes.

Table 2-3: Outline of the main test program (including the references = a total of 33 mixes) for matrix testing in Physica rheometer. The addition levels of fillers are given in volume % of powder (all particles ≤ 0.125 mm)

Filler	w/c=0.4 w/V _{powder} =1.18 0% of filler		w/c=0.4 w/V _{powder} =1.1 7% of filler		w/c=0.5 w/V _{powder} =1.18 20% of filler*		w/c=0.6 w/V _{powder} =1.18 33% of filler*	
	SP-130	SX-N	SP-130	SX-N	SP-130	SX-N	SP-130	SX-N
No filler	x	x						
Årdal (natural)			x	x	x	x	x	x
Årdal (crushed/ unwashed)					x	x	x	x
Årdal (crushed/ washed)					x	x	x	x
Tau					x	x	x	x
Jelsa					x	x	x	x
Hokksund					x	x	x	x
Limestone					x	x	x	x

* Total amount of filler including 7% of natural filler from Årdal as a filler part from 0/8 mm "low-filler" sand used for the later SCC mix design. 33^d mix is a cement paste (0% of filler) with a w/c=0.4, w/V_{powder} of 1.18 and no superplasticizer.

2.1.3 Rheometer

All matrix rheological measurements have been performed with a MCR 300 rheometer produced by Physica as illustrated on Figure 2-3. The resolution (accuracy) of the rheometer is 0.1 nNm for torque and 10 nrad for angular measurements.

A parallel plate measuring system was chosen. The lower plate is stationary, while the upper plate is rotating. The torque at the upper plate is measured continuously. The surfaces of both the rotor and the motionless plate were flat, but the upper plate had a serrated surface of 150 μm roughness. The gap between the plates was set to 1 mm for all measurements. The bottom plate was temperature controlled (+20 °C for all measurements).

In order to reduce evaporation of water from the matrix sample during the rather long measurement sequence (29.5 min) the upper and lower plates of the rheometer were covered with a plastic ring and a metallic lid, while a water trap attached to the upper plate was filled with water to ensure saturated vapour pressure above the fresh specimen.



Fig. 2-3: MCR 300 rheometer by Physica

2.1.4 Mixing and measurement sequence

The matrices were blended in a high shear blender by Braun (MR5550CA) as illustrated in Figure 2-4. Mixing intensity level 6 was used for the tests. The blending was performed by adding solids to the water (water and admixtures being previously mixed, the superplasticizers were diluted with water 1:10) and mixing for ½ minute, resting for 5 minutes and blending again for 1 minute. Total matrix volume was 185 ml.



Fig. 2-4: High shear blender MR5550CA by Braun

The rheological measurement sequence that was started 10 min after water addition is presented in Table 2-4.

Table 2-4: Rheological measurement sequence

Measuring profile	Time [min]
1 minute pre-shearing with constant shear rate ($\dot{\gamma}$) of 60 s^{-1} to produce uniform initial conditions	1
1 minute rest without shearing	1
Static yield stress: $\dot{\gamma} = 0.02 \text{ s}^{-1}$ in 30 points each lasting 5 seconds	2.5
Shearing $\dot{\gamma} = 60 \text{ s}^{-1}$ in 2 points each point lasting 15 s	0.5
Pause 30 seconds	0.5
Oscillation as an amplitude sweep to characterize the structure, to find the limit of linear viscoelastic range (LVE), and possibly to determine the yield point as the limit of the LVE shear stress range. Set frequency (f) = 1 s^{-1} . Strain amplitude within 0.1-100% in 36 logarithmic steps of 10 s	6
Up-down flow curve: <ul style="list-style-type: none"> ○ Stress (τ) – shear rate ($\dot{\gamma}$) curve with linear sweep of $\dot{\gamma}$ from 1 up to 100 s^{-1} in 30 points lasting 6 seconds each ○ Stress (τ) – shear rate ($\dot{\gamma}$) curve with linear sweep of $\dot{\gamma}$ from 100 down to 1 s^{-1} in 30 points lasting 6 seconds each 	6
Shearing $\dot{\gamma} = 250$ in 5 points each point lasting 6 s	0.5
Pause 30 seconds	0.5
Thixotropy: <ul style="list-style-type: none"> ○ $\dot{\gamma} = 0.1$ for t = 60 s with 5 measuring points ○ $\dot{\gamma} = 250$ for t = 30 s with 5 points ○ $\dot{\gamma} = 0.1$ for t = 200 s with 50 	5
10 seconds resting	
Shear rate ($\dot{\gamma}$) - stress (τ) curve with logarithmic sweep of τ from 0.5-250 Pa in 30 points each lasting 5 seconds in order to measure the gel strength (static yield stress) after 10 seconds rest	2.5
1 minute rest	1
Static yield stress: $\dot{\gamma} = 0.02 \text{ s}^{-1}$ in 30 points each lasting 5 seconds	2.5
Total	29.5

The measuring sequence is visualized in Figure 2-5.

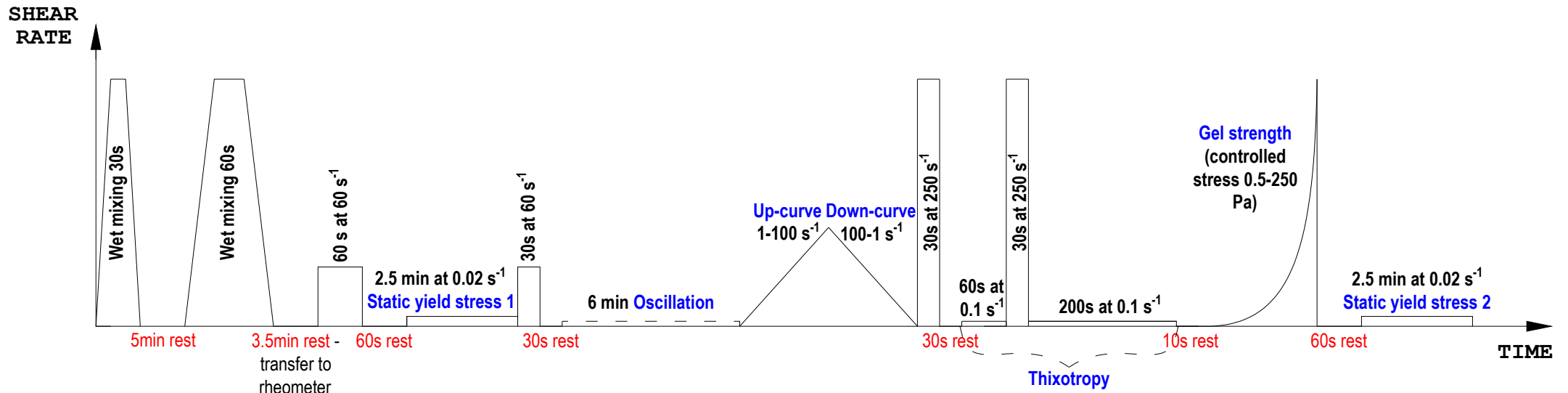


Fig.2-5: Schematic flow-chart of the measurement sequence

2.1.5 Oscillatory tests to determine complex shear modulus and critical strain

An oscillatory shear test as an amplitude sweep (see Table 2-4) was carried out with the Physica rheometer for the purpose of characterizing the structure and determining the limit of the linear viscoelastic range (LVE).

Oscillatory shear is a dynamic rheological technique in which strain is oscillated according to a sine function. By limiting the strain to a small amplitude (i.e., $< 1\%$ (= a shear strain $\gamma = 0.01$ – presumably below the fracture strain in the presumably elastic domain), the particles stay in close contact with one another and are able to recover elastically, so the microstructure is not disturbed and the matrices behave as a solid. At larger amplitudes the particles are separated and the paste becomes liquid in its behaviour. Thus the oscillatory shear provides information concerning the viscoelastic properties of the matrices both below yield (while behaviour is essentially elastic like a **solid**) and above yield (while behaviour is essentially viscous like a **liquid**).

The results of the tests were plotted as shown in Figure 2-6. The $\lg \gamma$ is plotted on the x-axis and both $\lg G'$ (storage modulus) and $\lg G''$ (loss modulus) are represented on the y-axis at the same scale.

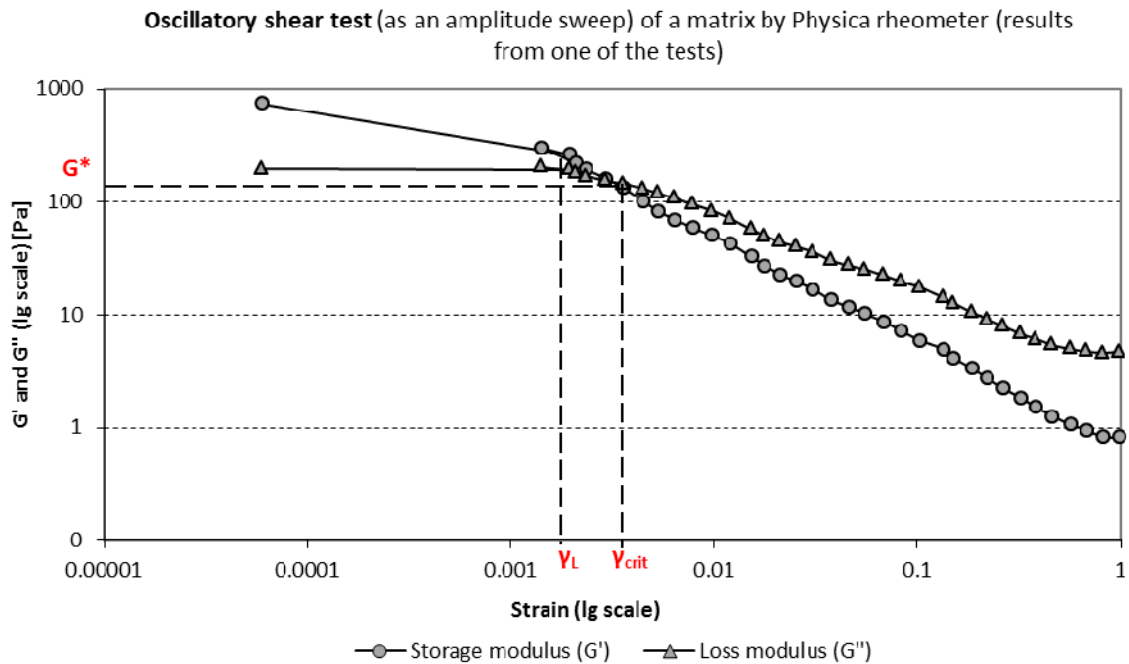


Fig.2-6: Relation $\lg G'(\gamma)$ and $\lg G''(\gamma) - \lg \gamma$

As long as the γ amplitudes remain below the limiting value γ_L , the G' and G'' curves should show a constantly high plateau value, i.e. the structure of the sample is stable under this low-deformation condition. At amplitudes higher than γ_L , the limit of the LVE range is exceeded. The structure of the sample has already been irreversibly changed or even completely destroyed. However, the value γ_L was not easily determinable for most of the matrices tested. That is why the critical strain value γ_{crit} (where $G^* = G' = G''$) was chosen as a parameter for further analysis of the results. Because of the mentioned it was also not possible to determine the yield point as the limit of the LVE shear stress range. The above definition of the end of the viscoelastic range as the critical strain is reached is based on writing Hookes law on the form:

$$G^* = \tau(t)/\gamma(t) \quad (2-1)$$

Values γ_{crit} and $G^*=G'=G''$ were determined graphically from the plots or calculated at the point where $G^*=G'=G''$. The usual interpretation of these parameters is (Barnes, Hutton and Walters 1989):

- **Gel character**, if $G' > G''$. Here, the elastic behaviour dominates over the viscous behaviour. The structure shows certain rigidity.
- **Liquid character**, if $G'' > G'$. In this case, the viscous behaviour dominates over elastic behaviour.

2.1.6 Rheological model functions for the flow curves

Two rheological models (see Figure 2-7) were applied to characterize the flow “down-curves” (see Table 2-4) of the matrices tested:

$$\text{Bingham: } \tau = \tau_B + \mu_B \dot{\gamma}; \quad (2-2)$$

flow curve model function from what the “Bingham yield point” τ_B (which is visible in Figure 2-7 as an intersection on the τ axis) and the “Bingham viscosity” μ_B were determined;

$$\text{Herschel / Bulkley: } \tau = \tau_{HB} + c \cdot \dot{\gamma}^p; \quad (2-3)$$

flow curve model function from what the “yield point according to Herschel/ Bulkley” τ_{HB} , the “flow coefficient” c [Pas] (also called the “Herschel/ Bulkley viscosity” μ_{HB}) and the exponent p (also called “Herschel/ Bulkley index”) were determined.

To characterize the structural breakdown during the flow curve test the area of the “hysteresis loop” between the up- and down curves was calculated. In order to simplify the calculations when determining the “hysteresis area”, up- and down-curves were approximated using two parameter power function (see Figure 2-7; or Herschel/ Bulkley function with a $\tau_{HB} = 0$). The “hysteresis area” was calculated by subtracting the area incorporated by the "down-curve" from the area incorporated by the "up-curve".

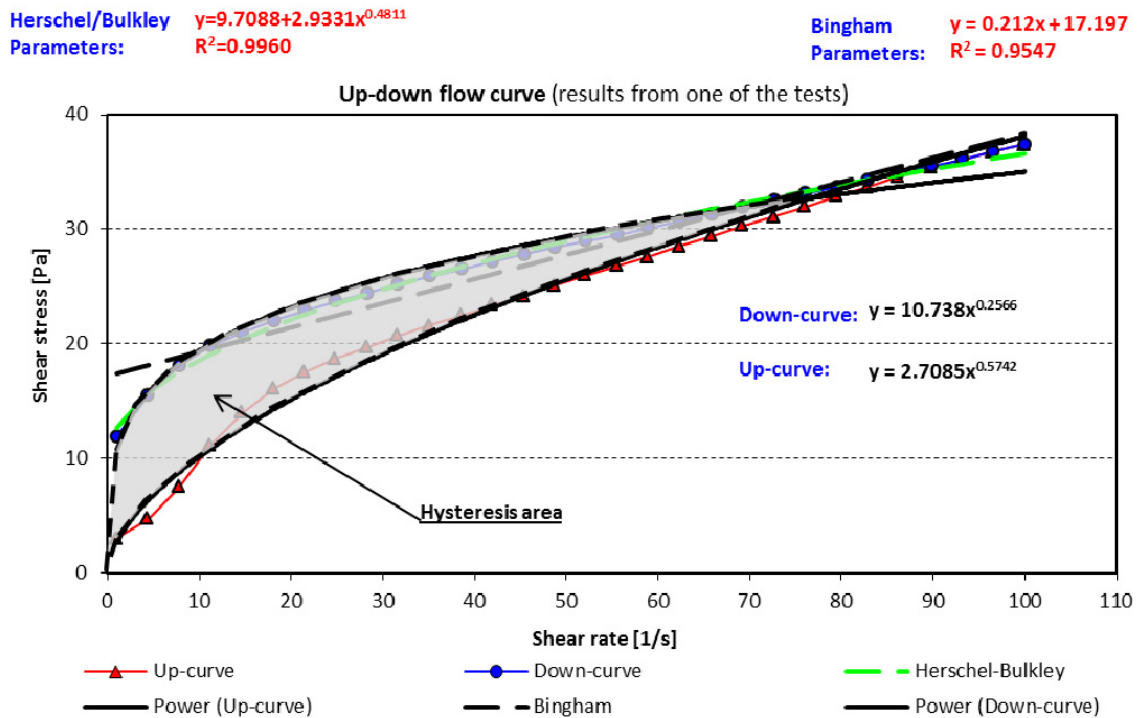


Fig.2-7: Use of rheological model functions to characterize the flow down-curves of the matrices tested

2.1.7 Gel strength, static yield stress and shear modulus

In this study yield values of the matrices were determined in three ways. First dynamic yield was determined by regression of the rheometer runs with a set shear rate range of 100 to 1 s^{-1} assuming that either Bingham or Herschel/ Bulkley model applies (see chapter 2.1.6).

In addition static tests were performed. First, very small and stepwise increasing shear loads were applied from the rest (see Table 2-4). The transition between elastic and plastic behaviour of fresh matrix (determined by controlled shear stress) was registered as the so-called **gel-strength**.

The **gel-strength** value was determined from the plots (see Figure 2-8) of γ on the x-axis and τ on the y-axis as the point where the relation of the two became obviously non-linear. The increase rate of the strain for the next point measured was checked to be more than two times greater than the increase rate in stress for all the gel-strengths registered. **Shear modulus** from the gel-strength tests is defined as the slope of the line drawn through the origin and a point in the plot where the shear stress is half of the gel-strength (**50% tangent shear modulus**).

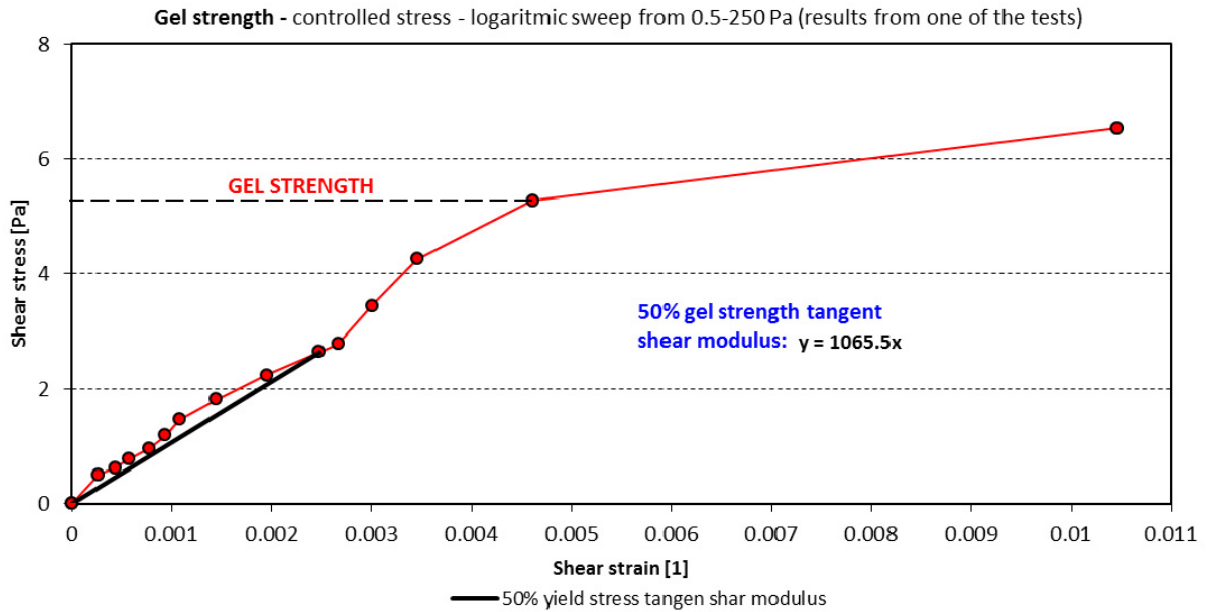


Fig.2-8: Determination of the gel strength and matrix shear modulus

The **static yield stress** was determined two times within the measurement sequence (see Table 2-4) in order to assess the aging of the matrices. The static yield stress was measured by applying small constant shear rate (0.02 s^{-1}) and registering the highest shear stress determined (see Figure 2-9). **Shear modulus** from the static yield stress tests is defined as the slope of the line drawn through the origin and a point in the plot where the shear stress is half of the maximum (**50% tangent shear modulus**).

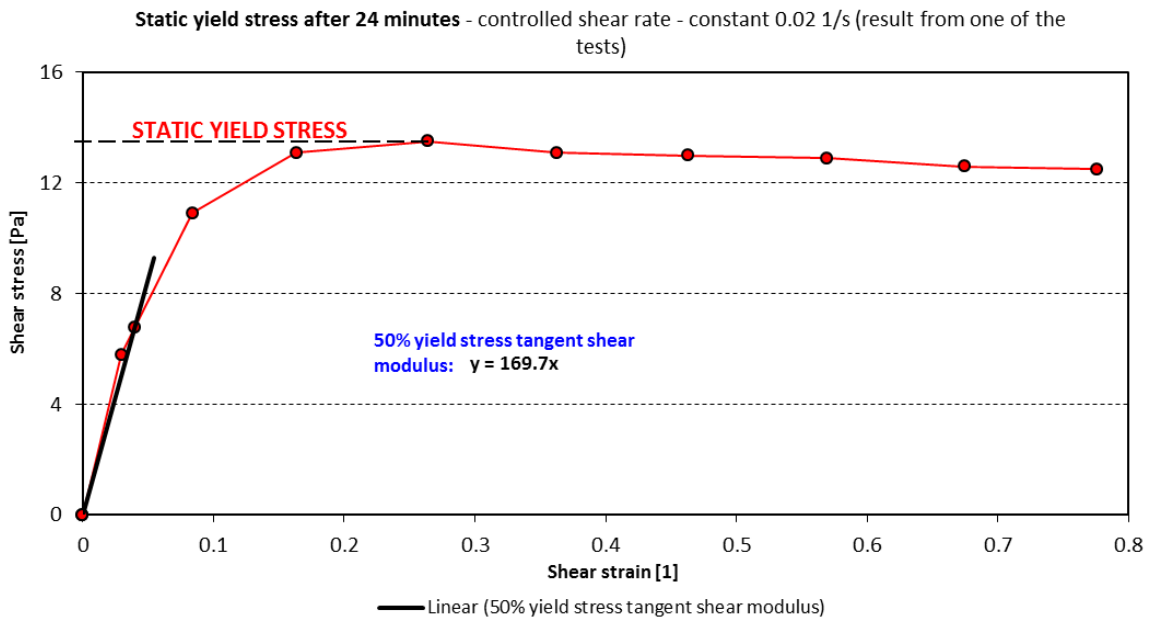


Fig.2-9: Determination of the static yield stress and matrix shear modulus

2.2 SCC rheology tests

2.2.1 Materials and mix composition

In order to assess the effect of different fillers on concrete rheology and see if it's possible to find a correlation between concrete and matrix rheological parameters all the fillers (Table 2-1) were tested in SCC mixes. Composition of concrete matrices with varying filler types and

quantities were copied directly from the previous tests (Table 2-3) – except for the SCC’s with a w/c ratio of 0.77.

In addition natural “low-filler” sand 0/8 mm (filler \leq 125 μ m content only 2.7% to minimize natural filler effect) and crushed coarse aggregate 8/16 mm from Årdal quarry (NorStone AS) were used in the mixes. Dynamon SP-130 from Rescon Mapei AS was chosen as the admixture (see Appendix B for material data sheets).

A total of 22 mixes have been tested. One mix is a reference mix with only filler from the natural “low-filler” sand. The other mixes form the main test program where each of the 7 fillers is tested at three different w/c ratios (0.5, 0.6 and 0.77). The matrix content was chosen 360 l/m³ for the w/c levels 0.5 and 0.6 and 400 l/m³ for the w/c ratio 0.77.

The superplasticizer dosage was accordingly 2.0%, 1.1% and 0.6% of binder by mass.

An outline of the main test program is given in Table 2-4 (see Appendix E for complete composition of all 22 mixes). Concrete compositions were designed to represent a cost-efficient SCC that would be usable for day-to-day real life concrete production.

Table 2-4: Outline of the concrete test program (a total of 22 mixes) for SCC testing in a coaxial cylinder viscometer by ConTec. The addition levels of fillers are given in volume % of powder (matrix = all liquids + particles \leq 0.125 mm), particles = granitic aggregate 0.125 – 16 mm)

Filler	w/c=0.4	w/c=0.5	w/c=0.6	w/c=0.77
	w/V _{powder} =1.1	w/V _{powder} =1.18	w/V _{powder} =1.18	w/V _{powder} =1.51
	7% of filler*	20% of filler*	33% of filler*	33% of filler*
	2.0% of SP-130	1.1% of SP-130	1.1% of SP-130	0.6% of SP-130
	360 l/m ³ of matrix	360 l/m ³ of matrix	360 l/m ³ of matrix	400 l/m ³ of matrix
Årdal (natural)	x	x	x	x
Årdal (crushed/unwashed)		x	x	x
Årdal (crushed/washed)		x	x	x
Tau		x	x	x
Jelsa		x	x	x
Hokksund		x	x	x
Limestone		x	x	x

* Total amount of filler including 7% of natural filler from Årdal as a filler part from 0/8 mm low-filer sand used for later SCC mix design.

2.2.2 Rheometer

All SCC rheological measurements have been performed with a Viscometer 5 by ConTec (Figure 2-10). The ConTec’s Viscometer 5 is a coaxial cylinder viscometer for course particle suspension that is suitable to measure the rheological properties of cement paste, mortar and concrete with about 120 mm slump or higher.

Both cylinders of the coaxial cylinder system contain ribs (or roughened surfaces) to reduce/prevent slippage.

The specified performance range of the ConTec Viscometer 5 is for torque 0.27 Nm to 27 Nm and for rotation velocity 0.1 revolutions per second (rps) to 0.6 rps under normal testing conditions. The absolute range for both the velocity and the torque can be optionally adjusted. The very low rotation velocity of the viscometer makes it possible to measure the stress-deformation curve of the sample mix, an important factor regarding consolidation of concrete. The high torque range of the viscometer is necessary when testing high performance concrete.

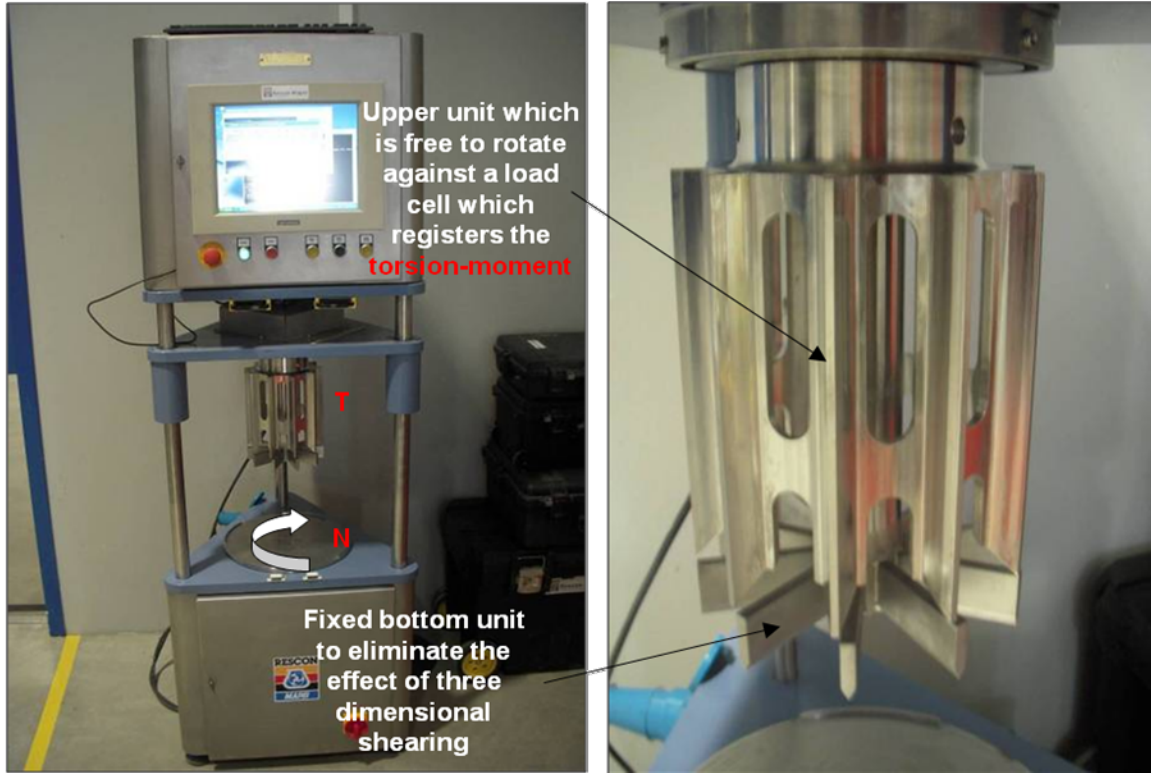


Fig. 2-10: Viscometer 5 by ConTec

2.2.3 Mixing, determination of fresh concrete properties and rheological parameters

Collomix ColloMatic® XM 2 - 650 forced action paddle-pan type mixer (Figure 2-11) was used to prepare the SCC mixes utilizing the standard mixing procedure according to EN 480-1 (2007). The concrete mixing sequence is presented in the Table 2-5 below.

Table 2-5: SCC mixing sequence

Mixing step No.	Time line	Action
1	0.00-0.10	10 sec mixing (all dry materials)
2	0.10-0.30	20 sec mixing (added water with admixture)
3	0.30-1.30	60 sec mixing
4	1.30-5.50	4 min and 20 sec rest*
5	5.50-6.00	10 sec mixing

* During the rest it was ensured that nothing was stuck at the bottom of the mixing bowl.

On the average 8 minutes were used for mixing and transfer to the rheometer.

The following fresh concrete properties were determined right away after mixing:

- Slump-flow according to EN 12350-8 (2010);
- Air void content according to EN 12350-7 (2009);
- Density according to EN 12350-6 (2009);

- Temperature.



Fig. 2-11: Collomix ColloMatic® XM 2 – 650 forced action mixer

The rheological measurement sequence lasted for 22 min including two down flow curves (at the beginning and after 22 min) and static yield stress measurement in between. At first down flow curve measurement was carried out (6 points from 0.45 to 0.04 RPS and a control for separation at 0.3 RPS), then the mix was covered with plastic and let rest for 20 min after what the static yield stress measurement was performed (with a controlled shear rate, i.e. very small constant speed of rotation = 0.08 RPS and then the static yield stress was determined from max torque at that speed) followed by another flow down curve (6 points at 0.45 to 0.04 RPS and control for separation at 0.3 RPS). The SCC was re-mixed by hand before each consecutive measurement.

The rheological properties were described by the fundamental parameters in the Bingham model (see chapter 2.1.7), the yield value τ_0 , and the plastic viscosity μ . They were calculated by the Reiner-Riwlin equation (Wallevik 2003). One can also choose to use the values **G** and **H** instead of the Bingham parameters, and they are often preferred, as they are simpler and easier to implement. The calculation process also qualified the proneness of the concrete-mix to segregate by the segregation factor (S), which can be considered as the change in viscosity during testing.

3. Results

3.1 Overview of the matrix test results

Tables 3-1, 3-2 and 3-3 show a compilation of rheological parameters determined according to the measurement sequence in Table 2-4 by means described in chapters 2.1.3 and 2.1.4.

Figures 3-1 to 3-4 illustrate structural decomposition and regeneration of matrices when a “thixotropy” measuring profile from Table 2-4 is applied. Tables 3-4 to 3-6 show regeneration of the structure of the matrices as a $\eta(t)$ in % after the application under high shear conditions.

Please see Appendix D for complete plots of oscillatory test results and up-down flow curves.

Table 3-1: Overview of the rheological parameters for matrices with Dynamon SR-N

Matrix No.	Filler	Bingham parameters		Herschel-Bulkley parameters				Hysteresis area [Pa/s]	Complex modulus, G* [Pa]	Critical strain γ_{crit} [1]	Gel strength [Pa]	Static yield stress [Pa]	Static yield s. (after 24 minutes) [Pa]	G (controlled stress) [Pa]	G (controlled shear rate) [Pa]	
		τ_y [Pa]	μ [Pa·s]	R ²	τ_y [Pa]	K [Pa·s]	n									R ²
1	2	3	4	5	6	7	8	9	10	11	12	13	14	15	16	17
0.4% of Dynamon SR-N w/c=0.4 w/V_{powder}=1.18 (Φ=0.459) or w/V_{powder}=1.1 (Φ=0.476)																
1	Cement paste; (w/V _{powder} =1.18)	45	1.03	0.9069	-18	30.48	0.35	0.9940	1046	not determ.	24	59	71	9623	5226	
2	Årdal (natural); (w/V _{powder} =1.1)	53	1.19	0.9058	-21	35.86	0.35	0.9933	1653	0.026	36	75	85	11215	1151	
0.4% of Dynamon SR-N w/c=0.5 w/V_{powder}=1.18 (Φ=0.459)																
3	Årdal (natural)	17	0.33	0.8860	-11	15.21	0.29	0.9947	262	0.014	5	19	28	3528	1025	
4	Årdal (crushed/unwashed)	22	0.45	0.8836	-14	19.57	0.29	0.9924	583	0.010	7	22	27	3072	986	
5	Årdal (crushed/washed)	21	0.36	0.8616	-18	24.36	0.23	0.9925	552	0.006	5	22	32	2925	1319	
6	Tau	26	0.58	0.8803	-18	23.78	0.30	0.9888	1274	0.013	10	27	36	4546	1403	
7	Jelsa	18	0.35	0.8849	-12	16.64	0.28	0.9949	976	0.012	8	29	36	3755	1400	
8	Hokksund	28	0.55	0.8584	-25	30.67	0.26	0.9855	607	0.001	10	34	44	4651	2066	
9	Limestone	24	0.47	0.8595	-24	28.72	0.25	0.9898	865	0.001	8	27	25	4238	391	
0.4% of Dynamon SR-N w/c=0.6 w/V_{powder}=1.18 (Φ=0.459)																
10	Årdal (natural)	8	0.20	0.8993	-5	6.81	0.33	0.9942	325	0.002	2	8	13	2894	298	
11	Årdal (crushed/unwashed)	14	0.32	0.8911	-9	11.94	0.32	0.9919	669	0.009	4	13	20	2067	521	
12	Årdal (crushed/washed)	7	0.19	0.9432	-1	3.15	0.44	0.9991	445	0.002	1	4	6	1992	71	
13	Tau	25	0.46	0.8743	-18	24.40	0.27	0.9930	570	0.012	7	22	26	3450	828	
14	Jelsa	22	0.31	0.8729	-12	20.99	0.23	0.9972	572	0.008	4	18	23	1996	640	
15	Hokksund	20	0.48	0.9041	-11	14.95	0.35	0.9938	805	0.002	7	17	25	2013	767	
16	Limestone	13	0.32	0.8876	-11	12.82	0.31	0.9925	456	0.011	4	10	19	2994	622	
AVERAGE: 0.8875												AVERAGE: 0.9930				

Table 3-2: Overview of the rheological parameters for matrices with Dynamon SP-130

Matrix No.	Filler	Bingham parameters			Herschel-Bulkley parameters				Hysteresis area [Pa/s]	Complex modulus, G* [Pa]	Critical strain γ_{crit} [1]	Gel strength [Pa]	Static yield stress [Pa]	Static yield s. (after 24 minutes) [Pa]	G (controlled stress) [Pa]	G (controlled shear rate) [Pa]
		τ_y [Pa]	μ [Pa·s]	R ²	τ_y [Pa]	K [Pa·s]	n	R ²								
1	2	3	4	5	6	7	8	9	10	11	12	13	14	15	16	17
0.4% of Dynamon SP-130 w/c=0.4 w/V_{powder}=1.18 (Φ=0.459) or w/V_{powder}=1.1 (Φ=0.476)																
17	Cement paste; (w/V _{powder} =1.18)	31	0.35	0.9676	22	3.16	0.56	0.9947	430	131	0.010	7	23	23	11511	404
18	Cement paste; <i>without</i> SP; (w/V _{powder} =1.18)	50	1.31	0.9047	-24	34.78	0.37	0.9885	202	not determ.	not determ.	29	62	78	15439	6588
19	Årdal (natural) (w/V _{powder} =1.1)	42	0.38	0.9574	31	4.11	0.52	0.9875	490	115	0.018	24	34	34	8337	668
0.4% of Dynamon SP-130 w/c=0.5 w/V_{powder}=1.18 (Φ=0.459)																
20	Årdal (natural)	14	0.19	0.9574	8	2.39	0.49	0.9983	202	82	0.004	3	9	9	985	115
21	Årdal (crushed/unwashed)	17	0.21	0.9547	10	2.93	0.48	0.9960	364	155	0.003	5	12	14	1066	170
22	Årdal (crushed/washed)	13	0.19	0.9593	6	2.36	0.50	0.9973	151	92	0.003	2	7	8	857	92
23	Tau	19	0.27	0.9473	7	4.58	0.45	0.9982	587	44	0.003	7	13	15	1488	193
24	Jelsa	19	0.23	0.9578	9	3.85	0.45	0.9953	220	107	0.003	7	12	14	1799	185
25	Hokksund	24	0.28	0.9235	8	8.03	0.36	0.9973	278	102	0.003	8	19	22	1819	352
26	Limestone	18	0.24	0.9533	9	3.45	0.47	0.9975	190	133	0.003	5	12	13	1481	177
0.4% of Dynamon SP-130 w/c=0.6 w/V_{powder}=1.18 (Φ=0.459)																
27	Årdal (natural)	8	0.13	0.9513	3	1.95	0.47	0.9983	85	54	0.003	2	4	6	907	68
28	Årdal (crushed/unwashed)	9	0.17	0.9586	4	2.05	0.50	0.9985	103	68	0.004	2	6	7	1065	77
29	Årdal (crushed/washed)	7	0.13	0.9503	2	2.00	0.47	0.9988	204	54	0.004	2	4	5	788	53
30	Tau	21	0.28	0.8928	-3	13.49	0.28	0.9973	226	61	0.002	3	16	18	900	278
31	Jelsa	12	0.19	0.9521	5	2.82	0.47	0.9985	236	34	0.005	3	8	9	1272	120
32	Hokksund	19	0.26	0.8852	-4	13.13	0.27	0.9959	484	22	0.004	7	18	22	1556	404
33	Limestone	14	0.18	0.9165	2	5.95	0.34	0.9997	588	15	0.006	4	10	12	1332	172
		AVERAGE: 0.9406				AVERAGE: 0.9963										

Table 3-3: Overview of the rheological parameters for matrices that were tested in order to see the correlation of the results with some previous research (Vikan 2005, Vikan and Jacobsen 2010)

Matrix No.	Filler	Bingham parameters			Herschel-Bulkley parameters				Hysteresis area [Pa/s]	Complex modulus, G^* [Pa]	Critical strain γ_{crit} [1]	Gel strength (after 10 min) [Pa]	Static yield stress [Pa]	Static yield s. (after 24 minutes) [Pa]	G (controlled stress) [Pa]	G (controlled shear rate) [Pa]	G (controlled shear rate; after 10 min) [Pa]	
		τ_y [Pa]	μ [Pa-s]	R^2	τ_y [Pa]	K [Pa-s]	n	R^2										
1	2	3	4	5	6	7	8	9	10	11	12	13	14	15	16	17	17-2	
0.4% of Dynamon SP-130 w/c=0.4 w/V_{powder}=1.18 ($\Phi=0.459$)																		
34 (17)	Cement paste; test sequence: see Table 2-4	31	0.35	0.9676	22	3.16	0.56	0.9947	430	131	0.010	7	23	23	11511	404	-	
35	Cement paste; test sequence: Vikan (2005)	37	0.28	0.9438	26	4.90	0.44	0.9891	33	-	-	5	-	-	-	14509	25740	
36	Cement paste; test sequence: Vikan and Jacobsen (2010)	32	0.28	0.9575	24	3.04	0.52	0.9877	-72	-	-	4	-	-	-	223925	9363	
Glenium 151 w/c=0.4 w/V_{powder}=1.18 ($\Phi=0.459$)																		
37	Cement paste; test sequence: see Table 2-4	38	0.33	0.9574	27	3.93	0.51	0.9908	478	110	0.004	19	31	28	4884	482	-	
38	Cement paste; test sequence: see Table 2-4	16	0.33	0.9845	11	1.57	0.68	0.9985	413	28	0.010	3	8	10	494	115	-	
		AVERAGE			0.9413			AVERAGE				0.9952						

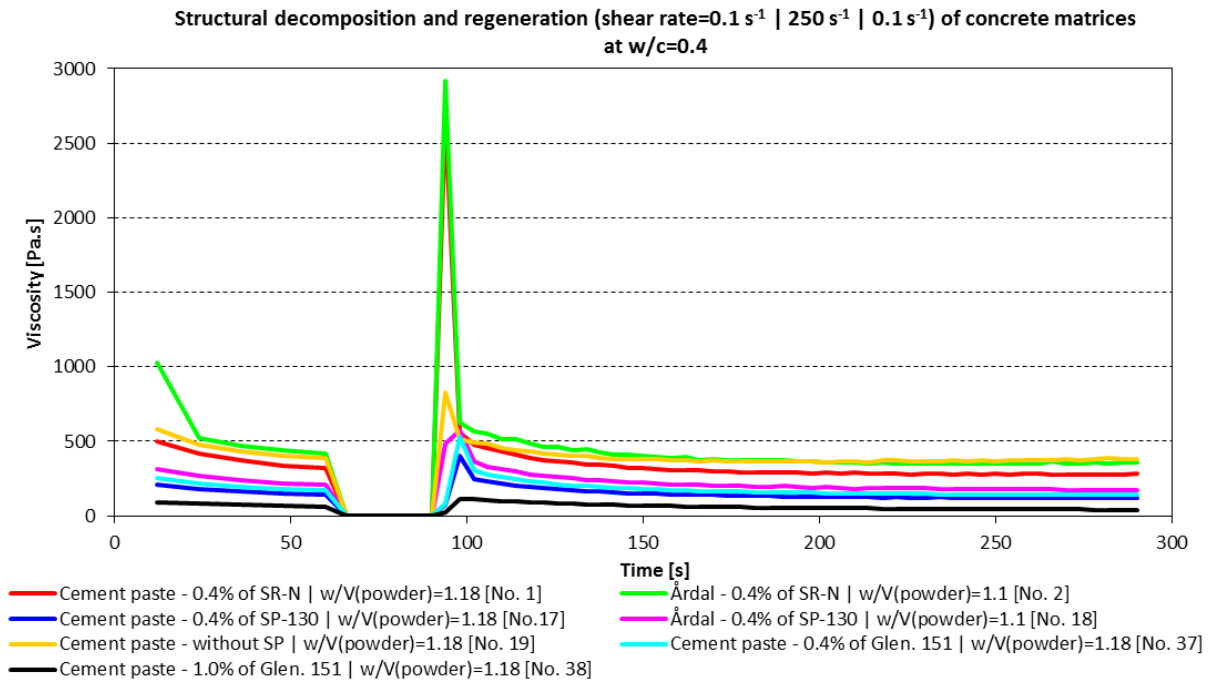


Fig.3-1: Structural decomposition and regeneration of matrices with different admixtures at $w/c=0.4$

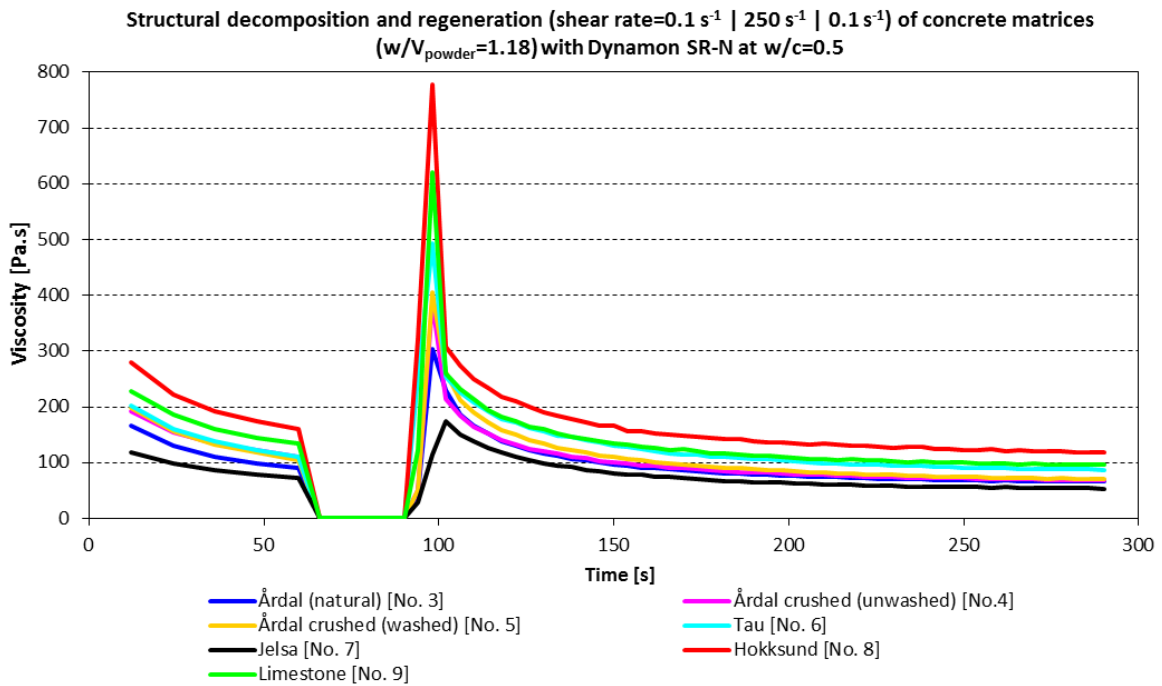


Fig.3-2: Structural decomposition and regeneration of matrices with Dynamon SR-N at $w/c=0.5$

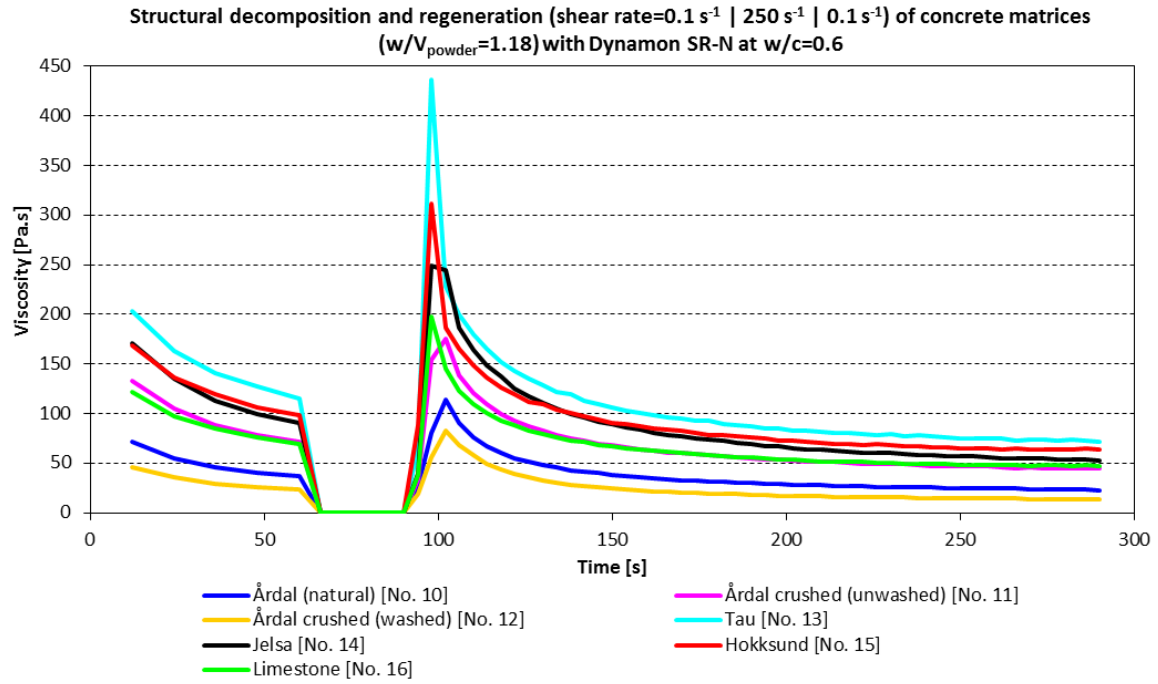


Fig.3-3: Structural decomposition and regeneration of matrices with Dynamon SR-N at $w/c=0.6$

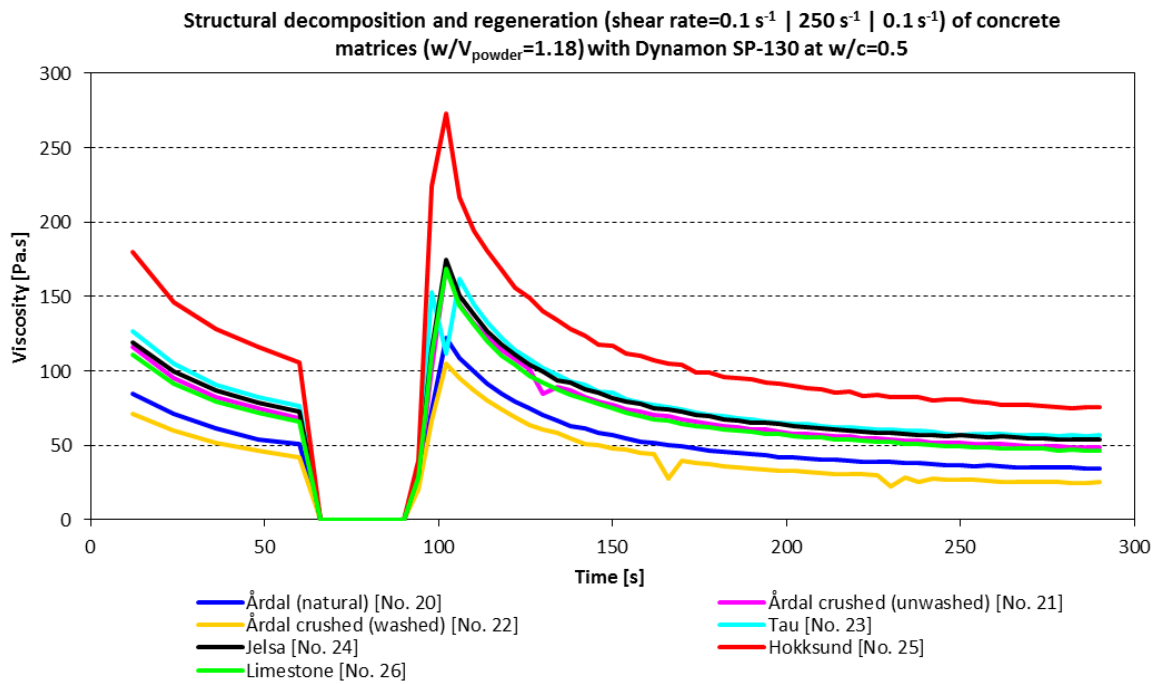


Fig.3-4: Structural decomposition and regeneration of matrices with Dynamon SP-130 at $w/c=0.5$

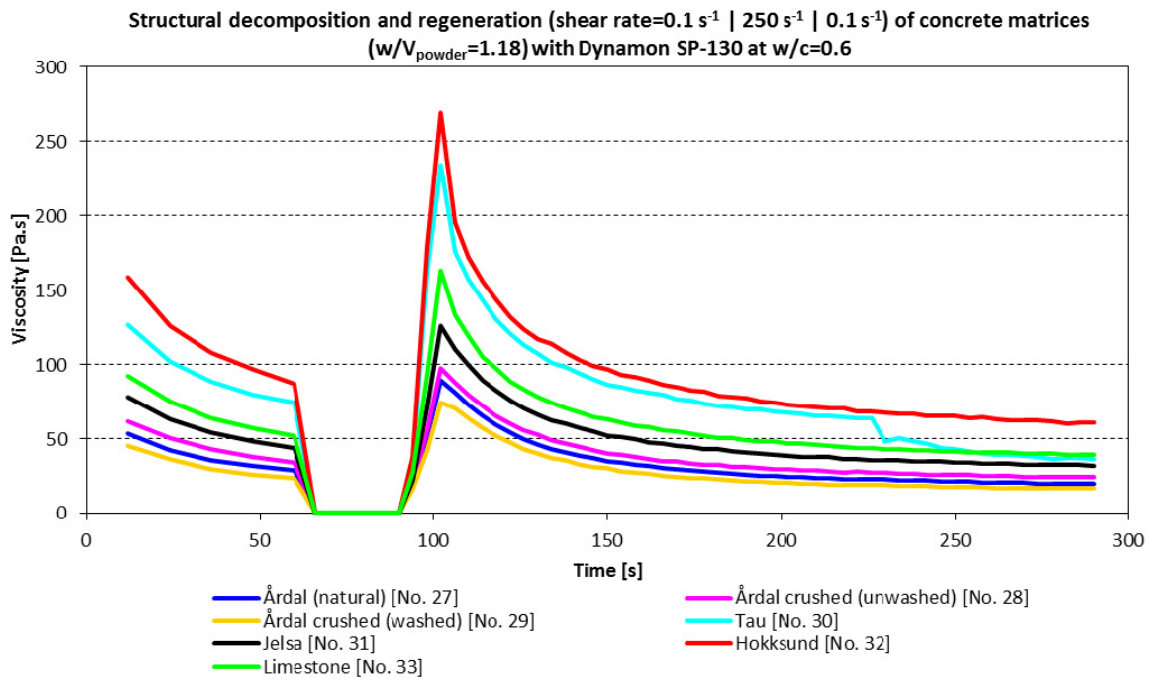


Fig.3-5: Structural decomposition and regeneration of matrices with Dynamon SP-130 at $w/c=0.6$

Table 3-4: Regeneration of the structure of the matrices ($w/c=0.4$) as a $\eta(t)$ in % after the application under high shear conditions

		Concrete matrices at $w/c=0.4$													
Matrix No.		1		2		17		18		19		37		38	
Matrix composition		Cement paste (0.4% of SR-N $w/V_{\text{powder}}=1.18$)		Árdal (0.4% of SR-N $w/V_{\text{powder}}=1.1$)		Cement paste (0.4% of SP-130 $w/V_{\text{powder}}= 1.18$)		Árdal (0.4% of SP-130 $w/V_{\text{powder}}=1.1$)		Cement paste (without SP $w/V_{\text{powder}}=1.18$)		Cement paste (0.4% of Glen. 151 $w/V_{\text{powder}}=1.18$)		Cement paste (1.0% of Glen. 151 $w/V_{\text{powder}}=1.18$)	
		η [Pas]	Reg. [%]	η [Pas]	Reg. [%]	η [Pas]	Reg. [%]	η [Pas]	Reg. [%]	η [Pas]	Reg. [%]	η [Pas]	Reg. [%]	η [Pas]	Reg. [%]
at the end of the first interval (under low shear)		322	100	414	100	208	100	208	100	391	100	171	100	60	100
at the end of the second interval (under high shear)		0.698	0.22	0.806	0.19	0.424	0.20	0.5	0.24	0.822	0.21	0.422	0.25	0.356	0.59
after $t=20$ s		435	135	515	124	219	105	311	150	451	115	260	152	100	166
after $t=40$ s		356	111	442	107	173	83	250	120	405	104	204	119	80	132
after $t=80$ s		296	92	378	91	139	67	201	97	374	96	166	97	59	99
after $t=100$ s		291	90	375	91	130	63	198	95	368	94	157	92	54	89

Table 3-5: Regeneration of the structure of the matrices (with Dynamon SR-N) as a $\mu(t)$ in % after the application under high shear conditions

Concrete matrices ($w/V_{\text{powder}}=1.18$) with Dynamon SR-N at $w/c=0.5$														
Matrix No.	3		4		5		6		7		8		9	
	Árdal (natural)		Árdal (crushed/unwashed)		Árdal (crushed/washed)		Tau		Jelsa		Hokksund		Limestone	
Filler	η [Pas]	Reg. [%]	η [Pas]	Reg. [%]	η [Pas]	Reg. [%]	η [Pas]	Reg. [%]	η [Pas]	Reg. [%]	η [Pas]	Reg. [%]	η [Pas]	Reg. [%]
at the end of the first interval (under low shear)	90	100	111	100	105	100	147	100	111	100	161	100	134	100
at the end of the second interval (under high shear)	0.326	0.36	0.362	0.33	0.345	0.33	0.453	0.31	0.443	0.40	0.443	0.28	0.413	0.31
after t=20 s	166	185	165	149	191	182	217	148	208	187	250	155	214	160
after t=40 s	117	130	120	108	135	129	165	112	157	141	190	118	160	119
after t=80 s	87	97	90	81	96	91	127	86	114	103	148	92	124	93
after t=100 s	79	88	83	75	88	84	119	81	107	96	138	86	113	84
Concrete matrices ($w/V_{\text{powder}}=1.18$) with Dynamon SR-N at $w/c=0.6$														
Matrix No.	10		11		12		13		14		15		16	
	Árdal (natural)		Árdal (crushed/unwashed)		Árdal (crushed/washed)		Tau		Jelsa		Hokksund		Limestone	
Filler	η [Pas]	Reg. [%]	η [Pas]	Reg. [%]	η [Pas]	Reg. [%]	η [Pas]	Reg. [%]	η [Pas]	Reg. [%]	η [Pas]	Reg. [%]	η [Pas]	Reg. [%]
at the end of the first interval (under low shear)	36	100	72	100	23	100	115	100	90	100	98	100	70	100
at the end of the second interval (under high shear)	0.207	0.57	0.278	0.39	0.194	0.84	0.389	0.34	0.316	0.35	0.413	0.42	0.312	0.45
after t=20 s	76	210	121	169	33	141	180	157	164	181	149	152	109	156
after t=40 s	48	132	60	84	33	141	129	112	111	123	109	111	80	114
after t=80 s	33	90	60	84	21	88	95	82	77	85	82	84	60	86
after t=100 s	30	82	55	77	18	78	87	76	69	76	76	77	56	80

Table 3-6: Regeneration of the structure of the matrices (with Dynamon SP-130) as a $\mu(t)$ in % after the application under high shear conditions

Concrete matrices ($w/V_{\text{powder}}=1.18$) with Dynamon SP-130 at $w/c=0.5$														
Matrix No.	20		21		22		23		24		25		26	
Filler	Årdal (natural)		Årdal (crushed/unwashed)		Årdal (crushed/washed)		Tau		Jelsa		Hokksund		Limestone	
	η [Pas]	Reg. [%]	η [Pas]	Reg. [%]	η [Pas]	Reg. [%]	η [Pas]	Reg. [%]	η [Pas]	Reg. [%]	η [Pas]	Reg. [%]	η [Pas]	Reg. [%]
at the end of the first interval (under low shear)	51	100	68	100	42	100	77	100	73	100	106	100	66	100
at the end of the second interval (under high shear)	0.206	0.41	0.246	0.36	0.209	0.50	0.295	0.39	0.265	0.37	0.313	0.30	0.259	0.39
after t=20 s	100	197	132	194	87	207	145	189	138	190	194	183	131	199
after t=40 s	70	138	85	125	61	144	102	133	100	137	140	132	92	140
after t=80 s	49	97	68	100	40	94	74	97	72	100	104	98	65	98
after t=100 s	44	87	61	89	34	81	68	88	66	90	95	89	59	90
Concrete matrices ($w/V_{\text{powder}}=1.18$) with Dynamon SP-130 at $w/c=0.6$														
Matrix No.	27		28		29		30		31		32		33	
Filler	Årdal (natural)		Årdal (crushed/unwashed)		Årdal (crushed/washed)		Tau		Jelsa		Hokksund		Limestone	
	η [Pas]	Reg. [%]	η [Pas]	Reg. [%]	η [Pas]	Reg. [%]	η [Pas]	Reg. [%]	η [Pas]	Reg. [%]	η [Pas]	Reg. [%]	η [Pas]	Reg. [%]
at the end of the first interval (under low shear)	28	100	34	100	24	100	74	100	44	100	87	100	52	100
at the end of the second interval (under high shear)	0.149	0.52	0.175	0.51	0.137	0.58	0.283	0.38	0.207	0.47	0.28	0.32	0.221	0.42
after t=20 s	73	257	80	233	64	271	157	211	100	229	172	197	119	228
after t=40 s	46	162	52	153	40	170	107	144	66	152	117	134	78	150
after t=80 s	30	104	35	101	24	104	77	103	45	103	85	97	55	105
after t=100 s	26	92	31	91	22	92	70	94	41	93	77	88	49	94

3.1.1 Repeatability of the matrix rheology test method

Repeatability tests with a constant matrix composition were carried out to find the order of result variation caused by the matrix mixing, rheological measurement procedures and accuracy of the Physica rheometer given in chapters 2.1.3 and 2.1.4. Results of the repeatability tests are presented in table 3-7.

Table 3-7: Repeatability of the matrix test method

Matrix No.	Filler	Test date	Bingham parameters		
			τ_y	μ	R^2
			[Pa]	[Pa·s]	[1]
0.4% of Dynamon SP-130 w/c=0.58 w/V_{powder}=1.38					
1	Limestone	30/04/2010	16	0.13	0.9312
2	Limestone	04/05/2010	13	0.17	0.9326
3	Limestone	04/05/2010	12	0.16	0.9427
4	Limestone	06/05/2010	14	0.20	0.9405
MEAN VALUE:			13	0.1654	0.9386
STANDARD DEVIATION (σ):			1	0.0261	0.0053
COEFFICIENT OF VARIATION (CV), [%]:			7.69	15.80	0.57

3.1.2 Overview of the test results

Tables 3-8 and 3-9 show a compilation of rheological parameters and fresh concrete properties determined according to the chapter 2.2.3.

Please see appendix F for complete plots of down flow curves.

Table 3-8: Overview of the rheological parameters and fresh concrete properties for mixes with w/c ratios 0.4 and 0.5

SCC mix No.	Filler	Fresh concrete properties				Mix design	Moment at initial yield of the fresh concrete		Rate of change		Segregation factor (S)		Bingham Parameters						Static yield stress [Pa]	No. of corresp. matrice
		Air content [%]	Slump-flow [mm]	Temp. [°C]	Density [kg/m ³]		Density [kg/m ³]	g ₁ [N·m]	g ₂ [N·m]	h ₁ [N·m·s]	h ₂ [N·m·s]	1 [%]	2 [%]	τ _{v1} [Pa]	τ _{v2} [Pa]	μ ₁ [Pa·s]	μ ₂ [Pa·s]	R ² ₁		
1	2	3	4	5	6	7	8	9	10	11	12	13	14	15	16	17	18	19	20	21
2.0% of Dynamon SP-130 w/c=0.4 w/V_{powder}=1.1																				
1	No additional filler	1.1	680	19	2338	2319	0.00	0.05	12.00	12.08	9	5	0	4	72.43	59.41	0.9958	0.9983	1312	17
1.1% of Dynamon SP-130 w/c=0.5 w/V_{powder}=1.18																				
2	Årdal (natural)	2.0	570	21.7	2358	2320	0.58	0.28	6.64	7.08	5	8	52	26	35,30	37.60	0.9974	0.9990	617	20
3	Årdal (crushed/unwashed)	3.8	390	24.7	2330	2320	1.48	1.39	13.21	12.97	6	3	133	124	70,20	68.94	0.9941	0.9985	1260	21
4	Årdal (crushed/washed)	2.9	520	21.9	2355	2320	1.07	2.06	9.81	7.84	6	18	96	185	52,15	41.66	0.9972	0.9674	1440	22
5	Tau	3.0	440	25.0	2360	2323	0.86	1.08	11.34	12.42	5	0	80	97	62,78	65.97	0.9940	0.9970	1179	23
6	Jelsa	3.3	460	24.4	2330	2323	0.72	0.69	9.86	10.58	7	6	62	60	50,36	54.03	0.9966	0.9965	883	24
7	Hokksund	3.6	380	23.6	2353	2323	1.54	3.95	11.51	8.17	6	20	133	341	58,80	41.73	0.9994	0.9982	1040	25
8	Limestone	3.8	395	21.9	2350	2321	0.47	0.52	8.30	8.57	7	2	46	51	47,95	49.50	0.9943	0.9948	649	26
AVERAGE:																0.9961	0.9937			

Table 3-9: Overview of the rheological parameters and fresh concrete properties for mixes with w/c ratios 0.6 and 0.77

SCC mix No.	Filler	Fresh concrete properties				Mix design	Moment at initial yield of the fresh concrete		Rate of change		Segregation factor (S)		Bingham Parameters						Static yield stress [Pa]	No. of coresp. matrice
		Air content [%]	Slump-flow [mm]	Temp. [°C]	Density [kg/m ³]		Density [kg/m ³]	g ₁ [N·m]	g ₂ [N·m]	h ₁ [N·m·s]	h ₂ [N·m·s]	1 [%]	2 [%]	τ _{y1} [Pa]	τ _{y2} [Pa]	μ ₁ [Pa·s]	μ ₂ [Pa·s]	R ² ₁		
1	2	3	4	5	6	7	8	9	10	11	12	13	14	15	16	17	18	19	20	21
1.1% of Dynamon SP-130 w/c=0.6 w/V_{powder}=1.18																				
9	Årdal (natural)	1.7	635	22.4	2343	2313	0.20	0.21	3.83	4.00	8	2	21	23	24.25	25.29	0.9939	0.9955	349	27
10	Årdal (crushed/unwashed)	1.5	485	21.7	2328	2313	0.43	0.41	8.16	8.39	8	-3	40	39	45.16	46.41	0.9957	0.9960	631	28
11	Årdal (crushed/washed)	2.8	515	21.4	2340	2313	0.44	0.41	6.96	7.78	7	7	41	25	38.52	43.08	0.9908	0.9968	657	29
12	Tau	3.2	455	21.7	2320	2319	0.85	0.81	7.24	8.30	8	2	73	70	37.01	42.38	0.9977	0.9972	636	30
13	Jelsa	2.8	515	21.1	2355	2319	0.44	0.44	8.94	9.04	9	1	40	40	47.50	48.03	0.9972	0.9974	729	31
14	Hokksund	3.8	465	20.4	2318	2321	0.75	0.86	6.03	6.45	7	5	65	74	30.80	32.96	0.9987	0.9934	523	32
15	Limestone	1.4	640	20.4	2338	2316	0.21	0.21	4.42	4.49	-8	0	20	21	25.52	25.95	0.9968	0.9964	322	33
0.6% of Dynamon SP-130 w/c=0.77 w/V_{powder}=1.51																				
16	Årdal (natural)	1.5	645	19.0	2315	2232	0.30	0.36	1.71	1.71	4	-2	34	40	11.34	11.37	0.9961	0.9976	126	-
17	Årdal (crushed/unwashed)	1.6	525	18.5	2335	2232	0.51	0.51	2.29	2.40	1	3	43	43	12.65	11.80	0.9942	0.9991	192	-
18	Årdal (crushed/washed)	1.5	655	18.0	2325	2232	0.47	0.41	2.19	2.42	-2	-5	46	40	12.64	14.00	0.9961	0.9898	195	-
19	Tau	1.4	510	18.4	2300	2237	0.61	0.68	2.16	2.26	6	10	60	67	12.49	13.03	0.9945	0.9986	218	-
20	Jelsa	1.6	575	20.0	2325	2237	0.51	0.54	2.47	2.47	5	4	50	53	14.25	14.29	0.9975	0.9971	185	-
21	Hokksund	1.5	495	21.0	2315	2237	0.86	1.05	2.47	2.47	10	10	81	98	14.77	14.97	0.9975	0.9958	240	-
22	Limestone	1.7	585	20.7	2308	2232	0.50	0.51	2.34	2.58	-2	5	47	46	12.92	12.70	0.9965	0.9979	170	-
AVERAGE:																	0.9959	0.9963		

3.1.3 Repeatability of the SCC rheology test method

Repeatability tests with a constant concrete composition were carried out to find the order of result variation caused by the concrete mixing, determination of fresh concrete properties and rheological measurement procedures given in chapter 2.2.3. Results of the repeatability tests are presented in table 3-10.

Table 3-10: Repeatability of the concrete test method

SCC mix No.	Filler	Test date	Fresh concrete properties				Segregation coefficient	Bingham Parameters	
			Air content	Slump-flow	T ₅₀₀	Density		τ_y	μ
			[%]	[mm]	[sec]	[kg/m ³]	[%]	[Pa]	[Pa·s]
0.8% of Dynamon SP-130 w/c=0.5 w/V_{powder}=1.18									
1	Tau	09/06/2010	4.0	580	2.00	2285	12	33	23
2	Tau	15/06/2010	3.7	600	1.97	2275	9	34	18
3	Tau	16/06/2010	3.8	510	4.31	2283	9	33	23
MEAN VALUE:			4	563	2.76	2281	10	33	21
STANDARD DEVIATION (σ):			0	47	1.34	5	2	0.58	3
COEFFICIENT OF VARIATION (CV):			3.98	8.39	48.64	0.23	17.32	1.73	13.53

4. Discussion

In the following an effort is made to discuss the results both in detail and hopefully to be able to learn something more about the effects of different fillers and different admixtures together.

4.1 Filler characterization

It has been suggested by most of the previous researchers (Nehdi, Mindess and Aitcin 1997, Zhang and Han 2000, Ferraris, Obla and Hill 2001, Bigas and Gillias 2002, Esping 2004, Pedersen 2004, Westerholm 2006, Esping 2008, Cepuritis 2011) that characteristics like mineral filler grading and specific surface area are found to be to some extent related to the rheology of fresh filler modified cement paste (matrix). Thus a series of tests were performed in order to determine those properties (see chapter 2.1.1). A total of four different methods have been used to measure both particle size distribution (PSD) and specific surface. The PSD results have also been recalculated into specific surface area by assuming that the particles are spherical in shape (Erdem, Khayat and Yahia 2009). The results of all the specific surface measurements and calculation are presented in Table 2-2.

Even though all of the used approaches give a rather different specific surface area values a relation between them seems to exist. Relation between different specific surface area determination methods is illustrated in Figures 4-1 to 4-6.

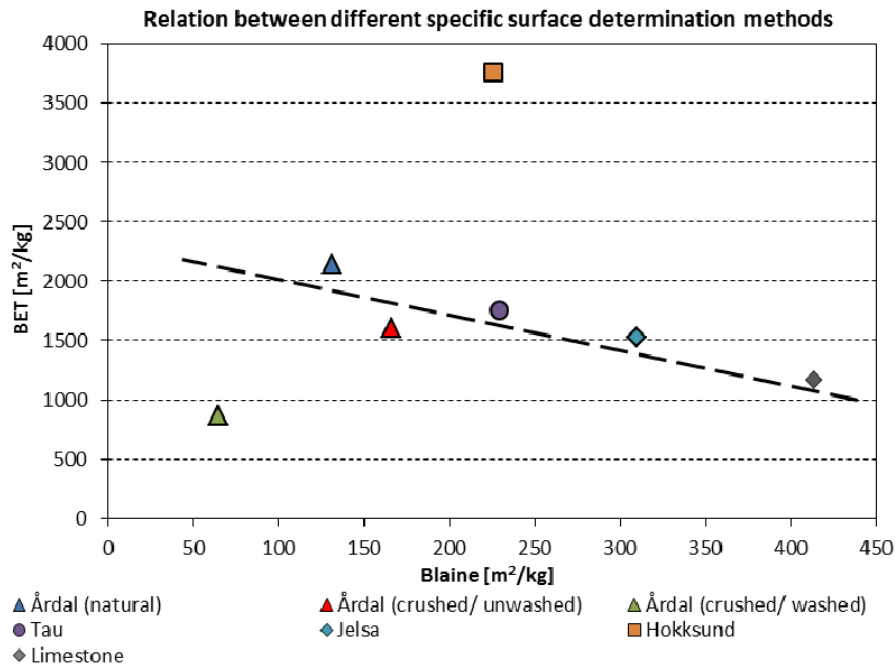


Fig.4-1: Relation between Blaine and BET specific surface area determination methods

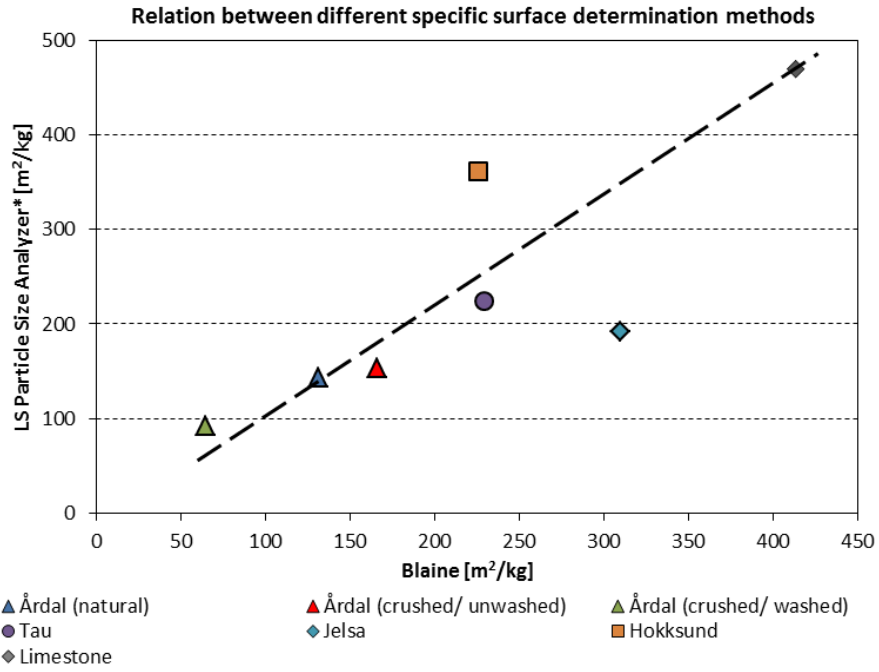


Fig.4-2: Relation between Blaine and LS Particle Size Analyzer specific surface area determination methods

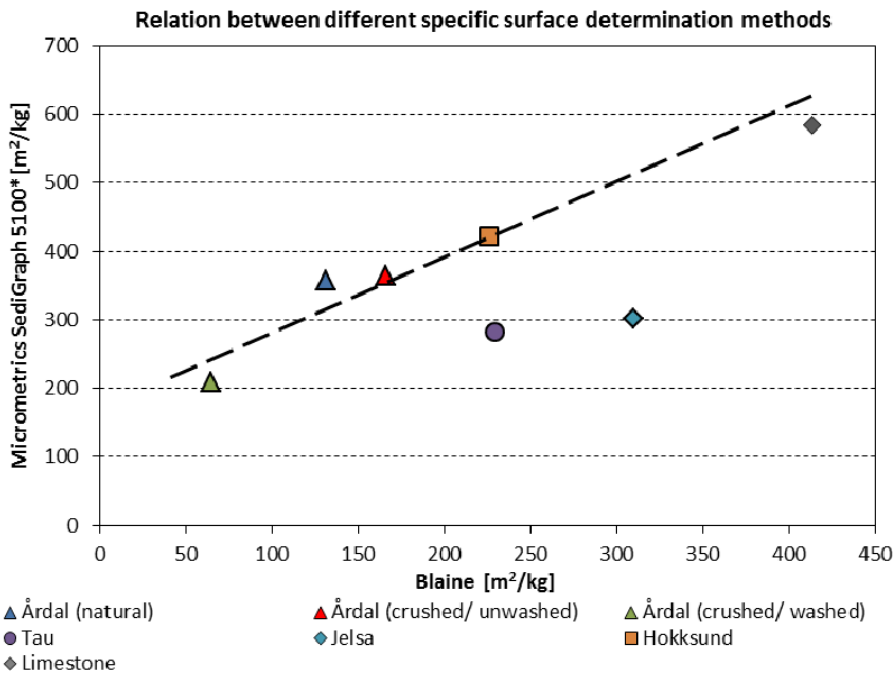


Fig.4-3: Relation between Blaine and Micrometrics SediGraph 5100 specific surface area determination methods

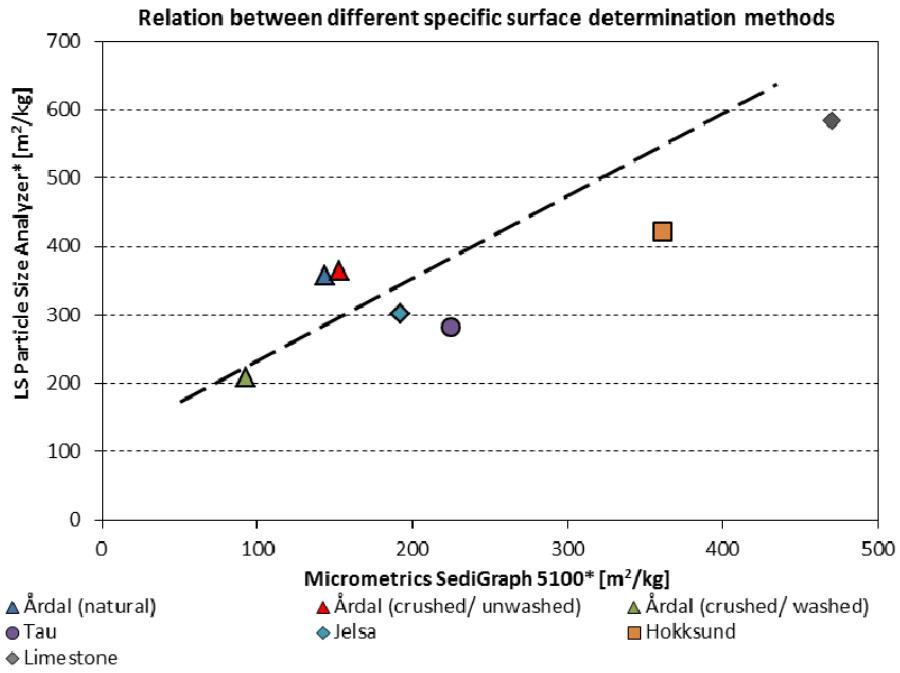


Fig.4-4: Relation between Micrometrics SediGraph 5100 and LS Particle Size Analyzer specific surface area determination methods

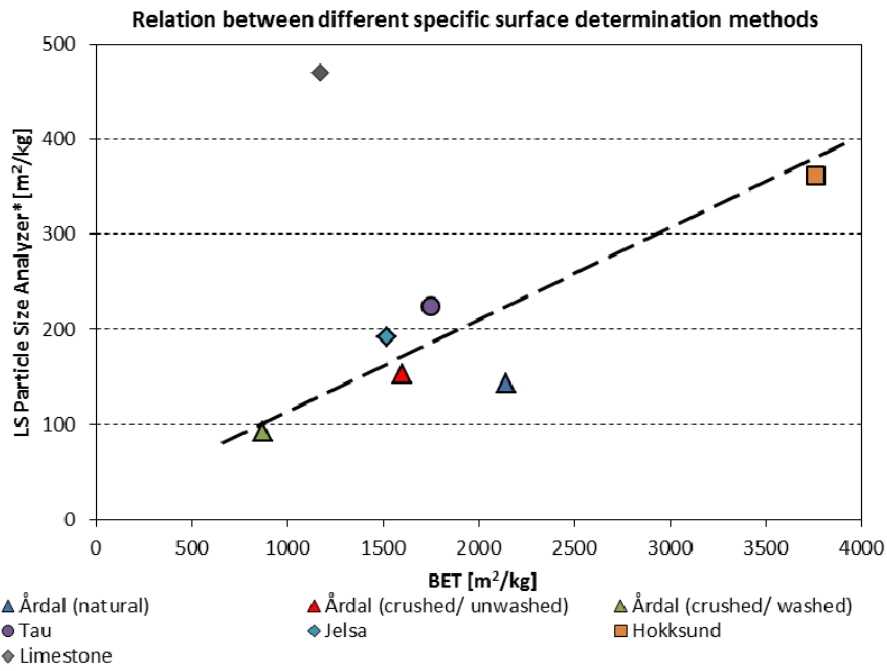


Fig.4-5: Relation between BET and LS Particle Size Analyzer specific surface area determination methods

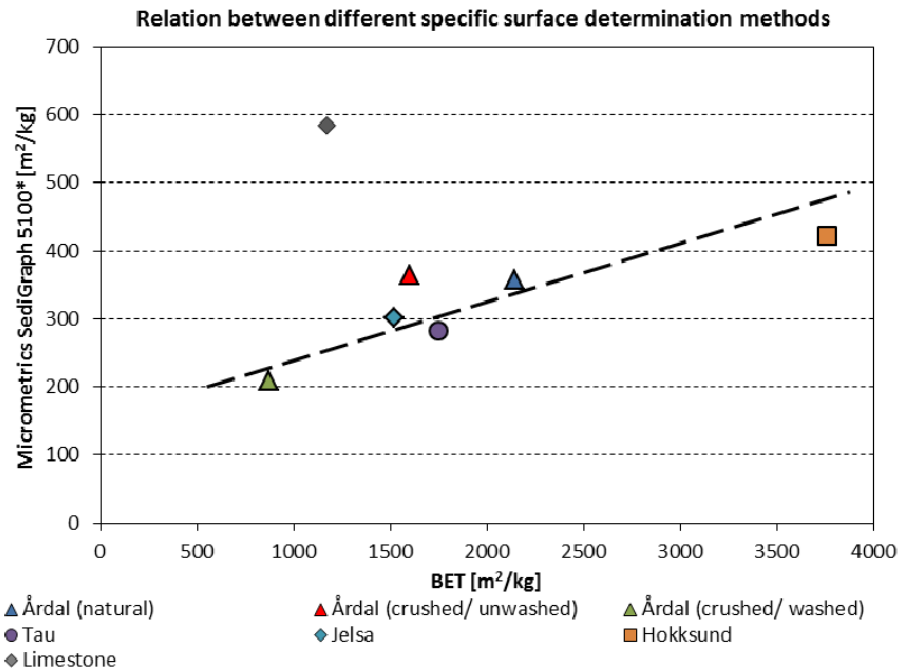


Fig.4-6: Relation between BET and Micrometrics SediGraph 5100 specific surface area determination methods

The first thing that is obvious from the results presented in Table 2-2 is that the values obtained by BET method are of an approx. 10 times higher order than values obtained by the other tests. This corresponds to the results from a similar fine particles characterization study presented by Wigum (2010).

The ratio of surface area to volume will increase exponentially with increased particle irregularity (shape, texture and porosity) and decreased size (Esping 2008). It is, however, obvious that in such test methods as Blaine where the specific surface area is determined from air permeability, based on packed spherical particles, information about the shape, texture and surface porosity is neglected. This is most likely true also for the SediGraph and LS Particle Size Analyser test methods, where differences in particle sedimentation rates in a suspension and laser diffraction angles are measured (see chapter 2.1.1) in order to determine the grain size.

In a previous Norwegian manufactured sand project (NORMIN 1995 cited in Wigum 2010) it was pointed out that various properties of the fines may influence upon the value of the specific surface, obtained by the BET method. Properties such as amount of particles < 10 μm in the tested material, mineralogy, and surface texture have been mentioned. Then based on the results obtained within this study and by Wigum (2010) we would have to assume that the big difference between BET and the other test methods is most likely due to the influence from the surface texture and/ or possibly also the “inner surface” (porosity) of the particle grains. The “inner surface” or porosity would have to be understood as the free space formed between the mineral grains where the nitrogen molecules can enter.

If we now look at the relation between BET measurements and results obtained by the other test methods (Figures 4-1, 4-5 and 4-6), it's obvious that the Flowsorb II 2300 nitrogen absorption by BET-method would report relatively very low (the second lowest within all the BET results) specific surface area for the limestone filler. While it is clear from the PSD analysis (see Figures 2-1 and 2-2) and some previous studies (Cepuritis 2011) that this is the finest material of all the tested. We would then eventually have to assume that limestone filler has the roundest particles, smoothest surface texture and/ or the largest mineral size, i.e. having no extra “inner surface” for the nitrogen molecules to penetrate. The fact that limestone filler is produced by grinding instead of crushing could be mentioned as the reason for better particle shape and surface

texture. This, however, does not comply with the fact that naturally weathered Árdal filler, that is also expected to have more rounded particle shape with comparably smooth surface, does not exhibit a low BET-method specific surface measurement result. Then as the last logically deductible reason the mineral composition of the fillers is left. This is to some extent approved by a research carried out by Géber and Gömze (2010). Within the study they have carried out BET and scanning electron microscope (SEM) tests on a number of different mineral fillers including limestone filler. Some of their results are illustrated on Figures 4-7 and 4-8.

It can be seen from Figure 4-7 that also in this study the limestone filler has shown the lowest specific surface area measured by the BET-method. No information of the filler PSD was given, though they were all of the same maximum grain size – 63 μm . Figure 4-8 holds SEM images of four different filler grains. It is obvious that the limestone filler surface texture is much smoother than in case of andesite, basalt or dolomite fines. However, it must also be noted that the above described deduction of the mineral composition being the main parameter affecting the BET measurement results is more of a speculation, since the fillers used for the current research are from a different origins than those studied by Géber and Gömze (2010). Thus thin-section studies of the filler mineralogical composition as well as SEM analysis is strongly recommend to be carried out also for fines used for the current research in order to approve the deducted hypothesis.

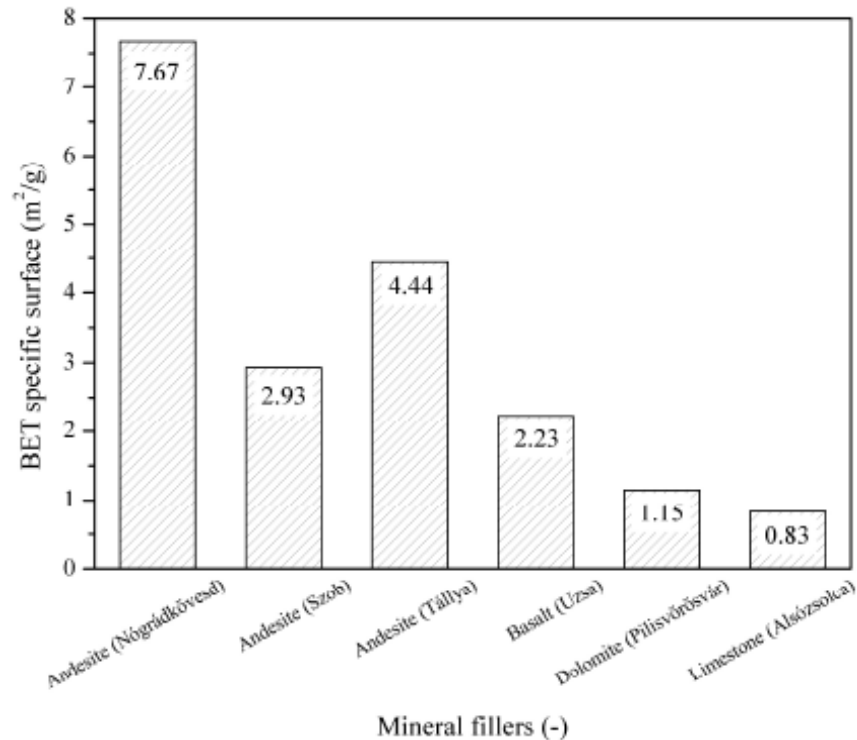


Fig.4-7: BET specific surface area determined in a study by Géber and Gömze (2010)

There is one more aspect worth noticing regarding the particle analysis results. It is known from the previous research that the fine aggregates (manufactured sand) from Hokksund quarry contain large amount of flaky mica particles (Cepuritis 2011). This is then expected to be true also for the filler part of the fine aggregate. As it can be seen from Figures 4-1 to 4-6, Blaine and SediGraph test methods are most likely not able to detect the high specific surface of the mica particles while BET and LS Particle Size Analyser show somewhat more trustable results. This is in particular important when looking for a relation between specific surface area of the fillers and various rheological properties of filler modified paste and SCC.

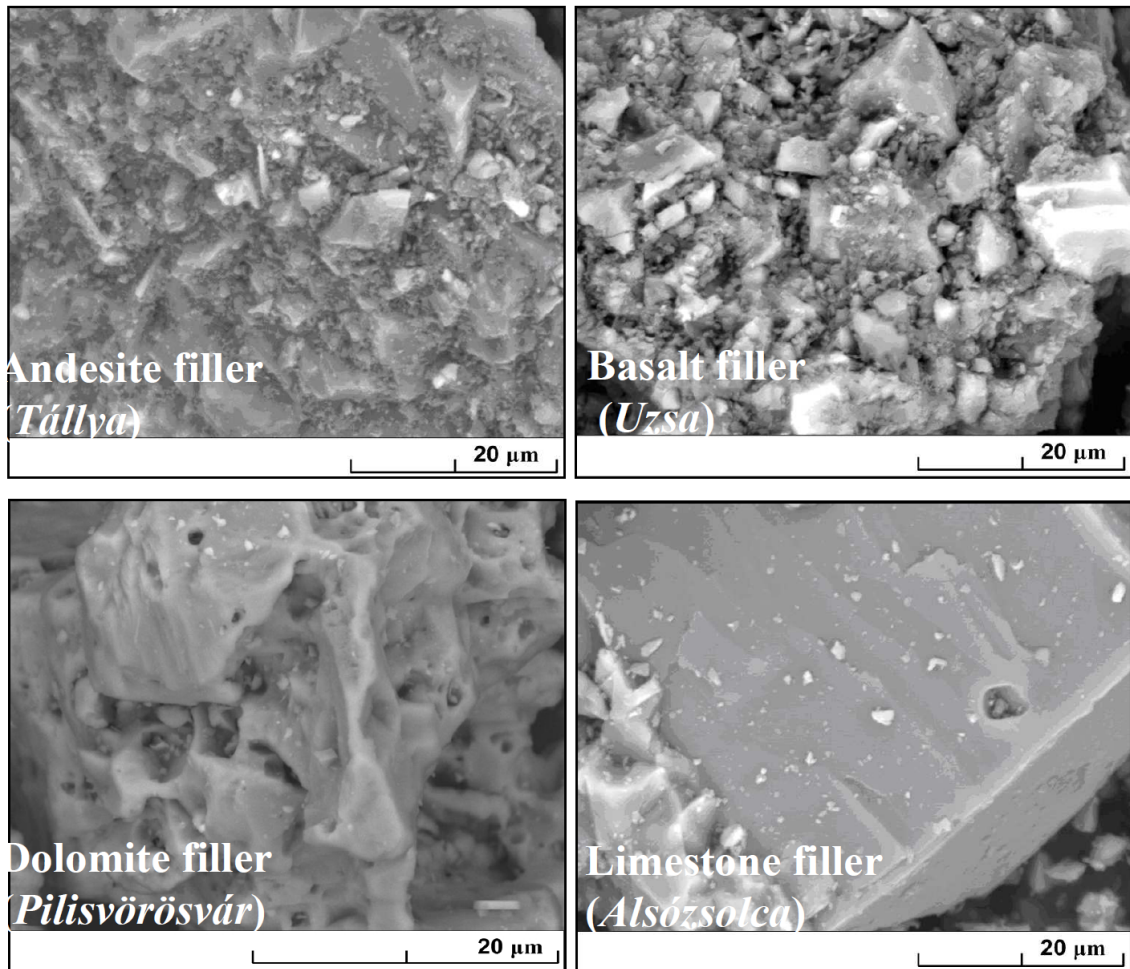


Fig.4-8: SEM micrographs from a study by Géber and Gömze (2010)

4.2 Matrix rheology tests

4.2.1 Influence of the rheological test sequence

A striking result of the quite long test cycle in the rheometer (almost 30 minutes, see Table 2-4 and Figure 2-5) is that it gave rheopex behaviour for barely all (37 from 38) of the tested matrix mixes. That is; the usual hysteresis loop with shear values of the down curve falling below the up curve (Vikan 2005; Jacobsen and Vikan 2010) was never seen with this test, but the opposite; see Figure 2-7. This “negative” thixotropy is remarkable and most probably a result of the long test cycle that was intended to incorporate as many studies as possible on one sample; possibly as a time dependant effect of the oscillatory test which run prior to the flow curve. A duplicate test with the test cycle (without oscillation) used by Jacobsen and Vikan (2010) was run showing a normal thixotropic flow curve; see Figure 4-9 below.

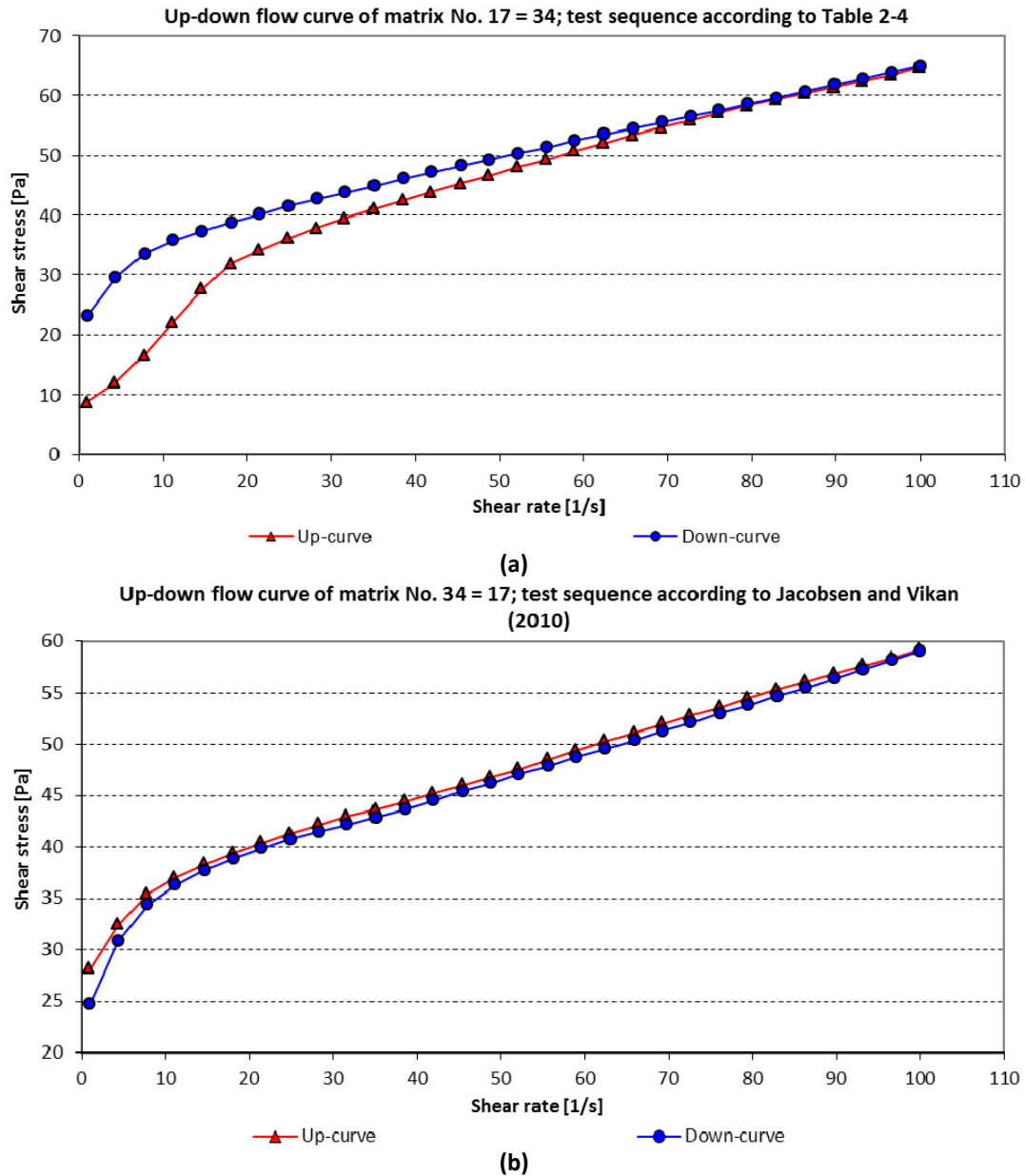


Fig.4-9: (a) rheopex behaviour in the test sequence with oscillation (see Table 2-4); (b) the same mix showing usual thixotropic behaviour in test sequence without oscillation (Jacobsen and Vikan 2010)

4.2.2 Influence of different fillers and superplasticizers

Table 4-1 shows a compilation of some main rheology results in an effort to analyse the effect of admixture and filler simultaneously for matrices with $\Phi = 0.459$, SP = 0.4 % of fly ash cement at $w/b = 0.50$ and 0.60 . The replacement levels of filler have been $V_{\text{filler}}/V_{\text{powder}} = 0.20$ and 0.33 , respectively.

From the data presented in Table 4-1 it seems that the differences in flow properties for different fillers are relatively small at constant Φ and SP-type and -dosage. This is seen by comparing the mean values (in parentheses) with the min and max values in each of the four columns of Table 4-1. Furthermore, the variation between different types of fillers is probably of the same order as the variation due to replacing fly ash cement with filler and associated w/b -increase. For Dynamon SP-130 the variation of μ between matrixes with different fillers was $0.19 - 0.28$ Pa.s for $w/b = 0.50$ and $V_{\text{filler}}/V_{\text{powder}} = 0.20$. The variation was slightly higher; $0.13 - 0.28$ Pa.s, at $w/b = 0.60$ and $V_{\text{filler}}/V_{\text{powder}} = 0.33$. This variation is only slightly larger than between 4 parallel

tests on a single material (0.13 – 0.20 Pa.s for matrix with limestone filler at w/b = 0.50, see Table 3-7 on repeatability of matrices).

Table 4-1: Rheology, min-max (mean), of the matrices

Rheology, min-max (mean)		w/b = 0.50 ($V_{\text{filler}}/V_{\text{powder}}=0.20$)		w/b = 0.60 ($V_{\text{filler}}/V_{\text{powder}}=0.33$)	
		<i>Dynamon SP-130</i>	<i>Dynamon SR-N</i>	<i>Dynamon SP-130</i>	<i>Dynamon SR-N</i>
Flow curves	τ_0 Bingham [Pa]	14-24 (18)	17-28 (22)	7-21 (13)	7-25 (16)
	μ [Pa·s]	0.19-0.28 (0.23)	0.33-0.58 (0.44)	0.13-0.28 (0.19)	0.19-0.48 (0.33)
	τ_0 Her.-Bulkl. [Pa]	6-10 (8)	-25 - -11 (-17)	-4-5 (1)	-18 - -1 (-9)
	Hyst. area [Pa/s]	151-587 (285)	262-1274 (731)	85-588 (275)	325-805 (549)
Static	τ_0 gel str. [Pa]	2-8 (5)	5-10 (8)	2-7 (3)	1-7 (4)
	τ_0 [Pa]	7-19 (12)	19-34 (26)	4-18 (9)	4-22 (13)
	$\tau_0 + 10$ min [Pa]	8-22 (14)	25-44 (33)	5-22 (11)	6-26 (19)
	G_r [Pa]	857-1819 (1356)	2925-4651 (3816)	788-1556 (1117)	1992-3450 (2487)
	G_r [Pa]	92-352 (183)	391-2066 (1227)	53-404 (167)	71-828 (535)
Visco-elastic	G^* [Pa]	44-155 (102)	26-151 (58)	15-68 (44)	26-158 (60)
	γ_{crit} [s^{-1}]	0.003-0.004 (0.003)	0.001-0.012 (0.008)	0.002-0.006 (0.004)	0.002-0.012 (0.006)

Table 4-1 also shows that the clearest effect on rheology was when changing w/b while keeping the type of SP, and also when changing the type of SP and keeping w/b constant. Furthermore, the natural material gave higher consistency than the crushed fillers as expected (see Tables 3-1 and 3-2). The increased w/b with filler replacement seemed to slightly increase consistency at the actual reduction of total SP (SP constant dosage as percentage of cement) when keeping Φ constant.

The static tests showed highest static yield stress values at highest age as expected. The static shear moduli, G , were determined as tangent at 50 % of maximum stress. Highest G was observed in the stress controlled test with lower rate of shear than in the measurements at constant rate of shear. It seems that static shear moduli G were increased more by changing SP from long-chained SP-130 to the short side-chained SR-N than the rheological properties taken from the flow curves (Bingham yield, plastic viscosity, thixotropy).

The reference paste (w/b = 0.40, $\Phi=0.459$, 0.4 % SP, no filler) was tested a number of times with different types of SP and test sequences. Generally, higher values for most rheological properties shown in Table 5-1 (i.e lower consistency) were obtained compared to when using filler. That is, when filler replaces fly ash cement (but keeping total particle volume fraction constant ($\Phi = 0.459$)), the consistency increases even if the SP-content of the mix-volume reduces. Thus all fillers showed a positive effect by increasing the consistency when replacing cement and keeping SP-percentage as a constant dosage of cement.

The complex modulus G^* was determined as a function of time dependant shear stress and shear rate: $G^* = \tau(t)/\dot{\gamma}(t)$ at increasing strain amplitude. We used oscillatory amplitude sweeps at $1 s^{-1}$ frequency that gave storage- (G') and loss- (G'') modulus at the critical strain amplitude where $G' = G'' = G^*$. Starting from very low oscillatory shear deformations this usually is taken as the transition from solid or gel to liquid behaviour at the end of the linear viscoelastic range. The G^* - values were all significantly lower than the static G -values. There was a tendency of lowest G for the natural fillers whereas no such effect could be seen on G^* .

In Table 4-1 the Herschel-Bulkley (H-B) model gave the best flow curve fit ($R^2 = 0.995-0.995$) compared to the Bingham model ($R^2 = 0.924-0.958$) due to shear thinning. On the other hand

this often gave negative yield stress so the H-B model is probably not applicable to describe yield. Also the determination of static G could be uncertain due to the nature of the stress-strain curves.

4.2.3 Structural decomposition and regeneration

Results of the structural decomposition and regeneration tests are presented on Figures 3-1 to 3-5 and in Tables 3-4 to 3-6.

According to an accepted definition proposed by Barnes, Hutton and Walters (1989), a gradual decrease of the viscosity under shear stress followed by a gradual recovery of structure when the stress is removed is called thixotropy. They also state that the opposite type of behaviour, involving a gradual increase in viscosity, under stress, followed by recovery, is called negative thixotropy, anti-thixotropy or sometimes also rheopexy (Mezger 2006). Rheoplectic behaviour would then mean an increase in the structural strength when performing a high-shear process which is followed by a complete decomposition of the increased structural strength during the subsequent period of rest (Mezger 2006).

As described in the chapter 4.2.1 most of the tested matrices exhibited rheoplectic behaviour if this is to be evaluated from the up-down flow curve tests. This was explained as a possible time dependant effect of the oscillatory test which was run prior to the flow curves. However, it is known from previous studies that cement pastes generally show thixotropic behaviour (Vikan 2004, Banfil 1994, Collepardi 1971). In his paper Banfil (1994) has stressed that the rheological data measured at any instant depend upon the previous shear history of the sample. Then the area in the hysteresis loop that was determined for the matrices would have the dimensions of “energy” related to the volume of the sample sheared which indicates that energy is required to break down the thixotropic structure. By this meaning that a hysteresis loop (hysteresis area) gives evidence only that the structural breakdown has occurred during the test and an infinite number of different loops are possible depending on the experimental details. Banfil (1994) stresses that therefore hysteresis loops cannot unambiguously characterize structural breakdown. Later Mezger (2006) has defined that in order to correctly determine a time dependent thixotropic behaviour in a scientific sense:

- both the decomposition and the regeneration of the specimen structure have to be taken into consideration;
- the test must be performed under constant shear rate (load) in each test interval.

As it can be seen from Table 2-4 and Figure 2-5 the above mentioned criteria are met within the selected test cycle.

It can be seen from Figures 3-1 to 3-5 that according to the selected structural regeneration and decomposition test sequence all of the tested cement pastes and matrices show the expected thixotropic behaviour. It must also be noted that for all of the tested specimens the structural regeneration occurs completely (i.e. to 100%) which is important since in the opposite case such a behaviour would be referred to “incomplete” or “false ” thixotropy (Mezger 2006) and we would be speaking only about “partial regeneration”.

In order to give a meaningful specification for thixotropy, i.e. to quantify it, Mezger (2006) has proposed to determine the % of structural regeneration after a certain period (t) of rest in seconds (that follows the high shear phase) compared to the initial viscosity value of the structural strength at rest before the shearing. Such values for rest periods of t=20, 40, 80 and 100 s are presented in Tables 3-4 to 3-6 or in illustrated in a more demonstrative way on Figures 4-10 to 4-13.

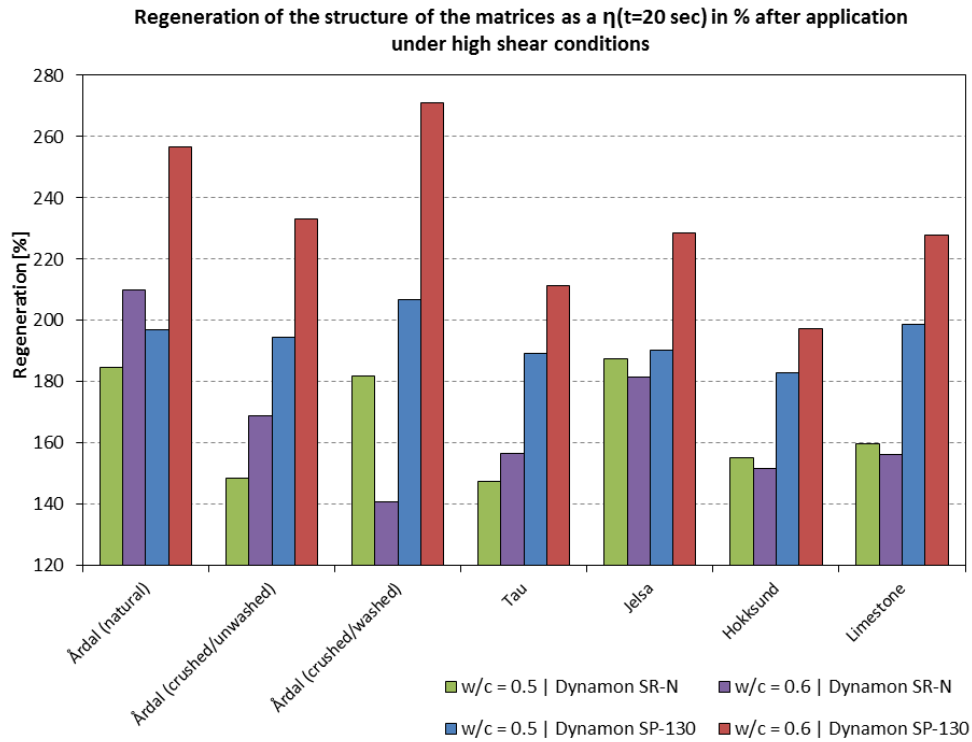


Fig.4-10: Regeneration of the structure of the matrices as a $\eta(t=20 \text{ sec})$ in % after application under high shear conditions

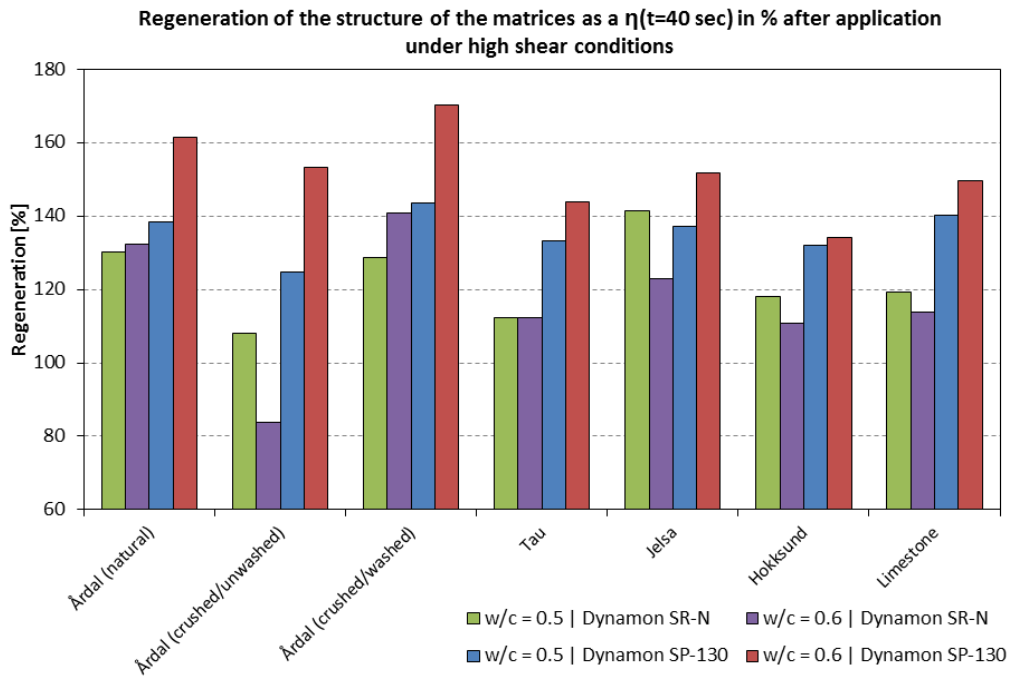


Fig.4-11: Regeneration of the structure of the matrices as a $\eta(t=40 \text{ sec})$ in % after application under high shear conditions

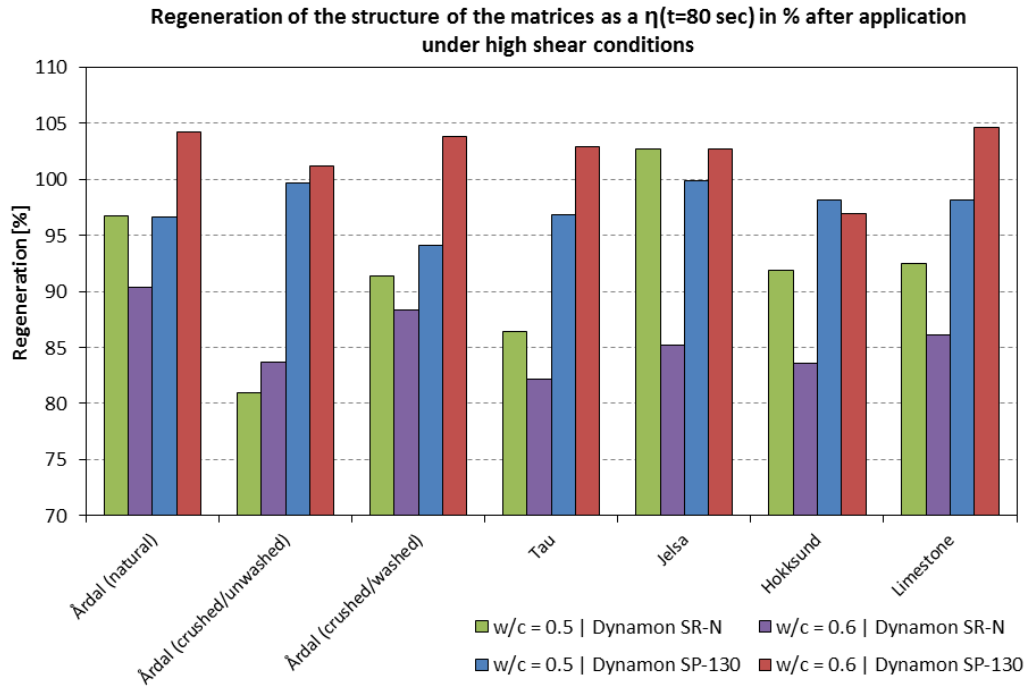


Fig.4-12: Regeneration of the structure of the matrices as a $\eta(t=80 \text{ sec})$ in % after application under high shear conditions

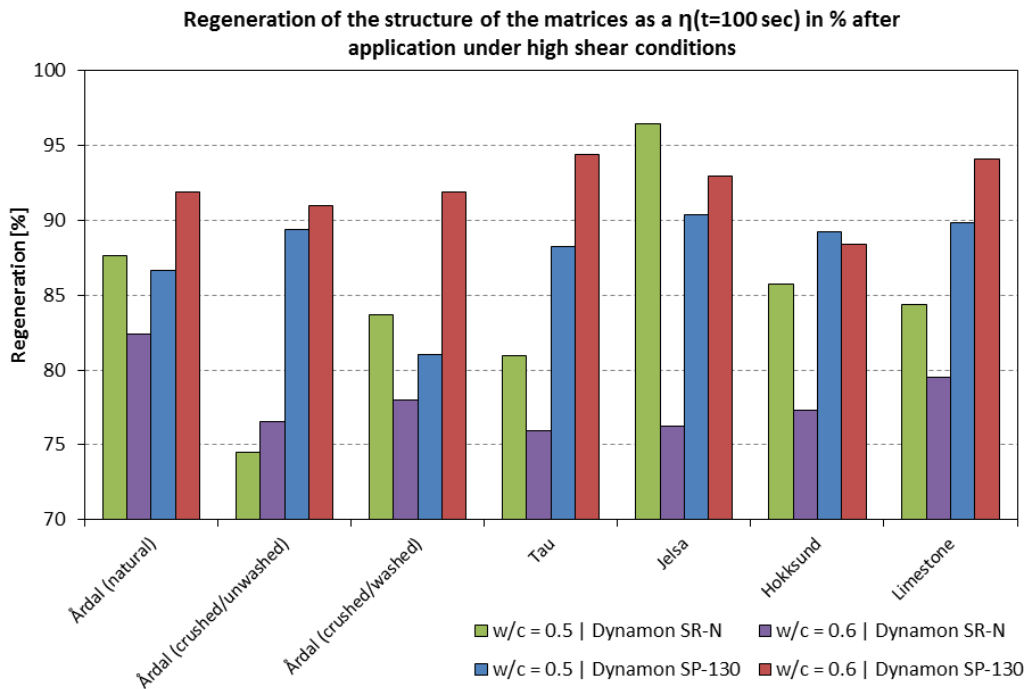


Fig.4-13: Regeneration of the structure of the matrices as a $\eta(t=100 \text{ sec})$ in % after application under high shear conditions

It can be seen from Figures 4-10 to 4-13 that both SP type and fines used can affect the structural regeneration (thixotropy) of the tested filler modified pastes. Matrices with long-chained Dynamon SP-130 display higher thixotropy (slower regeneration) than matrices with short side-chained Dynamon SR-N. It's also possible to notice some relations between structural regeneration rate and filler type. In order to investigate if a relation between specific surface of the fillers and structural regeneration exists – series of correlation analysis were performed. An overview of the results is given in Tables 4-2 to 4-5. Since the amount of data points for each correlation was not high (=7) it was chosen at first check if there is a linear correlation and then

pay closer attention by actually plotting the relation with high enough squared linear correlation coefficient (R^2) values if necessary.

Table 4-2: Correlation analysis between regeneration of the structure of the matrices (w/c=0.5 | Dynamon SR-N) and specific surface of the fillers

Correlation analysis				
Regeneration of the structure of the matrices (w/c=0.5 Dynamon SR-N) as a $\eta(t)$ in % after application under high shear conditions				
Method	t=20 [sec]	t=40 [sec]	t=80 [sec]	t=100 [sec]
	Squared linear correlation coefficient [R^2]			
Blaine	0.0501	0.0002	0.0692	0.0907
BET	0.0743	0.0325	0.0009	0.0067
LS Particle Size Analyzer	0.1862	0.0664	0.0022	0.0028
Micrometrics SediGraph 5100	0.0043	0.0756	0.0001	0.0043

Table 4-3: Correlation analysis between regeneration of the structure of the matrices (w/c=0.6 | Dynamon SR-N) and specific surface of the fillers

Correlation analysis				
Regeneration of the structure of the matrices (w/c=0.6 Dynamon SR-N) as a $\eta(t)$ in % after application under high shear conditions				
Method	t=20 [sec]	t=40 [sec]	t=80 [sec]	t=100 [sec]
	Squared linear correlation coefficient [R^2]			
Blaine	0.0028	0.0728	0.1327	0.0167
BET	0.0079	0.0079	0.0436	0.0743
LS Particle Size Analyzer	0.1770	0.0652	0.1028	0.0019
Micrometrics SediGraph 5100	0.0006	0.1337	0.0058	0.1061

Table 4-4: Correlation analysis between regeneration of the structure of the matrices (w/c=0.5 | Dynamon SP-130) and specific surface of the fillers

Correlation analysis				
Regeneration of the structure of the matrices (w/c=0.5 Dynamon SP-130) as a $\eta(t)$ in % after application under high shear conditions				
Method	t=20 [sec]	t=40 [sec]	t=80 [sec]	t=100 [sec]
	Squared linear correlation coefficient [R^2]			
Blaine	0.1121	0.0004	0.3555	0.5761
BET	0.6296	0.1726	0.0517	0.1219
LS Particle Size Analyzer	0.1246	0.0002	0.1067	0.3257
Micrometrics SediGraph 5100	0.0316	0.0062	0.1917	0.3601

Table 4-5: Correlation analysis between regeneration of the structure of the matrices (w/c=0.6 | Dynamon SP-130) and specific surface of the fillers

Correlation analysis				
Regeneration of the structure of the matrices (w/c=0.6 Dynamon SP-130) as a $\eta(t)$ in % after application under high shear conditions				
Method	t=20 [sec]	t=40 [sec]	t=80 [sec]	t=100 [sec]
	Squared linear correlation coefficient [R^2]			
Blaine	0.3135	0.2973	0.0037	0.1599
BET	0.4157	0.5069	0.7180	0.5454
LS Particle Size Analyzer	0.4027	0.4487	0.0478	0.0023
Micrometrics SediGraph 5100	0.1592	0.2033	0.0049	0.0001

As it can be seen from Tables 4-2 to 4-5 the relation is generally very poor and even if in a number of cases a limited correlation seems to exist – it does not follow any logical rules. Since for some of the filler specific surface area determination methods a reasonable doubt was discussed if correct values for the Hokksund and Limestone fines have been found (see chapter 4.1) it was decided to repeat the correlation analysis and exclude the results from those fillers. Results of the analysis are presented in Tables 4-6 to 4-9.

Table 4-6: Correlation analysis between regeneration of the structure of the matrices (w/c=0.5 | Dynamon SR-N) and specific surface of the fillers (excluding Hokksund and Limestone filler results)

Correlation analysis				
Regeneration of the structure of the matrices (w/c=0.5 Dynamon SR-N) as a $\eta(t)$ in % after application under high shear conditions				
Method	t=20 [sec]	t=40 [sec]	t=80 [sec]	t=100 [sec]
	Squared linear correlation coefficient [R^2]			
Blaine	0.0074	0.0432	0.1188	0.2250
BET	0.0212	0.0148	0.0064	0.0029
LS Particle Size Analyzer	0.1954	0.0331	0.0001	0.0187
Micrometrics SediGraph 5100	0.0227	0.0595	0.0147	0.0227

Table 4-7: Correlation analysis between regeneration of the structure of the matrices (w/c=0.6 | Dynamon SR-N) and specific surface of the fillers (excluding Hokksund and Limestone filler results)

Correlation analysis				
Regeneration of the structure of the matrices (w/c=0.6 Dynamon SR-N) as a $\eta(t)$ in % after application under high shear conditions				
Method	t=20 [sec]	t=40 [sec]	t=80 [sec]	t=100 [sec]
	Squared linear correlation coefficient [R ²]			
Blaine	0.0517	0.0926	0.3504	0.2766
BET	0.6875	0.6875	0.0618	0.0004
LS Particle Size Analyzer	0.8119	0.1569	0.5185	0.2206
Micrometrics SediGraph 5100	0.5953	0.3604	0.0035	0.0801

Table 4-8: Correlation analysis between regeneration of the structure of the matrices (w/c=0.5 | Dynamon SP-130) and specific surface of the fillers (excluding Hokksund and Limestone filler results)

Correlation analysis				
Regeneration of the structure of the matrices (w/c=0.5 Dynamon SP-130) as a $\eta(t)$ in % after application under high shear conditions				
Method	t=20 [sec]	t=40 [sec]	t=80 [sec]	t=100 [sec]
	Squared linear correlation coefficient [R ²]			
Blaine	0.7875	0.0969	0.5656	0.7175
BET	0.3893	0.1419	0.1549	0.3614
LS Particle Size Analyzer	0.9138	0.1915	0.2973	0.6139
Micrometrics SediGraph 5100	0.2783	0.4704	0.4777	0.5020

Table 4-9: Correlation analysis between regeneration of the structure of the matrices (w/c=0.6 | Dynamon SP-130) and specific surface of the fillers (excluding Hokksund and Limestone filler results)

Correlation analysis				
Regeneration of the structure of the matrices (w/c=0.6 Dynamon SP-130) as a $\eta(t)$ in % after application under high shear conditions				
Method	t=20 [sec]	t=40 [sec]	t=80 [sec]	t=100 [sec]
	Squared linear correlation coefficient [R ²]			
Blaine	0.6563	0.6446	0.1373	0.2947
BET	0.1521	0.2246	0.0010	0.0200
LS Particle Size Analyzer	0.9118	0.9307	0.0956	0.5571
Micrometrics SediGraph 5100	0.0969	0.1436	0.1671	0.1135

As it can be seen from Tables 4-6 to 4-9 after excluding the doubtful specific surface results the relation in some cases has improved. It seems the best for the specific surface values obtained by the LS Particle Size Analyzer at the beginning of the regeneration process, i.e. after 20 sec. It also seems that the relation seems to be better for the matrices prepared with Dynamon SP-130 and matrices with the w/c ratio of 0.6. It must also be steady noted that this is just an indication and the correlations analysed in Tables 4-6 to 4-9 are based on very few data points (=5) and most probably other important phenomena that govern the regeneration exist.

However, it might still be interesting to study in what way the specific surface can affect the structural regeneration (thixotropy) of the matrices. Therefore two of the correlations from Tables 4-8 (linear $R^2=0.9138$) and 4-9 (linear $R^2=0.9118$) were plotted and analysed. The plots are presented on Figures 4-14 and 4-15.

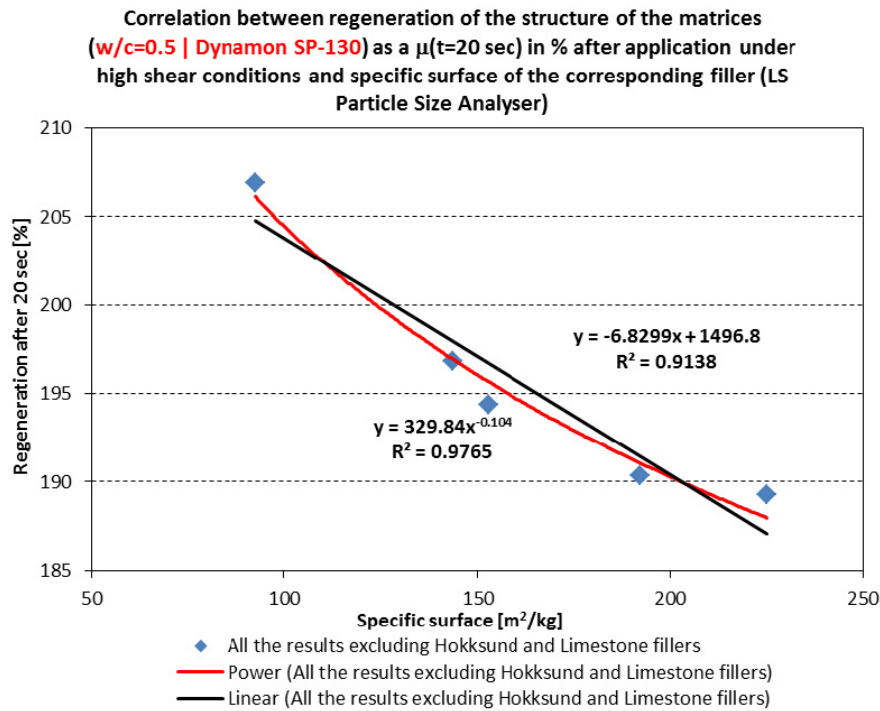


Fig.4-14: Correlation between regeneration of the structure of the matrices (w/c=0.5 | Dynamon SP-130) as a $\eta(t=20 \text{ sec})$ in % after application under high shear conditions and specific surface of the corresponding filler (LS Particle Size Analyser)

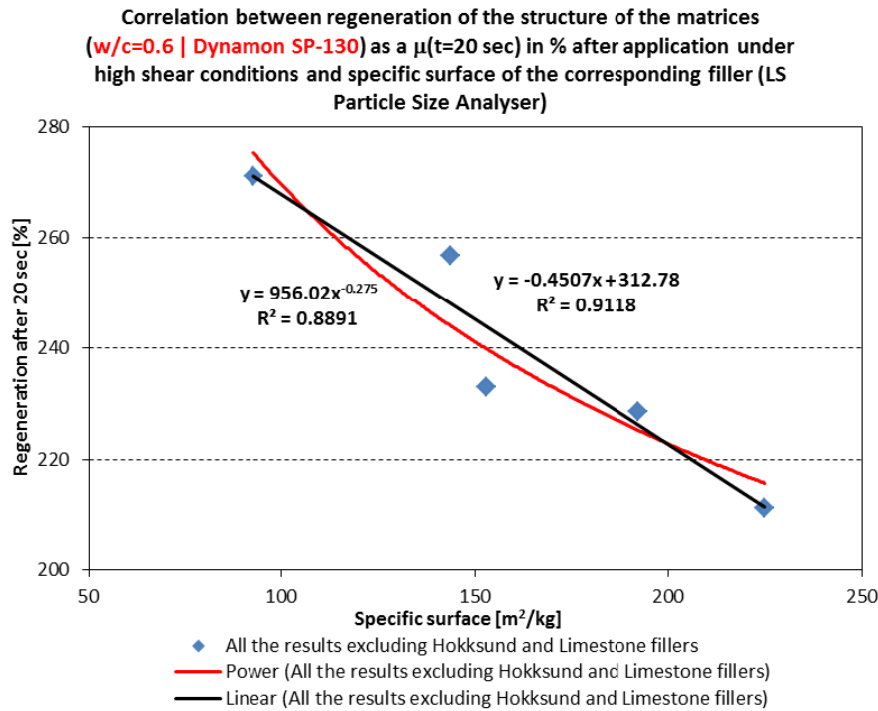


Fig.4-15: Correlation between regeneration of the structure of the matrices ($w/c=0.6$ | Dynamon SP-130) as a $\eta(t=20 \text{ sec})$ in % after application under high shear conditions and specific surface of the corresponding filler (LS Particle Size Analyser)

As it can be seen from Figures 4-14 and 4-15 the higher is the specific surface area of the filler, the longer time it takes in order to reach the same structural strength in terms of viscosity as before application under high shear rate. The reason for this is probably due to that a lot higher number of contacts between the particles exists in case when the filler is finer. Such a system is then less dynamic in changing its state and as a result exhibits more thixotropic behaviour. If the filler is finer it would eventually incorporate a lot more of very fine particles. From basic physical chemistry there is an upper limit to the dominance of electrostatic and repulsive forces beyond which the viscous and other mechanical forces will dominate the rheology of the fresh mix. There are indications that the limit is in order of 0.1 - 1 micron (Billberg 2006). However, it will vary depending on the properties of liquid and particles (surface characteristics, reactivity etc.). This means that the number of contacts between the particles is not the only reason for slower regeneration or decomposition what was approved by the different regeneration test results when the SP type is kept as the only variable (see Figures 4-10 to 4-13).

4.2.4 Stability

The fourth rheological sequence (see Table 2-4 and Figure 2-5) aimed at relating to stability was also used where the evolution of apparent time dependant viscosity was recorded in consecutive tests at high, low and high shear rate. This also gives information about thixotropy as discussed in the previous chapter

However, the aim of this test sequence was to investigate the stability of the matrices. The principle to study this is based on assumption that if a filler modified cement paste is sheared at a very low rate ($=0.1 \text{ s}^{-1}$) in the small rheometer gap ($=1 \text{ mm}$) for a certain period of time, a layer of water may appear at the top of the sample. Then instead of shearing the matrix sample the rheometer would rather run only in the top layer of water. Thus viscosity values close to the one of water at 20°C ($=1.002 \text{ mPa}\cdot\text{s}$) should appear in the results (Figures 3-1 to 3-5 and in Tables 3-4 to 3-6). For a “normal-sized” concrete or matrix sample appearance of a less than 1 mm thick water layer on the top is usually caused by the bleed water, however, if the sample is

only 1 mm high and the time of observation relatively short (60 sec) then it is assumed to be as a results of stability issues.

As it can be seen from the results (Figures 3-1 to 3-5 and in Tables 3-4 to 3-6), no apparent viscosity values even close to the viscosity of water have been observed. Though this does not mean that the above introduced stability estimation method or approach is not applicable since the aim of the study was to produce very stable matrices. According to the visual observations at the laboratory during the experiments, all of the matrices can be classified as very stable.

4.2.5 Correlation to specific surface area of the fillers

An extensive correlation analysis has been performed in order to investigate if relation between the specific surface area of the fillers and different determined rheological properties of the matrices (see Tables 3-1 to 3-3) can be found. Since the amount of data points for each correlation was not high (=7) it was chosen at first check if there is a linear correlation and then pay closer attention by actually plotting the relation with high enough squared linear correlation coefficient (R^2) values if necessary. An overview of the analysis results is given in Tables 4-10 and 4-11.

As it can be seen from Tables 4-10 to 4-11, the relation is generally very poor and even if in a number of cases correlation seems to exist, as for the complex modulus G^* , it does not follow any logical rules since the relation is not valid for all types of the matrices (with the respect to w/c and SP type). Since for some of the filler specific surface area determination methods a reasonable doubt was discussed if correct values for the Hokksund and Limestone fines have been found (see chapter 4.1) it was decided to repeat the correlation analysis and exclude the results from those fillers. Results of the analysis are presented in Tables 4-12 to 4-13.

Table 4-10: Correlation analysis between specific surface area of the fillers and rheological parameters of matrices with Dynamon SR-N

Correlation analysis														
Method	Bingham parameters			Herschel-Bulkley parameters			Hysteresis area	Complex modulus, G*	Critical strain γ_{crit}	Gel strength	Static yield stress	Static yield s. (after 24 minutes)	G (controlled stress)	G (controlled shear rate)
	τ_y	μ	τ_y	K	n									
	1	2	3	4	5	6								
	Squared linear correlation coefficient [R²] for matrices with Dynamon SR-N at w/c=0.5													
Blaine	0.0763	0.0844	0.1272	0.0941	0.0007	0.3161	0.0000	0.1257	0.3033	0.3015	0.0011	0.3726	0.1196	0.1479
BET	0.1784	0.2071	0.1068	0.0910	0.0346	0.0425	0.7904	0.0768	0.2653	0.3092	0.4749	0.3283	0.4811	0.2605
LS Particle Size Analyzer	0.3829	0.2961	0.5775	0.5091	0.0754	0.0893	0.1865	0.5333	0.3607	0.3969	0.0114	0.5563	0.0326	0.3083
Micrometrics SediGraph 5100	0.1101	0.0803	0.2451	0.1958	0.0350	0.0006	0.1123	0.3680	0.0746	0.0759	0.0738	0.2083	0.2229	0.1387
MIN=	0.0763	0.0803	0.1068	0.0910	0.0007	0.0006	0.0000	0.0768	0.0746	0.0759	0.0011	0.2083	0.0326	
MAX=	0.3829	0.2961	0.5775	0.5091	0.0754	0.3161	0.7904	0.5333	0.3607	0.3969	0.4749	0.5563	0.4811	
AVERAGE=	0.1869	0.1670	0.2642	0.2225	0.0364	0.1121	0.2723	0.2759	0.2510	0.2709	0.1403	0.3664	0.2141	0.1387
	Squared linear correlation coefficient [R²] for matrices with Dynamon SR-N at w/c=0.6													
Blaine	0.2443	0.1821	0.4063	0.3239	0.4353	0.0194	0.0364	0.3933	0.1912	0.1737	0.3542	0.0853	0.4459	0.2532
BET	0.1176	0.3610	0.0507	0.0386	0.0058	0.3750	0.7362	0.1989	0.3706	0.1669	0.2486	0.0190	0.2196	0.2237
LS Particle Size Analyzer	0.0924	0.2933	0.2058	0.0905	0.0667	0.0739	0.1838	0.0831	0.2751	0.0592	0.2408	0.0788	0.3687	0.1625
Micrometrics SediGraph 5100	0.0000	0.0638	0.0579	0.0020	0.0514	0.0059	0.0159	0.0579	0.0641	0.0001	0.0948	0.0641	0.1554	0.0487
MIN=	0.0000	0.0638	0.0507	0.0020	0.0058	0.0059	0.0159	0.0579	0.0641	0.0001	0.0948	0.0190	0.1554	
MAX=	0.2443	0.3610	0.4063	0.3239	0.4353	0.3750	0.7362	0.3933	0.3706	0.1737	0.3542	0.0853	0.4459	
AVERAGE=	0.1136	0.2250	0.1802	0.1138	0.1398	0.1185	0.2431	0.1833	0.2252	0.1000	0.2346	0.0618	0.2974	0.1625

Table 4-11: Correlation analysis between specific surface area of the fillers and rheological parameters of matrices with Dynamon SP-130

Correlation analysis													
Method	Bingham parameters		Herschel-Bulkley parameters			Hysteresis area	Complex modulus, G*	Critical strain γ_{crit}	Gel strength	Static yield stress	Static yield s. (after 24 minutes)	G (controlled stress)	G (controlled shear rate)
	τ_y	μ	τ_y	K	n								
	1	2	3	4	5	6	7	8	9	10	11	12	13
	Squared linear correlation coefficient [R²] for matrices with Dynamon SP-130 at w/c=0.5												
Blaine	0.2720	0.2878	0.2593	0.0706	0.0867	0.0006	0.0654	0.1657	0.3116	0.1763	0.1512	0.5110	0.1303
BET	0.5297	0.3307	0.0056	0.7203	0.7507	0.0233	0.0168	0.0442	0.3367	0.6680	0.6104	0.2454	0.7109
LS Particle Size Analyzer	0.4025	0.4380	0.0891	0.2849	0.2766	0.0007	0.0518	0.1220	0.2453	0.3799	0.3153	0.3883	0.3531
Micrometrics SediGraph 5100	0.1451	0.1029	0.3267	0.0564	0.0653	0.0354	0.2517	0.0320	0.0549	0.1724	0.1140	0.1166	0.1350
	MIN=	0.1029	0.0056	0.0564	0.0653	0.0006	0.0168	0.0320	0.0549	0.1724	0.1140	0.1166	0.1303
	MAX=	0.4380	0.3267	0.7203	0.7507	0.0354	0.2517	0.1657	0.3367	0.6680	0.6104	0.5110	0.7109
	AVERAGE=	0.2899	0.1702	0.2830	0.2948	0.0150	0.0964	0.0910	0.2371	0.3492	0.2977	0.3153	0.3323
	Squared linear correlation coefficient [R²] for matrices with Dynamon SP-130 at w/c=0.6												
Blaine	0.2265	0.1360	0.0000	0.0769	0.1836	0.5173	0.5194	0.5162	0.1688	0.1684	0.1486	0.4405	0.1137
BET	0.2590	0.2875	0.3945	0.3549	0.2680	0.0592	0.0850	0.0340	0.6084	0.4113	0.4948	0.3542	0.5771
LS Particle Size Analyzer	0.3466	0.2014	0.1554	0.2736	0.5005	0.8802	0.6893	0.3892	0.5316	0.3708	0.3948	0.5853	0.3796
Micrometrics SediGraph 5100	0.0575	0.0104	0.0038	0.0285	0.1385	0.5318	0.4679	0.4410	0.2294	0.0681	0.0883	0.4408	0.0835
	MIN=	0.0104	0.0000	0.0285	0.1385	0.0592	0.0850	0.0340	0.1688	0.0681	0.0883	0.3542	0.0835
	MAX=	0.3466	0.3945	0.3549	0.5005	0.8802	0.6893	0.5162	0.6084	0.4113	0.4948	0.5853	0.5771
	AVERAGE=	0.2224	0.1588	0.1384	0.1835	0.4971	0.4404	0.3451	0.3845	0.2546	0.2816	0.4552	0.2884

Table 4-12: Correlation analysis between specific surface area of the fillers and rheological parameters of matrices with Dynamon SR-N (excluding Hokksund and Limestone filler results)

Correlation analysis															
Method	Bingham parameters			Herschel-Bulkley parameters			Hysteresis area	Complex modulus, G*	Critical strain γ_{crit}	Gel strength	Static yield stress	Static yield s. (after 24 minutes)	G (controlled stress)	G (controlled shear rate)	AVERAGE
	τ_y	μ	τ_y	K	n										
	1	2	3	4	5	6	7	8	9	10	11	12	13		
Squared linear correlation coefficient [R²] for matrices with Dynamon SR-N at w/c=0.5															
Blaine	0.0011	0.0509	0.0884	0.1100	0.3460	0.4919	0.2002	0.3394	0.5634	0.6951	0.3763	0.4177	0.1932	0.2980	
BET	0.0343	0.0181	0.3458	0.4247	0.7131	0.0069	0.1622	0.8684	0.0374	0.0366	0.0702	0.2387	0.1873	0.2418	
LS Particle Size Analyzer	0.1618	0.4019	0.0005	0.0082	0.6751	0.6427	0.2381	0.5810	0.8556	0.4893	0.3216	0.8206	0.1463	0.4110	
Micrometrics SediGraph 5100	0.0794	0.0003	0.5188	0.5467	0.5484	0.0820	0.0847	0.4236	0.0003	0.0774	0.3257	0.0028	0.5393	0.2484	
MIN=	0.0011	0.0003	0.0005	0.0082	0.3460	0.0069	0.0847	0.3394	0.0003	0.0366	0.0702	0.0028	0.1463		
MAX=	0.1618	0.4019	0.5188	0.5467	0.7131	0.6427	0.2381	0.8684	0.8556	0.6951	0.3763	0.8206	0.5393		
AVERAGE=	0.0692	0.1178	0.2384	0.2724	0.5707	0.3059	0.1713	0.5531	0.3642	0.3246	0.2734	0.3699	0.2665	0.2484	
Squared linear correlation coefficient [R²] for matrices with Dynamon SR-N at w/c=0.6															
Blaine	0.7878	0.4331	0.6659	0.8055	0.9016	0.2566	0.7569	0.5343	0.4709	0.7574	0.7616	0.0119	0.7130	0.6044	
BET	0.0511	0.0625	0.1694	0.0883	0.3428	0.0379	0.0140	0.0294	0.1268	0.1288	0.2089	0.3910	0.1922	0.1418	
LS Particle Size Analyzer	0.8993	0.8034	0.9710	0.9381	0.8357	0.2054	0.8043	0.7392	0.8721	0.9592	0.9212	0.3303	0.9571	0.7874	
Micrometrics SediGraph 5100	0.0059	0.0150	0.0543	0.0162	0.2484	0.0176	0.0110	0.0313	0.0389	0.0455	0.1601	0.0217	0.1042	0.0592	
MIN=	0.0059	0.0150	0.0543	0.0162	0.2484	0.0176	0.0110	0.0294	0.0389	0.0455	0.1601	0.0119	0.1042		
MAX=	0.8993	0.8034	0.9710	0.9381	0.9016	0.2566	0.8043	0.7392	0.8721	0.9592	0.9212	0.3910	0.9571		
AVERAGE=	0.4360	0.3285	0.4651	0.4620	0.5821	0.1294	0.3966	0.3336	0.3772	0.4727	0.5129	0.1887	0.4916	0.4916	

Table 4-13: Correlation analysis between specific surface area of the fillers and rheological parameters of matrices with Dynamon SP-130 (excluding Hokksund and Limestone filler results)

Correlation analysis															
Method	Bingham parameters			Herschel-Bulkley parameters			Hysteresis area	Complex modulus, G*	Critical strain γ_{crit}	Gel strength	Static yield stress	Static yield s. (after 24 minutes)	G (controlled stress)	G (controlled shear rate)	AVERAGE
	τ_y	μ	2	τ_y	K	n									
	1	2	3	4	5	6	7	8	9	10	11	12	13		
	Squared linear correlation coefficient [R²] for matrices with Dynamon SP-130 at w/c=0.5														
Blaine	0.8520	0.4960	0.2272	0.6488	0.8945	0.1414	0.0031	0.0567	0.8800	0.6760	0.6602	0.9557	0.7713	0.5587	
BET	0.0705	0.0388	0.1779	0.0348	0.0801	0.1058	0.0320	0.5361	0.0850	0.1889	0.0708	0.0344	0.1080	0.1202	
LS Particle Size Analyzer	0.8462	0.8390	0.0766	0.8730	0.8979	0.5892	0.1314	0.0000	0.8808	0.8302	0.7483	0.6846	0.8360	0.6333	
Micrometrics SediGraph 5100	0.0594	0.0024	0.6792	0.0015	0.0149	0.0249	0.1724	0.1430	0.0526	0.2071	0.1122	0.0037	0.1178	0.1224	
MIN=	0.0594	0.0024	0.0766	0.0015	0.0149	0.0249	0.0031	0.0000	0.0526	0.1889	0.0708	0.0037	0.1080		
MAX=	0.8520	0.8390	0.6792	0.8730	0.8979	0.5892	0.1724	0.5361	0.8808	0.8302	0.7483	0.9557	0.8360		
AVERAGE=	0.4570	0.3441	0.2902	0.3895	0.4719	0.2153	0.0847	0.1839	0.4746	0.4755	0.3979	0.4196	0.4583		
	Squared linear correlation coefficient [R²] for matrices with Dynamon SP-130 at w/c=0.6														
Blaine	0.3497	0.3986	0.0030	0.1264	0.0857	0.2184	0.2639	0.1194	0.7580	0.3351	0.3024	0.6889	0.2923	0.3032	
BET	0.0697	0.0434	0.0055	0.0426	0.0386	0.2621	0.0130	0.1225	0.0136	0.0433	0.0751	0.0365	0.0683	0.0642	
LS Particle Size Analyzer	0.7840	0.7981	0.1724	0.5546	0.4734	0.1379	0.0127	0.0386	0.7372	0.7569	0.7568	0.2196	0.7389	0.4755	
Micrometrics SediGraph 5100	0.0056	0.0015	0.1195	0.0320	0.0617	0.5284	0.0531	0.0006	0.0232	0.0092	0.0043	0.1880	0.0095	0.0797	
MIN=	0.0056	0.0015	0.0030	0.0320	0.0386	0.1379	0.0127	0.0006	0.0136	0.0092	0.0043	0.0365	0.0095		
MAX=	0.7840	0.7981	0.1724	0.5546	0.4734	0.5284	0.2639	0.1225	0.7580	0.7569	0.7568	0.6889	0.7389		
AVERAGE=	0.3023	0.3104	0.0751	0.1889	0.1648	0.2867	0.0857	0.0702	0.3830	0.2861	0.2846	0.2833	0.2773		

As it can be seen from Tables 4-12 and 4-13 the relation in a lot of cases has noticeably improved if the results from Hokksund and Limestone filler are excluded. However, only one of the parameters (gel strength) shows indication of existing correlation for the entire matrix types with respect to the w/c ration and SP. Though it seems that on overall static yield values are easier to be related to specific surface measurements than the dynamic ones. The relation seems to be the best for specific surface area measures obtained by the LS Particle Size Analyzer and for the matrices prepared with Dynamon SR-N at w/c ratio of 0.6. Quite opposite the rheologic properties of the matrices with Dynamon SP-130 and w/c ratio of 0.5 seem to be much more related to the specific surface measurements than those with w/c ratio of 0.6. Specific surface area values determined by the BET method and by Micrometrics SediGraph 5100 seem to have no relation at all. This is opposite to a study by Cepuritis (2011) where specific surface values calculated from SediGraph PSD measurements showed a limited relation to dynamic (Bingham and Herschel-Bulkley) and static yield values of the corresponding matrices. However, matrix composition and measurements sequence was very different for that study.

Some of the other authors who have come to a conclusion that the effect on rheology of the filler depends largely on its specific surface have used different ways of expressing the surface/ PSD of the filler. Like, for example, Pedersen (2004) has used D_{50} value that is a median particle size meaning that 50% of the filler particles are smaller or bigger than the median particle size. D_{50} values were calculated from SediGraph and LS Particle Size Analyzer results (Table 2-2) by means of linear interpolation. Results of the calculation are presented in Table 4-14.

Table 4-14: Median particle size D_{50} of the fillers

D_{50} median particle size (50 % smaller particles)*							
PSD determinaton method	Filler						
	Årdal (natural)	Årdal (crushed/washed)	Årdal (crushed/unwashed)	Tau	Jelsa	Hokksund	Limestone
	[μm]						
LS Particle Size Analyzer	73.10	46.71	78.07	26.60	23.80	36.61	18.78
Micrometrics SediGraph 5100	72.54	44.72	72.43	22.28	19.41	24.95	19.36

* Obtained by linear interpolation

Linear correlation analysis between the determined D_{50} values and rheological parameters of the matrices is presented in Tables 4-15 to 4-16. Tables 4-17 and 4-18 include the same analysis if the results from Hokksund and Limestone fillers are excluded.

Table 4-15: Correlation analysis between median particle size D_{50} of the fillers and rheological parameters of matrices with Dynamon SR-N

PSD determination method	Correlation analysis													AVERAGE	
	Bingham parameters			Herschel-Bulkley parameters			Hysteresis area	Complex modulus, G^*	Critical strain γ_{crit}	Gel strength	Static yield stress	Static yield s. (after 24 minutes)	G (controlled stress)		G (controlled shear rate)
	τ_y	μ	τ_y	K	n										
	1	2	3	4	5	6	7	8	9	10	11	12	13		
	Squared linear correlation coefficient $[R^2]$ for matrices with Dynamon SR-N at $w/c=0.5$														
LS Particle Size Analyzer	0.2242	0.2994	0.1342	0.1089	0.0430	0.6055	0.0005	0.0498	0.6498	0.4976	0.0502	0.4911	0.0045	0.2430	
Micrometrics SediGraph 5100	0.3008	0.3657	0.1885	0.1622	0.0298	0.5973	0.0082	0.0780	0.7643	0.6546	0.1422	0.5582	0.0083	0.2968	
MIN=	0.2242	0.2994	0.1342	0.1089	0.0298	0.5973	0.0005	0.0498	0.6498	0.4976	0.0502	0.4911	0.0045		
MAX=	0.3008	0.3657	0.1885	0.1622	0.0430	0.6055	0.0082	0.0780	0.7643	0.6546	0.1422	0.5582	0.0083		
AVERAGE=	0.2625	0.3326	0.1614	0.1355	0.0364	0.6014	0.0044	0.0639	0.7071	0.5761	0.0962	0.5246	0.0064		
	Squared linear correlation coefficient $[R^2]$ for matrices with Dynamon SR-N at $w/c=0.6$														
LS Particle Size Analyzer	0.6351	0.5112	0.7551	0.6929	0.5883	0.1998	0.1567	0.5465	0.5205	0.5436	0.7099	0.0650	0.7816	0.5159	
Micrometrics SediGraph 5100	0.7154	0.6259	0.7491	0.7178	0.5142	0.3137	0.2847	0.4210	0.6226	0.6125	0.7656	0.0289	0.8310	0.5540	
MIN=	0.6351	0.5112	0.7491	0.6929	0.5142	0.1998	0.1567	0.4210	0.5205	0.5436	0.7099	0.0289	0.7816		
MAX=	0.7154	0.6259	0.7551	0.7178	0.5883	0.3137	0.2847	0.5465	0.6226	0.6125	0.7656	0.0650	0.8310		
AVERAGE=	0.6753	0.5686	0.7521	0.7053	0.5513	0.2567	0.2207	0.4838	0.5715	0.5781	0.7377	0.0469	0.8063		

Table 4-16: Correlation analysis between median particle size D_{50} of the fillers and rheological parameters of matrices with Dynamon SP-130

Correlation analysis													
PSD determination method	Bingham parameters		Herschel-Bulkley parameters			Hysteresis area	Complex modulus, G^*	Critical strain γ_{crit}	Gel strength	Static yield stress	Static yield s. (after 24 minutes)	G (controlled stress)	G (controlled shear rate)
	τ_y	μ	τ_y	K	n								
	1	2	3	4	5	6	7	8	9	10	11	12	13
Squared linear correlation coefficient [R^2] for matrices with Dynamon SP-130 at $w/c=0.5$													
LS Particle Size Analyzer	0.5121	0.5708	0.2192	0.2087	0.2198	0.1475	0.0163	0.2553	0.6551	0.3724	0.3786	0.6897	0.2894
Micrometrics SediGraph 5100	0.6517	0.6926	0.1604	0.3414	0.3523	0.1558	0.0072	0.2888	0.7725	0.4956	0.5133	0.7963	0.4202
MIN=	0.5121	0.5708	0.1604	0.2087	0.2198	0.1475	0.0072	0.2553	0.6551	0.3724	0.3786	0.6897	0.2894
MAX=	0.6517	0.6926	0.2192	0.3414	0.3523	0.1558	0.0163	0.2888	0.7725	0.4956	0.5133	0.7963	0.4202
AVERAGE=	0.5819	0.6317	0.1898	0.2751	0.2860	0.1516	0.0117	0.2721	0.7138	0.4340	0.4459	0.7430	0.3548
Squared linear correlation coefficient [R^2] for matrices with Dynamon SP-130 at $w/c=0.6$													
LS Particle Size Analyzer**	0.4953	0.4551	0.0428	0.2600	0.3021	0.3562	0.2636	0.2047	0.2150	0.4102	0.3491	0.4090	0.2806
Micrometrics SediGraph 5100**	0.5888	0.5675	0.0968	0.3549	0.3775	0.3902	0.2910	0.1702	0.3259	0.5331	0.4685	0.4835	0.4033
MIN=	0.4953	0.4551	0.0428	0.2600	0.3021	0.3562	0.2636	0.1702	0.2150	0.4102	0.3491	0.4090	0.2806
MAX=	0.5888	0.5675	0.0968	0.3549	0.3775	0.3902	0.2910	0.2047	0.3259	0.5331	0.4685	0.4835	0.4033
AVERAGE=	0.5420	0.5113	0.0698	0.3075	0.3398	0.3732	0.2773	0.1874	0.2705	0.4717	0.4088	0.4463	0.3419
AVERAGE													
													0.3488
													0.4345
													0.3110
													0.3886

Table 4-17: Correlation analysis between median particle size D_{50} of the fillers and rheological parameters of matrices with Dynamon SR-N (excluding Hokksund and Limestone filler results)

Method	Correlation analysis														
	Bingham parameters			Herschel-Bulkley parameters			Squared linear correlation coefficient $[R^2]$ for matrices with Dynamon SR-N at $w/c=0.5$							G (controlled shear rate)	AVERAGE
	τ_y	μ	2	τ_y	K	n	Hysteresis area	Complex modulus, G^*	Critical strain γ_{crit}	Gel strength	Static yield stress	Static yield s. (after 24 minutes)	G (controlled stress)		
	1			3	4	5	6	7	8	9	10	11	12	13	
LS Particle Size Analyzer	0.1410	0.2775		0.0000	0.0009	0.3852	0.7377	0.5024	0.2316	0.8342	0.7769	0.4139	0.4803	0.2289	0.3854
Micrometrics SediGraph 5100	0.1597	0.2805		0.0037	0.0007	0.3183	0.7873	0.5526	0.1819	0.8428	0.8333	0.4769	0.4704	0.2887	0.3998
MIN=	0.1410	0.2775		0.0000	0.0007	0.3183	0.7377	0.5024	0.1819	0.8342	0.7769	0.4139	0.4704	0.2289	
MAX=	0.1597	0.2805		0.0037	0.0009	0.3852	0.7873	0.5526	0.2316	0.8428	0.8333	0.4769	0.4803	0.2887	
AVERAGE=	0.1504	0.2790		0.0019	0.0008	0.3517	0.7625	0.5275	0.2067	0.8385	0.8051	0.4454	0.4753	0.2588	AVERAGE
															AVERAGE
LS Particle Size Analyzer	0.9527	0.7435		0.8556	0.9405	0.7884	0.5111	0.8648	0.8486	0.7449	0.9260	0.9027	0.0363	0.8876	0.7694
Micrometrics SediGraph 5100	0.9554	0.7372		0.8317	0.9342	0.7319	0.5186	0.8913	0.8412	0.7268	0.9069	0.8591	0.0283	0.8530	0.7550
MIN=	0.9527	0.7372		0.8317	0.9342	0.7319	0.5111	0.8648	0.8412	0.7268	0.9069	0.8591	0.0283	0.8530	
MAX=	0.9554	0.7435		0.8556	0.9405	0.7884	0.5186	0.8913	0.8486	0.7449	0.9260	0.9027	0.0363	0.8876	
AVERAGE=	0.9540	0.7403		0.8436	0.9373	0.7602	0.5148	0.8780	0.8449	0.7359	0.9165	0.8809	0.0323	0.8703	

Table 4-18: Correlation analysis between median particle size D_{50} of the fillers and rheological parameters of matrices with Dynamon SP-130 (excluding Hokksund and Limestone filler results)

Correlation analysis													
Method	Bingham parameters		Herschel-Bulkley parameters			Hysteresis area	Complex modulus, G^*	Critical strain γ_{crit}	Gel strength	Static yield stress	Static yield s. (after 24 minutes)	G (controlled stress)	G (controlled shear rate)
	τ_y	μ	τ_y	K	n								
	1	2	3	4	5	6	7	8	9	10	11	12	13
Squared linear correlation coefficient [R²] for matrices with Dynamon SP-130 at w/c=0.5													
LS Particle Size Analyzer	0.9921	0.7507	0.1674	0.8526	0.9474	0.3973	0.0053	0.1606	0.9908	0.8575	0.8962	0.8438	0.9466
Micrometrics SediGraph 5100	0.9745	0.7642	0.1270	0.8680	0.9427	0.3840	0.0087	0.1983	0.9737	0.8096	0.8681	0.8498	0.9147
MIN=	0.9745	0.7507	0.1270	0.8526	0.9427	0.3840	0.0053	0.1606	0.9737	0.8096	0.8681	0.8438	0.9147
MAX=	0.9921	0.7642	0.1674	0.8680	0.9474	0.3973	0.0087	0.1983	0.9908	0.8575	0.8962	0.8498	0.9466
AVERAGE=	0.9833	0.7574	0.1472	0.8603	0.9450	0.3906	0.0070	0.1795	0.9823	0.8335	0.8822	0.8468	0.9307
Squared linear correlation coefficient [R²] for matrices with Dynamon SP-130 at w/c=0.6													
LS Particle Size Analyzer	0.5695	0.6741	0.0307	0.3144	0.2252	0.2804	0.0598	0.0213	0.7769	0.5853	0.5267	0.4765	0.5051
Micrometrics SediGraph 5100	0.5787	0.6843	0.0377	0.3269	0.2389	0.3486	0.0701	0.0252	0.8063	0.5988	0.5339	0.4484	0.5150
MIN=	0.5695	0.6741	0.0307	0.3144	0.2252	0.2804	0.0598	0.0213	0.7769	0.5853	0.5267	0.4484	0.5051
MAX=	0.5787	0.6843	0.0377	0.3269	0.2389	0.3486	0.0701	0.0252	0.8063	0.5988	0.5339	0.4765	0.5150
AVERAGE=	0.5741	0.6792	0.0342	0.3206	0.2320	0.3145	0.0649	0.0233	0.7916	0.5921	0.5303	0.4624	0.5101
												AVERAGE	
												0.6776	
												0.6680	
												AVERAGE	
												0.3881	
												0.4010	

It can be seen from Tables 4-15 and 4-16 that if D_{50} is used as a parameter to describe the filler properties the relation to the matrix rheological properties is somewhat improved (when compared to relation to specific surface), even if all the results obtained are used for the analysis. Also the results obtained by the Micrometrics Sedigraph show a lot better relation to matrix rheological properties compared to when the specific surface was used to describe the filler properties (Tables 4-10 to 4-13). The relation seems to be the best for D_{50} values obtained by the SediGraph and for the matrices prepared with Dynamon SR-N at w/c ratio of 0.6. However, none of the relations seems to be valid for all of the matrix types and the order of relation in terms of linear R^2 is only between 0.6-0.8. The same as for relation to specific surface measurements the gel strength seems to be the most promising parameter in this sense and the static yield tests tend to give us better relation to the D_{50} value than the dynamic ones. As a possible explanation here could be that some plasticizer steric hindrance effects are different when the matrices are sheared at higher rates, i.e. flowing. Or alternatively, more trivial reasons related to the measuring technique – using a model (Bingham, Herschel-Bulkley) vs. a “true” measurement depending on the accuracy of the test equipment can be thought of.

When the doubtful Hokksund and Limestone filler characterization results (see chapter 4.1) are excluded from the analysis (Tables 4-17 and 4-18) the correlation between D_{50} values and rheologic properties of the matrices is considerably improved. Now D_{50} values obtained from SediGraph and LS Particle Size Analyser indicate the same relation. Even though that in a number of cases the liner R^2 has value of higher than 0.9 we have to take into account that the amount of data points used for the analysis is quite low (=5) and that in the same way as in previous analysis (see above) Gel strength is the only parameter where the relation is independent from the w/c or SP type.

On the overall it seems that D_{50} values of the filler can give us a better indication of the rheological properties of the corresponding matrix phase than the specific surface measurements. Especially in case of the BET method, that is believed to be the most accurate with respect to describing the surface texture and “inner surface” (porosity) of the fillers. As a reason a hypothesis that particles below a certain size, surface texture and porosity do not noticeably contribute to the measured rheological properties can be proposed.

4.3 Concrete

4.3.1 Influence of different fillers

Table 4-19 shows a compilation of the determined SCC rheological parameters in an effort to analyse the effect of different fillers.

Table 4-19: Rheology, min-max (mean), of SCC

Rheology, min-max (mean)			
SP =	Dynamon SP-130		
w/V _{powder} =	1.18		1.51
w/b =	0.50	0.60	0.77
V _{filler} /V _{powder} =	0.20	0.33	0.33
Slump-flow, [mm]	395-570 (451)	465-640 (530)	495-655 (570)
τ_{01} Bingham, [Pa]	52-133 (86)	20-73 (43)	34-81 (51)
$\tau_{02} + 22$ min Bingham, [Pa]	26-341 (126)	21-74 (42)	40-98 (55)
μ_1 Bingham, [Pas]	35.30-62.78 (53.93)	24.25-47.50 (35.54)	11.34-14.77 (13.01)
$\mu_2 + 22$ min Bingham, [Pas]	37.60-65.96 (51.35)	25.29-48.03 (37.73)	11.37-14.97 (13.17)
static yield stress, [Pa]	369-862 (605)	193-437	76-144 (113)

Table 4-19 shows that the differences in SCC flow properties for different fillers seem to be of a higher order than when compared to the in rheological properties of the corresponding matrices (see Table 4-1). This is first seen by the slump-flow values that, based on some large practical experience, allow to conclude that the differences in the workability would have large practical influence on the real life concreting operations. Second of all, the values can be compared to the repeatability testing results presented in Table 3-10. According to Table 3-10 slump-flow value seems to be the measure with the lowest repeatability – the variation within 3 equal mixes has been up to 90 mm (510-600 mm). However, the results of the Bingham parameters show excellent repeatability – the yield stress τ_0 has been varying in the order of 1 Pa but the plastic viscosity for all of the three mixes is 18-23 Pa.s.

Table 4-19 also shows that the effect on SCC rheology when exchanging part of the cement with filler while solids volume Φ is kept constant is probably of the same order as varying the filler type. It is clear from Tables 3-8 and 3-9 that when cement is replaced by filler the flowability of the concrete is considerably increased. According to the filler and cement test results (see Table 2-2 and Appendix B) the specific surface of the fly ash cement is much larger than specific surface area of the tested fillers. SCC prepared with natural filler gave the best flowability as expected.

The repeated dynamic yield stress measurements show higher values at the highest age as expected. Static yield stress values are in all cases higher than the dynamic yield values. Some reasons for this being related to thixotropic rebuild, as a consequence of (reversible) coagulation of the cement particles and to the additional resistance, because of the concomitant change in particle packing, when going from zero rate of deformation state as reported by Wallevik (2003).

4.3.2 Correlation to specific surface area of the fillers

In the same manner as for the matrices relation between the measured specific surface values of the fillers (Table 2-2) and rheological properties of the SCC was analysed. Tables 4-20 and 4-21 present the results if all of the results are included in the analysis. Tables 4-22 and 4-23 hold the results if measurements from Limestone and Hokksund fillers are excluded from the correlation calculation.

Table 4-20: Correlation analysis between specific surface area of the fillers and rheological parameters of SCC with Dynamon SP-130 at $w/c = 0.5$

Correlation analysis										
Method	Fresh concrete properties		Segregation coefficient		Bingham Parameters				Static yield stress	AVERAGE
	Air content	Slump-flow	1	2	τ_{y1}	τ_{y2}	μ_1	μ_2		
	1	2	3	4	5	6	7	8	9	
	Squared linear correlation coefficient [R^2] for SCC matrices with Dynamon SP-130 at $w/c=0.5$									
Blaine	0.3055	0.3253	0.3974	0.2144	0.1835	0.0676	0.0016	0.0416	0.3344	0.2079
BET	0.0015	0.0832	0.1130	0.2102	0.2099	0.4253	0.0087	0.0695	0.0238	0.1272
LS Particle Size Analyzer	0.3202	0.4312	0.1387	0.0084	0.0249	0.0245	0.0001	0.0053	0.2416	0.1328
Micrometrics SediGraph 5100	0.2275	0.2847	0.0822	0.0497	0.0452	0.0060	0.0193	0.0065	0.4368	0.1287
MIN=	0.0015	0.0832	0.0822	0.0084	0.0249	0.0060	0.0001	0.0053	0.0238	
MAX=	0.3202	0.4312	0.3974	0.2144	0.2099	0.4253	0.0193	0.0695	0.4368	
AVERAGE=	0.2137	0.2811	0.1828	0.1207	0.1159	0.1309	0.0074	0.0307	0.2591	

Table 4-21: Correlation analysis between specific surface area of the fillers and rheological parameters of SCC with Dynamon SP-130 at w/c=0.6 and 0.77

Correlation analysis											
Method	Fresh concrete properties		Segregation coefficient		Bingham Parameters				Static yield stress	AVERAGE	
	Air content	Slump-flow	1	2	τ_{y1}	τ_{y2}	μ_1	μ_2			
	1	2	3	4	5	6	7	8	9		
Squared linear correlation coefficient [R ²] for SCC matrices with Dynamon SP-130 at w/c=0.6										AVERAGE	
Blaine	0.0208	0.0714	0.4655	0.2167	0.0175	0.0024	0.0182	0.0530	0.0765		0.1047
BET	0.2788	0.0895	0.0654	0.0293	0.2035	0.4724	0.0841	0.0874	0.0270		0.1486
LS Particle Size Analyzer	0.0000	0.0607	0.6224	0.0460	0.0003	0.0370	0.2490	0.2965	0.2920		0.1782
Micrometrics SediGraph 5100	0.1814	0.2772	0.6931	0.2462	0.1480	0.0172	0.3243	0.4539	0.5577		0.3221
MIN=	0.0000	0.0607	0.0654	0.0293	0.0003	0.0024	0.0182	0.0530	0.0270		AVERAGE
MAX=	0.2788	0.2772	0.6931	0.2462	0.2035	0.4724	0.3243	0.4539	0.5577		
AVERAGE=	0.1202	0.1247	0.4616	0.1346	0.0923	0.1322	0.1689	0.2227	0.2383		
Squared linear correlation coefficient [R ²] for SCC matrices with Dynamon SP-130 at w/c=0.77											AVERAGE
Blaine	0.3703	0.1159	0.0000	0.3427	0.0432	0.0346	0.1647	0.0178	0.0016		
BET	0.1040	0.3061	0.7151	0.2813	0.5189	0.7232	0.2161	0.1031	0.1719	0.3489	
LS Particle Size Analyzer	0.2071	0.1641	0.0075	0.4022	0.2248	0.2093	0.1750	0.0460	0.0493	0.1650	
Micrometrics SediGraph 5100	0.4497	0.0492	0.0172	0.1381	0.0109	0.0194	0.0196	0.0336	0.0223	0.0844	
MIN=	0.1040	0.0492	0.0000	0.1381	0.0109	0.0194	0.0196	0.0178	0.0016	AVERAGE	
MAX=	0.4497	0.3061	0.7151	0.4022	0.5189	0.7232	0.2161	0.1031	0.1719		
AVERAGE=	0.2828	0.1588	0.1850	0.2911	0.1995	0.2466	0.1438	0.0501	0.0613		

Table 4-22: Correlation analysis between specific surface area of the fillers and rheological parameters of SCC with Dynamon SP-130 at w/c =0.5 (excluding Hokksund and Limestone filler results)

Correlation analysis											
Method	Fresh concrete properties		Segregation coefficient		Bingham Parameters				Static yield stress	AVERAGE	
	Air content	Slump-flow	1	2	τ_{y1}	τ_{y2}	μ_1	μ_2			
	1	2	3	4	5	6	7	8	9		
Squared linear correlation coefficient [R ²] for SCC matrices with Dynamon SP-130 at w/c=0.5										AVERAGE	
Blaine	0.1264	0.2183	0.2363	0.4590	0.0883	0.2683	0.0298	0.2460	0.1185		0.1990
BET	0.1629	0.0126	0.3079	0.4283	0.1813	0.7788	0.0844	0.0054	0.6437		0.2895
LS Particle Size Analyzer	0.0415	0.2281	0.0004	0.7799	0.0631	0.2516	0.0826	0.3958	0.0741		0.2130
Micrometrics SediGraph 5100	0.0005	0.0402	0.0735	0.3823	0.0006	0.4559	0.0000	0.0712	0.3655		0.1544
MIN=	0.0005	0.0126	0.0004	0.3823	0.0006	0.2516	0.0000	0.0054	0.0741		AVERAGE
MAX=	0.1629	0.2281	0.3079	0.7799	0.1813	0.7788	0.0844	0.3958	0.6437		
AVERAGE=	0.0828	0.1248	0.1545	0.5124	0.0833	0.4387	0.0492	0.1796	0.3004		

Table 4-23: Correlation analysis between specific surface area of the fillers and rheological parameters of SCC with Dynamon SP-130 at w/c=0.6 and 0.77 (excluding Hokksund and Limestone filler results)

Correlation analysis										
Method	Fresh concrete properties		Segregation coefficient		Bingham Parameters				Static yield stress	AVERAGE
	Air content	Slump-flow	1	2	τ_{y1}	τ_{y2}	μ_1	μ_2		
	1	2	3	4	5	6	7	8	9	
Squared linear correlation coefficient [R^2] for SCC matrices with Dynamon SP-130 at w/c=0.6										AVERAGE
Blaine	0.1071	0.1074	0.6812	0.1950	0.1204	0.3322	0.2466	0.1755	0.1886	0.2393
BET	0.1762	0.2006	0.0011	0.2635	0.0251	0.0333	0.2663	0.3797	0.4575	0.2004
LS Particle Size Analyzer	0.1352	0.1702	0.1663	0.1836	0.3965	0.7409	0.0424	0.0460	0.0490	0.2145
Micrometrics SediGraph 5100	0.5993	0.1157	0.0326	0.7228	0.1340	0.0012	0.0233	0.1076	0.2379	0.2194
MIN=	0.1071	0.1074	0.0011	0.1836	0.0251	0.0012	0.0233	0.0460	0.0490	AVERAGE
MAX=	0.5993	0.2006	0.6812	0.7228	0.3965	0.7409	0.2663	0.3797	0.4575	
AVERAGE=	0.2544	0.1485	0.2203	0.3412	0.1690	0.2769	0.1446	0.1772	0.2333	
Squared linear correlation coefficient [R^2] for SCC matrices with Dynamon SP-130 at w/c=0.77										AVERAGE
Blaine	0.0441	0.3676	0.5527	0.5513	0.2790	0.4738	0.4640	0.0940	0.0660	0.3214
BET	0.0178	0.0576	0.5022	0.1291	0.0628	0.0376	0.1965	0.5213	0.2940	0.2021
LS Particle Size Analyzer	0.0598	0.6075	0.8308	0.9110	0.4408	0.8122	0.0911	0.0018	0.1225	0.4308
Micrometrics SediGraph 5100	0.1420	0.1066	0.1132	0.0412	0.2088	0.0157	0.0684	0.6246	0.2540	0.1749
MIN=	0.0178	0.0576	0.1132	0.0412	0.0628	0.0157	0.0684	0.0018	0.0660	AVERAGE
MAX=	0.1420	0.6075	0.8308	0.9110	0.4408	0.8122	0.4640	0.6246	0.2940	
AVERAGE=	0.0659	0.2848	0.4997	0.4082	0.2479	0.3348	0.2050	0.3104	0.1841	

As it can be seen from Tables 4-21 to 4-23, no direct relation between specific surface areas of the fillers used and fresh SCC characteristics seem to exist and some of the promising squared linear correlation coefficients R^2 determined are most probably of an accidental character. This is opposite to what was observed in efforts of relating the specific surface of the filler to rheological properties of the corresponding matrices where much better relation was observed. This would only emphasize that concrete and matrix are two very different particle suspension systems. Meaning that properties of fresh concrete are and matrix might be dominated by different forces and thus be related to different filler properties.

In the same way as for the matrix mixes (see chapter 4.2.5), efforts were made to relate the fresh SCC properties to median particle size D_{50} of the fillers. However, this did not improve the correlation like in case of the matrices. Results of this correlation analysis are presented in Appendix G.

4.4 Correlation between concrete and matrix rheology

Relationship between concrete and matrix rheology is reported to be a very complex subject (Pedersen 2004) and still not completely investigated. Even though it is clear that when the Particle-Matrix proportioning model is used a variation in the yield stress (consistency) of matrix gives a large effect on concrete workability at constant aggregate composition and volume fraction especially if the concrete is “matrix dominated” as in the case of SCC (Mørtzell 1996, Smepllass and Mørtzell 2001, Pedersen 2004, Hammer and Wallevik 2005).

Several authors have tried to study the hypothesis that there is a direct correlation between yield stress (consistency) of matrix and concrete workability (Smepllass and Mørtzell 2001, Hammer and Wallevik 2005, Cepuritis 2011). However, the hypothesis has not been confirmed. Smepllass and Mørtzell (2001) studied the applicability of the Particle-Matrix model to self-compacting concrete and the relationship between the rheology of the matrix phase and the workability of the corresponding concrete. Some uncertainties on the matrix phase characterization were later verified by Hammer and Wallevik (2005). Their results indicated that a given matrix consistency does not always give one and the same independent mortar or concrete consistency, for the given particle phase. Hammer and Wallevik (2005) suggest that it is expected the correlation to improve when cement particles are well dispersed or when the matrix contains coarser particles.

Pedersen (2004) has also studied the relationship between the rheological properties of the matrix phase with different fillers and the corresponding self-compacting concrete. The studies indicated that the yield-stress of the matrix phase has a crucial effect on the slump-flow measure. No straightforward correlation between the rheological properties of self-compacting concrete and the corresponding matrix phase was found. Pedersen (2004) suggests considering studies on rheological properties of the matrix phase useful to gain fundamental knowledge regarding the effect of different constituents. Pedersen (2004) also points out that matrix rheology testing may to some extent be useful to predict the effects in self-compacting concrete, but the limitations should be kept in mind when using matrix rheology to predict the behaviour of a given constituent in concrete.

Cepuritis (2011) investigated relationship between the rheological properties of concrete prepared with 100% crushed aggregates and the corresponding matrix phases. He came to the same conclusions as Pedersen (2011).

Even though the previous attempts have been unsuccessful efforts were made to relate concrete and matrix rheological parameters determined within this study. Correlation between Bingham yield stress and dynamic yield values of the corresponding matrices is presented on Figures 4-16 and 4-17 but relation of the fresh concrete static yield stress to the static yield values of the matrices on Figures 4-18 and 4-19. Relation of the SCC viscosity to the viscosity of the corresponding matrices is illustrated on Figures 4-20 and 4-21.

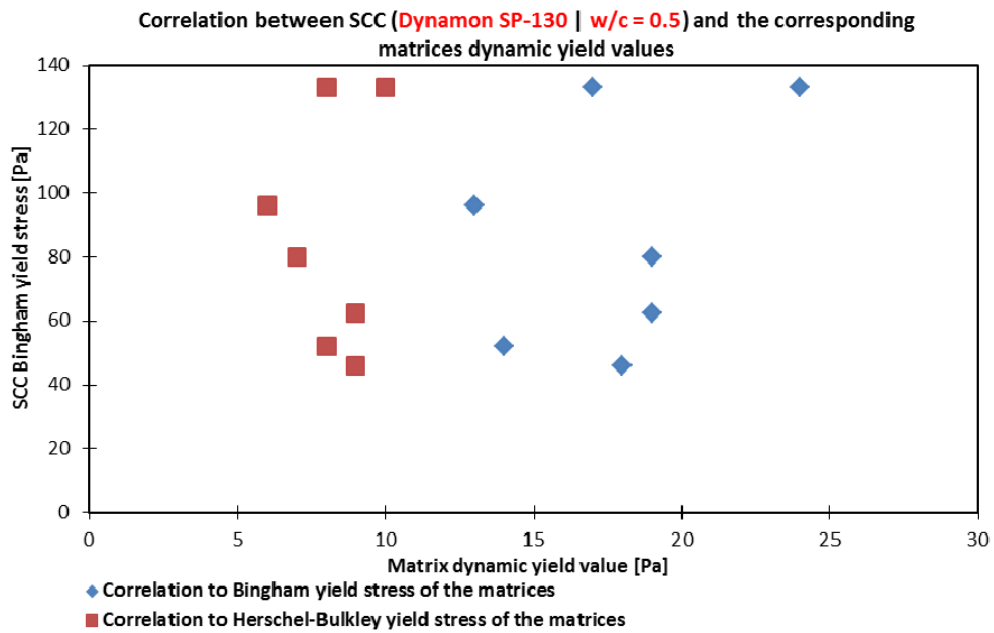


Fig. 4-16: Correlation between SCC (Dynamon SP-130 | w/c=0.5) Bingham yield stress and corresponding dynamic yield values of matrices

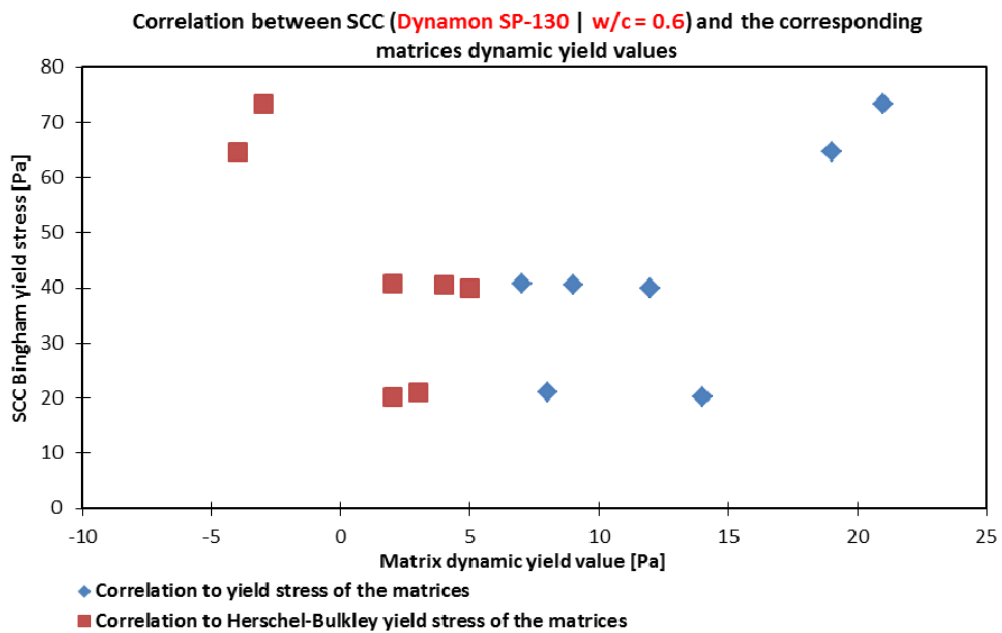


Fig. 4-17: Correlation between SCC (Dynamon SP-130 | w/c=0.6) Bingham yield stress and corresponding dynamic yield values of matrices

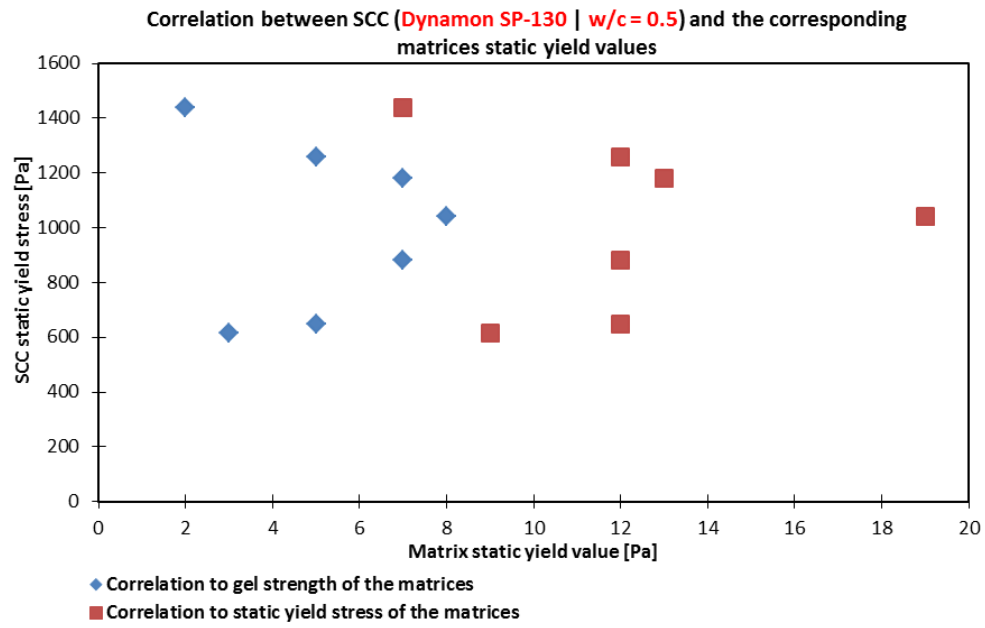


Fig. 4-18: Correlation between SCC (Dynamon SP-130 | w/c=0.5) and the corresponding matrices static yield values

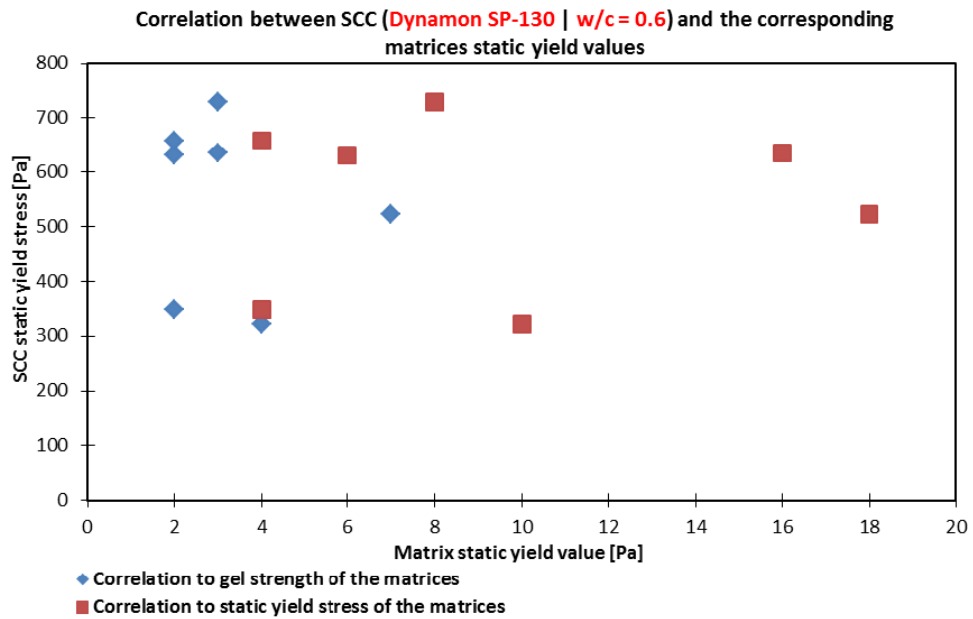


Fig. 4-19: Correlation between SCC (Dynamon SP-130 | w/c=0.5) and the corresponding matrices static yield values

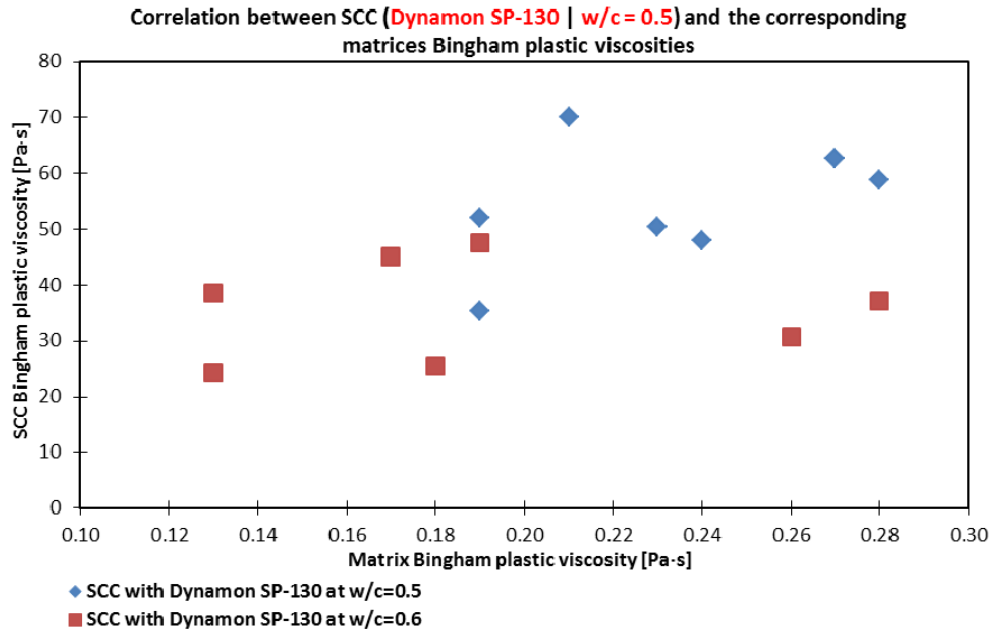


Fig. 4-20: Correlation between SCC and the corresponding matrices Bingham plastic viscosities

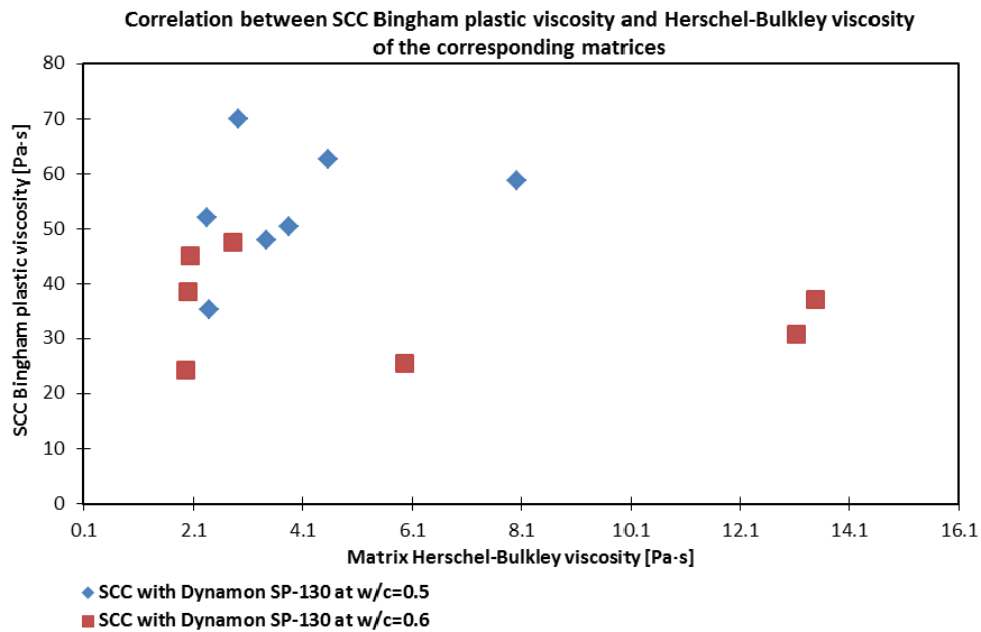


Fig. 4-21: Correlation between SCC Bingham plastic viscosity and Herschel-Bulkley viscosity of the corresponding matrices

Correlation analysis presented on Figures 4-16 to 4-21 indicate that no simple and straight forward relation between concrete and matrix rheological parameters can be found. This agrees with the previous research done (Smeplass and Mørtzell 2001, Pedersen 2004, Hammer and Wallevik 2005, Cepuritis 2011). Thus matrix rheology studies at the moment should more likely be considered useful only to gain fundamental knowledge regarding the effect of different constituents as suggested by Pedersen (2004) and Cepuritis (2011). The knowledge of the relation between concrete and matrix rheology needs to be extended by further research in order to use matrix rheological parameters to predict behaviour of fresh concrete. This means that a distinction between research on matrix and concrete rheology must be made when planning further experiments. Matrix studies, as suggested above, can be considered relevant for more fundamental studies of interaction between fines (fillers, cements etc.) and admixtures with respect to overall effect on rheology and to obtain more knowledge on what other (except

specific surface) main parameters of the filler actually are important for choice of micro-proportioning (size, moisture adsorption, admixture adsorption, shape, packing etc.). On the other hand, concrete rheology studies should be chosen when studies with more practical and of a direct industrial meaning must be conducted. The above mentioned distinction, however, does not exclude that further research should also be carried out to get better understanding of the actual relation between the characteristics of fresh matrix and concrete.

4.5 Summary and concluding discussion

The research carried out within this study is a strong foundation in order to fully understand the interaction between different types of mineral fillers and admixtures one hand and rheological properties of cement based particle suspensions such as matrix and concrete on the other. However, based on the results so far it's still more new questions than answers.

First, it is rather clear that most of the available mineral particle characterization methods give very different results. The amount of mineral particle characterization studies is rather limited especially if this is to be related to the properties of a cement based suspensions. Most of the authors choose only one surface area determination method. In most of the cases this is the very simple Blaine or the much more advanced BET methods. According to this study all of the four used methods can give questionable results and it is still a challenge to explain why certain approaches give such a different values. Mineral composition of the tested fines was proposed as a reason for some strange results of the specific surface measurements. Thus thin-section studies of the filler mineralogical composition as well as SEM analysis is strongly recommend to be carried out as the next step to get better understanding of the topic. Then the results of those analyses have to be looked at in the light of the specific surface area determination methodology. Separate attention must be paid to topics like adsorption of nitrogen (N_2) and water (H_2O) on the surface of the mineral fillers.

The obtained results confirmed that it is possible to some extent relate the rheological differences of matrices to the specific surfaces of the fillers used to mix them. This seems to also be true for the structural regeneration and decomposition of the matrices. The results indicated that the higher the filler specific surface area the longer time it takes in order to reach a certain regeneration of matrix structural strength after decomposition at high shear conditions. LS Particle Size Analyser that uses laser diffraction angles in order to determine the PSD of fines was proven to express the specific surfaces of the fillers in a way that was the best related to the rheological parameters of the matrix. While a static yield value – gel strength that was determined by controlled stress (0.5 to 250 Pa in logarithmic steps) was indicated as the most relevant parameter that can be related to the specific surface of the fillers independent on the quality of the matrix with the respect to SP type and w/b ratio. The natural filler gave the best flowability of the matrix and concrete as expected.

When the filler particle size distribution was described by other means than the specific surface area, i.e. the mean particle diameter D_{50} the relation to the rheological properties of matrix was improved. However, it still stayed to some extent limited to the w/b ration and the SP type. Thus we would have to assume that other properties than the specific surface can be used to better describe the particle phase. This also indicates that very fine particles below a certain size, surface texture and porosity of the fillers might not noticeably contribute to the rheological properties of the matrix. Packing measurements of the whole particle composition (=cement+filler) would be recommended for further studies as it can then be expressed as the maximum packing value Φ/Φ_{max} that is known to be a fundamental parameter governing the rheological properties of suspensions (Barnes, Hutton and Walters 1989). It is also known to be related to the specific surface area of the particles.

The variation of a filler type seems to change the rheology and thixotropy of a matrix by approximately the same order as if one superplasticizer is exchanged by another – with the

condition that the admixtures are of a different type. For example if the length of the polymer molecule side chains and solid volume concentration is considerably varying as within this study. Furthermore when the fly ash cement was partly replaced by the coarser fillers (while keeping the total particle volume fraction constant) the flow of the matrices and SCC was greatly improved. However, the matrix and concrete rheology seem to have no simple relation even it is often stated to be like that for the “matrix-dominated” mixes like SCC. Thus a clear distinction must be made when designing a new research plan. It is proposed to use matrix rheology for more fundamental studies and concrete rheology when studies for a direct industrial application are carried out. This shouldn't exclude research in order to further understand the relation between matrix and concrete properties.

Some of the determined matrix rheological parameters turned out to be strongly dependent on the used test method. This was due to the unexpectedly high effect from the shear history of the samples since a comparably very long (=29.5 min) test sequence was used. This caused all of the samples show negative “thixotropy” or rheopexic behaviour, i.e. the shear values of the down flow curves were falling below the up curves. This is opposite to what has been experienced before and what was determined by the structural regeneration and decomposition experiments. Some evidence exists that this could be as a time dependent effect of oscillatory test which was run prior to flow curve. This means that one should be very careful when designing a test sequence and perhaps it is not a good practice to incorporate a lot of parameters in one cycle.

5. Conclusions

Most of the widely available fine mineral particle characterization methods give different and questionable results and it is still a challenge to explain why certain approaches give such a different values. Mineral composition of the tested fines was proposed as a reason for some strange results of the specific surface measurements.

The obtained results confirmed that it is possible to some extent relate the rheological differences of matrices to the specific surfaces of the fillers used to mix them. This seems to also be true for the structural regeneration and decomposition of the matrices. The results indicated that the higher the filler specific surface area the longer time it takes in order to reach a certain regeneration of matrix structural strength after decomposition at high shear conditions. The type of the superplasticizer also seemed to affect the regeneration.

LS Particle Size Analyser that uses laser diffraction angles in order to determine the PSD of fines was proven to express the specific surfaces of the fillers in a way that was the best related to the rheological parameters of the matrix. While a static yield value – gel strength that was determined by controlled stress (0.5 to 250 Pa in logarithmic steps) was indicated as the most relevant parameter that can be related to the specific surface of the fillers independent on the quality of the matrix with the respect to SP type and w/b ratio.

When the filler particle size distribution was described by other means than the specific surface area, i.e. the mean particle diameter D_{50} the relation to the rheological properties of matrix was improved. However, it still stayed to some extent limited to the w/b ration and the SP type. Thus we would have to assume that other properties than the specific surface can be used to better describe the particle phase. This also indicates that very fine particles below a certain size, surface texture and porosity of the fillers might not noticeably contribute to the rheological properties of the matrix.

The variation of a filler type seems to change the rheology and thixotropy of a matrix by approximately the same order as if one superplasticizer is exchanged by another – with the condition that the admixtures are of a different type. For example, if the length of the polymer molecule side chains and solid volume concentration is considerably varying as within this study. Furthermore when the fly ash cement was partly replaced by the coarser fillers (while keeping the total particle volume fraction constant) the flow of the matrices and SCC was greatly improved. The natural filler gave the best flowabilty of the matrix and concrete as expected.

The rheological properties of matrix and concrete seem to have no simple relation even it is often stated to be like that for the “matrix-dominated” mixes like SCC. Thus a clear distinction must be made when designing a new research plan. It is proposed to use matrix rheology for more fundamental studies and concrete rheology when studies for a direct industrial application are carried out.

Some of the determined matrix rheological parameters turned out to be strongly dependent on the used test method. This means that one should be very careful when designing a test sequence and perhaps it is not a good practice to incorporate a lot of parameters in one cycle.

Herschel-Bulkley (H-B) model gave the best flow curve fit ($R^2 = 0.995-0.995$) compared to the Bingham model ($R^2 = 0.924-0.958$) for the matrices due to shear thinning. On the other hand this often gave negative yield stress so the H-B model is probably not applicable to describe the dynamic yield.

6. Further research needs

The following topics are of interest for further research and development:

- The questions raised within the study regarding the different fine mineral particle characterization methods must be answered. In particular the effect of mineral composition and grain surface texture on the measurements carried out with Flowsorb II 2300 nitrogen absorption by BET-method is thought to give some answers. Thus thin-section studies of the filler mineralogical composition as well as SEM analysis are strongly recommended to be carried out as part of the future studies.
- Since the specific surface area of the mineral fines can't be used as a single factor affecting the rheology of filler modified paste, different parameter/-s must be found. Packing measurements of the whole particle composition (=cement+filler) would be recommended for further studies as it can then be expressed as the maximum packing value Φ/Φ_{\max} that is known to be a fundamental parameter governing the rheological properties of suspensions (Barnes, Hutton and Walters 1989). It is also known to be related to the specific surface area of the particles.
- A new approach of measuring the stability of matrix/ paste was discussed in this paper (see chapter 4.2.4). However, matrices tested within the study were designed in order to produce very stable mixes what was achieved. Thus it was not possible to fully investigate the applicability of the described test method. It is recommended to carry out a separate study with wider variety (with respect to the stability) of the tested mixes in order to understand if the used approach can be applied.
- The results of the study have once again emphasized that, even though the Particle-Matrix model has proven to show excellent applicability for concrete mix design and has been used by practitioners by more than a decade, the understanding of how to relate the rheological properties of matrix and concrete is still weak. Thus further research on this topic is still necessary.

7. References

- American Society for Testing and Materials, 2011. ASTM C33 / C33M – 11 Standard Specification for Concrete Aggregates. Pennsylvania: ASTM.
- American Concrete Institute (ACI) Committee 552, 2010. ACI 522R-10 *Report on Pervious Concrete*. Farmington Hills: ACI.
- Bager, D.H., Geiker, M.R., and Jensen, R.M, 2001. Rheology of self-compacting mortars, influence of particle packing. *Nordic Concrete Research*, 26, pp. 1-16.
- Banfil, P. F. G., 1994. *Rheological methods for assessing the Flow Properties of Mortar and Related Materials*. Construction and Building Materials, 8 (1), pp. 43-50.
- Barnes, H.A, Hutton, J.F. and Walters, K., 1989. *An Introduction to Rheology*, Amsterdam: Elsevier Science.
- Berg, S.A. and Jacobsen, S., 2010. Packing and Aggregate/Fibre – Void Saturation to Proportion Self-Compacting Fibre Reinforced Concrete. In: *Second International Conference on Sustainable Construction Materials and Technologies*. Ancona, Italy 28th-30th June 2010. Ancona: Università Politecnica delle Marche.
- Bigas, J.P. and Gillias, J.L., 2002. Effect of fine mineral additions on granular packing of cement mixtures. *Magazine of Concrete Research*. V. 54., 3, pp. 155-164.
- Billberg, P., 2006. *Form Pressure Generated by Self-Compacting Concrete – Influence of Thixotropy and Structural Behaviour at Rest*. Ph. D. School of Architecture and Built Environment Division of Concrete Structures, Royal Institute of Technology.
- Carman, P. C., 1938. The determination of the specific surface of powders I. *Journal of the Society of Chemical Industry*, 57, pp. 225-234.
- Cepuritis, R., 2011. *Effects of Concrete Aggregate Crushing on Rheological Properties of Concrete and Matrix*. Master thesis. Norwegian University of Science and Technology.
- Colleparidi, M., 1971. The rheological behaviour of cement pastes. *Il Cemento*, 68, pp. 99-106.
- Danielsen, S.W., 2008. Concrete aggregates from crushed hard rock - why, - where, - how? In: Wigum, B.J. ed, 2008. *Manufactured sand – Workshop, Stavanger, Norway, October 30th and 31st 2008. Summary of Presentations*. Trondheim: SINTEF.
- De Larrard, F., 1999. *Concrete mixture proportioning: a scientific approach*. London, E & FN Spon.
- Erdem, T.K., Khayat, K.H. and Yahia, A., 2009. Correlation of Self-Consolidating Concrete to Corresponding Concrete-Equivalent Mortar. *ACI Materials Journal*, V. 106, 2 (March-April), pp. 154-160.
- Esping, O., 2004. Rheology of cementitious materials: Effects of geometrical properties of filler and fine aggregates. Licentiate thesis. Chalmers University of Technology.
- Esping, O., 2008. Effect of limestone filler BET(H₂O)-area on the fresh and hardened properties of self-compacting concrete. *Cement and Concrete Research*, 38, pp. 938-944.

European Committee for Standardization, 2002. EN 12620:2008 *Aggregates for concrete*. Brussels: CEN.

European Committee for Standardization, 2007. EN 480-1:2008 *Admixtures for concrete, mortar and grout - Test methods - Part 1: Reference concrete and reference mortar for testing*. Brussels: CEN.

European Committee for Standardization, 2009. EN 12350-7:2010 *Testing fresh concrete - Part 7: Air content - Pressure methods*. Brussels: CEN.

European Committee for Standardization, 2009. EN 12350-6:2010 *Testing fresh concrete - Part 6: Density*. Brussels: CEN.

European Committee for Standardization, 2010. EN 12350-8:2010 *Testing fresh concrete - Part 8: Self-compacting concrete - Slump-flow test*. Brussels: CEN.

Ferraris C.F., Obla K. H. and Hill R., 2001. The influence of mineral admixtures on the rheology of cement paste and concrete. *Cement and Concrete Research*, V. 31, pp 245-255.

Fuller, W. and Thompson, S. E., 1907. The laws of proportioning concrete. *Transactions of the American Society of Civil Engineers. Paper no 1053*, pp 67-143.

Féret, R., 1892. Sur la compacité des mortiers hydrauliques, *Annales des Ponts et Chaussées*, Série 7, vol. 4, pp. 5-164 (in French).

Glavind, M., Olsen, G. S. and Munch-Petersen, C., 1993. Packing calculations and concrete mix design. *Nordic Concrete Research*, 13, pp. 21-34.

Géber, R. and Gömze, L.A, 2010. Characterization of mineral materials as asphalt fillers. *Materials Science Forum*, vol. 659, pp. 471-476.

Hammer, T.A. and Wallevik, J.E., 2005. On the Correlation Between Rheology of Paste, Mortar and Concrete. In: *Proceedings of the Second North American Conference on the Design and Use of Self-Consolidating Concrete (SCC) and the Fourth International RILEM Symposium on Self-Compacting Concrete*. Chicago: Hanley Wood Publication.

Hotvedt, O., 2009. Manufactured sand – Two cases; The Concrete Dam; “Førrevassdammen”, 1982-1986 & Norsk Stein 1993. In: Wigum, B.J. ed, 2008. *Manufactured sand – Workshop, Stavanger, Norway, October 30th and 31st 2008. Summary of Presentations*. Trondheim: SINTEF.

Jacobsen, S., Haugan, L. C. and Arntsen, B., 2005. Developing Ultra High Performance Concrete for Concrete Products. In: Kanstad T. and Hansen E. A., eds., *Proceedings of XIX Nordic Concrete Research Symposium*. Sandefjord, Norway 13th-15th June 2005.

Jacobsen, S. and Arntsen, B., 2008. Aggregate packing and – void saturation in mortar and concrete proportioning. *Materials and Structures*, 41, pp. 703-716.

Lyse, I., 1932. Test on consistency and strength of concrete having constant water content. In: *Proc. ASTM Vol. 32*, pp. 629-636.

Mezger, T. G., 2006. *The rheology handbook: for users of rotational and oscillatory rheometers*. Amsterdam: Elsevier Science.

- Mørtzell, E., 1996. *Modelling the effect of concrete part materials on concrete consistency*. Ph. D. Norwegian University of Science and Technology (in Norwegian).
- Nehdi, M., Mindess, S. and Aitcin, P.C., 1997. Statistical modelling of the microfiller effect on the rheology of composite cement pastes. *Advances in Cement Research*, V. 9, pp. 37-46.
- Pedersen, B., 2004. *Alkali-reactive and inert fillers in concrete. Rheology of fresh mixtures and expansive reactions*. Ph. D. Norwegian University of Science and Technology.
- Powers, T.C., 1968. *Properties of fresh concrete*. New York: John Wiley & Sons.
- Roussel, N., 2006. A theoretical frame to study stability of fresh concrete. *RILEM Materials and Structures*, 41, pp. 75-83.
- Smeplass, S. and Mørtzell, E., 2001. The particle matrix model applied on SCC. In: The University of Tokyo, *Second international symposium on self-compacting concrete*. Tokyo: University of Tokyo.
- Vikan, H. and Jacobsen, S., 2010. *Influence of rheology on the pumpability of mortar. COINProject report 21 – 2010*. Trondheim: SINTEF.
- Vikan, H., 2005. *Rheology and reactivity of cementitious binders with plasticizers*. Ph. D. Norwegian University of Science and Technology.
- Wallevik, J., 2003a. *Rheology of Particle Suspensions. Fresh Concrete, Mortar and Cement Paste with Various Types of Lignosulfonates*. Ph. D. Norwegian University of Science and Technology.
- Westerholm, M., 2006. *Rheology of the Mortar Phase of Concrete with Crushed Aggregate*, Licentiate thesis. Luleå University of Technology.
- Wigum, B.J., Danielsen, S.W. eds., Hotvedt, O. and Pedersen, B., 2009. *Production and utilisation of manufactured sand. COIN Project report 12 – 2009*. Trondheim: SINTEF.
- Wigum, B.J., 2010. *Classification and particle properties of fine aggregates*. Trondheim: NTNU.
- Zhang, X, Han, J., 2000. The effect of ultra-fine admixture on the rheological property of cement paste. *Cement and Concrete Research*, V. 30, pp. 827-830.

APPENDIX A – Example Calculation for Surface Area of Filler

In the following (Table A-1) a numerical example of specific surface calculation (using LS Particle Size Analyzer results as an input) for one of the fillers (Limestone) is given.

Table A-1: Example calculation for specific surface area of limestone filler

A	B	C	D	E	F	G	H	I	J	K					
Measuring method	Sieve aperture size, mm	Cumulative % passing	Percent passing among two sieves	Amount of 1 kg of sand passing among two sieves, kg	Volume passing among two sieves, m ³	Average diameter D _i , m	Volume of one particle, m ³	No. of particles	Surface area of one particle, m ²	Specific surface area m ² /kg					
				2740	Particle density, kg/m ³										
											1 x D/100	E/ρ	mean size	πD _i ³ /6	F/H
LS Particle Size Analyzer	0.125	100.00	6.2	0.0620	2.26E-05	1.13E-04	7.46E-13	3.04E+07	3.98E-08	1.21					
	0.100	93.80	3.6	0.0360	1.31E-05	9.00E-05	3.82E-13	3.44E+07	2.54E-08	0.88					
	0.080	90.20	6.4	0.0640	2.34E-05	7.00E-05	1.80E-13	1.30E+08	1.54E-08	2.00					
	0.060	83.80	11.6	0.1160	4.23E-05	5.00E-05	6.54E-14	6.47E+08	7.85E-09	5.08					
	0.040	72.20	20.1	0.2010	7.34E-05	3.00E-05	1.41E-14	5.19E+09	2.83E-09	14.67					
	0.020	52.10	17.2	0.1720	6.28E-05	1.50E-05	1.77E-15	3.55E+10	7.07E-10	25.11					
	0.010	34.90	12.8	0.1280	4.67E-05	7.50E-06	2.21E-16	2.11E+11	1.77E-10	37.37					
	0.005	22.10	17.2	0.1715	6.26E-05	3.00E-06	1.41E-17	4.43E+12	2.83E-11	125.18					
	0.001	4.95	3.0	0.0300	1.09E-05	7.50E-07	2.21E-19	4.96E+13	1.77E-12	87.59					
	0.001	1.95	2.0	0.0195	7.12E-06	2.50E-07	8.18E-21	8.70E+14	1.96E-13	170.80					
		Σ=	100.0	1.0					Σ=	469.90					

APPENDIX B – Material data sheets

Natural “low-filler” sand 0/8 mm from Årdal quarry (NorStone AS)

Particle density: 2650 kg/m³;

Saturated-surface-dry water absorption: 0.3%;

Please see figure B-1 for particle size distribution of the aggregate.

Crushed coarse aggregate 8/16 mm from Årdal quarry (NorStone AS)

Particle density: 2650 kg/m³;

Saturated-surface-dry water absorption: 0.3%;

Please see figure B-1 for particle size distribution of the aggregate.

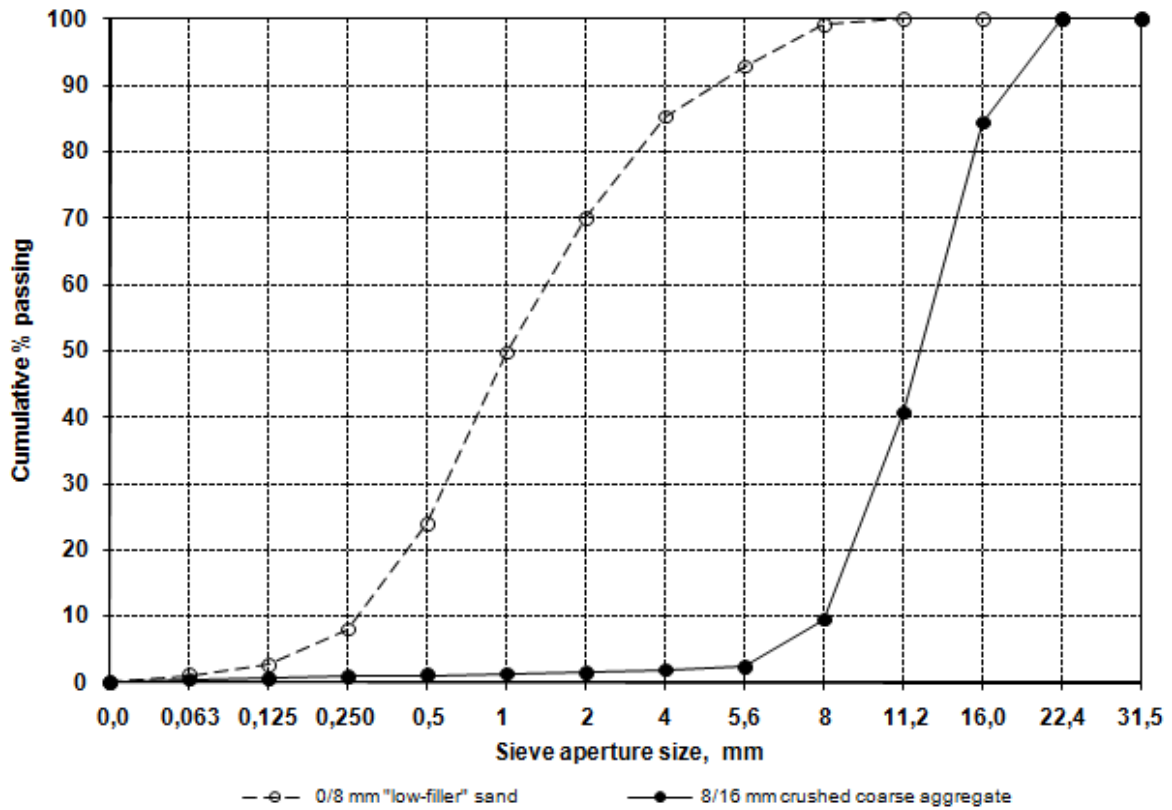


Fig. B-1: Particle size distribution of the aggregates used for the study

Portland cement of type CEM II/A-V from Norcem AS

The test report of the cement batch used for the study is presented on Figure B-2.

PRØVNINGSRAPPORT	
Oppdragsgiver:	KOK
Prøven merket:	STD FA sement fra Rescon Mapei
Prøve kode:	AZ15-11
	Ref: 71-11
KJEMISK ANALYSE EN 196-2	FYSIKALSK PRØVNING EN 196
Glødetap	2.04 %
Fri kalk	1.26 %
Flyveaske	18.20 %
Svovel trioksyd (SO ₃)	3.41 %
Silika (SiO ₂)	25.57 %
Aluminiumoksyd (Al ₂ O ₃)	8.40 %
Jernoksyd (Fe ₂ O ₃)	4.06 %
Kalsiumoksyd (CaO)	52.32 %
Magnesiumoksyd (MgO)	2.45 %
Fosfor pentoksyd (P ₂ O ₅)	0.27 %
Kaliumoksyd (K ₂ O)	1.11 %
Natriumoksyd (Na ₂ O)	0.56 %
Alkali	1.29 %
	FINHET
	Partikkelanalyse +90my 0.1 %
	" " +64my 1 %
	" " -24my 77.6 %
	" " -30 my 85.1 %
	Spesifikk overflate; Blaine 503 m²/kg
	NORMAL KONSISTENS
	Vannbehov - %
	VOLUMBESTANDIGHET
	Le Chatelier - mm
	BINDETIDER
	Størkning begynt - min.
	TRYKKFASTHET
	1 døgn - MPa
	2 døgn - MPa
	7 døgn - MPa
	28 døgn - MPa
Norcem A.S Brevik, Sement- og betonglaboratoriet, 4. july 2011	
ae.	_____ Laboratoriesjef

Fig. B-2: Test report of the cement batch used for the study

Superplasticizer Dynamon SP-130 from Rescon Mapei AS

Dynamon SP-130 is a high performance superplasticizing admixture based on modified acrylic polymers. Please see figure B-3 for technical specifications.


TEKNISKE SPESIFIKASJONER		
Produktspesifikasjoner		
Form:		Væske
Farge:		Gulbrun
Viskositet (Brookfield Viscometer DV-1, LV1, 100rpm ved 20±2°C)		Lettflytende; < 30 cP
Tørrestoffinnhold, %:		30 ± 1,5
Spesifikk vekt, g/cm ³ :		1,09 ± 0.02
pH-verdi:		6,5 ± 1
Kloridinnhold, %:		< 0,01
Alkaliinnhold (Na ₂ O-ekvivalenter), %:	< 2,5	
Bruksegenskaper i betong		
Som vannreducerer (lik konsistens)		
Sementmengde, kg/m ³ (CEM I):	350	350
Tilsetningsmengde (i % av sementvekt):	0	0,6
Masseforhold	0,59	0,43
% vannreduksjon		27
Konsistens, mm		
- synkmål, 5 min	220	230
- synkmål, 30 min	200	200
Trykkfasthet, 1 døgn	18	25
Trykkfasthet, 7 døgn	38	58
Trykkfasthet, 28 døgn	50	73

Fig. B-3: Technical specifications of Dynamon SP-130 from Rescon Mapei AS

Superplasticizer Dynamon SR-N from Rescon Mapei AS

Dynamon SR-N is a high performance superplasticizing admixture based on modified acrylic polymers. Please see figure B-4 for technical specifications.


TECHNICAL SPECIFICATIONS			
Form:		Liquid	
Colour:		Yellowish brown	
Viscosity (Brookfield Viscometer DV-1, LV1, 100rpm at 20±2°C):		Low viscosity;<30 cP	
Dry solids content, %:		19.5 ± 1.0	
Density, g/cm ³ :		1.05 ± 0.02	
pH-value:		6.5 ± 1	
Chloride content, %:		< 0.01	
Alkali content (equiv. Na ₂ O) %:		< 2.0	
CHARACTERISTICS OF CONCRETE CONTAINING DYNAMON SR-N			
<i>As water reducing admixture</i>			
Quantity of cement kg/m ³ (CEM I- 42.5R):	350	350	
Admixture dosage (% by weight of cement)	0	1,1	
Mass ratio (w/c ratio):	0.5	0.41	
Compressive strength (N/mm ²):			
1 day	26	37	
7 days	43	56	
28 days	52	66	
CHARACTERISTICS OF CONCRETE CONTAINING DYNAMON SR-N			
<i>As superplasticising admixture</i>			
Quantity of cement, kg/m ³ (CEM I-42.5R):	350	350	
Admixture dosage (in % of cement weight):	0	1.1	
Mass ratio (w/c ratio):	0.49	0.49	
Air content:	2.4	1.9	
Workability, mm:			
- slump, 5 min	40	200	
- slump, 30 min	30	200	
- slump, 60 min	20	210	
- slump, 90 min	20	180	
- slump flow, 5 min	200	430	
- slump flow, 30 min	200	340	
- slump flow, 60 min	200	330	
- slump flow, 90 min	200	320	

Fig. B-4: Technical specifications of Dynamon SR-N from Rescon Mapei AS

Superplasticizer Glenium 151 from BASF Construction Chemicals GmbH

Glenium 151 is a high performance superplasticizing admixture based on modified polycarboxylate polymers. Please see figure B-5 for technical specifications.



The Chemical Company

GLENIUM C151

Nov. 2009

SUPERPLASTISERENDE TILSETNINGSSTOFF FOR BETONG.

Tekniske data:

Konsistens:	Viskøs væske.	pH-verdi:	6,6 ± 1,0.
Farge:	Gullig.	Ekvivalent Na ₂ O:	< 2,0%.
Tørrestoff:	15,0 ± 1,5%.	Kloridinnhold:	< 0,01%.
Densitet:	1,03 ± 0,02kg/l.		

Produktbeskrivelse.

Glenium C151 er basert på en kjede av modifiserte polykarboxylater. Produktet er primært utviklet til bruk ved produksjon av høyfast betong, men kan godt benyttes i ordinære betonger.

Glenium C151 har en elektrostatisk virkemåte som forbedrer effektiviteten av sementdispersjonen.

Bruksområder.

Den gode dispergeringseffekten gjør Glenium C151 til det ideelle tilsetningsstoff der det ønskes stor vannreducerende evne.

Egenskaper.

- God flyt med lave w/c-forhold.
- Glenium C151 forbedrer de fysiske egenskaper og derved betongens bestandighet.

Andre anbefalte kombinasjoner.

Kan kombineres med alle Glenium produkter, samt

- Luftinnførende.
- Plastiserende.
- Akselererende.
- Retarderende.
- Fiber.

Dosering.

Anbefalt doseringsmengde 0,2-2,0% av sementmengden, avhengig av betongsammensetning og krav.

Andre doseringer kan være aktuelle i særlige tilfeller og under særlige utførelsesforhold.

Prøveblandinger anbefales.

Bruksanvisning.

Den optimale effekten oppnås ved å tilsette Glenium C151 straks etter tilsetting av ca. 50% av blandevannet. Unngå å tilsette Glenium C151 til de tørre materialer.

Glenium C151 kan tilsettes på bilen på byggeplass. For å få full utnyttelse av stoffet bør betongen blandes godt, 1-2min pr m³.

Forpakning.

- 1000 liters containere.
- Tank.

Lagring.

Oppbevares i tett lukket beholder ved vanlig temperatur, min. +5 °C, i 12 mnd.

Sikkerhetstiltak.

Se produktets sikkerhetsdatablad.

Fig. B-5: Technical specifications of Dynamon SR-N from Glenium 151 from BASF Construction Chemicals GmbH

APPENDIX C – Composition of the tested matrices

Table C-1: Matrices with Dynamon SP-130 (Main test program)

MASS BASED FRACTIONS		VOLUME BASED FRACTIONS				CONSTITUENTS IN GRAMS											
w/c	w/b	w/p (for Årdal)	w/V _{powder}	V _{cem} /V _{powder}	V _{filler} /V _{powder}	Mix volume, ml	water	W _{corrected}	STD FA	FILLER							
										1	2	3	4	5	6	7	SP1
0.40	0.40	0.400	1.18	1	0	185	100	90.3	250.00								10.00
		0.376		0.93	0.07		96.86	87.4	242.14	15.23							
0.50	0.50	0.408	1.18	0.80	0.20	185	100	92.2	200.00								8.00
		0.414		0.67	0.33												
0.60	0.60	0.414	1.18	0.67	0.33	185	100	93.5	166.67								6.67
		0.414		0.67	0.33												

Table C-2: Matrices with Dynamon SR-N (Main test program)

MASS BASED FRACTIONS		VOLUME BASED FRACTIONS				CONSTITUENTS IN GRAMS											
w/c	w/b	w/p (for Årdal)	w/V _{powder}	V _{cem} /V _{powder}	V _{filler} /V _{powder}	Mix volume, ml	water	W _{corrected}	STD FA	FILLER							
										1	2	3	4	5	6	7	SP2
0.40	0.40	0.400	1.18	1	0	185	100	90.2	250.00								10.00
		0.376		0.93	0.07		96.86	87.3	242.14	15.23							
0.50	0.50	0.408	1.18	0.80	0.20	185	100	92.1	200.00								8.00
		0.414		0.67	0.33												
0.60	0.60	0.414	1.18	0.67	0.33	185	100	93.5	166.67								6.67
		0.414		0.67	0.33												

SYMBOLS USED IN THE TABLES:

w/c – water/cement ratio by mass;

w/b – water/binder ratio by mass;

w/p – water/powder (all solids in the mix – filler and cement) ratio by mass;

w/V_{powder} – water/powder ratio by volume;

V_{cem}/V_{powde} – cement/powder ratio by volume;

V_{filler}/V_{powder} – filler/powder ratio by volume;

w_{corrected} – corrected water dosage used for the real mix (excludes water from the admixtures);

STD FA – portland cement of type CEM II/A-V from Norcem AS;

SP1 – Superplasticizer Dynamon SP-130 (dry solids content 30%) from Rescon Mapei AS (diluted 1:10 with water);

SP2 – Superplasticizer Dynamon SR-N (dry solids content 19.5%) from Rescon Mapei AS (diluted 1:10 with water).

FILLERS:

1. Årdal (natural);

2. Årdal (crushed/ unwashed);

3. Årdal (crushed/ washed);

4. Tau;

5. Jelsa;

6. Hokksund;

7. Limestone.

APPENDIX D – Plots of oscillatory test results and up-down flow curves for the tested matrices

In the following (figures D-1 to D-72), you will find complete plots of oscillatory test results and up-down flow curves for all matrix mixes. Matrix mix numbers are according to Tables 3-1 to 3-3.

MATRIX No. 1

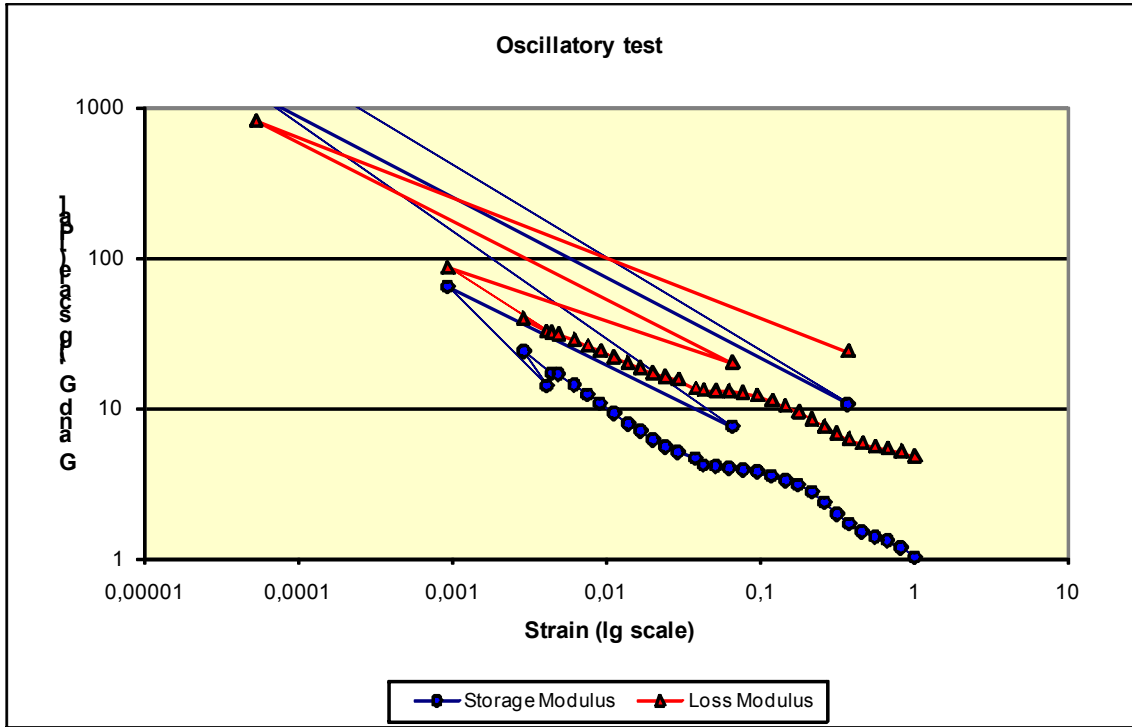


Fig. D-1: Oscillatory test results of matrix No. 1

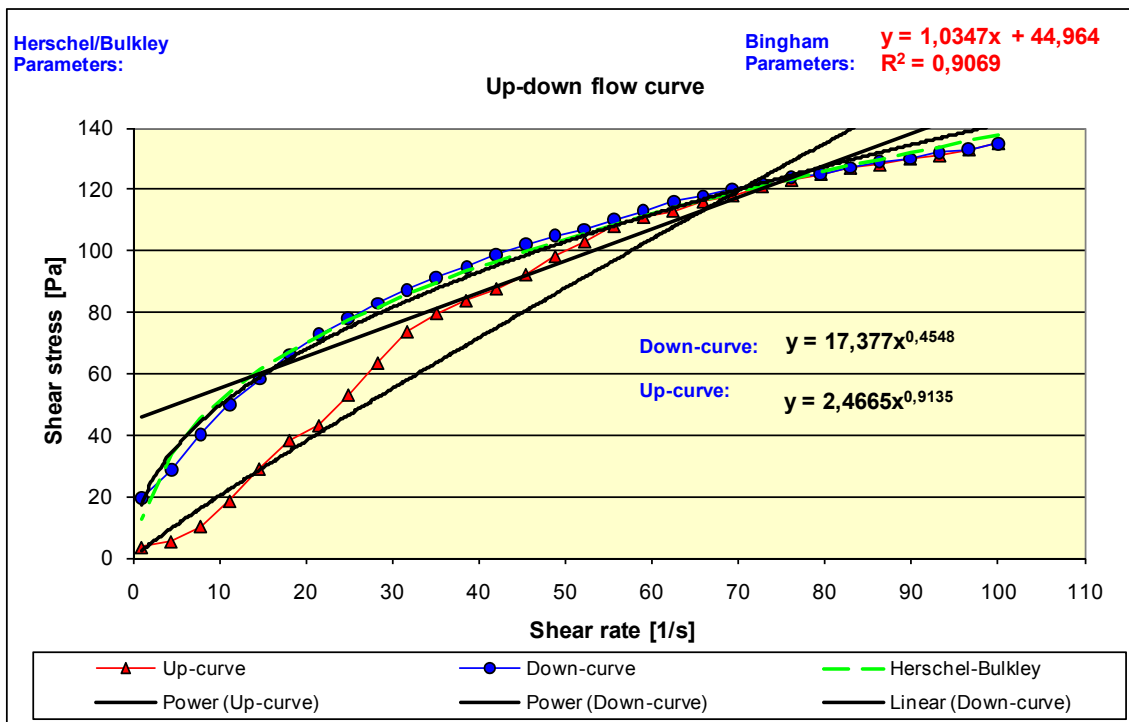


Fig. D-2: Up-down flow curves of matrix No. 1

MATRIX No. 2

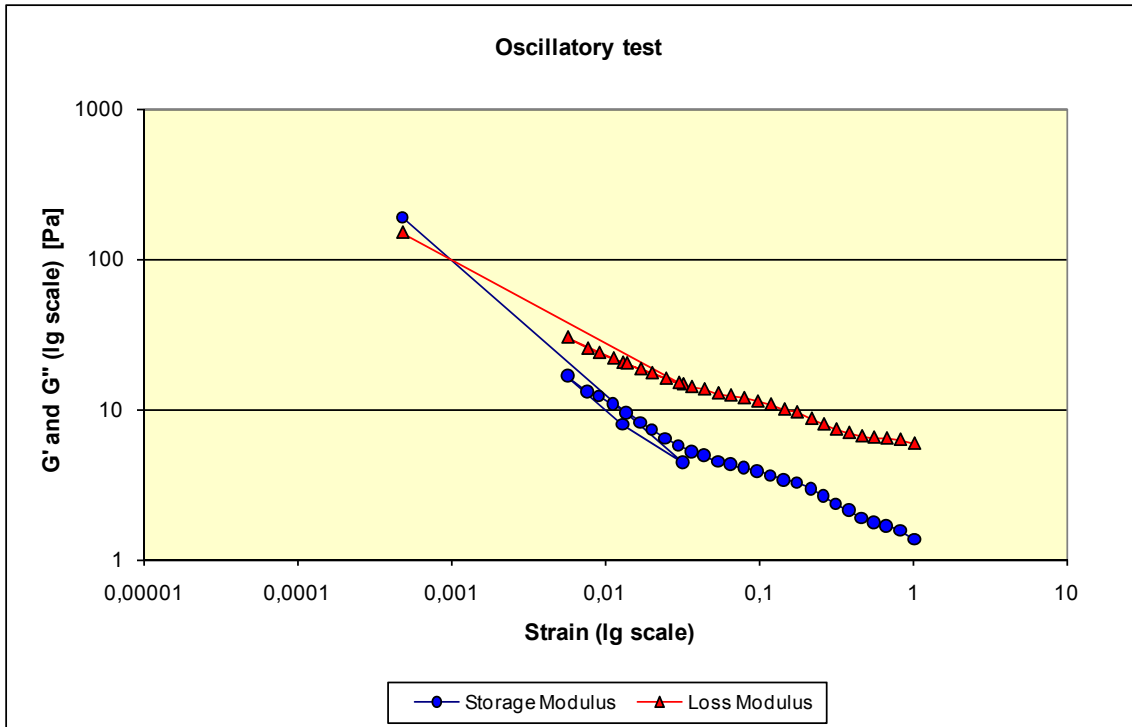


Fig. D-3: Oscillatory test results of matrix No. 2

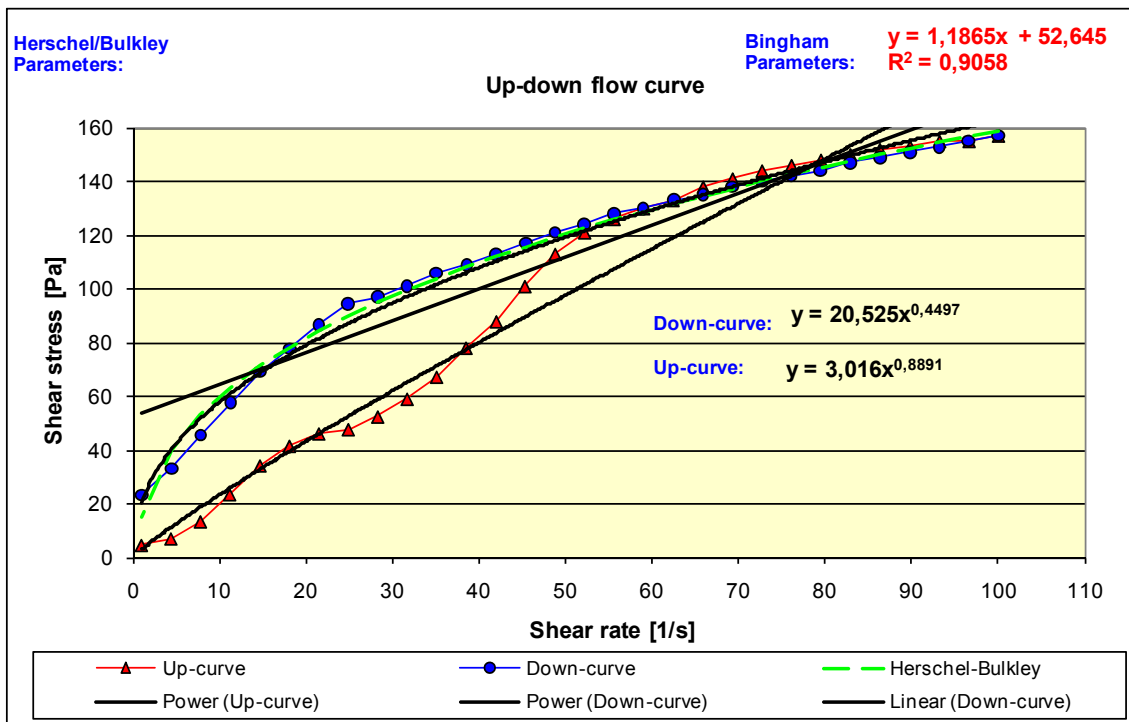


Fig. D-4: Up-down flow curves of matrix No. 2

MATRIX No. 3

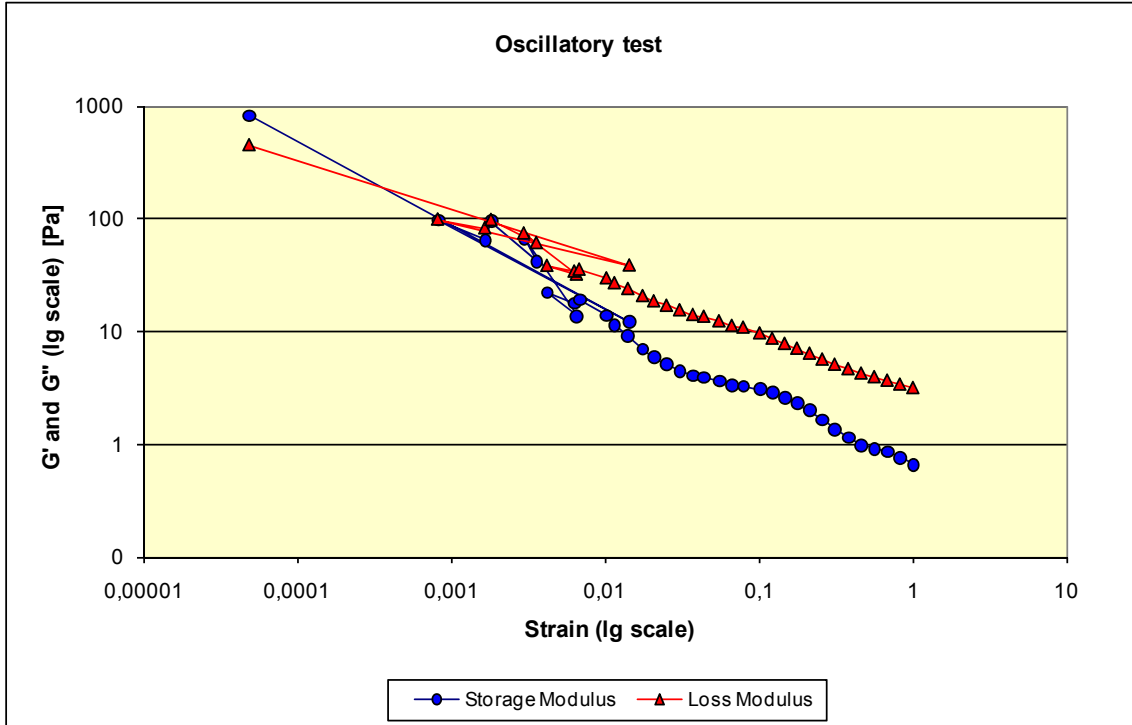


Fig. D-5: Oscillatory test results of matrix No. 3

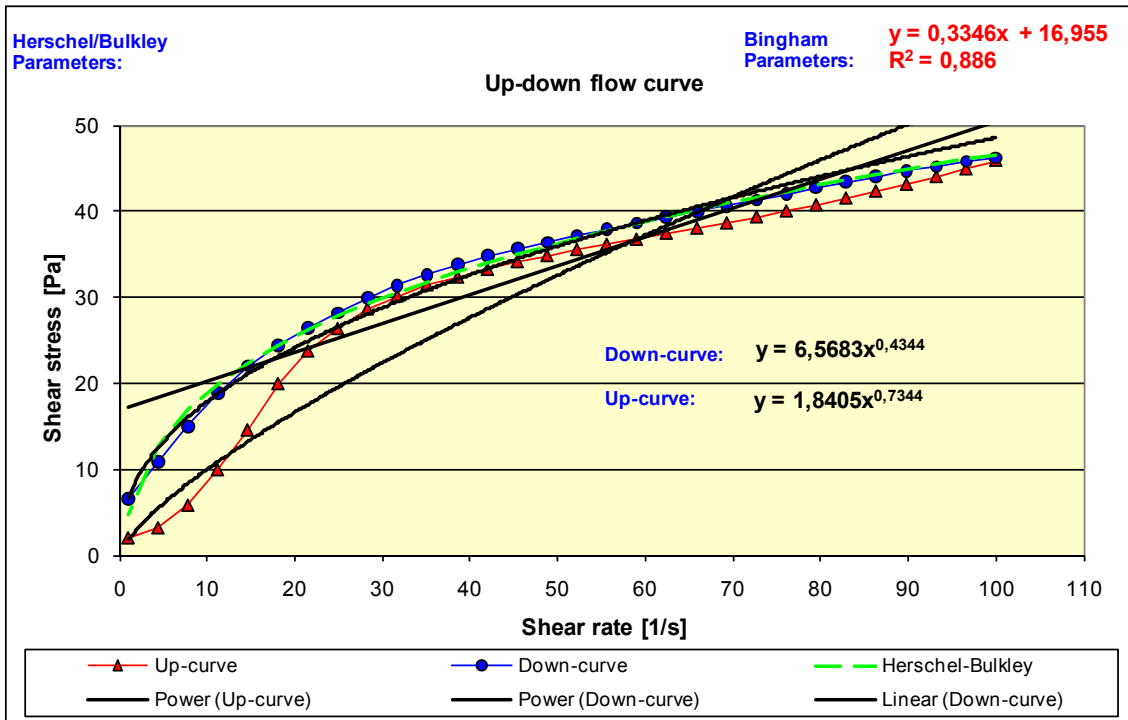


Fig. D-6: Up-down flow curves of matrix No. 3

MATRIX No. 4

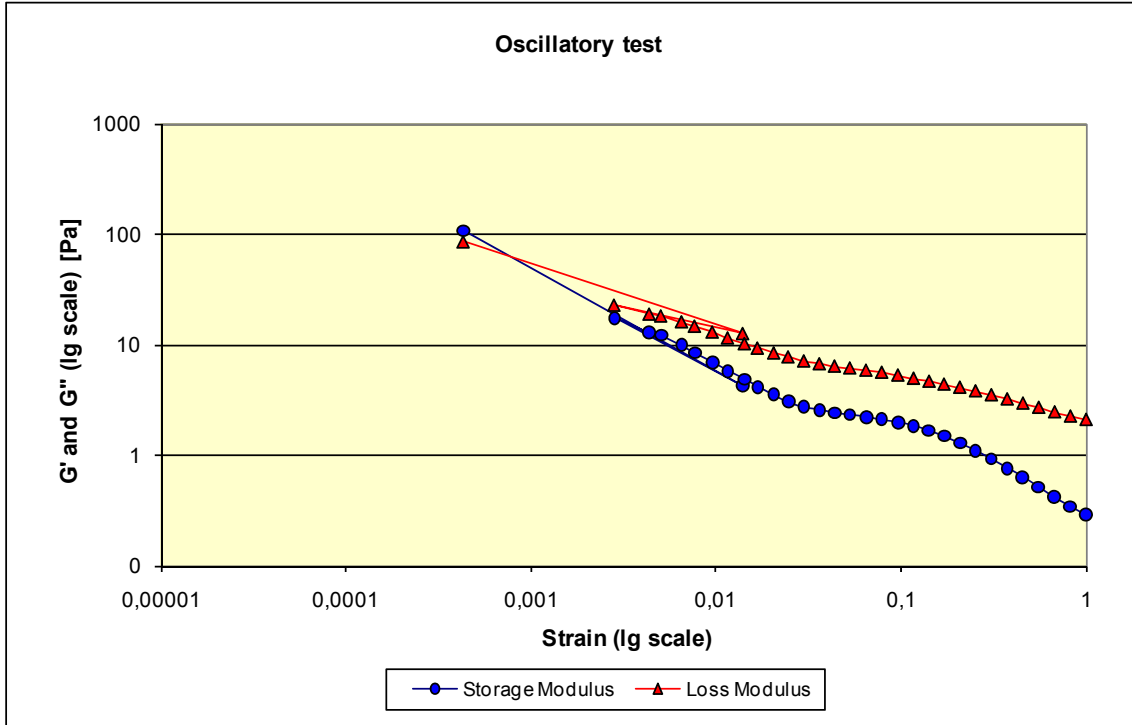


Fig. D-7: Oscillatory test results of matrix No. 4

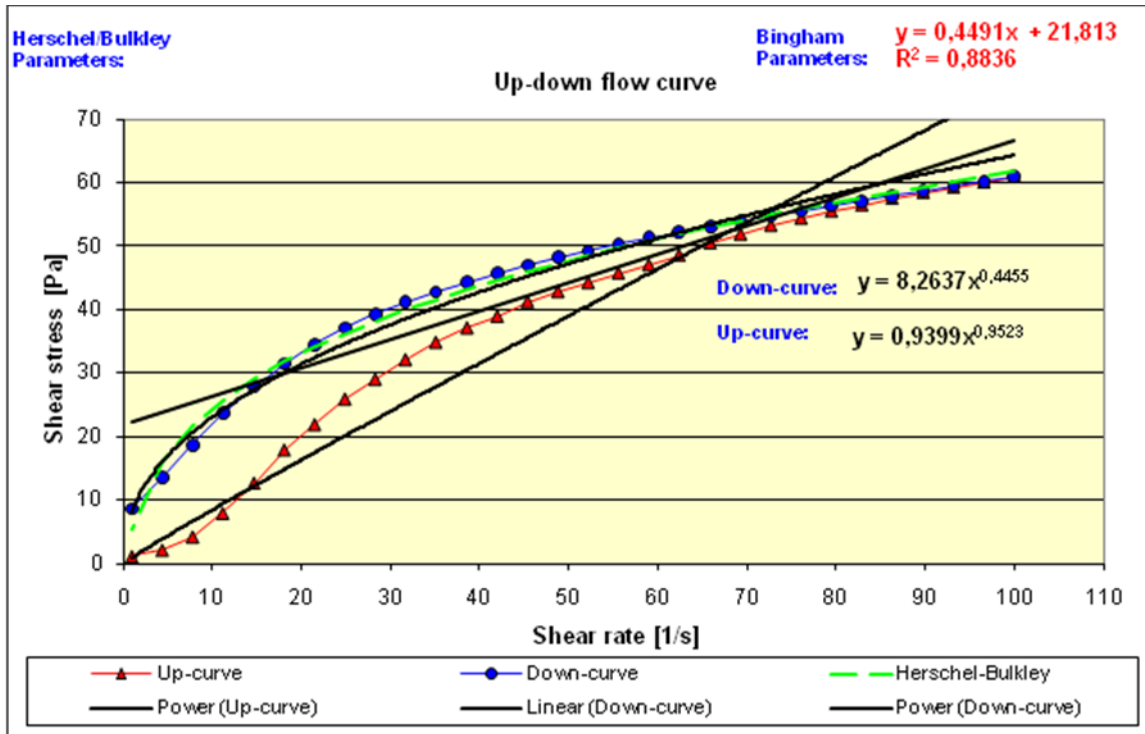


Fig. D-8: Up-down flow curves of matrix No. 4

MATRIX No. 5

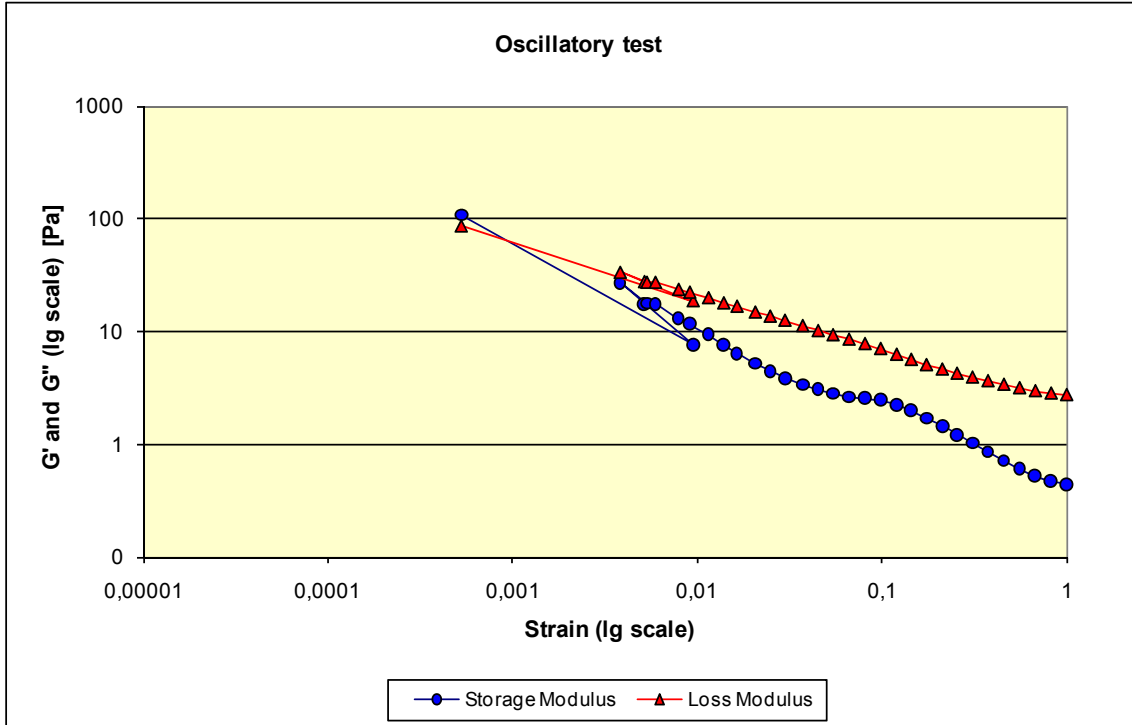


Fig. D-9: Oscillatory test results of matrix No. 5

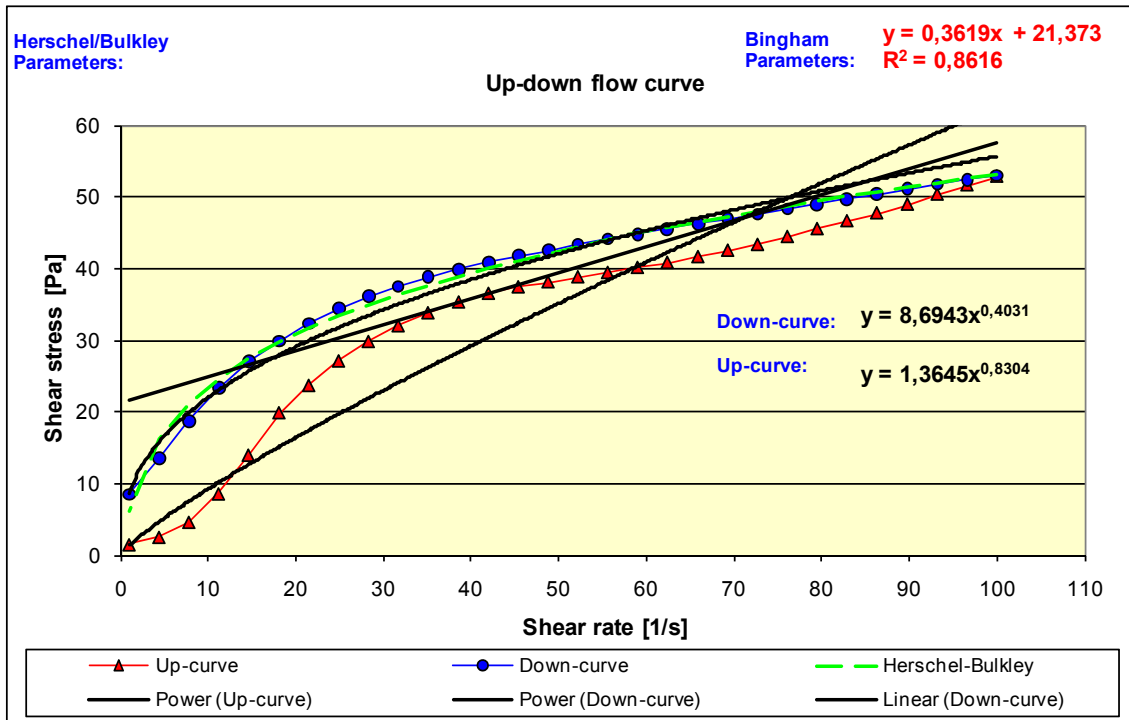


Fig. D-10: Up-down flow curves of matrix No. 5

MATRIX No. 6

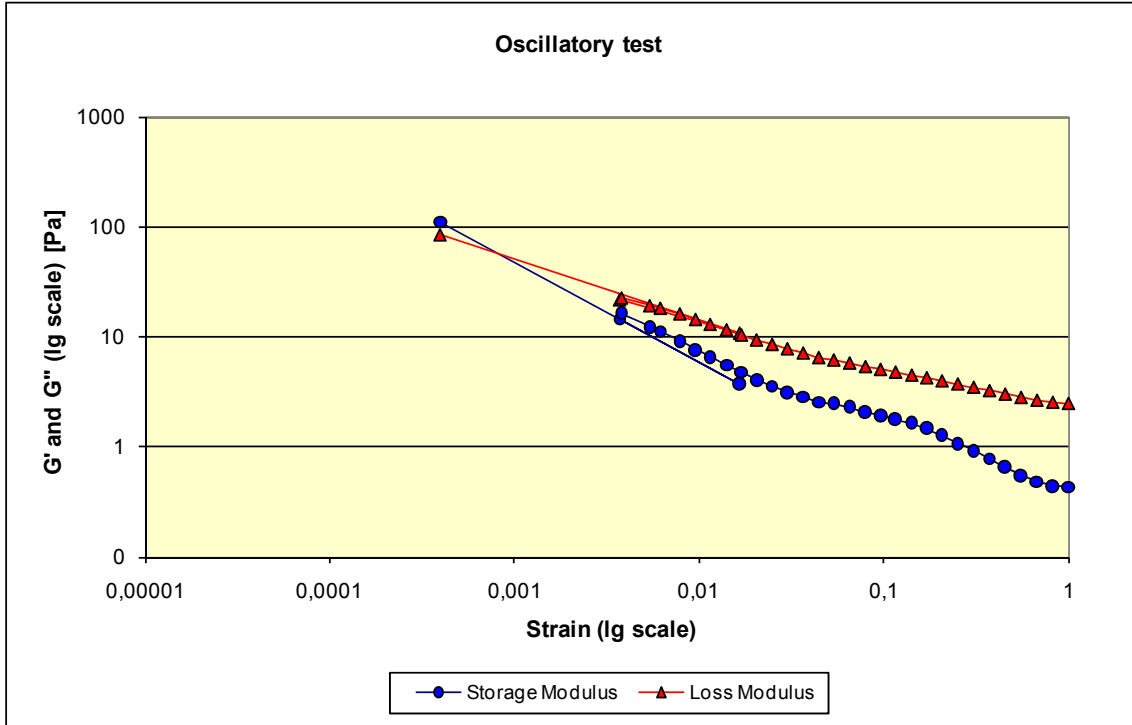


Fig. D-11: Oscillatory test results of matrix No. 6

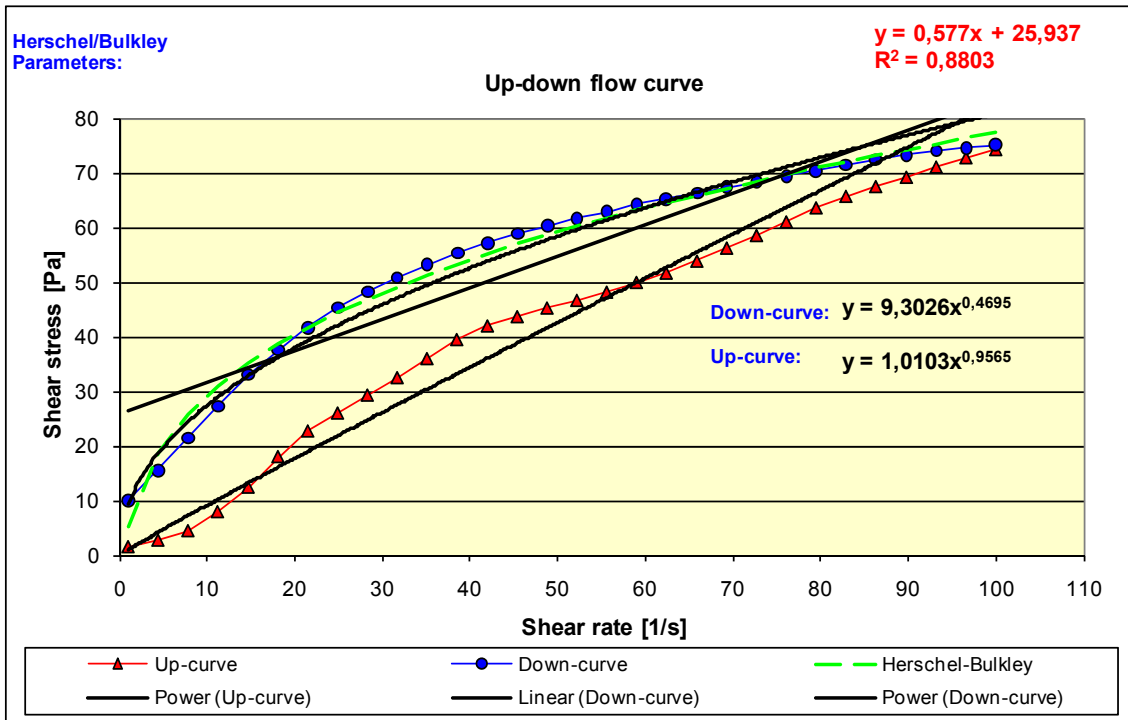


Fig. D-12: Up-down flow curves of matrix No. 6

MATRIX No. 7

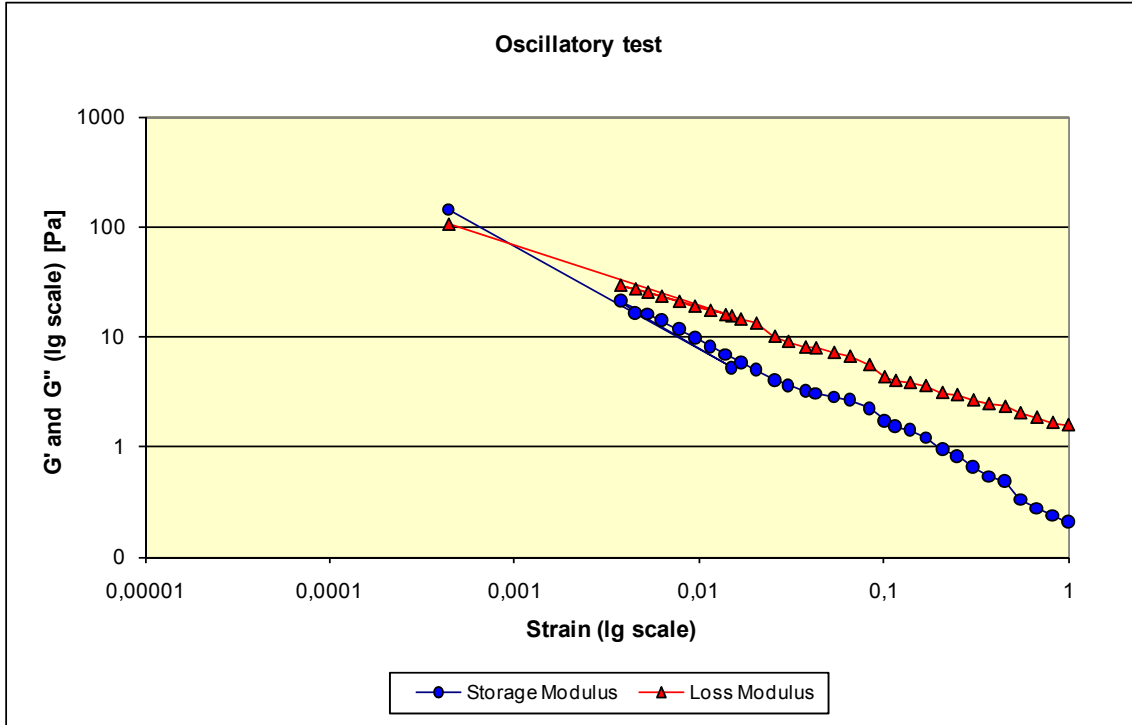


Fig. D-13: Oscillatory test results of matrix No. 7

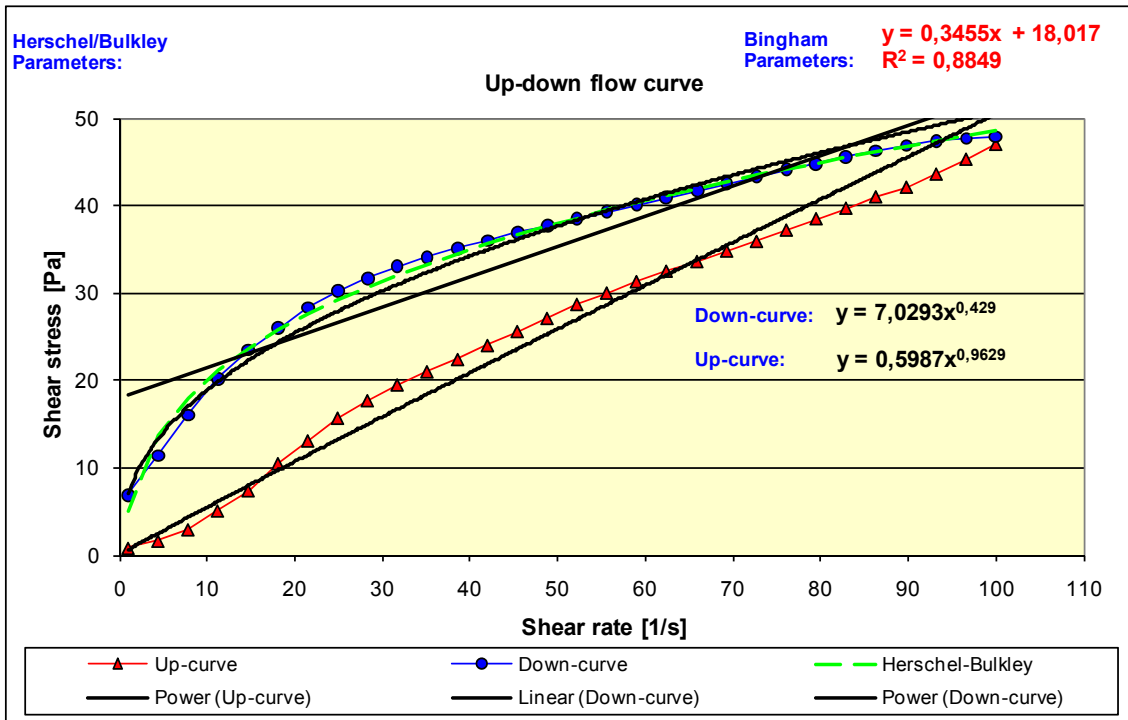


Fig. D-14: Up-down flow curves of matrix No. 7

MATRIX No. 8

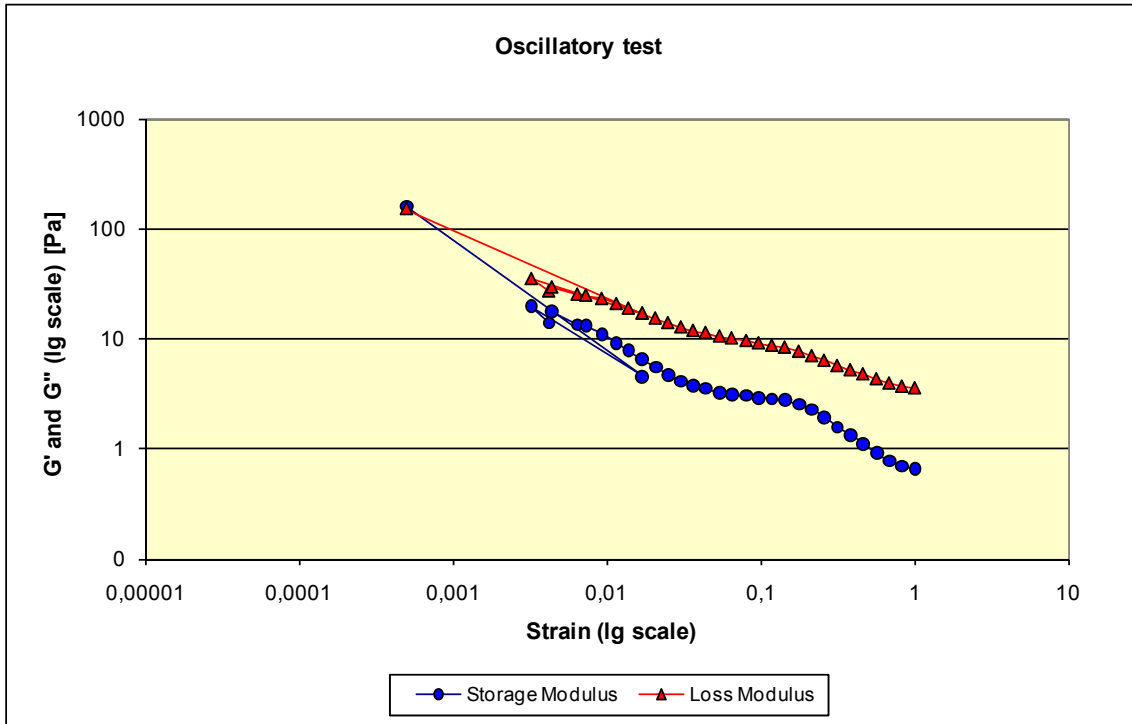


Fig. D-15: Oscillatory test results of matrix No. 8

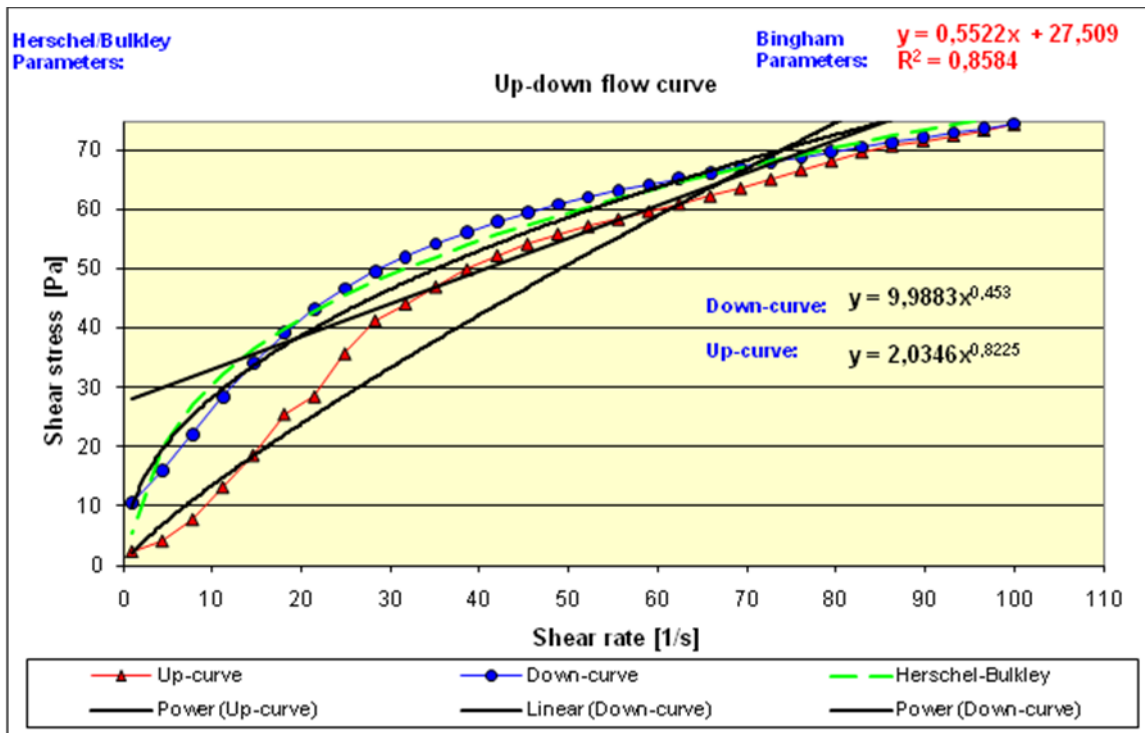


Fig. D-16: Up-down flow curves of matrix No. 8

MATRIX No. 9

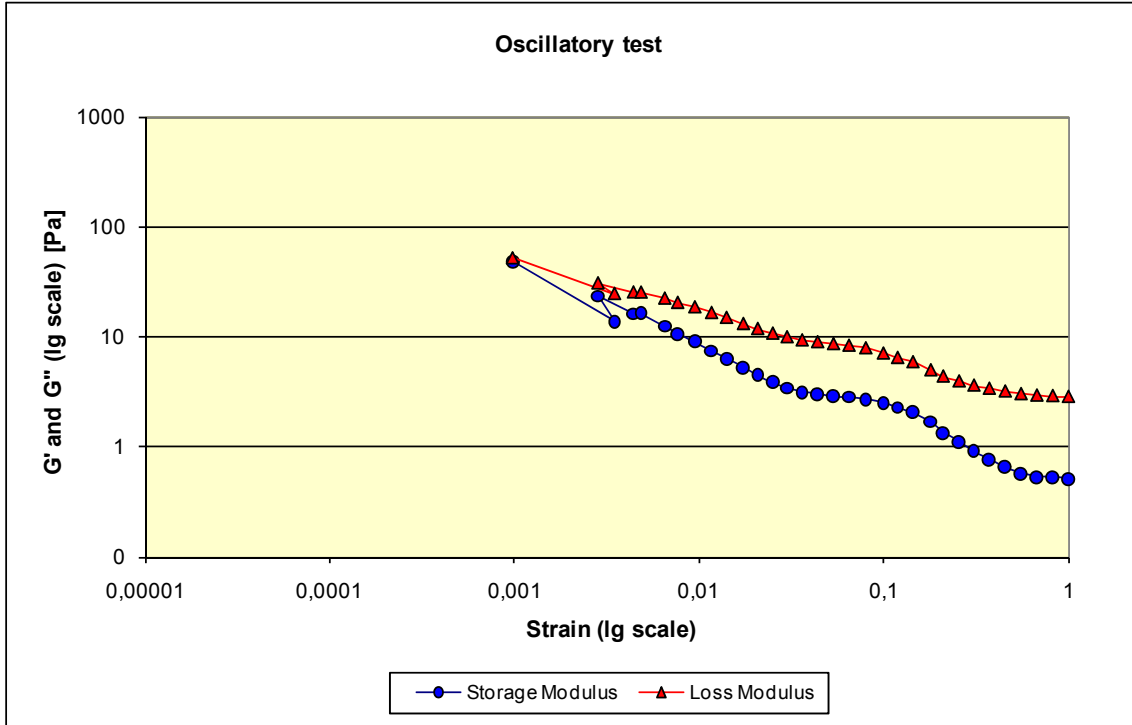


Fig. D-17: Oscillatory test results of matrix No. 9

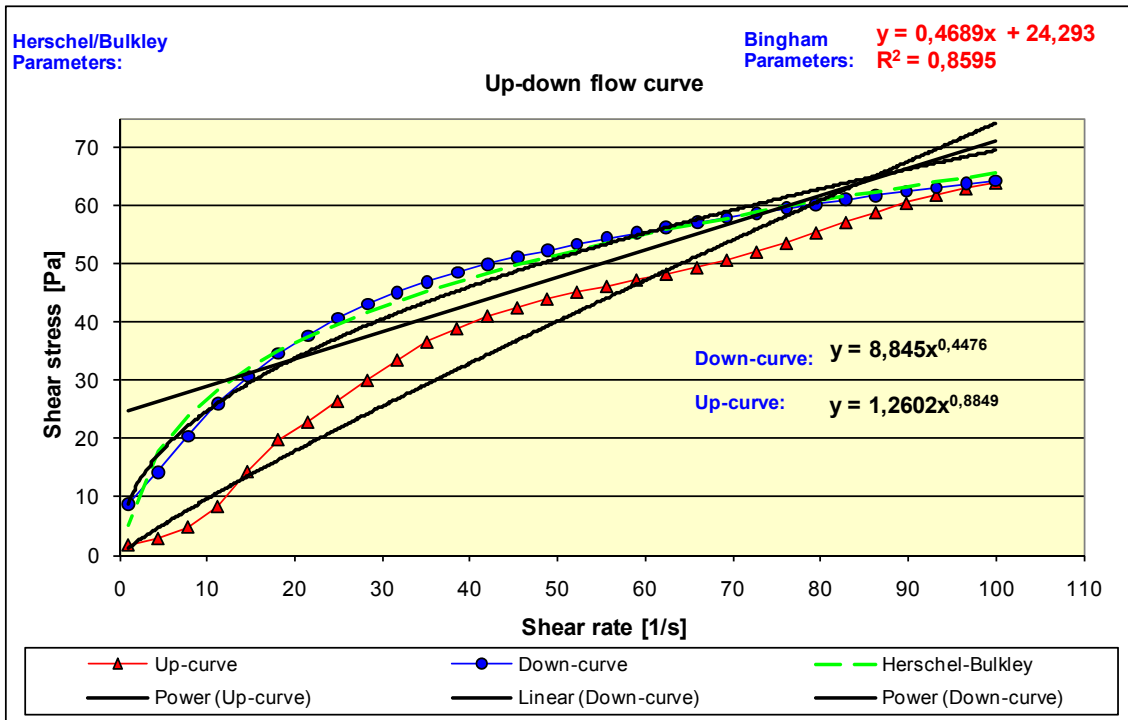


Fig. D-18: Up-down flow curves of matrix No. 9

MATRIX No. 10

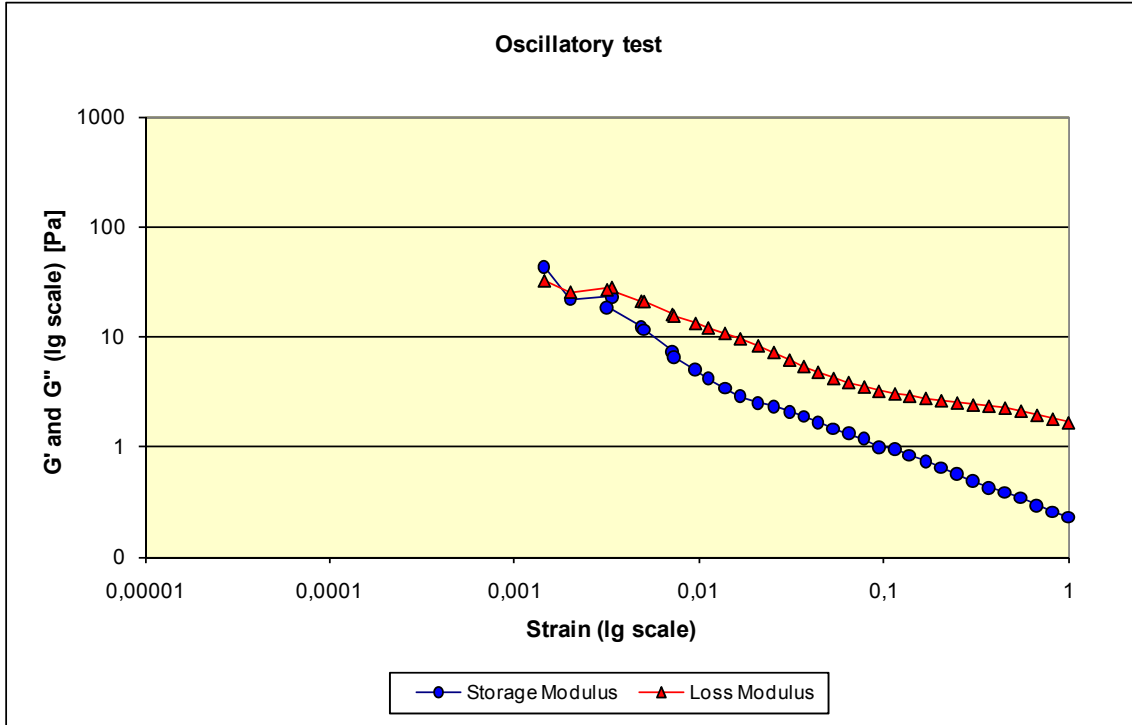


Fig. D-19: Oscillatory test results of matrix No. 10

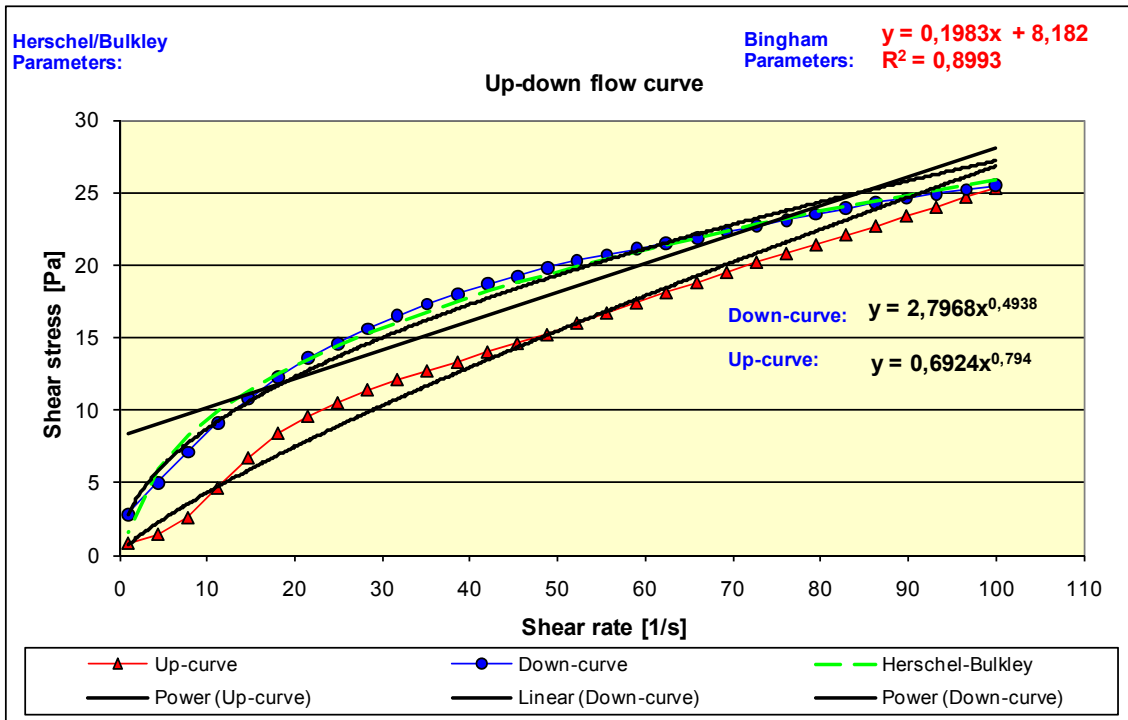


Fig. D-20: Up-down flow curves of matrix No. 10

MATRIX No. 11

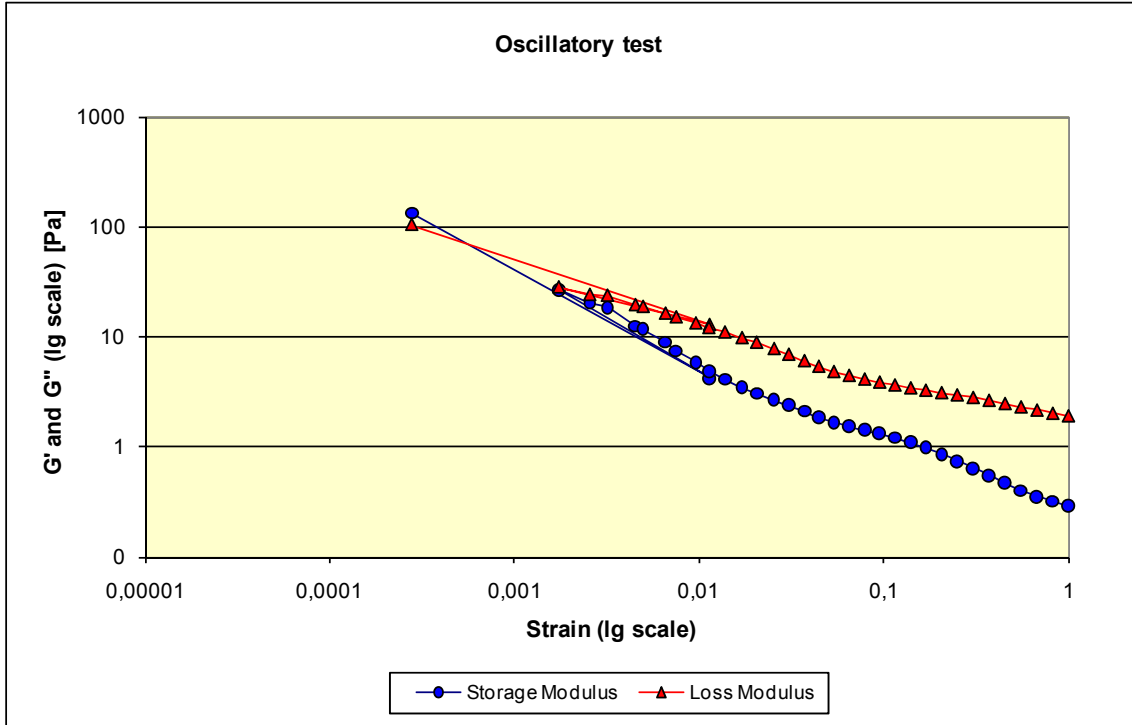


Fig. D-21: Oscillatory test results of matrix No. 11

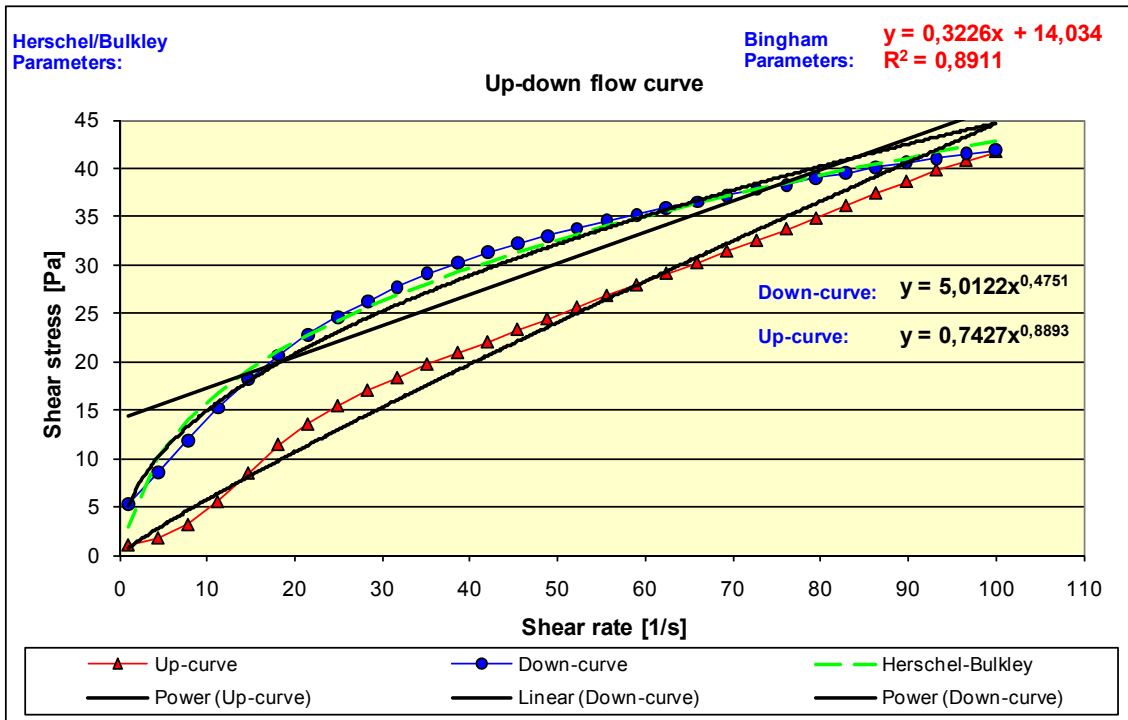


Fig. D-22: Up-down flow curves of matrix No. 11

MATRIX No. 12

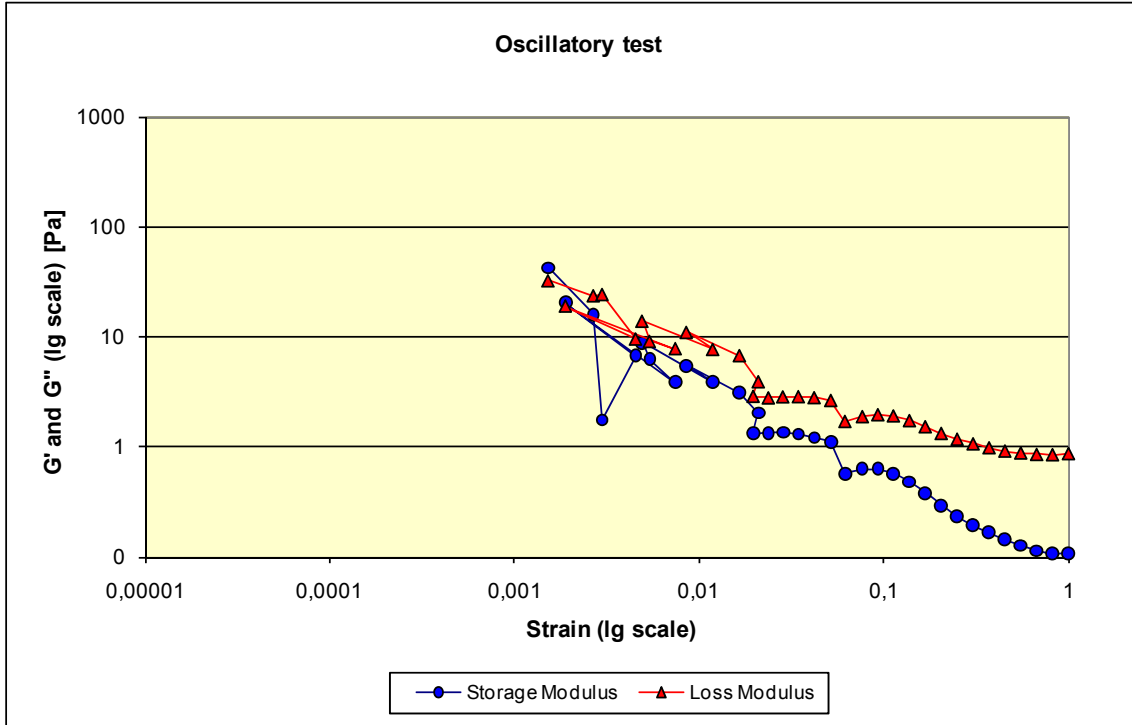


Fig. D-23: Oscillatory test results of matrix No. 12

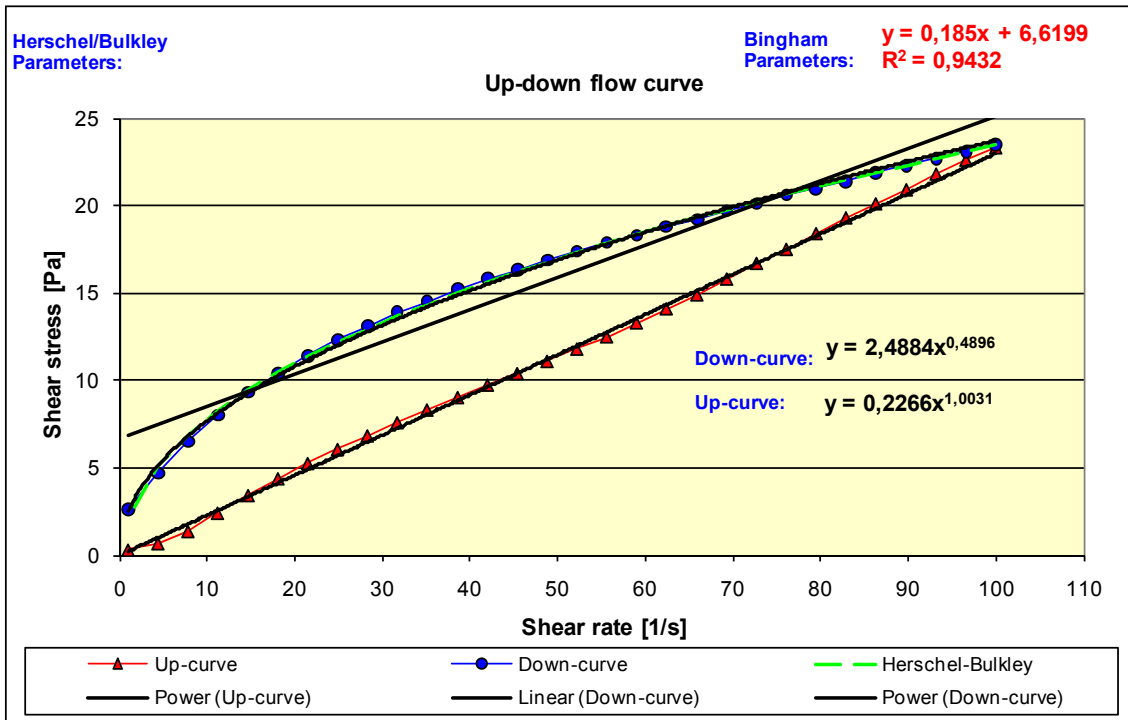


Fig. D-24: Up-down flow curves of matrix No. 12

MATRIX No. 13

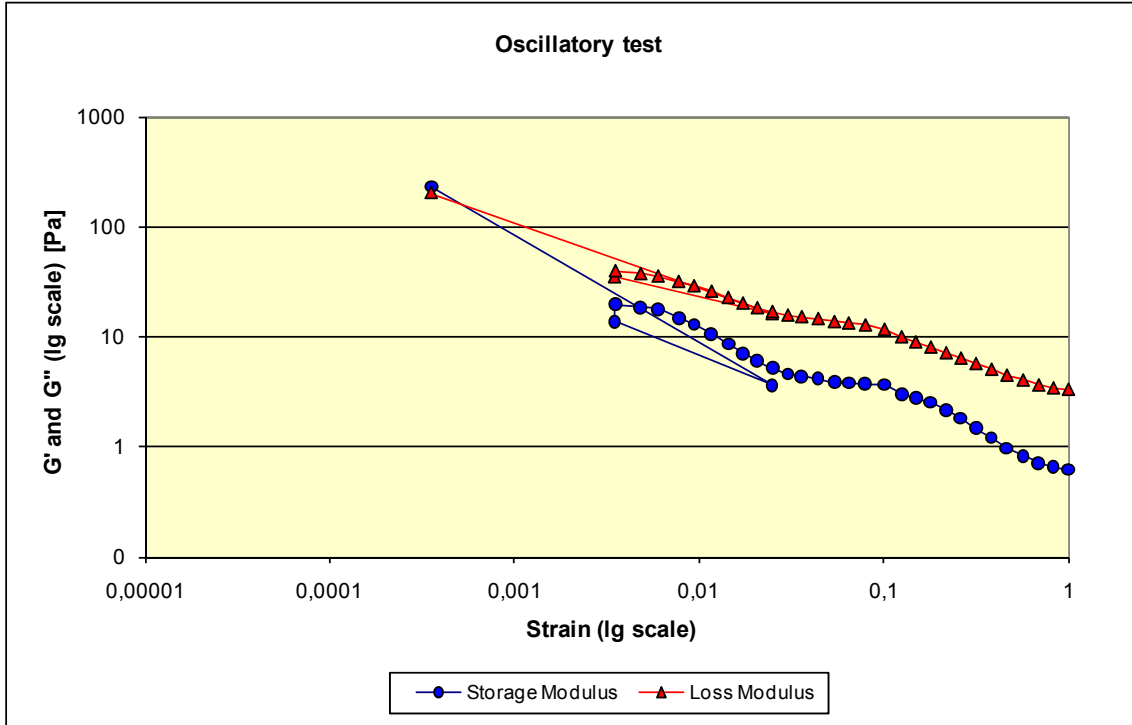


Fig. D-25: Oscillatory test results of matrix No. 13

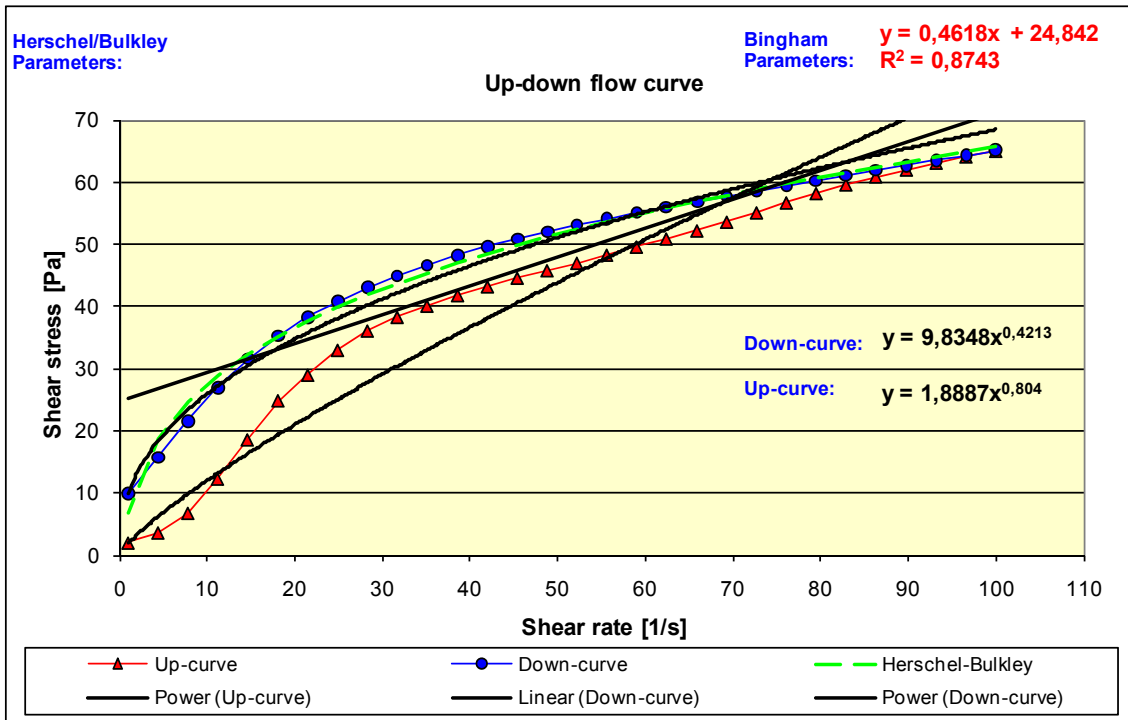


Fig. D-26: Up-down flow curves of matrix No. 13

MATRIX No. 14

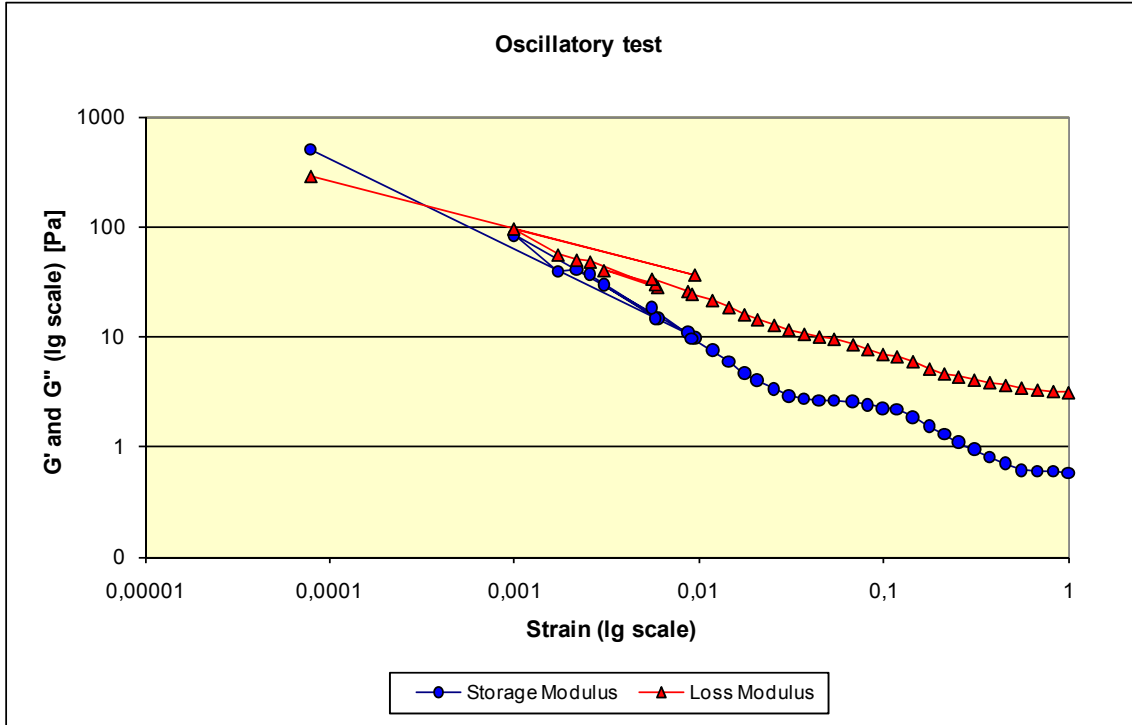


Fig. D-27: Oscillatory test results of matrix No. 14

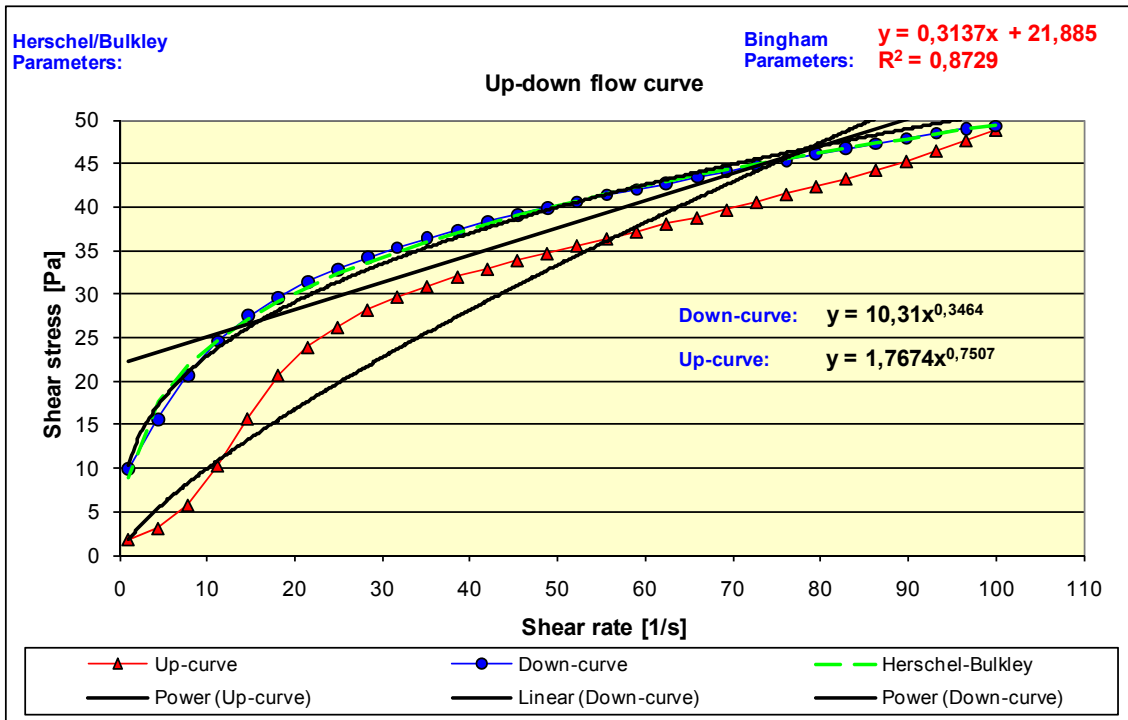


Fig. D-28: Up-down flow curves of matrix No. 14

MATRIX No. 15

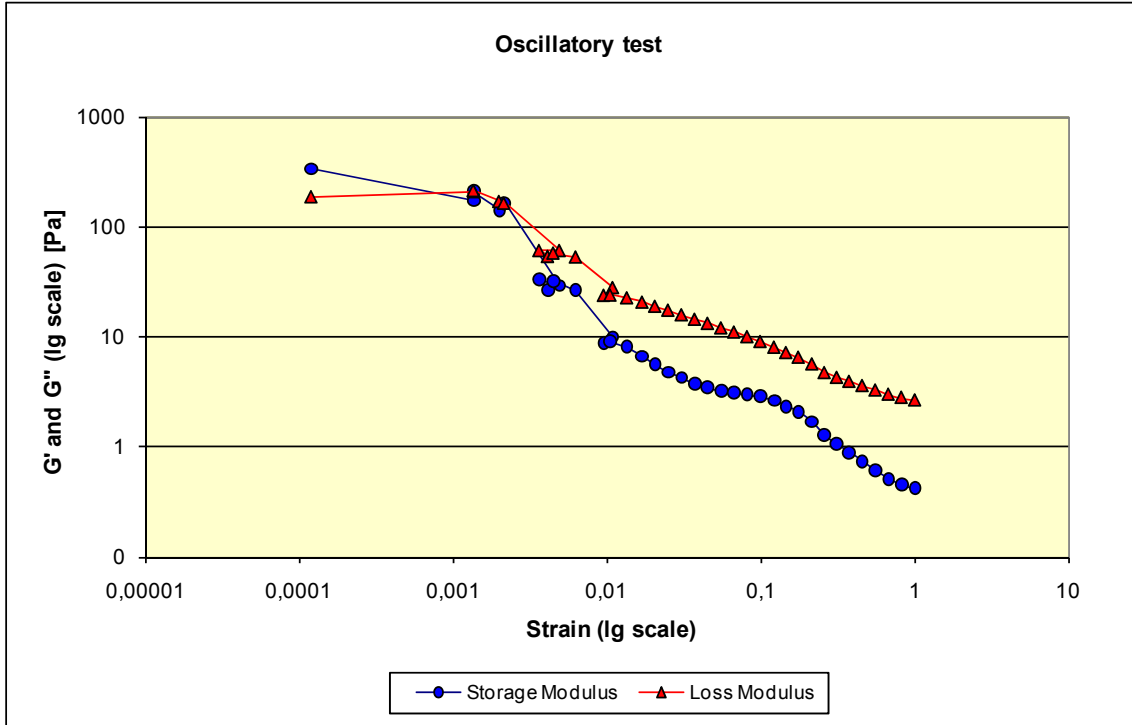


Fig. D-29: Oscillatory test results of matrix No. 15

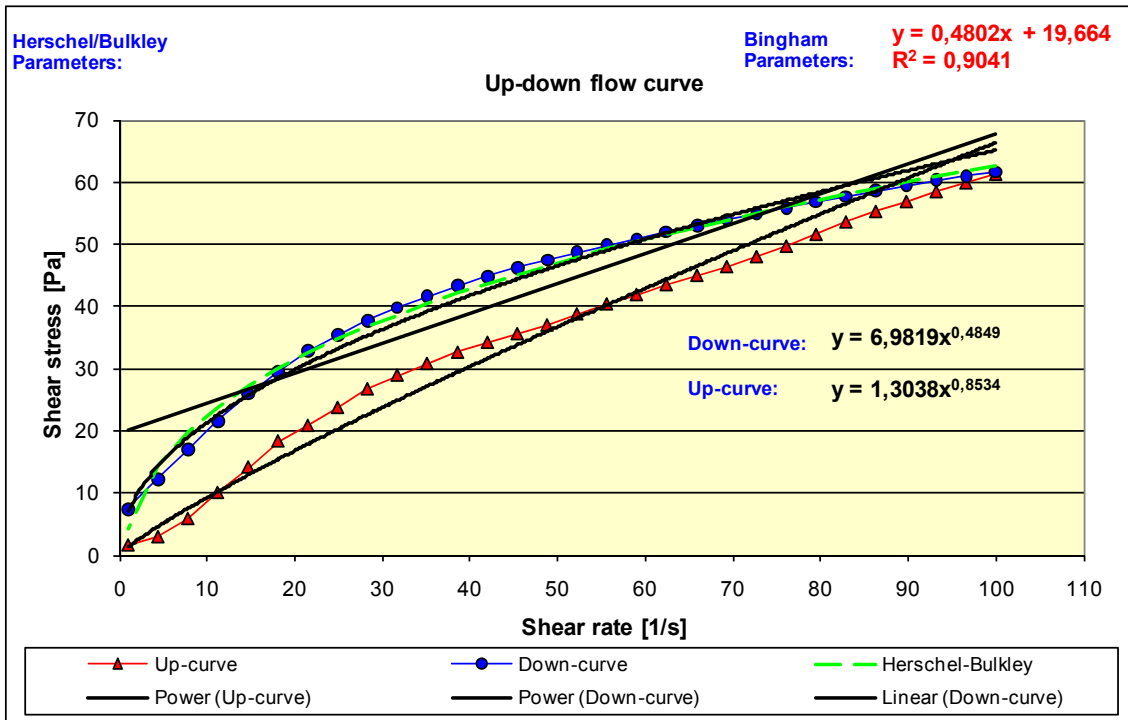


Fig. D-30: Up-down flow curves of matrix No. 15

MATRIX No. 16

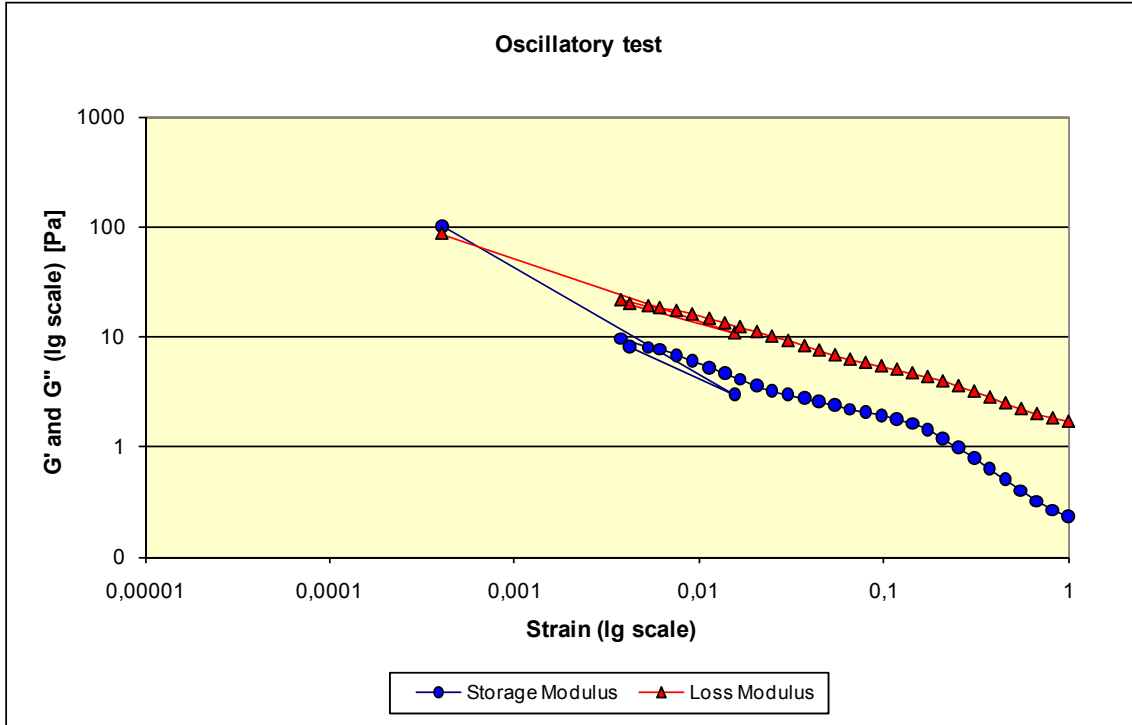


Fig. D-31: Oscillatory test results of matrix No. 16

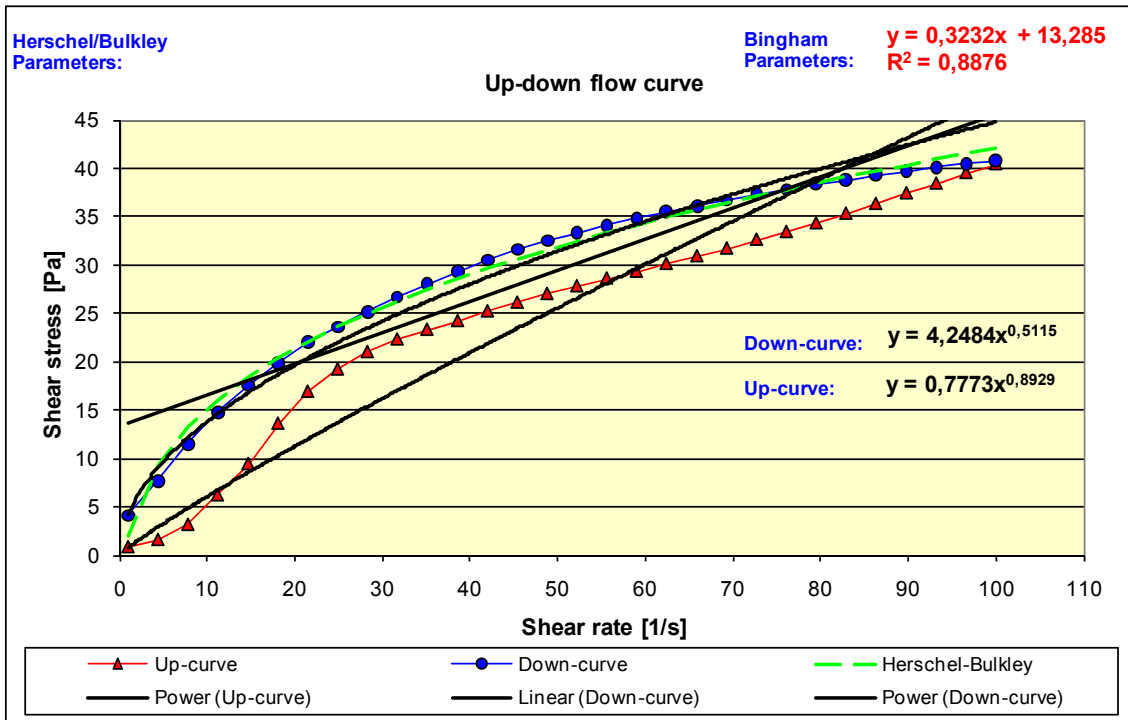


Fig. D-32: Up-down flow curves of matrix No. 16

MATRIX No. 17 (the same as 34)

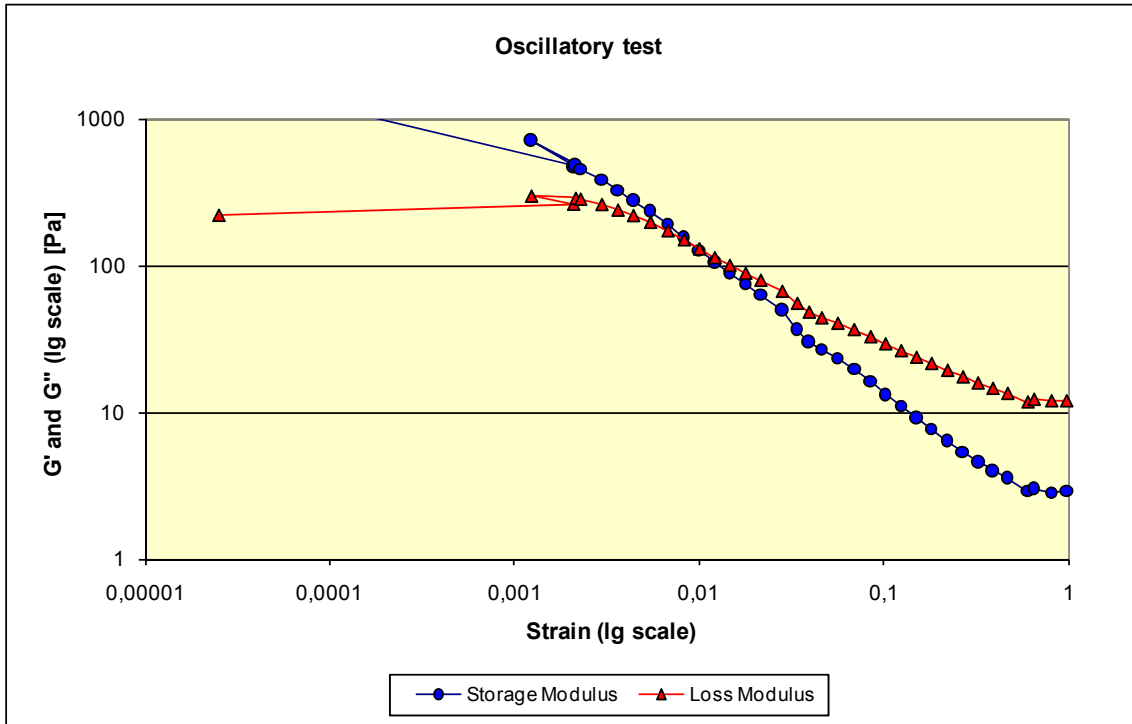


Fig. D-33: Oscillatory test results of matrix No. 17

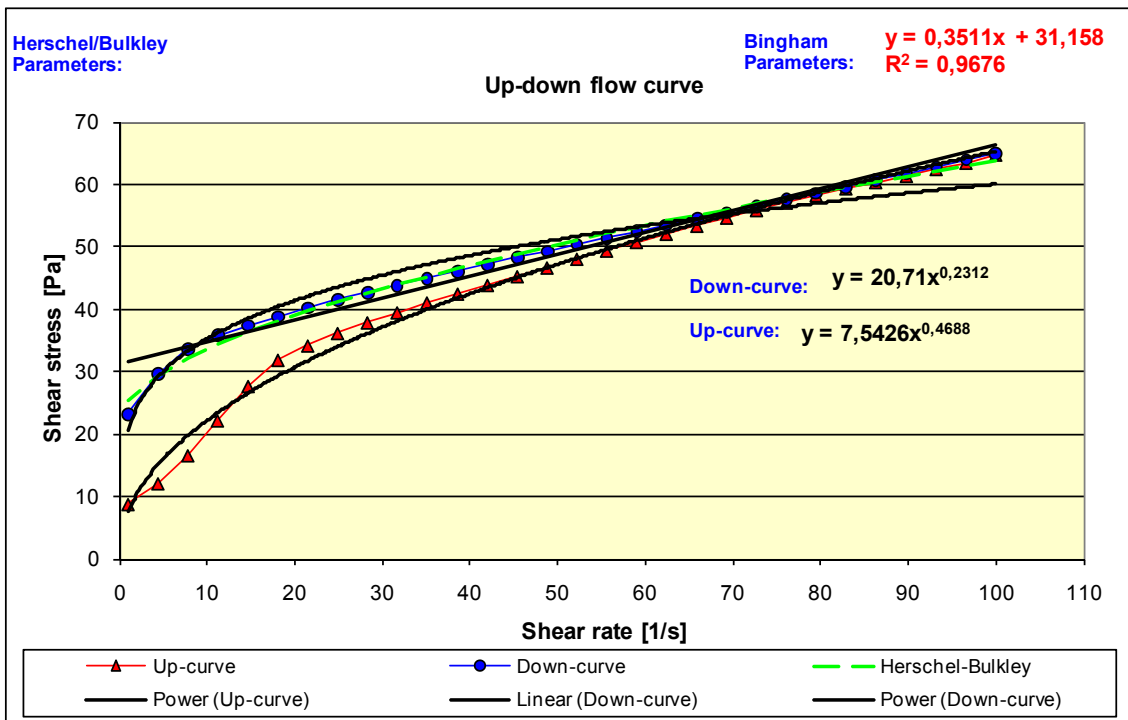


Fig. D-34: Up-down flow curves of matrix No. 17

MATRIX No. 18

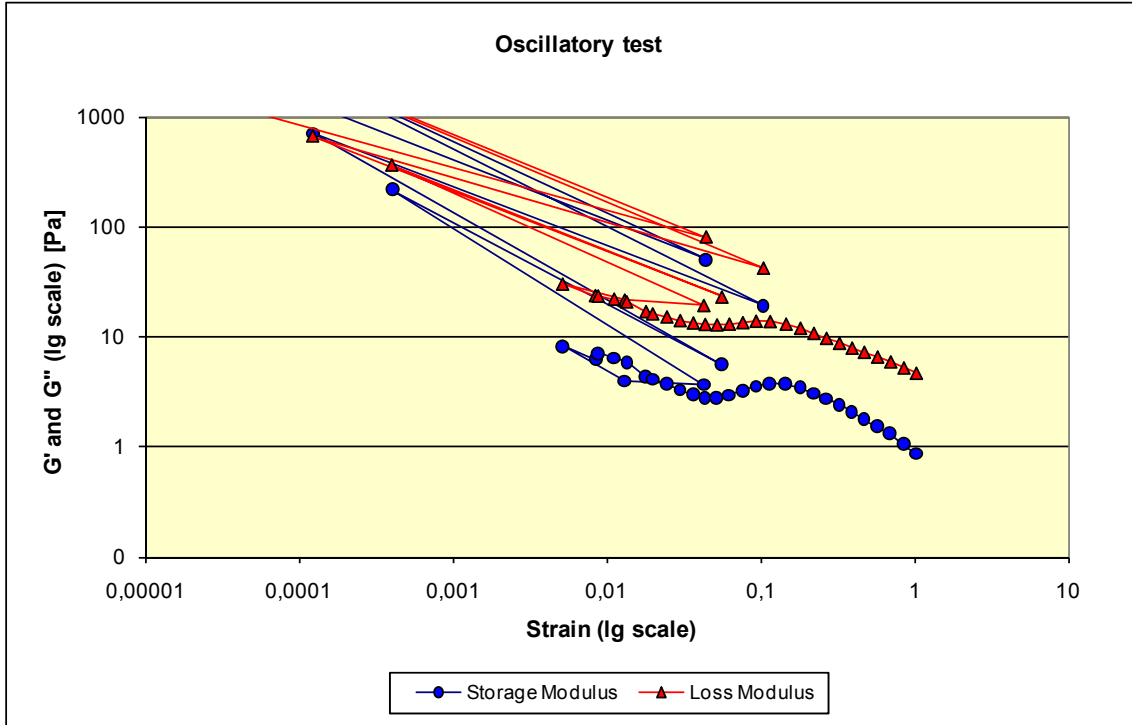


Fig. D-35: Oscillatory test results of matrix No. 18

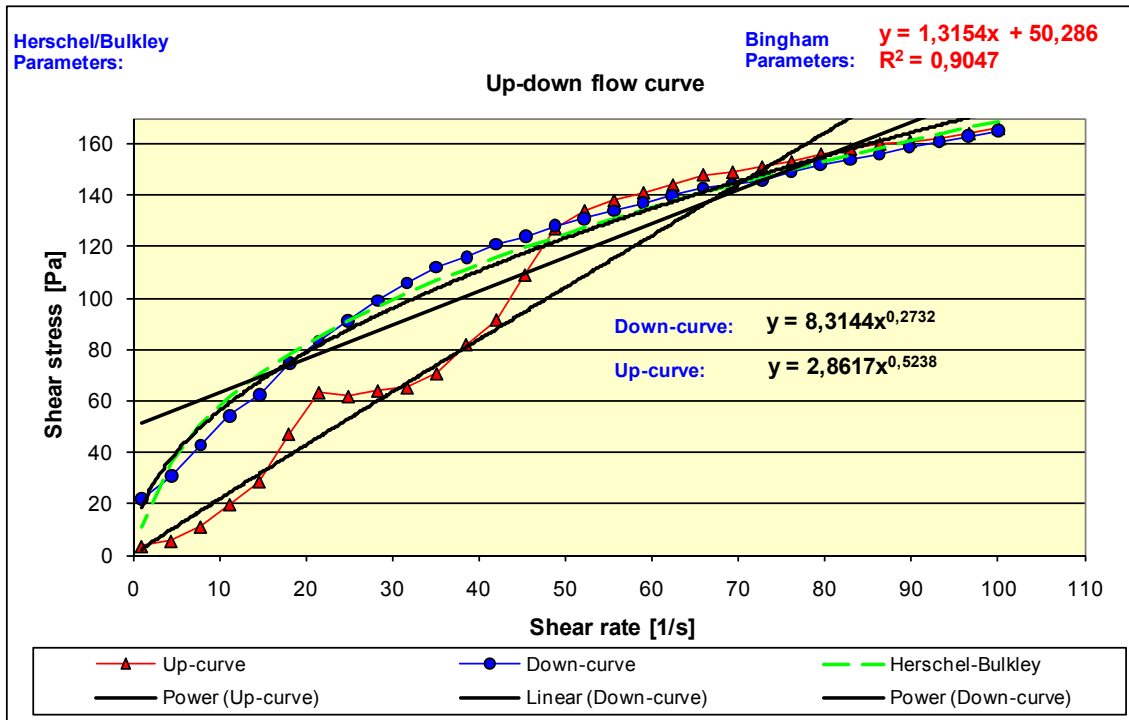


Fig. D-36: Up-down flow curves of matrix No. 18

MATRIX No. 19

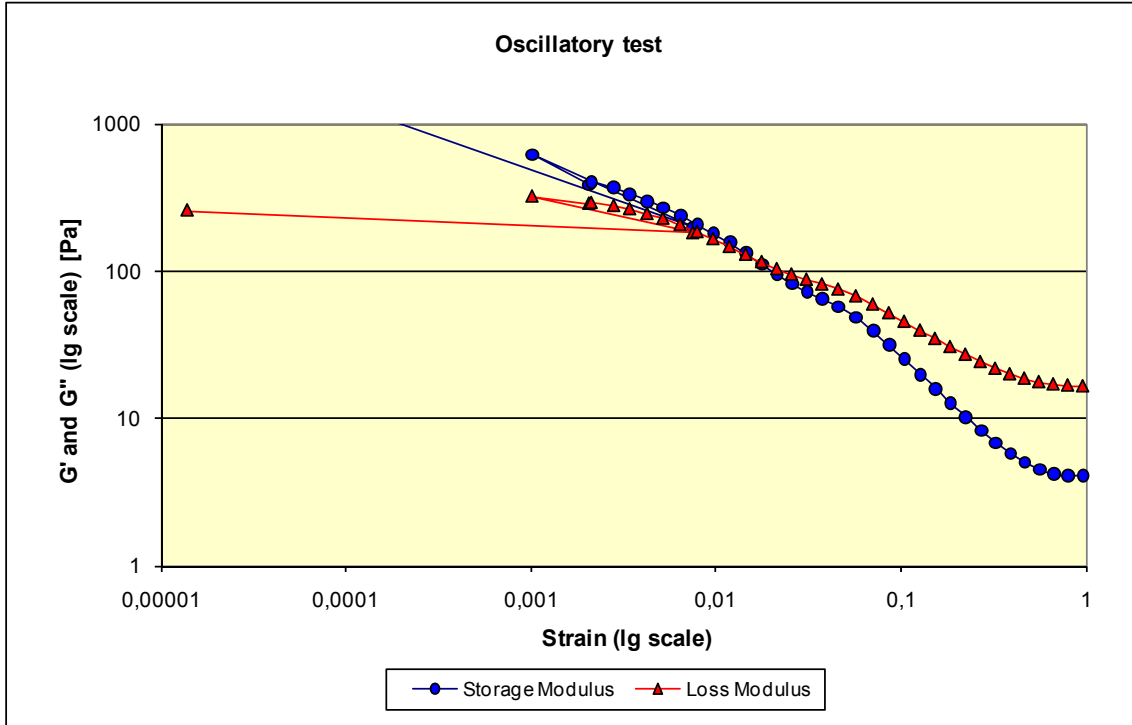


Fig. D-37: Oscillatory test results of matrix No. 19

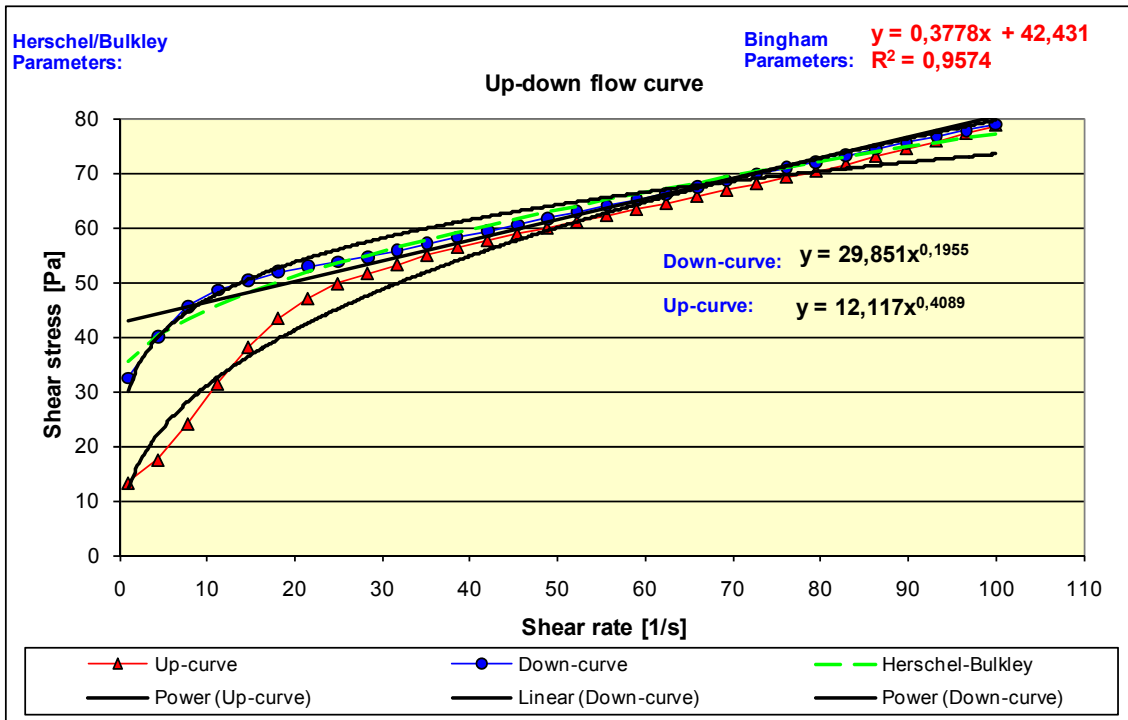


Fig. D-38: Up-down flow curves of matrix No. 19

MATRIX No. 20

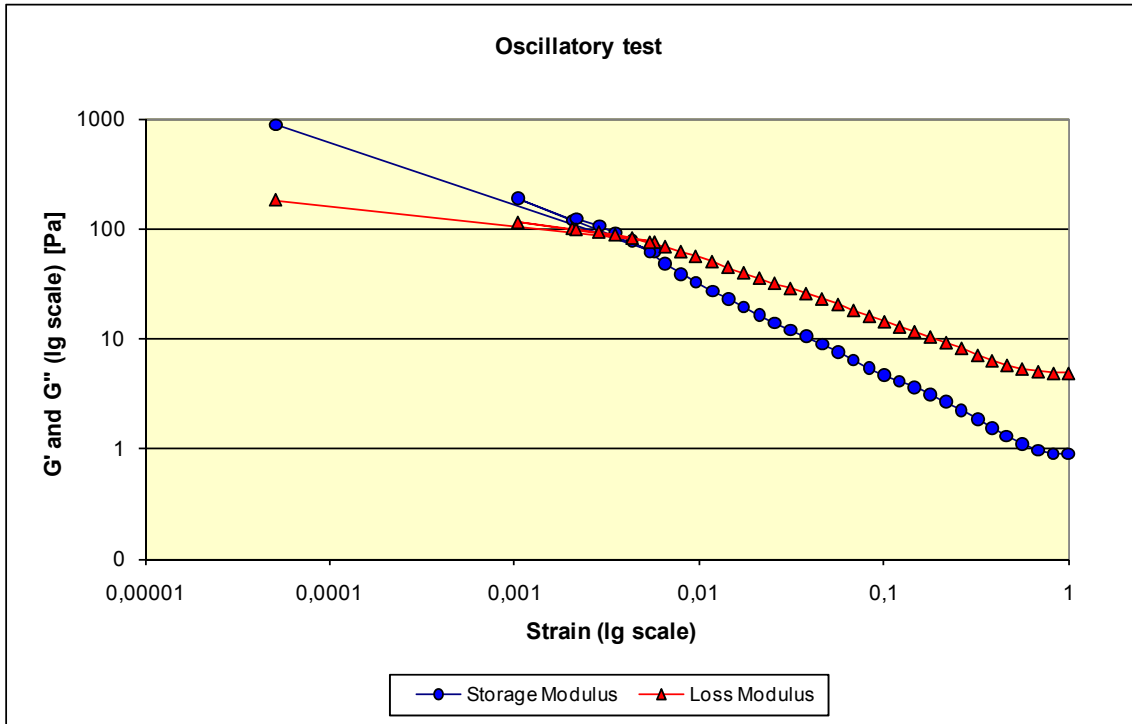


Fig. D-39: Oscillatory test results of matrix No. 20

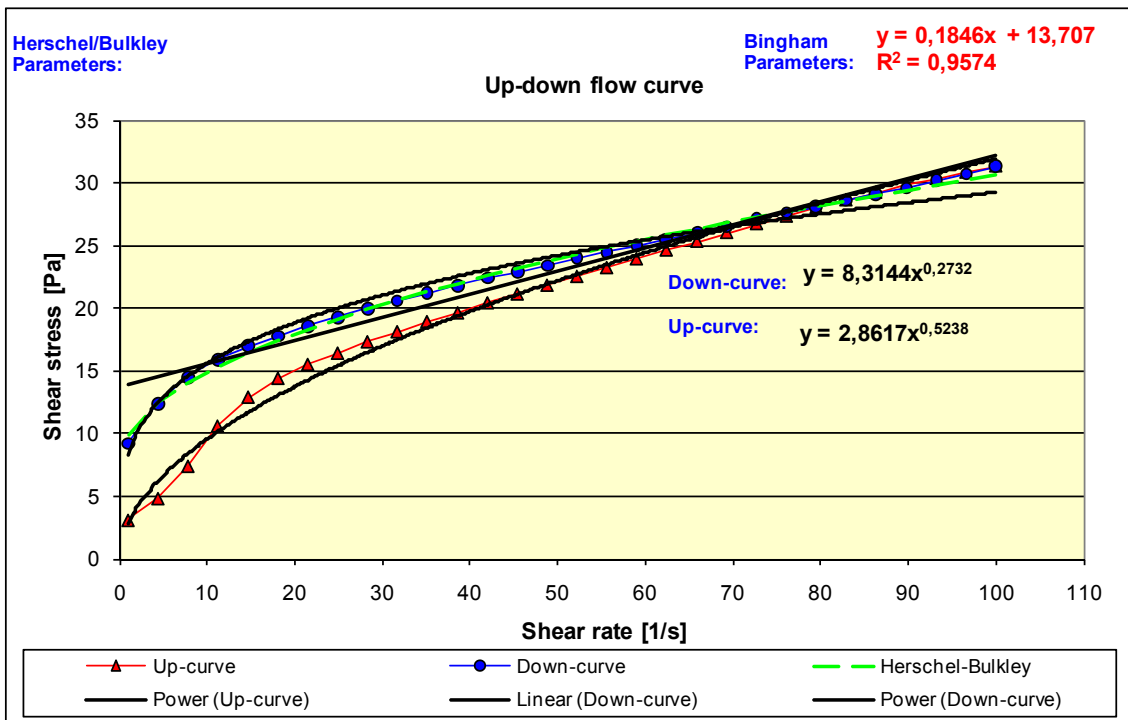


Fig. D-40: Up-down flow curves of matrix No. 20

MATRIX No. 21

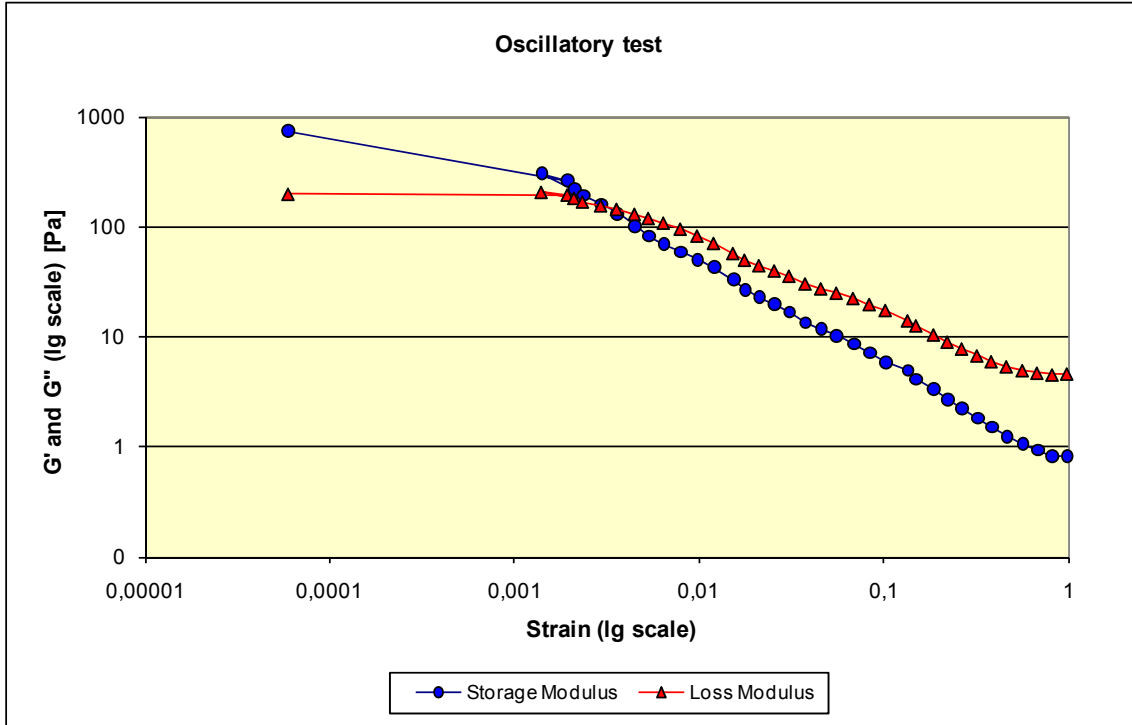


Fig. D-41: Oscillatory test results of matrix No. 21

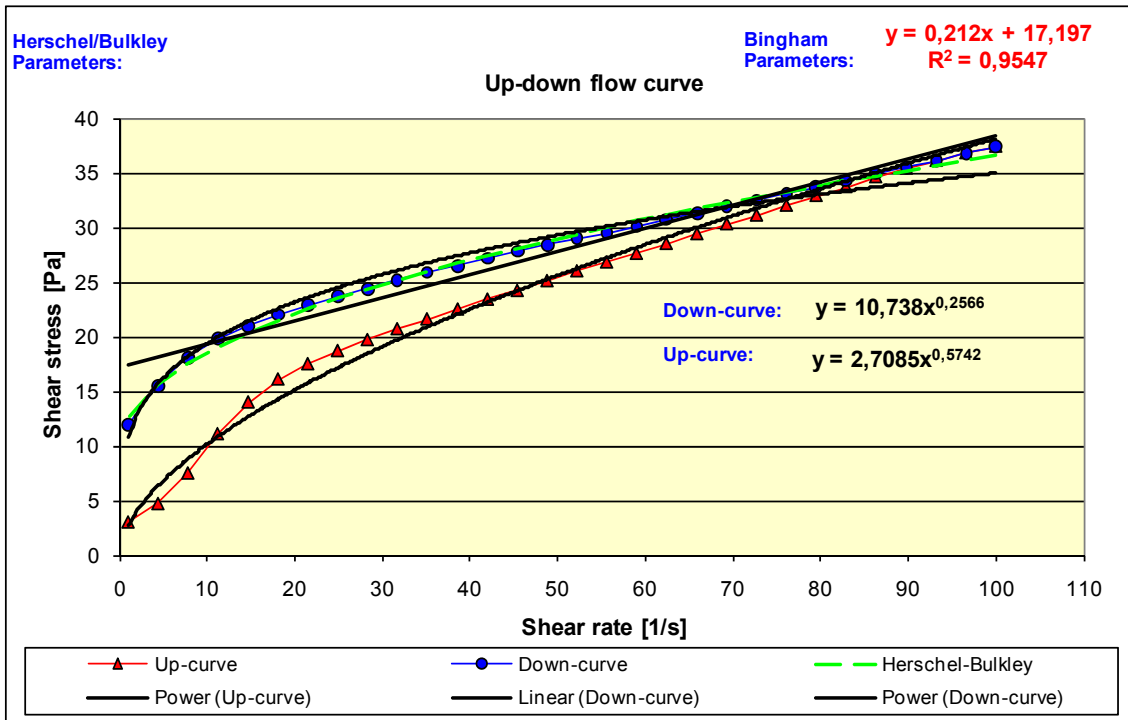


Fig. D-42: Up-down flow curves of matrix No. 21

MATRIX No. 22

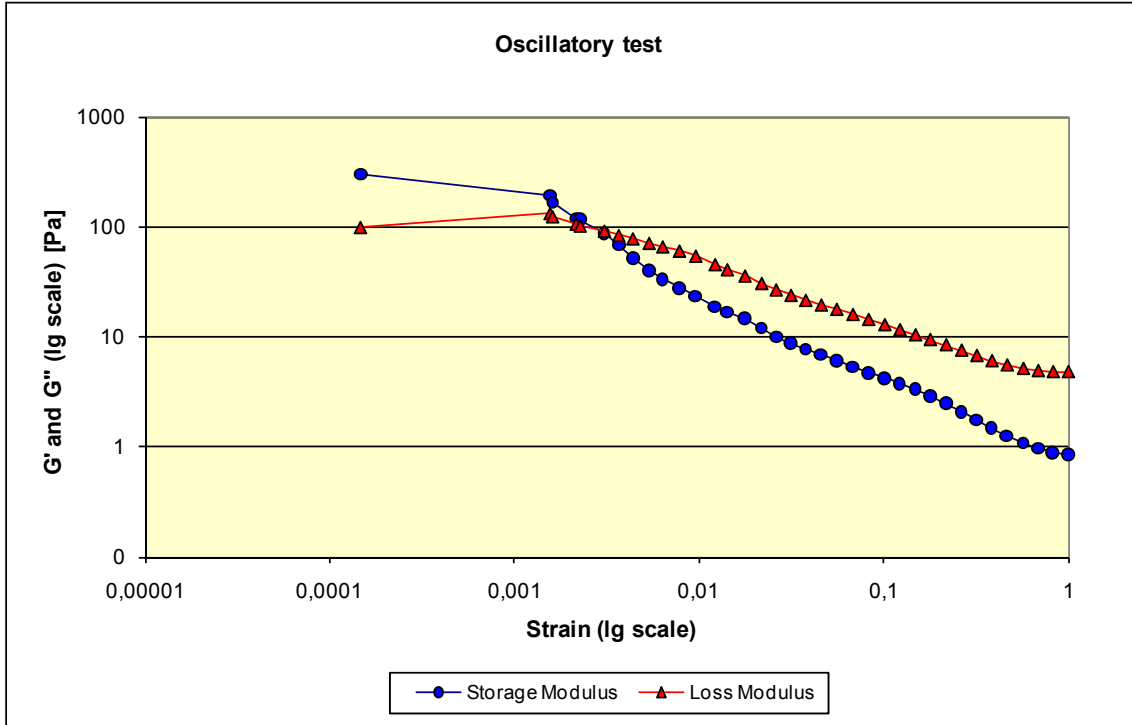


Fig. D-43: Oscillatory test results of matrix No. 22

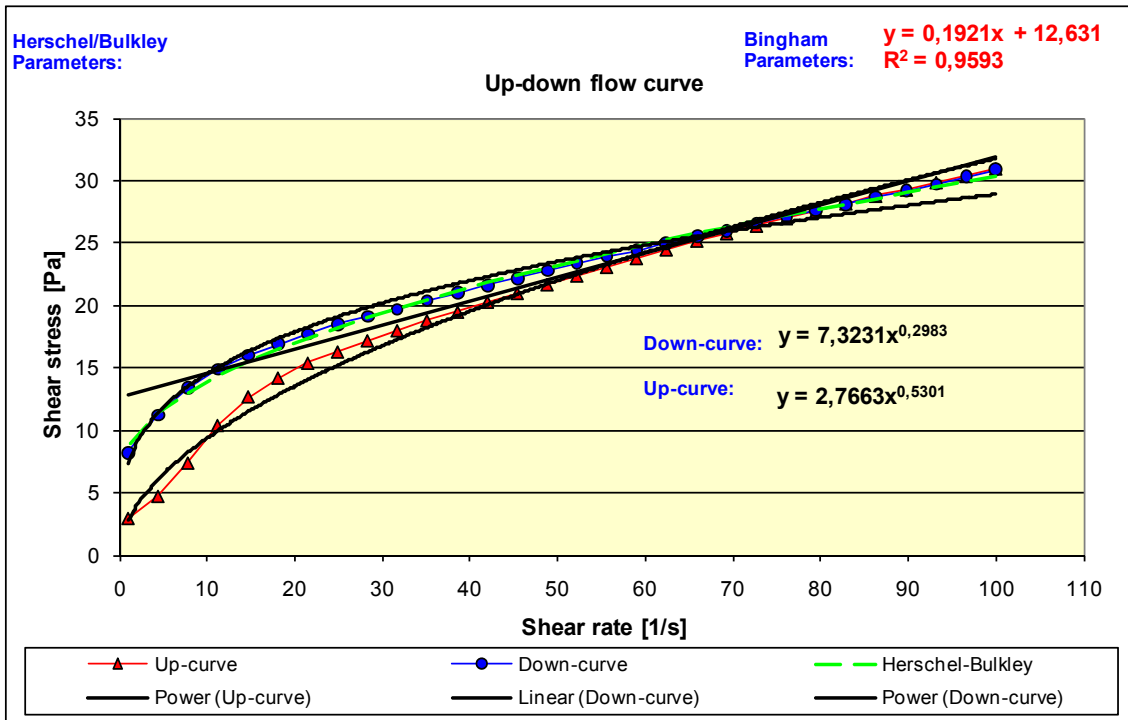


Fig. D-44: Up-down flow curves of matrix No. 22

MATRIX No. 23

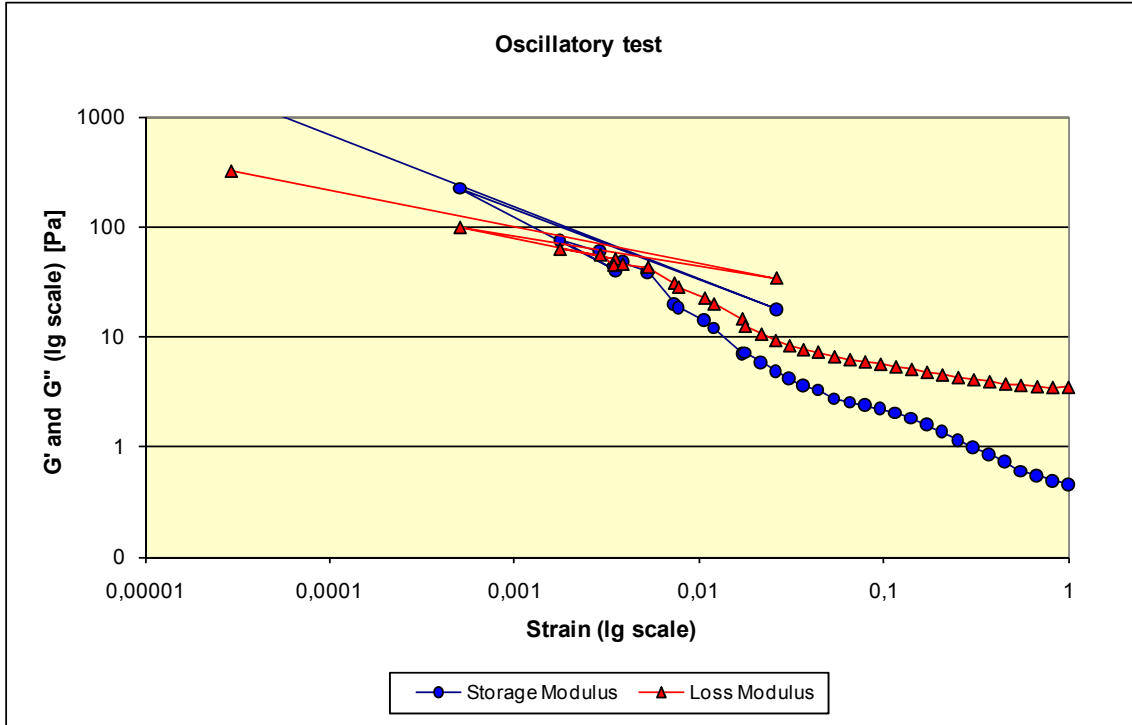


Fig. D-45: Oscillatory test results of matrix No. 23

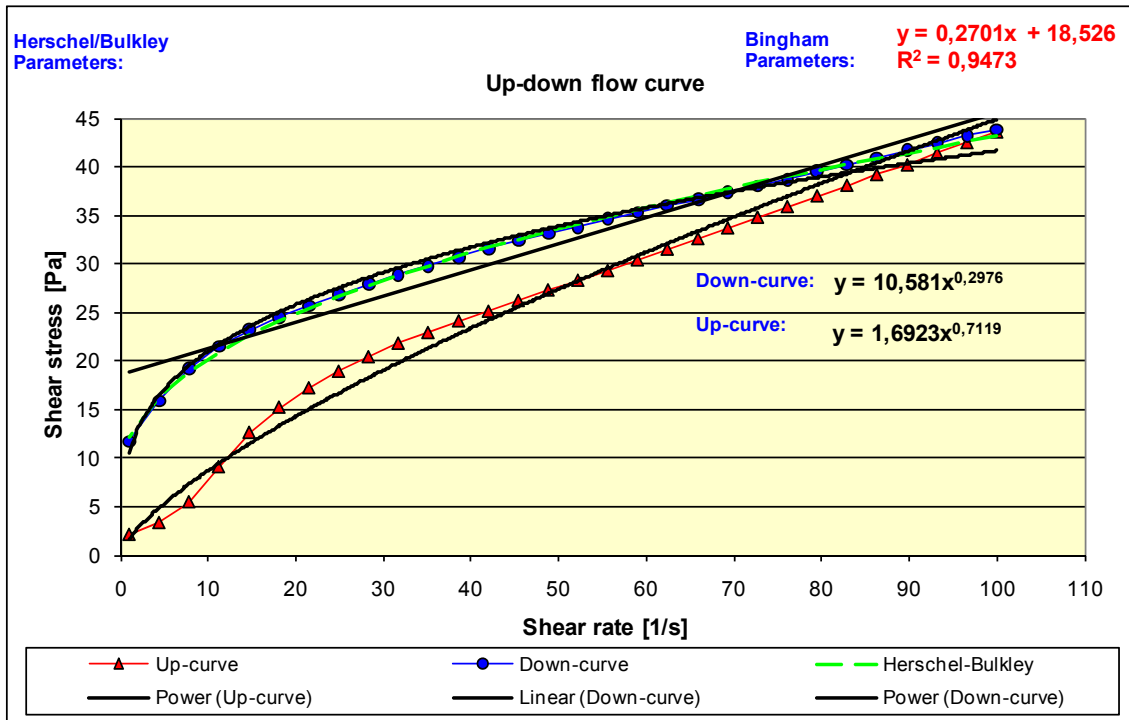


Fig. D-46: Up-down flow curves of matrix No. 23

MATRIX No. 24

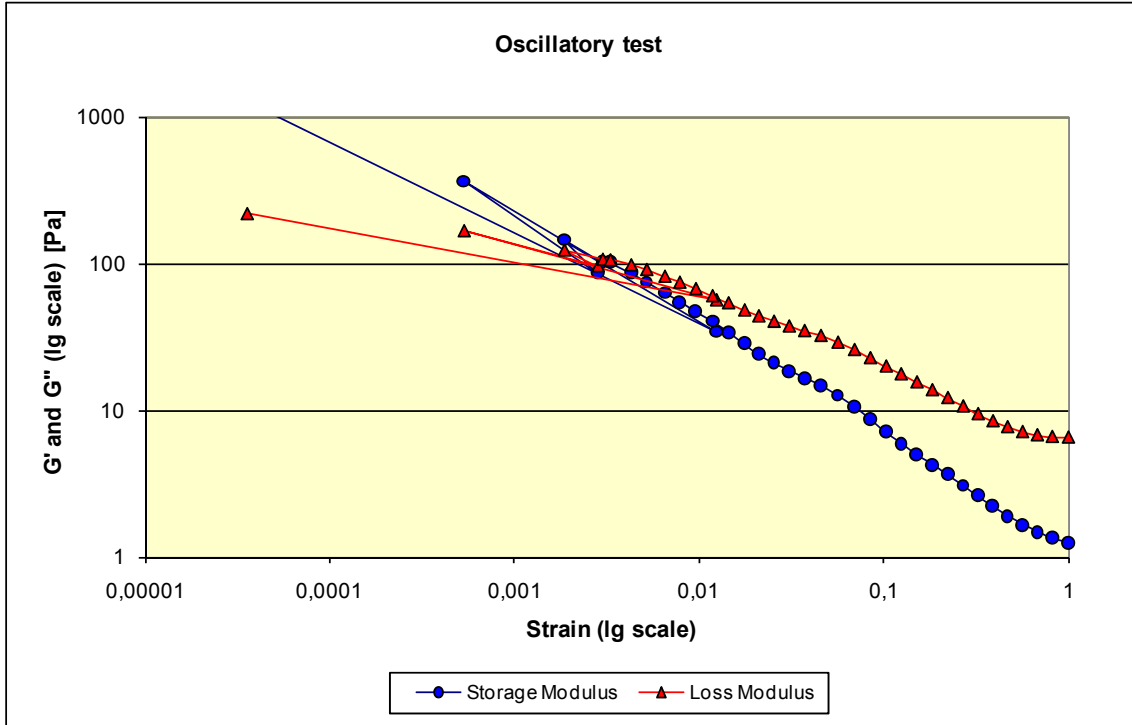


Fig. D-47: Oscillatory test results of matrix No. 24

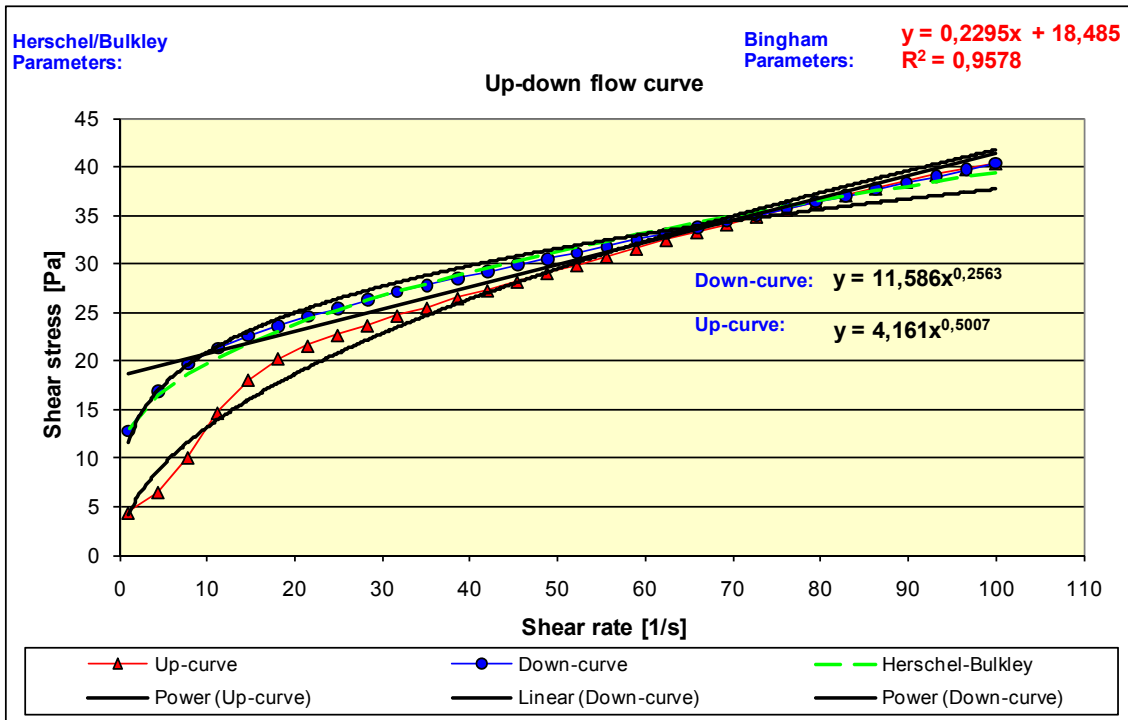


Fig. D-48: Up-down flow curves of matrix No. 24

MATRIX No. 25

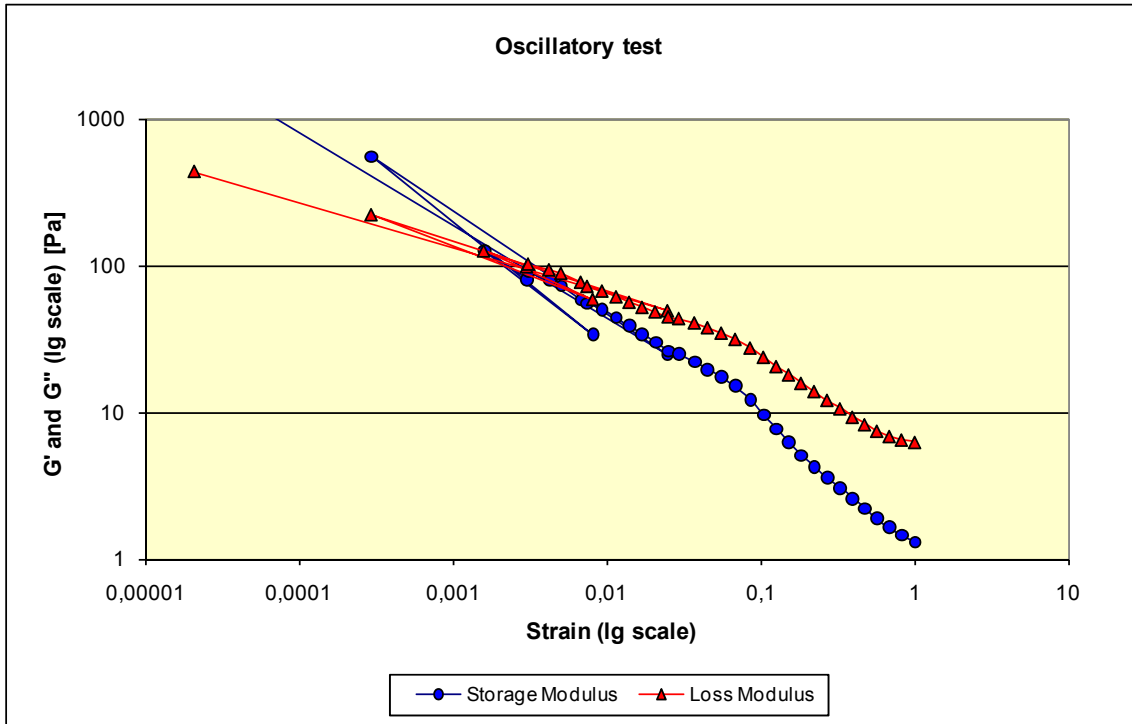


Fig. D-49: Oscillatory test results of matrix No. 25

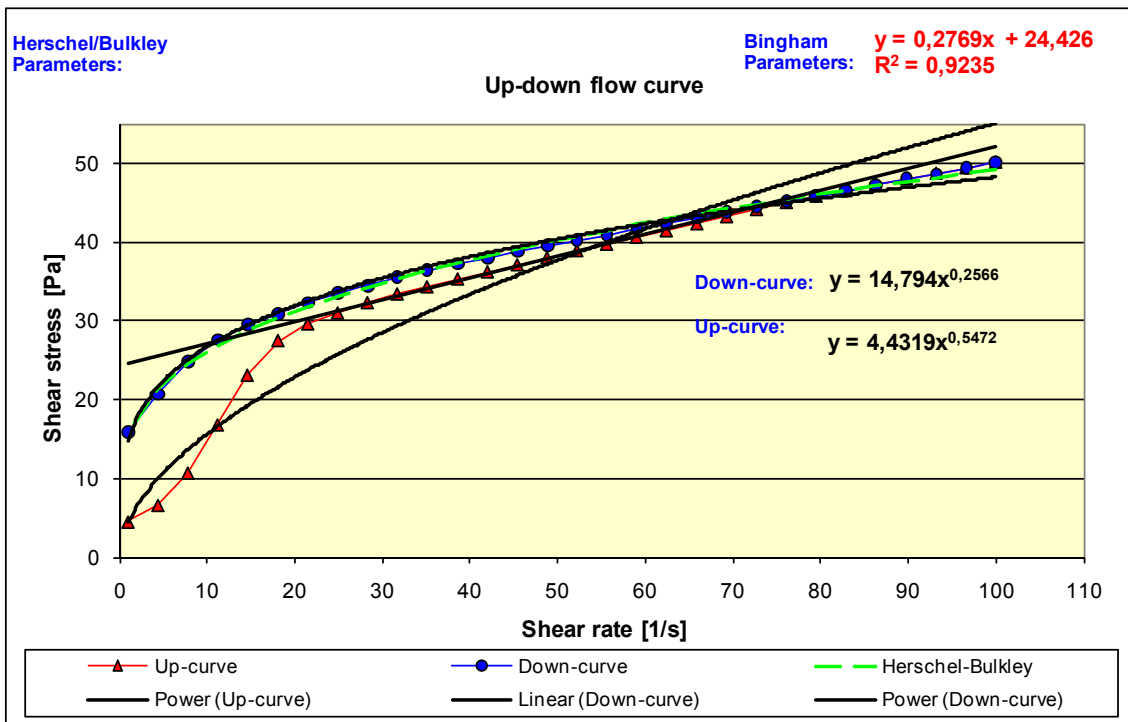


Fig. D-50: Up-down flow curves of matrix No. 25

MATRIX No. 26

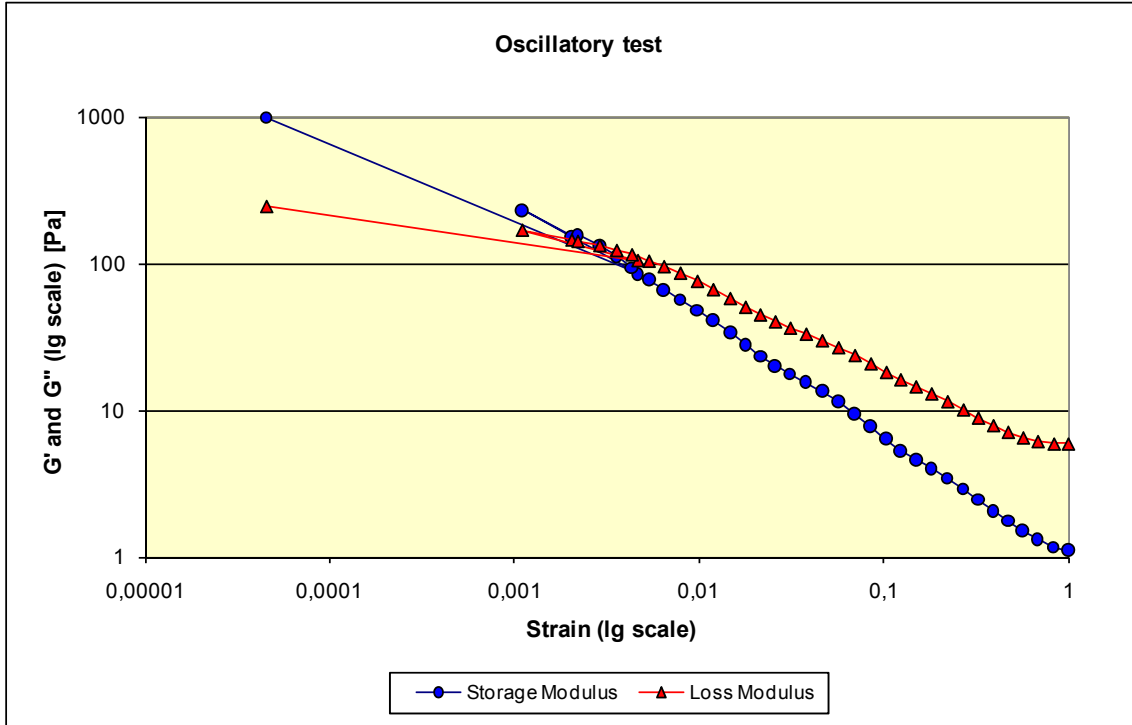


Fig. D-51: Oscillatory test results of matrix No. 26

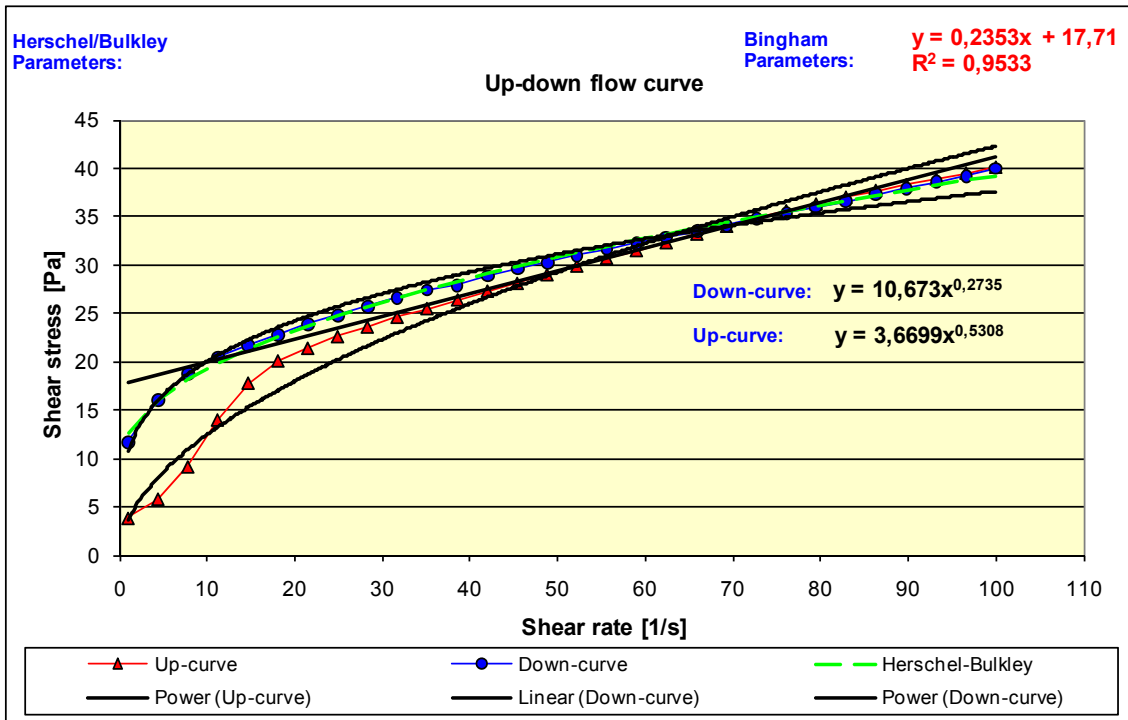


Fig. D-52: Up-down flow curves of matrix No. 26

MATRIX No. 27

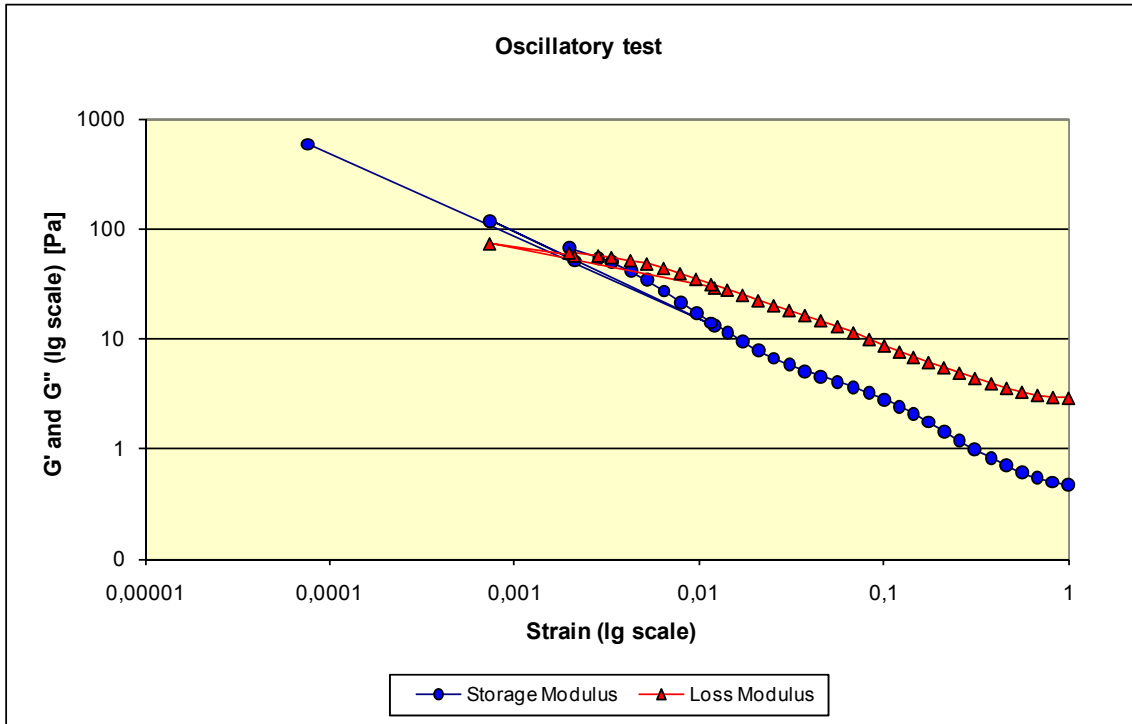


Fig. D-53: Oscillatory test results of matrix No. 27

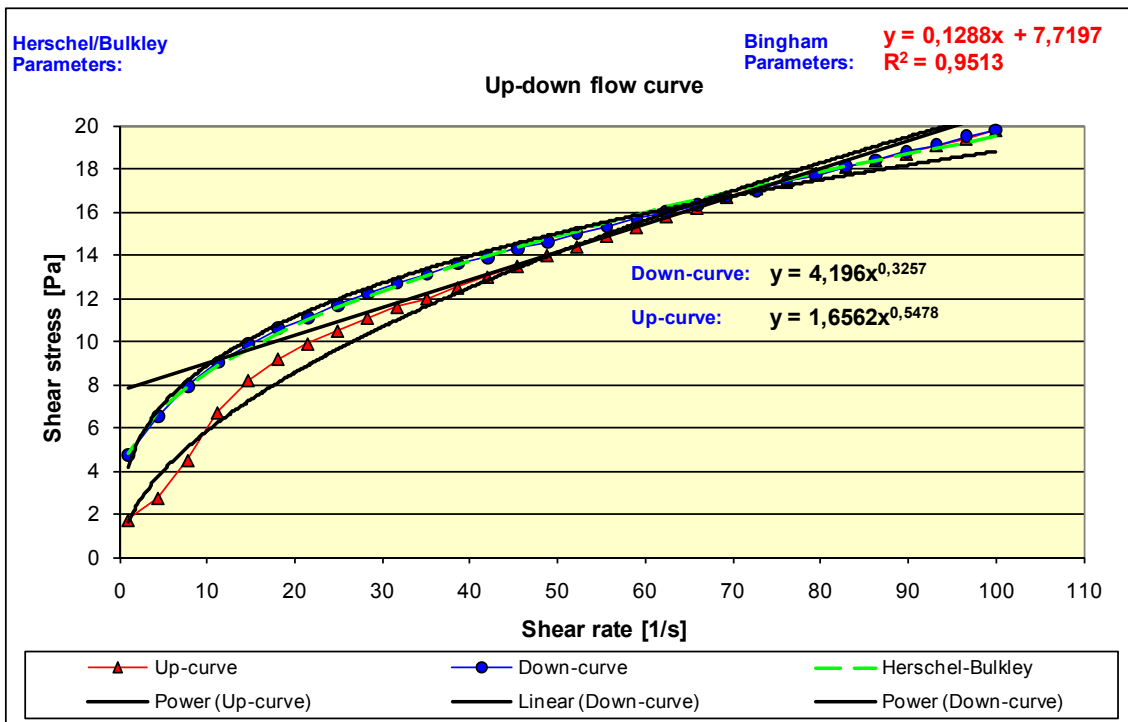


Fig. D-54: Up-down flow curves of matrix No. 27

MATRIX No. 28

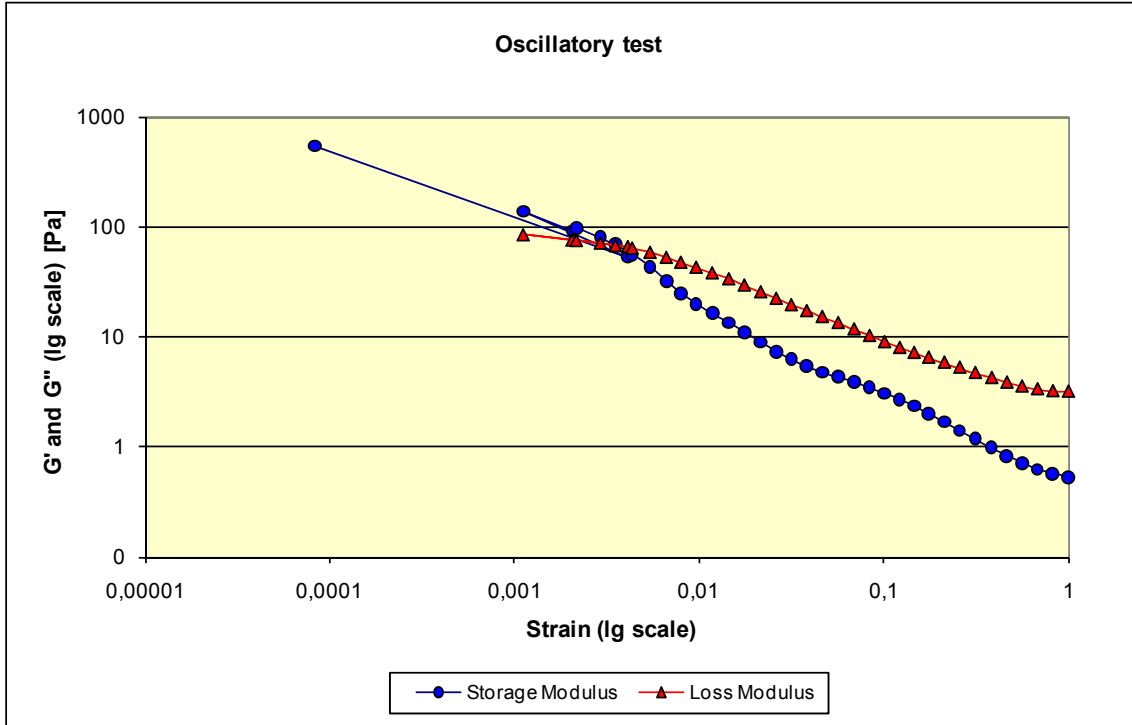


Fig. D-55: Oscillatory test results of matrix No. 28

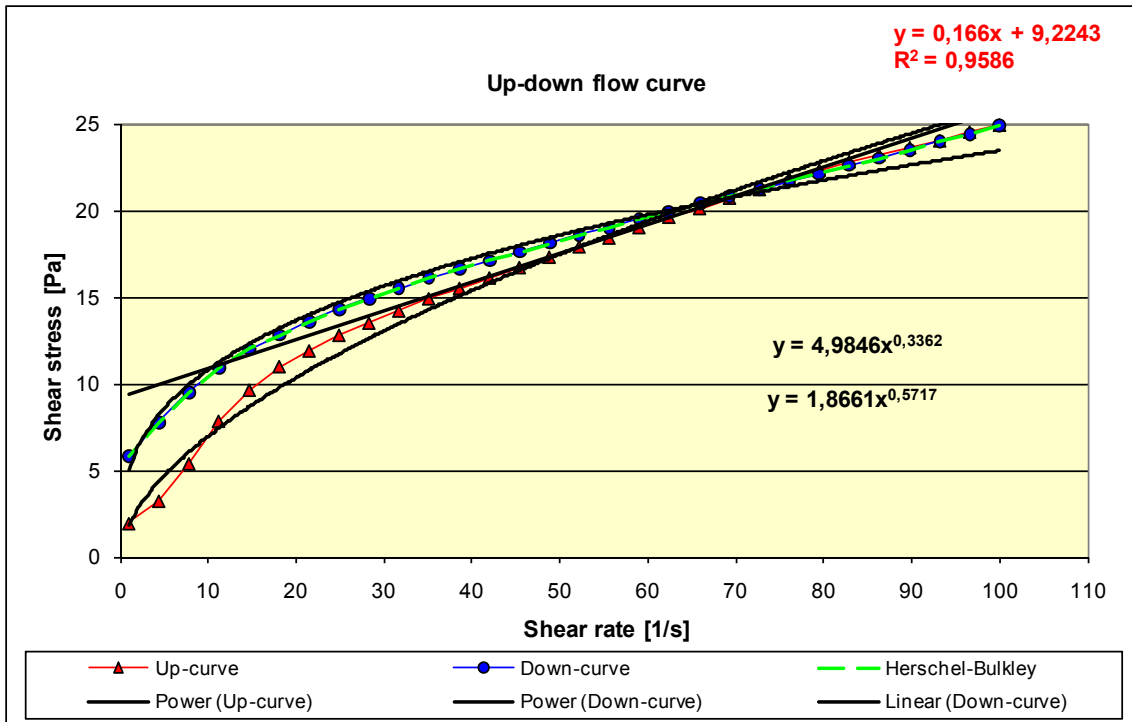


Fig. D-56: Up-down flow curves of matrix No. 28

MATRIX No. 29

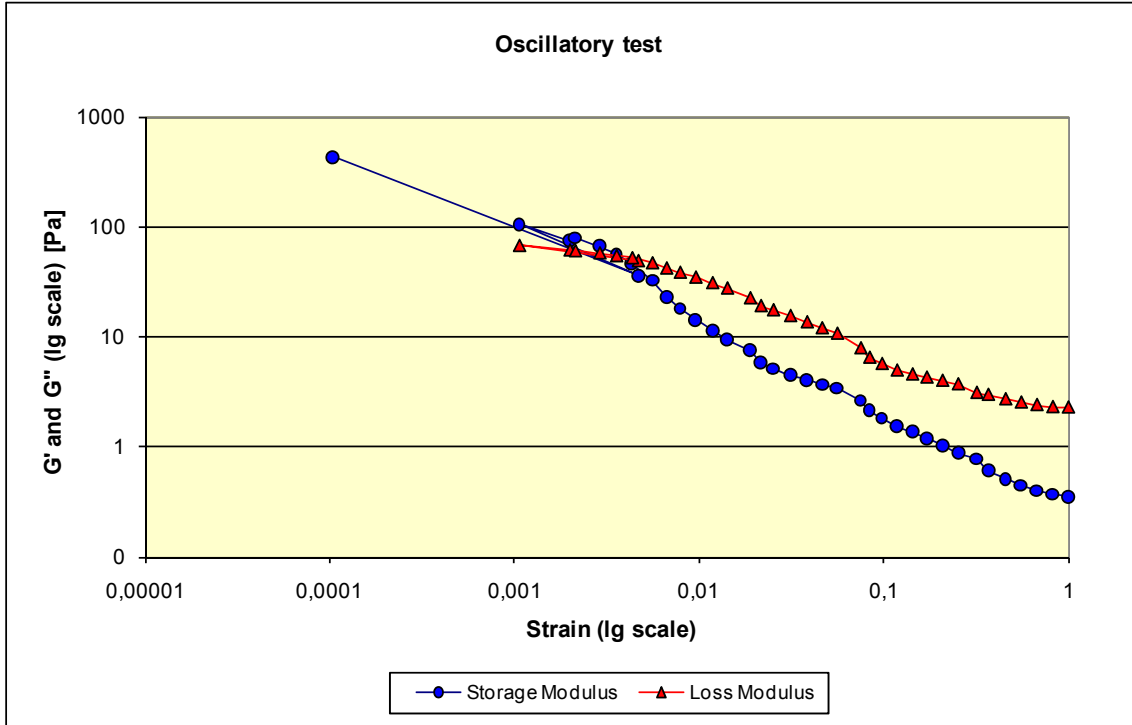


Fig. D-57: Oscillatory test results of matrix No. 29

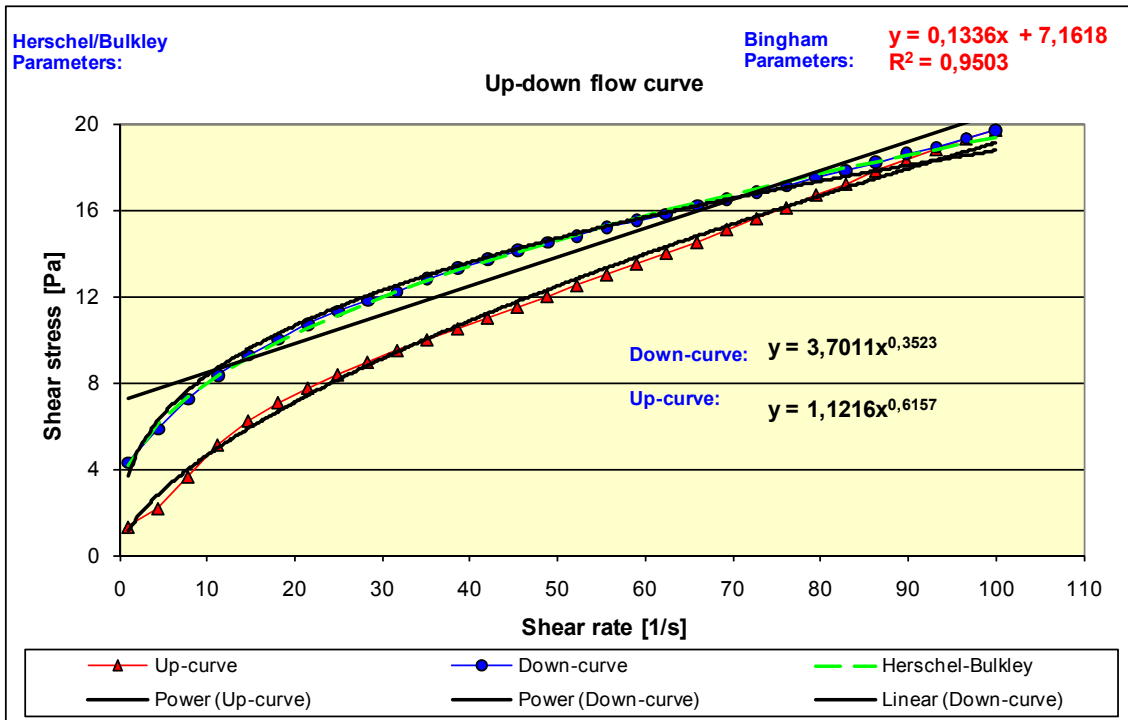


Fig. D-58: Up-down flow curves of matrix No. 29

MATRIX No. 30

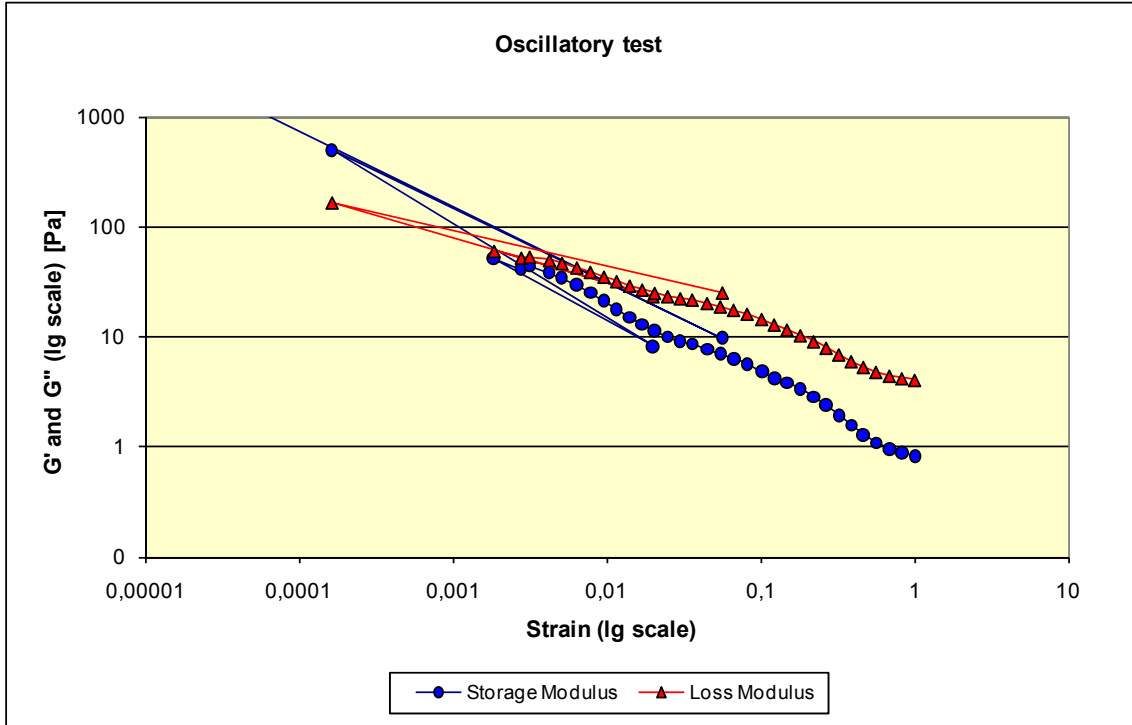


Fig. D-59: Oscillatory test results of matrix No. 30

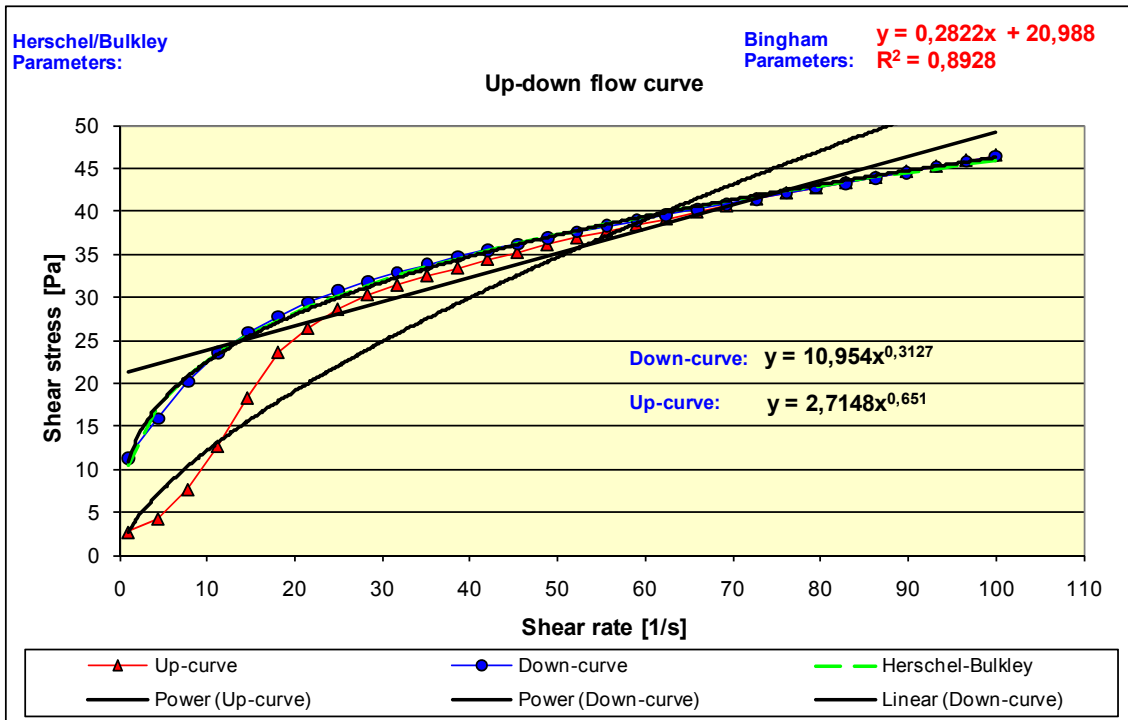


Fig. D-60: Up-down flow curves of matrix No. 30

MATRIX No. 31

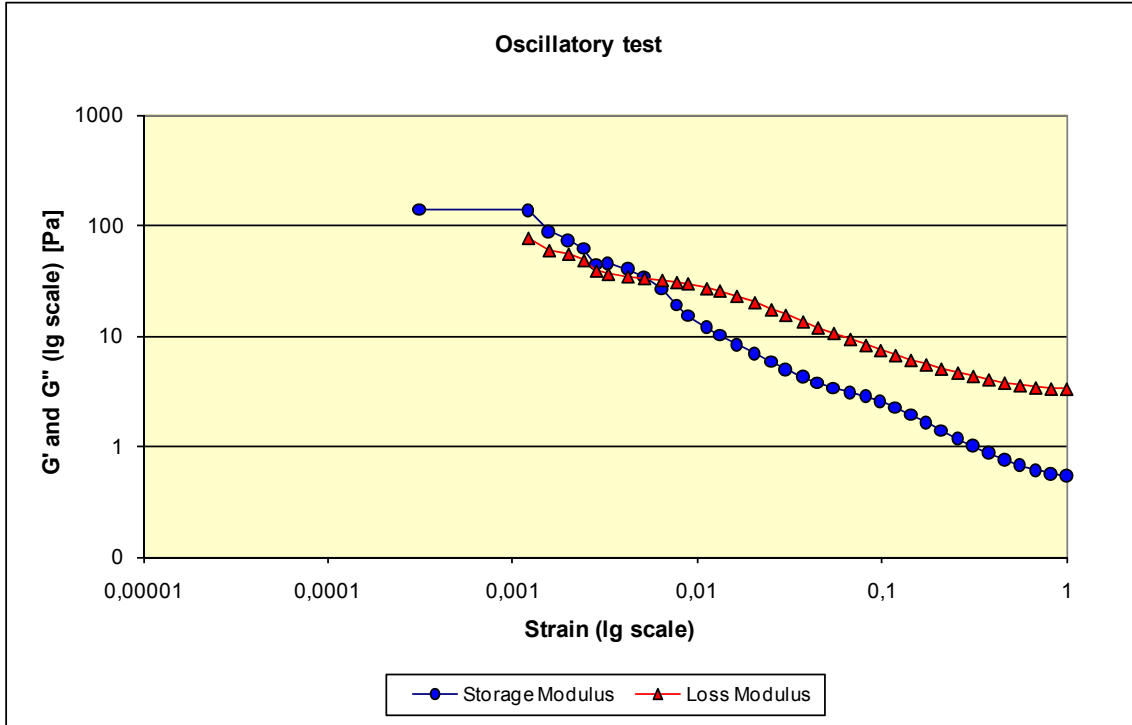


Fig. D-61: Oscillatory test results of matrix No. 31

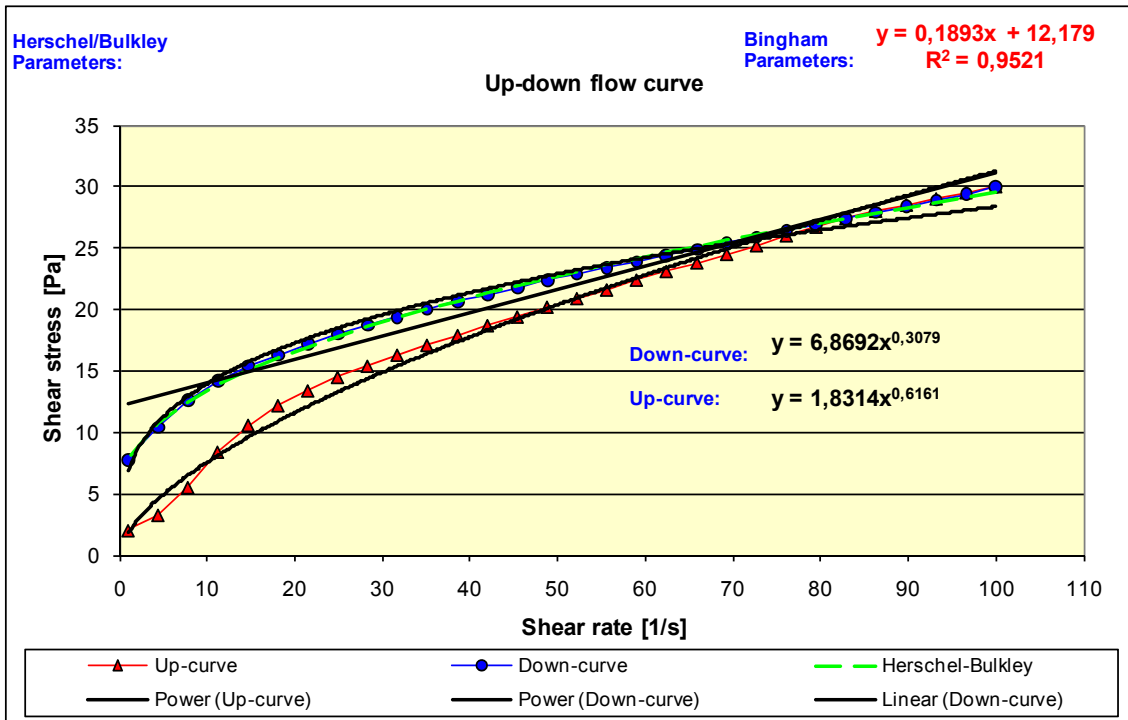


Fig. D-62: Up-down flow curves of matrix No. 31

MATRIX No. 32

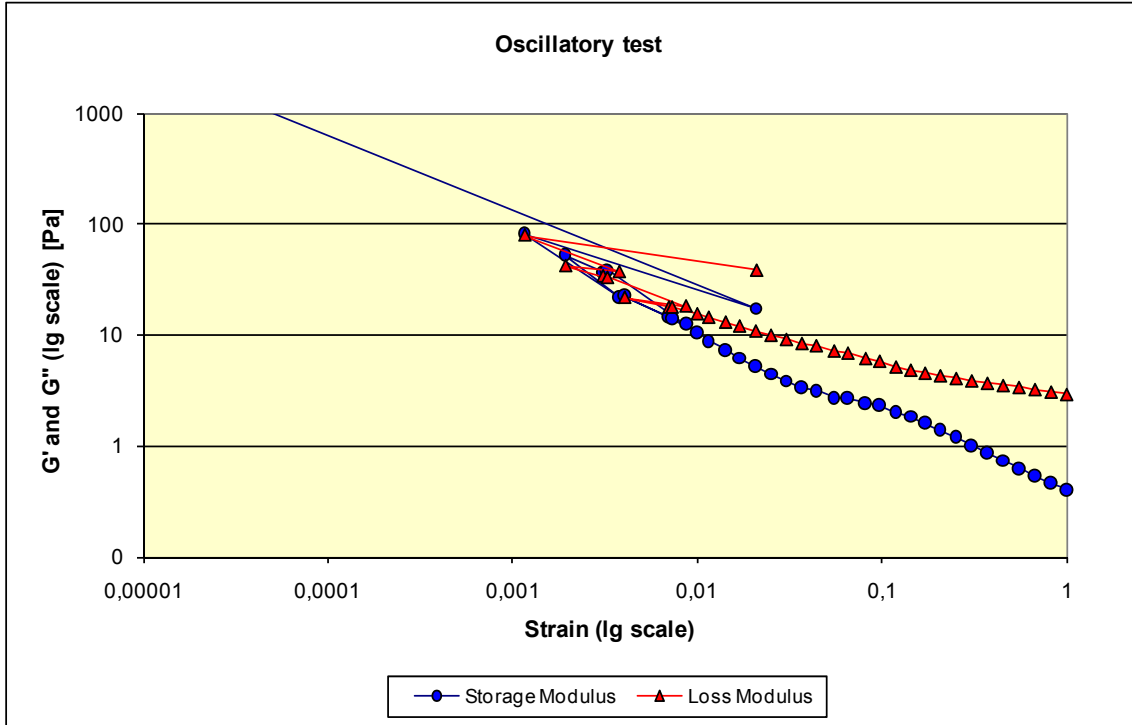


Fig. D-63: Oscillatory test results of matrix No. 32

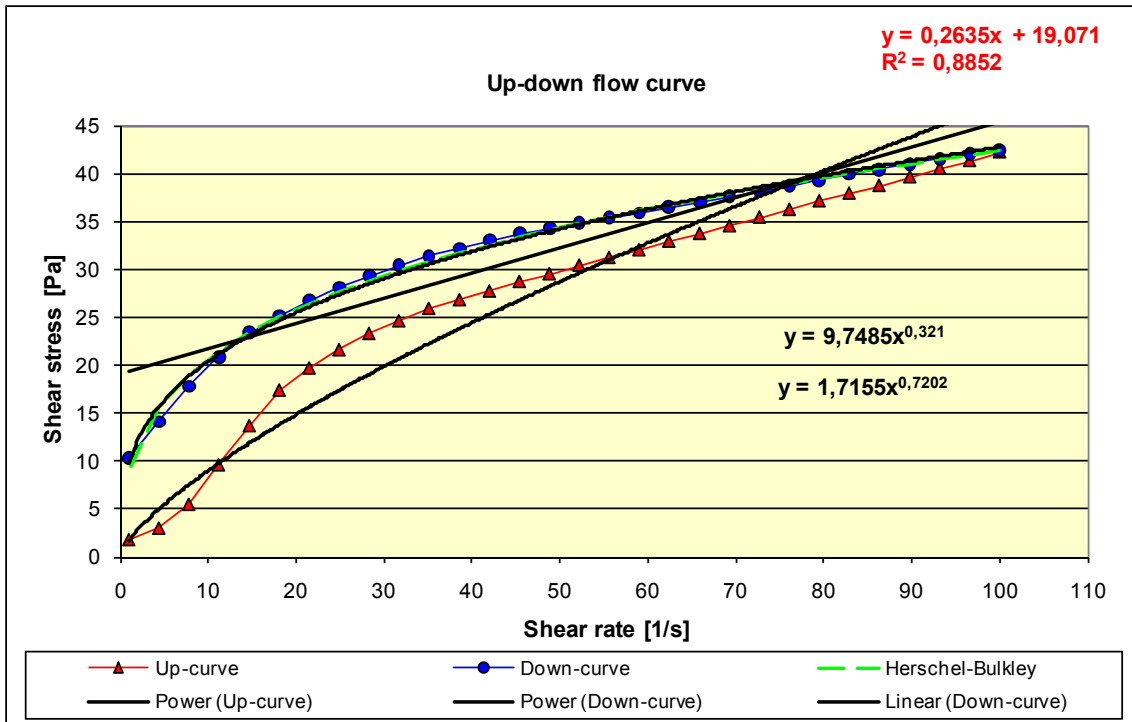


Fig. D-64: Up-down flow curves of matrix No. 32

MATRIX No. 33

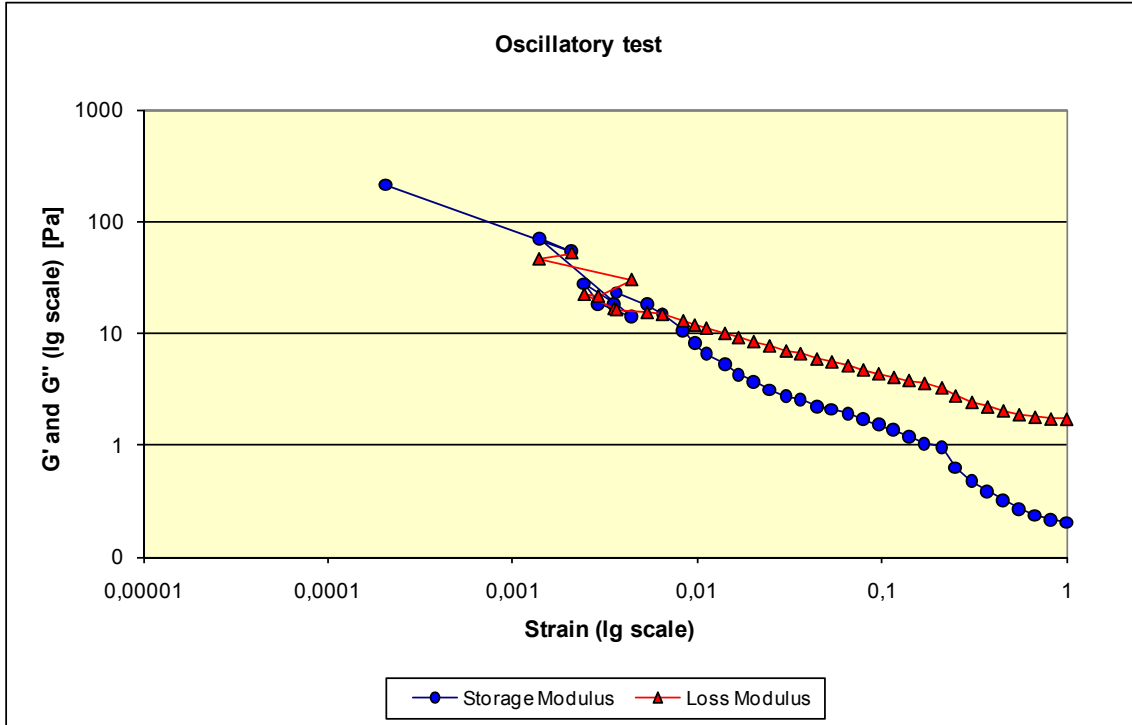


Fig. D-65: Oscillatory test results of matrix No. 33

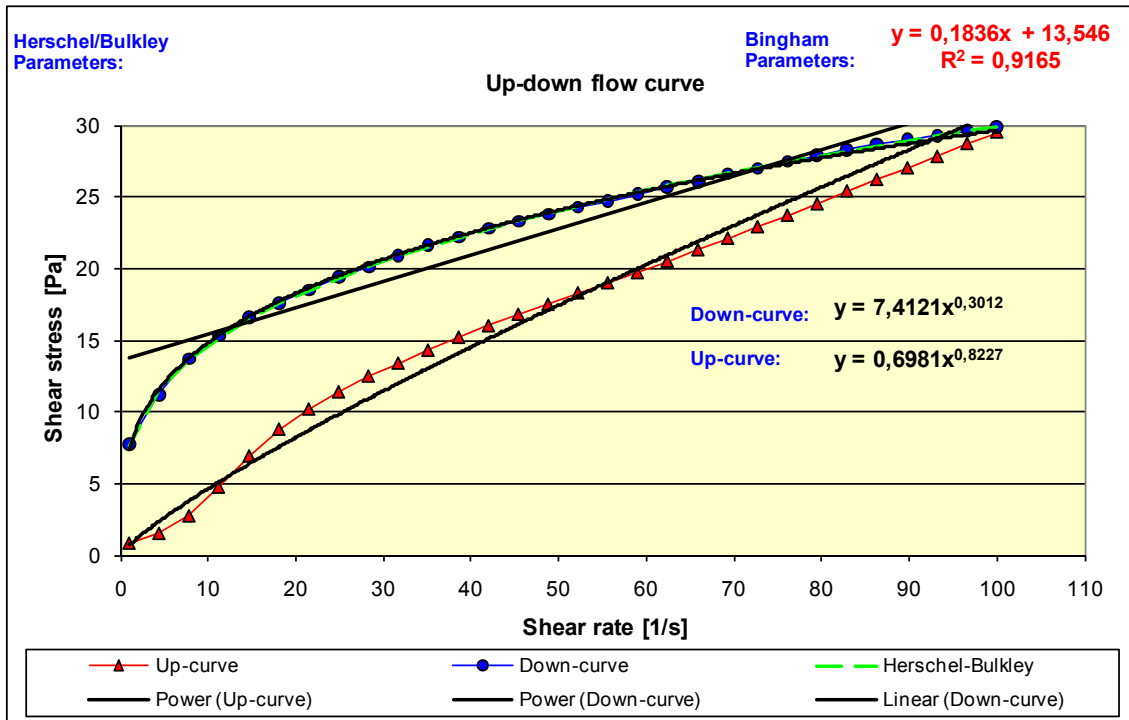


Fig. D-66: Up-down flow curves of matrix No. 33

MATRIX No. 34 (see MATRIX No. 17)

MATRIX No. 35

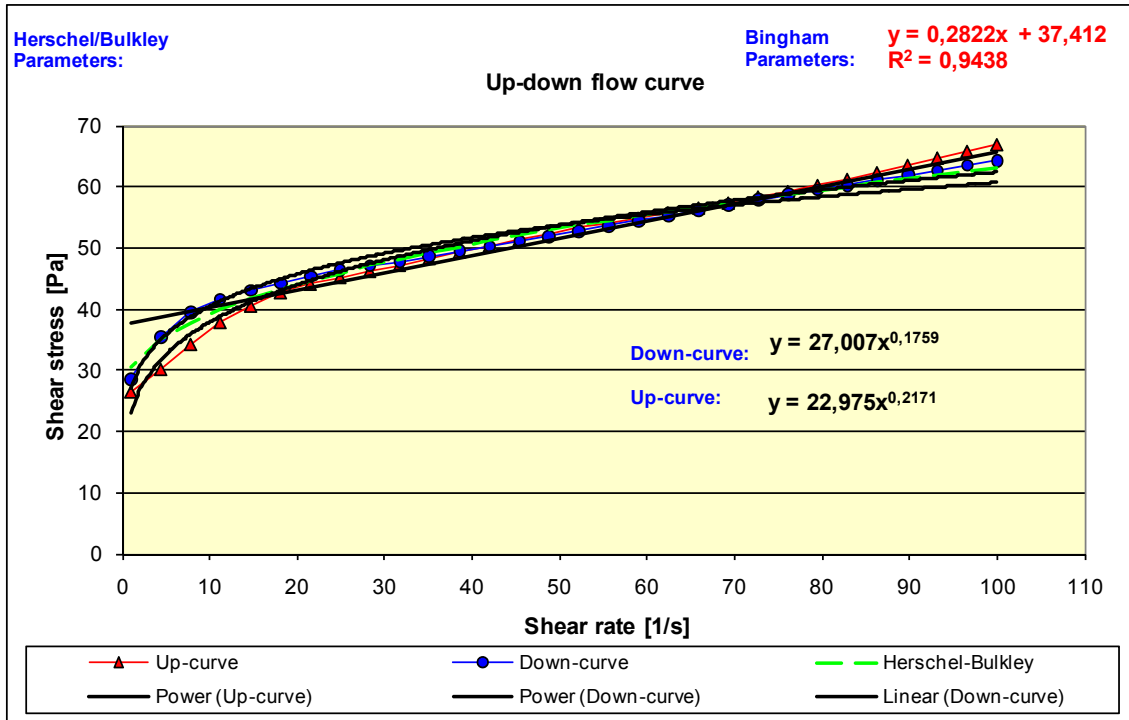


Fig. D-67: Up-down flow curves of matrix No. 35

MATRIX No. 36

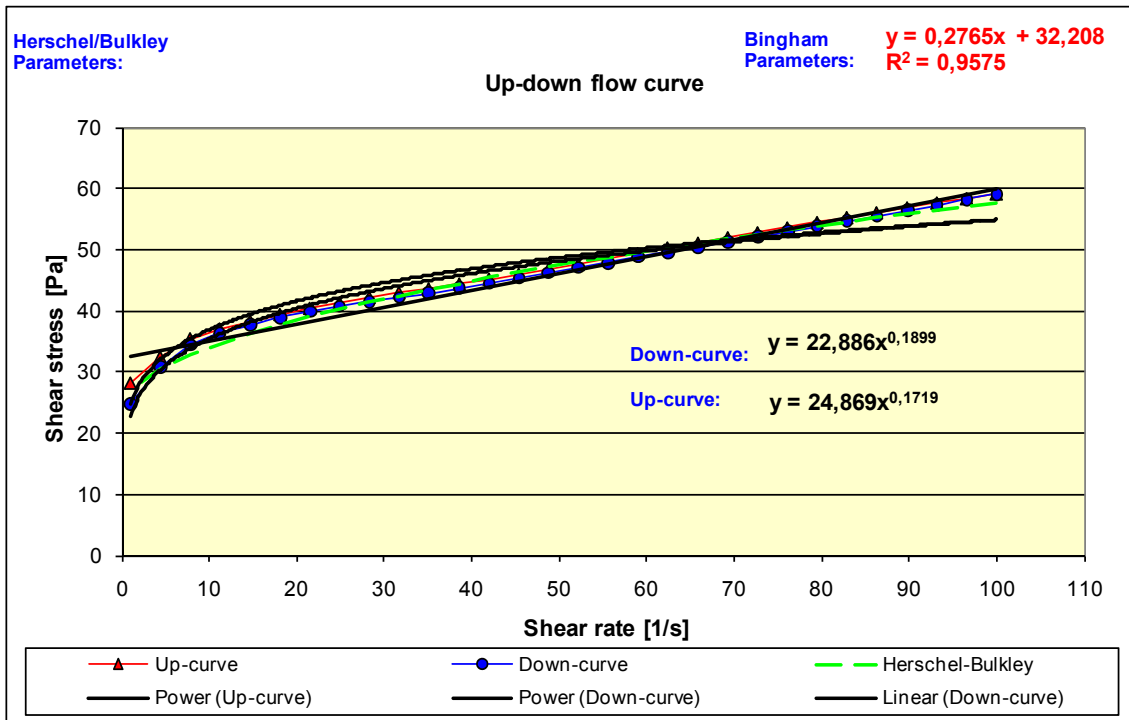


Fig. D-68: Up-down flow curves of matrix No. 36

MATRIX No. 37

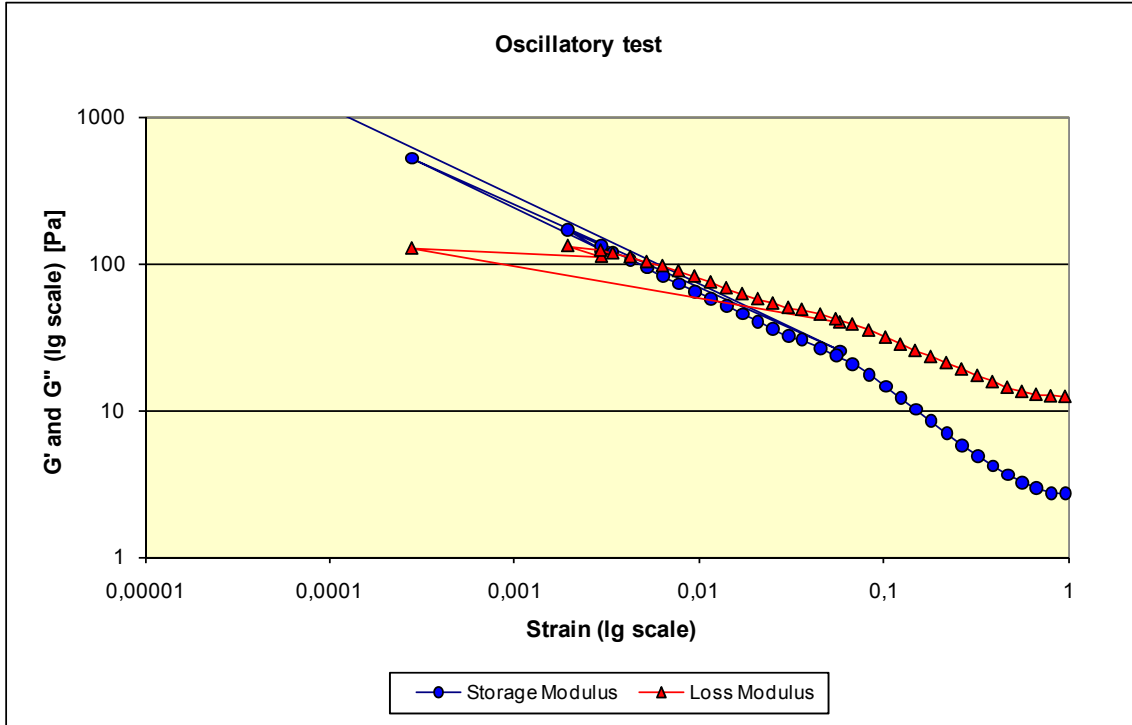


Fig. D-69: Oscillatory test results of matrix No. 37

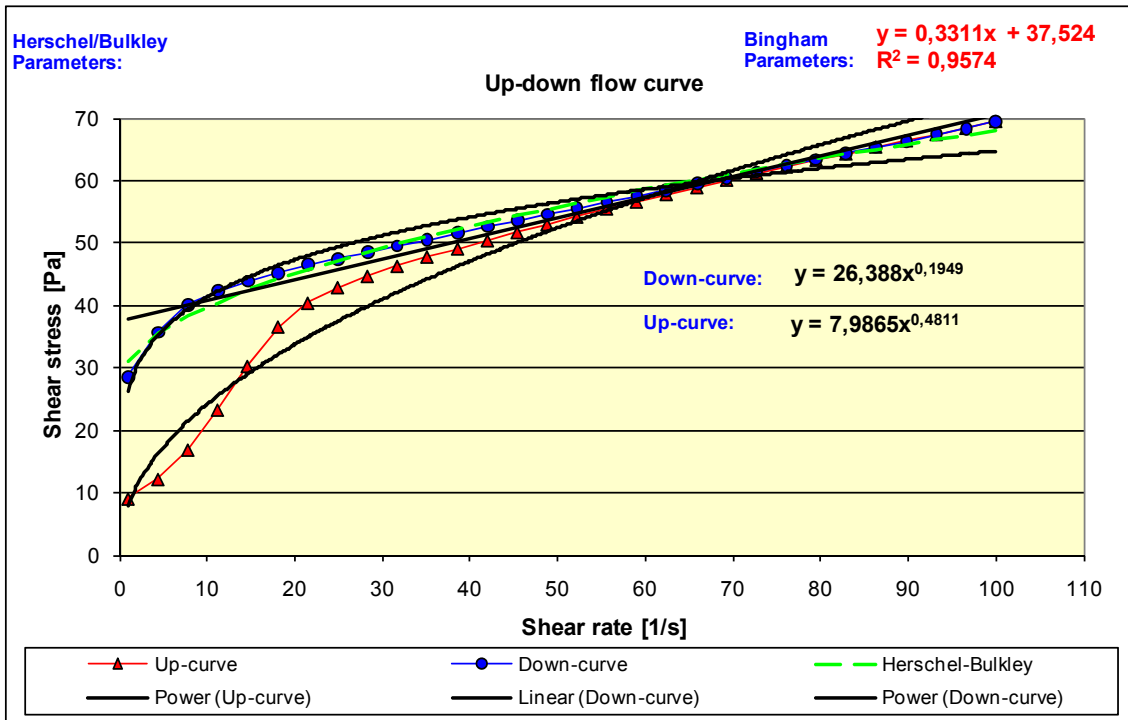


Fig. D-70: Up-down flow curves of matrix No. 37

MATRIX No. 38

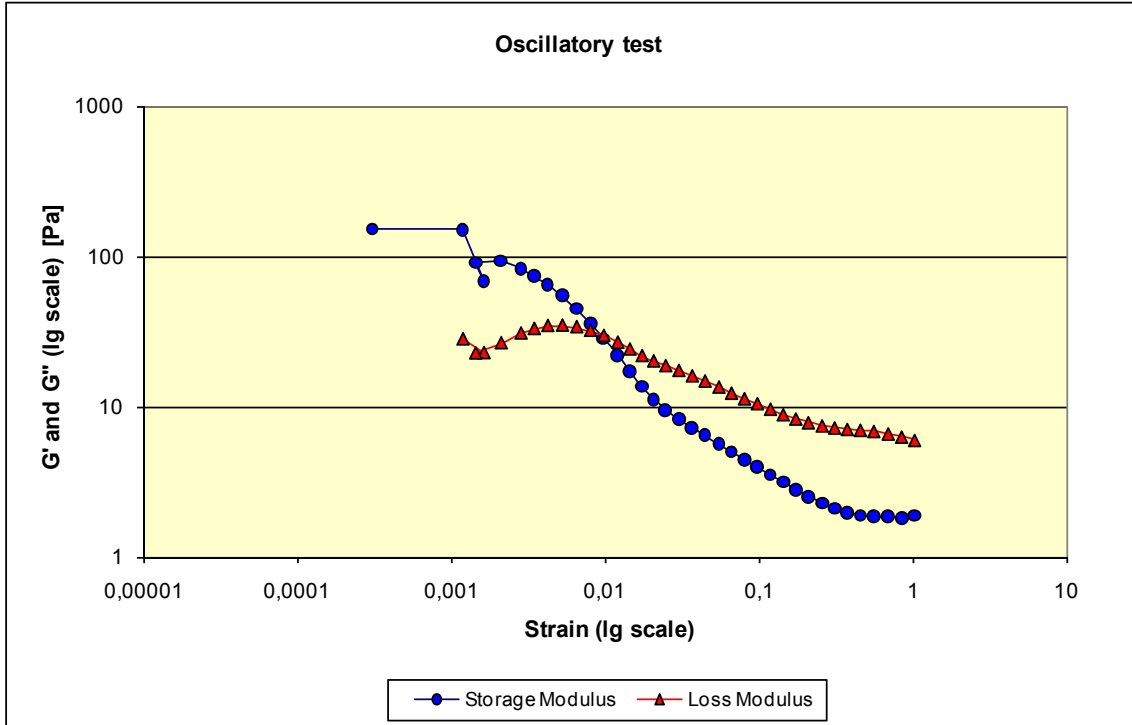


Fig. D-71: Oscillatory test results of matrix No. 38

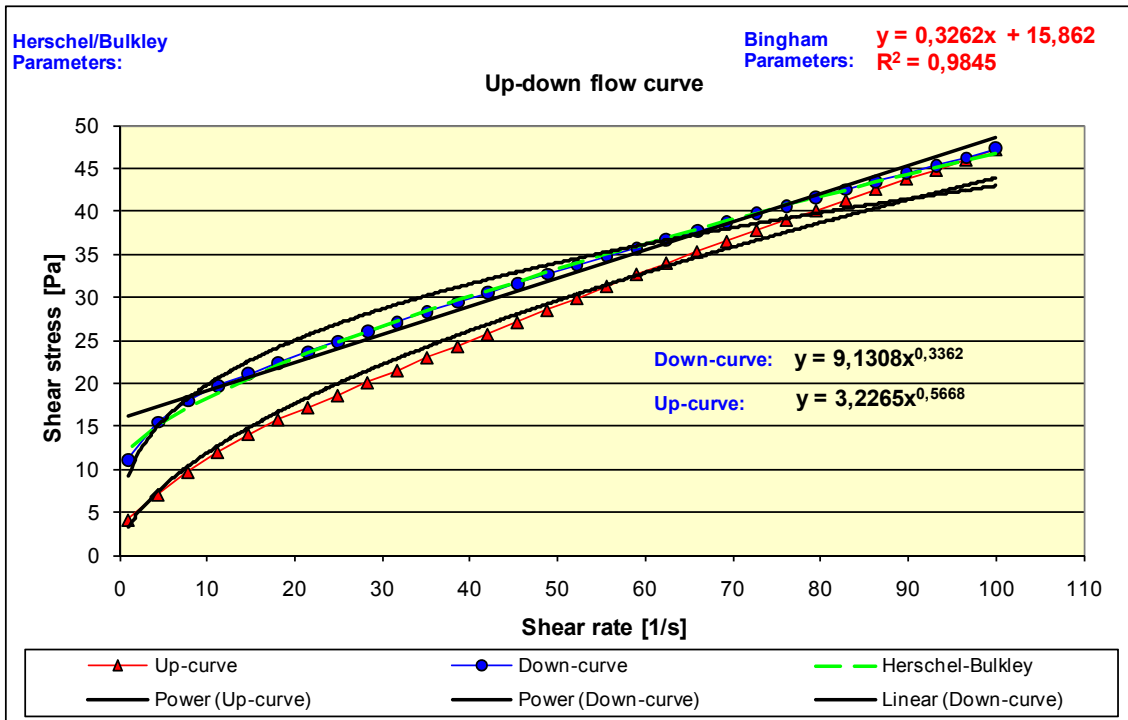


Fig. D-72: Up-down flow curves of matrix No. 38

APPENDIX E – Mix design of the tested SCC

In the following (table E-1), you will find complete mix designs for all SCC mixes. SCC mix numbers are according to Tables 3-8 and 3-9.

Table E-1: SCC mix design

SCC mix No.	w/c=w/b	"Low-filler" sand 0/8 mm, kg/m ³	8/16 mm coarse aggregate, kg/m ³	Extra filler, kg/m ³	Filler type	CEM II/A-V (STD FA), kg/m ³	Effective Water, kg/m ³	Dynamon SP-130, %	Matrix, l/m ³
1	0.40	1155	519	no extra f.	no extra f.	468	187	2.0	360
2	0.50	1137	536	57	Årdal natural	389	194	1.1	360
3	0.50	1137	536	57	Årdal natural (crushed/unwashed)	389	194	1.1	360
4	0.50	1137	536	57	Årdal natural (crushed/washed)	389	194	1.1	360
5	0.50	1139	535	59	Tau	389	194	1.1	360
6	0.50	1139	535	59	Jelsa	389	194	1.1	360
7	0.50	1140	534	60	Hokksund	389	194	1.1	360
8	0.50	1138	536	58	Limestone	389	194	1.1	360
9	0.60	1125	548	115	Årdal natural	324	194	1.1	360
10	0.60	1125	548	115	Årdal natural (crushed/unwashed)	324	194	1.1	360
11	0.60	1125	548	115	Årdal natural (crushed/washed)	324	194	1.1	360
12	0.60	1125	549	120	Tau	324	195	1.1	360
13	0.60	1126	547	120	Jelsa	324	194	1.1	360
14	0.60	1128	546	122	Hokksund	324	194	1.1	360
15	0.60	1125	549	117	Limestone	324	194	1.1	360
16	0.77	1039	525	112	Årdal natural	314	240	0.6	400
17	0.77	1039	525	112	Årdal natural (crushed/unwashed)	314	240	0.6	400
18	0.77	1039	525	112	Årdal natural (crushed/washed)	314	240	0.6	400
19	0.77	1039	525	117	Tau	314	240	0.6	400
20	0.77	1039	525	117	Jelsa	314	240	0.6	400
21	0.77	1041	522	119	Hokksund	314	240	0.6	400
22	0.77	1038	525	114	Limestone	314	240	0.6	400

APPENDIX F – SCC down flow curves

In the following (figures F-1 to F-22), you will find complete plots of down flow curves for all SCC mixes. SCC mix numbers are according to Tables 3-8 and 3-9.

SCC mix No. 1

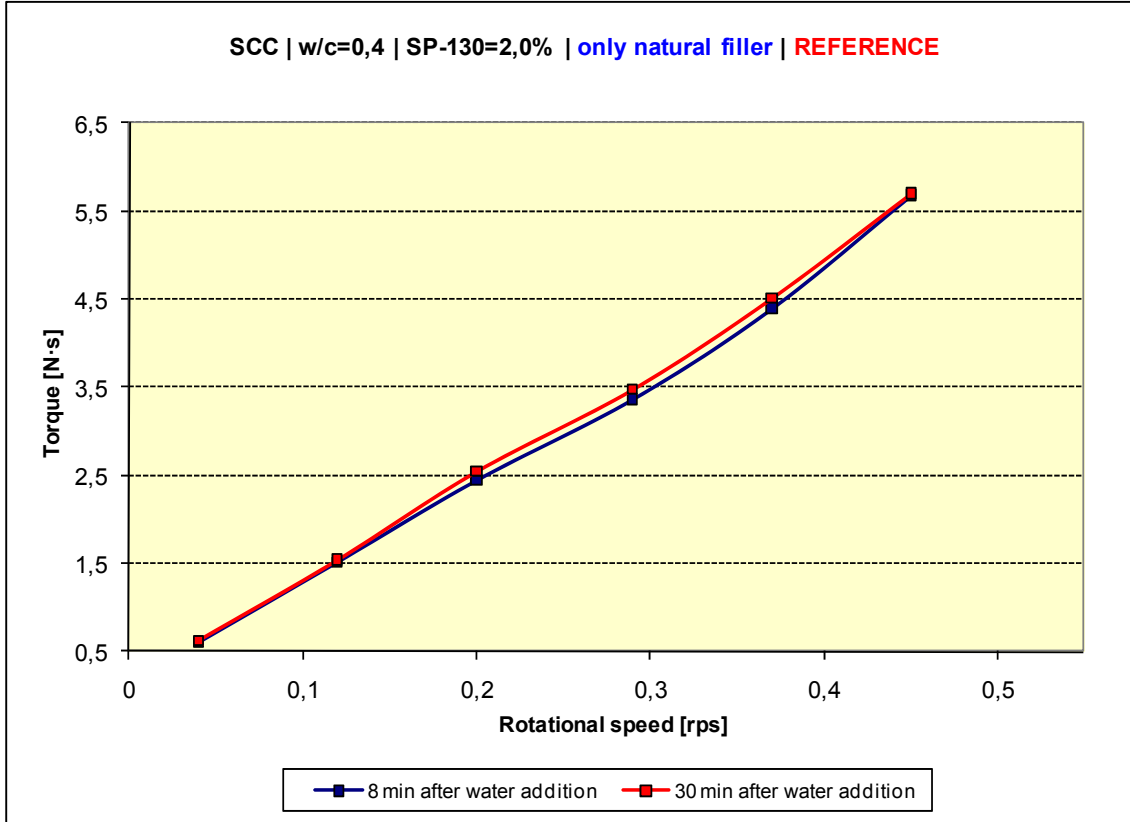


Fig. F-1: Relation torque (T) - rotational speed (N) of SCC mix No. 1

SCC mix No. 2

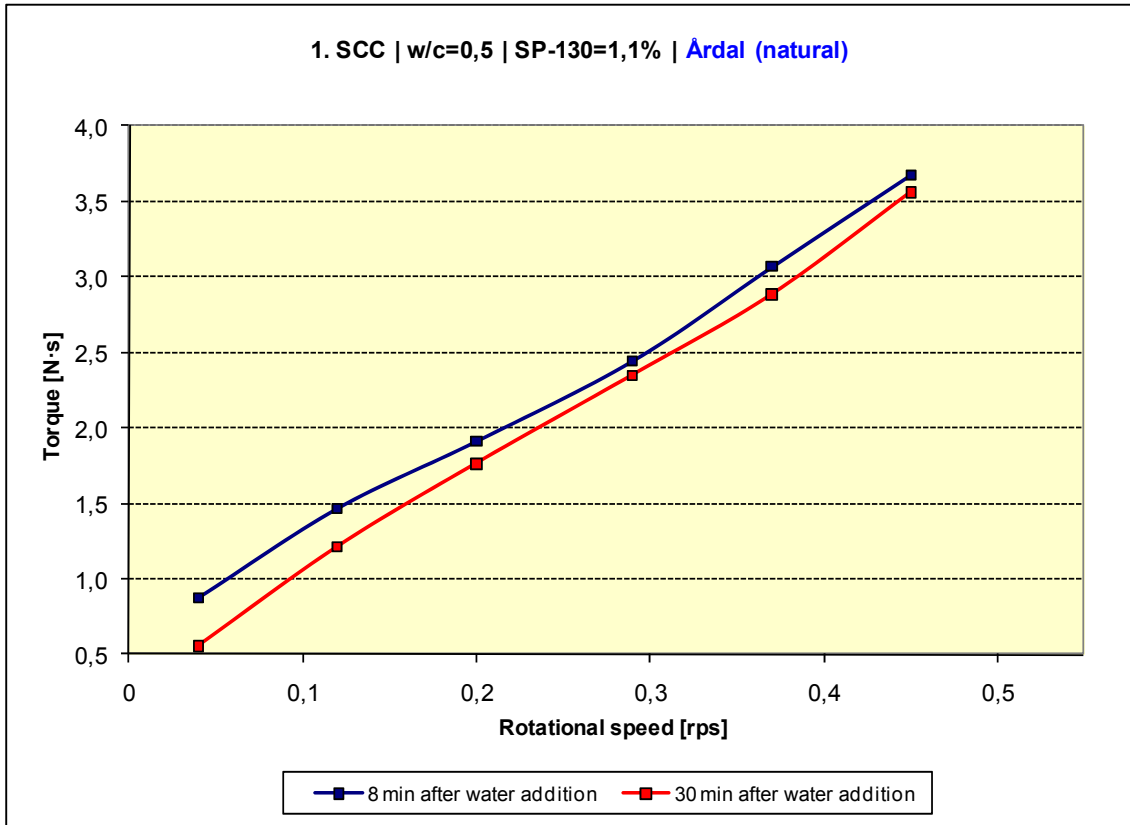


Fig. F-2: Relation torque (T) - rotational speed (N) of SCC mix No. 2

SCC mix No. 3

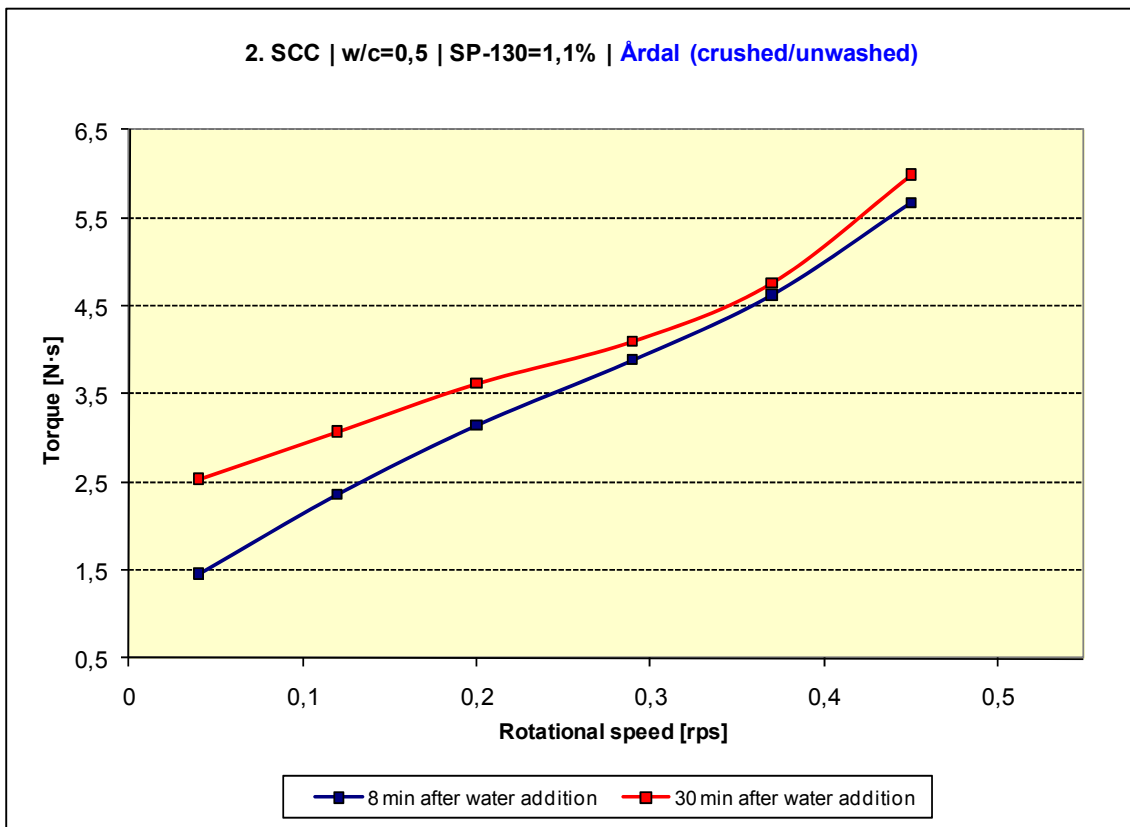


Fig. F-3: Relation torque (T) - rotational speed (N) of SCC mix No. 3

SCC mix No. 4

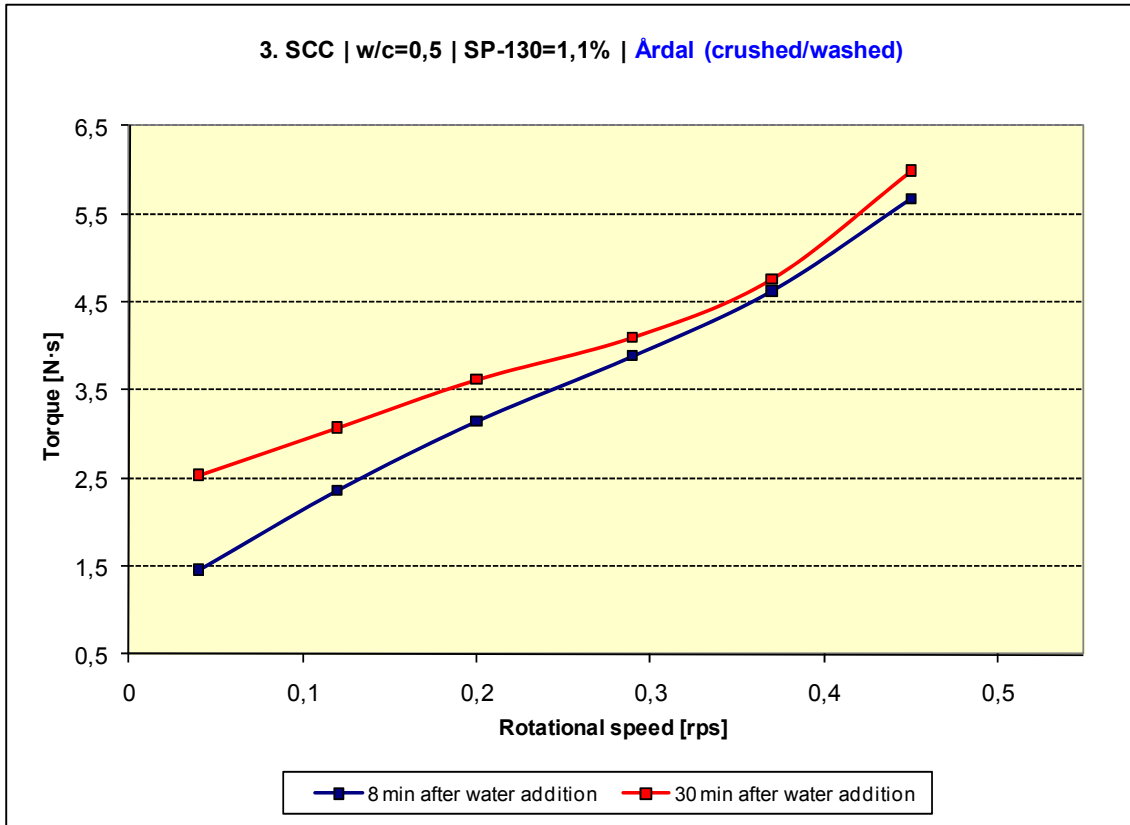


Fig. F-4: Relation torque (T) - rotational speed (N) of SCC mix No. 4

SCC mix No. 5

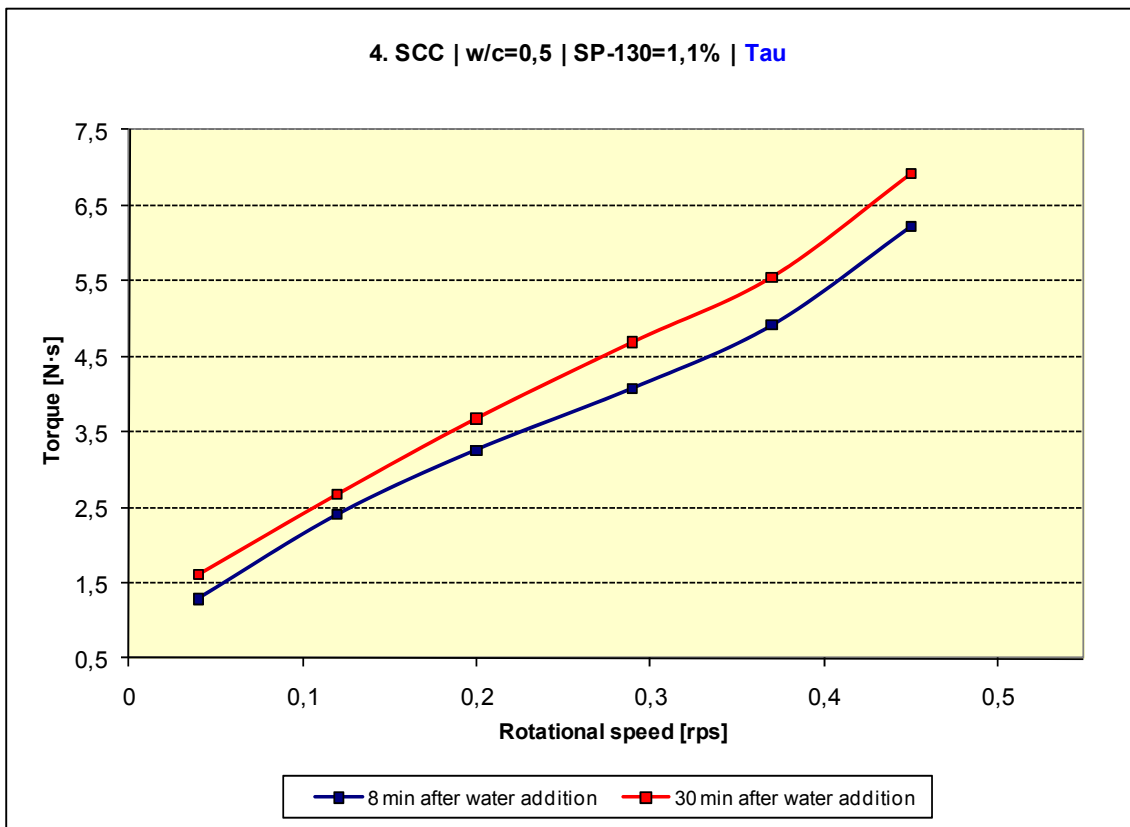


Fig. F-5: Relation torque (T) - rotational speed (N) of SCC mix No. 5

SCC mix No. 6

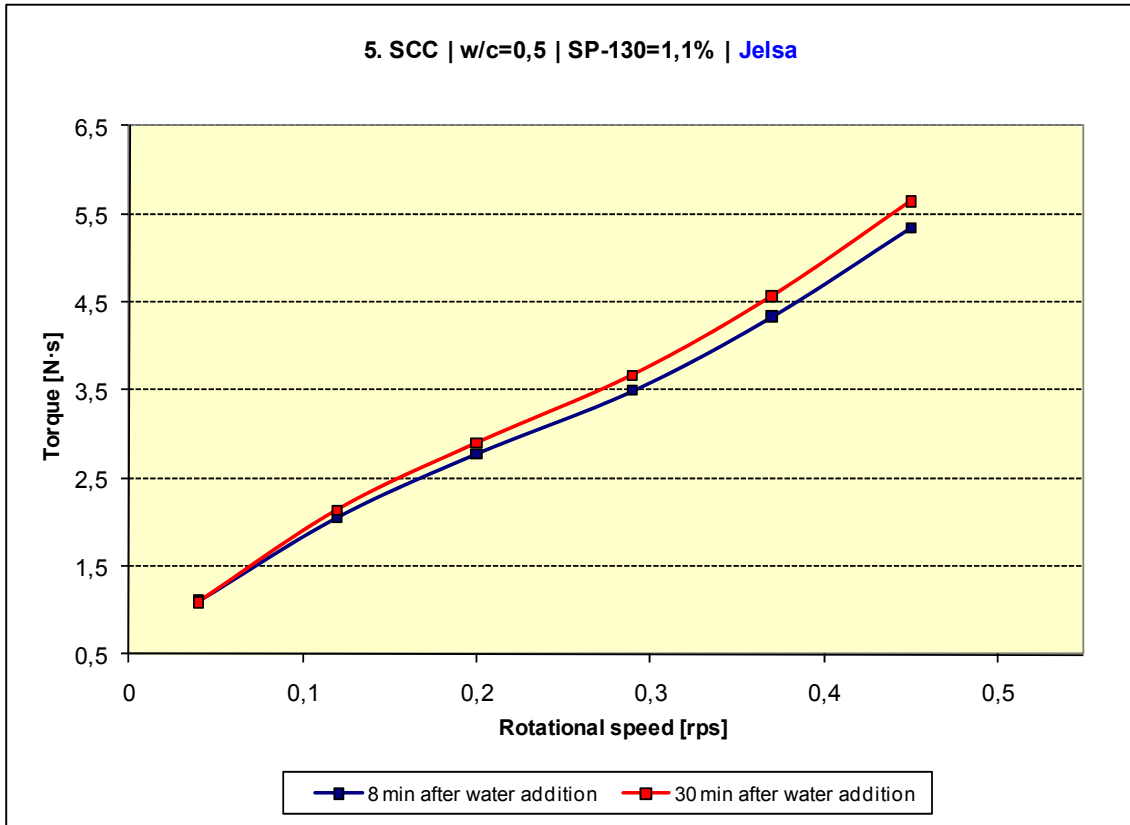


Fig. F-6: Relation torque (T) - rotational speed (N) of SCC mix No. 6

SCC mix No. 7

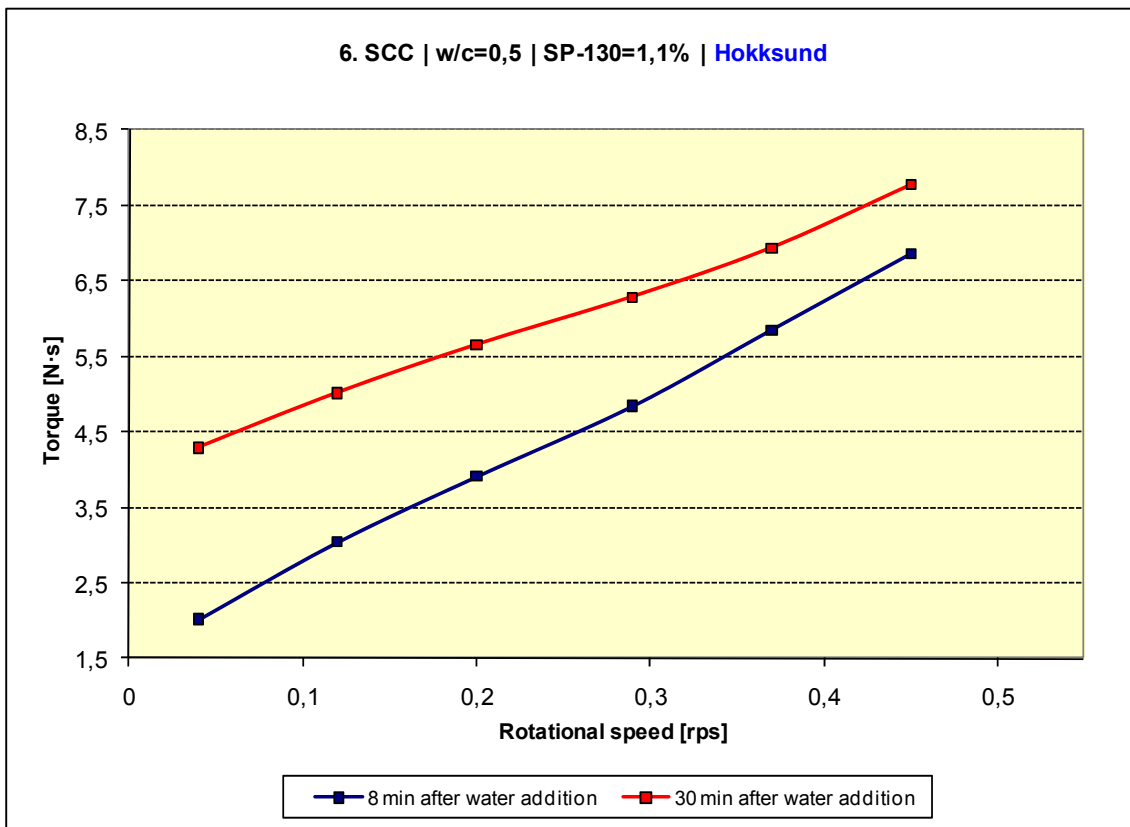


Fig. F-7: Relation torque (T) - rotational speed (N) of SCC mix No. 7

SCC mix No. 8

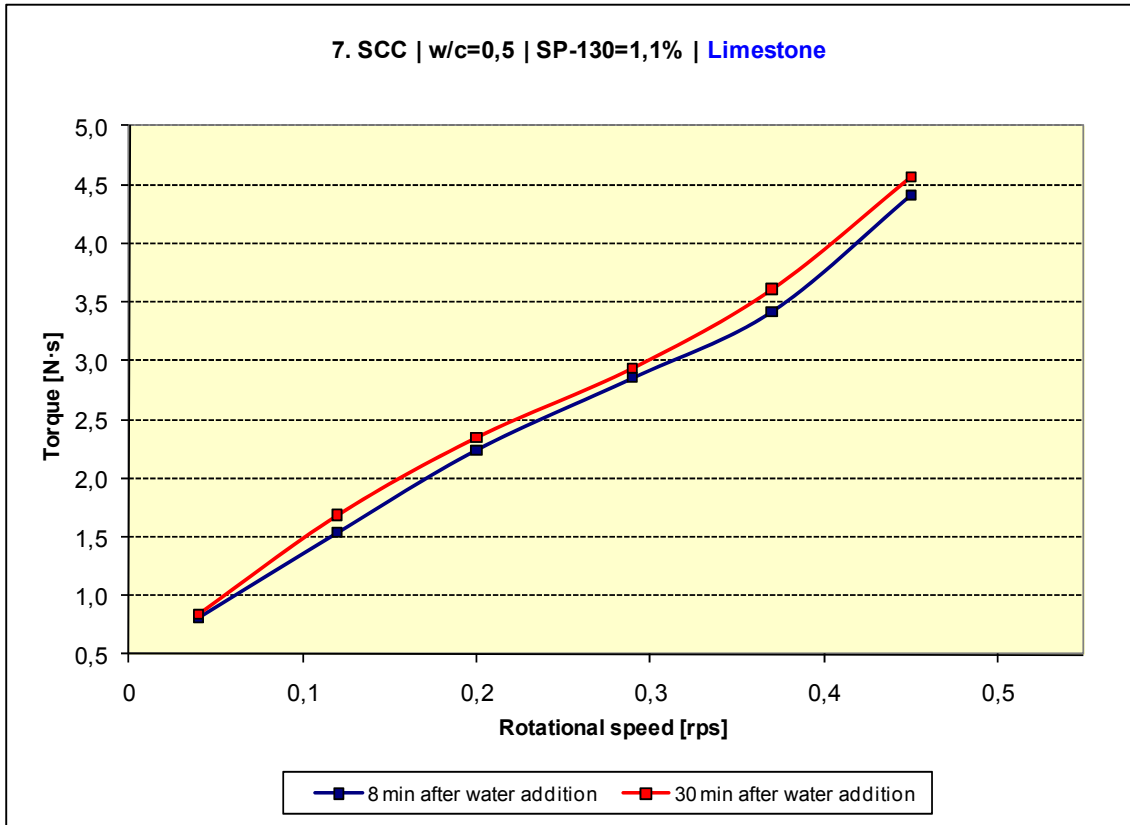


Fig. F-8: Relation torque (T) - rotational speed (N) of SCC mix No. 8

SCC mix No. 9

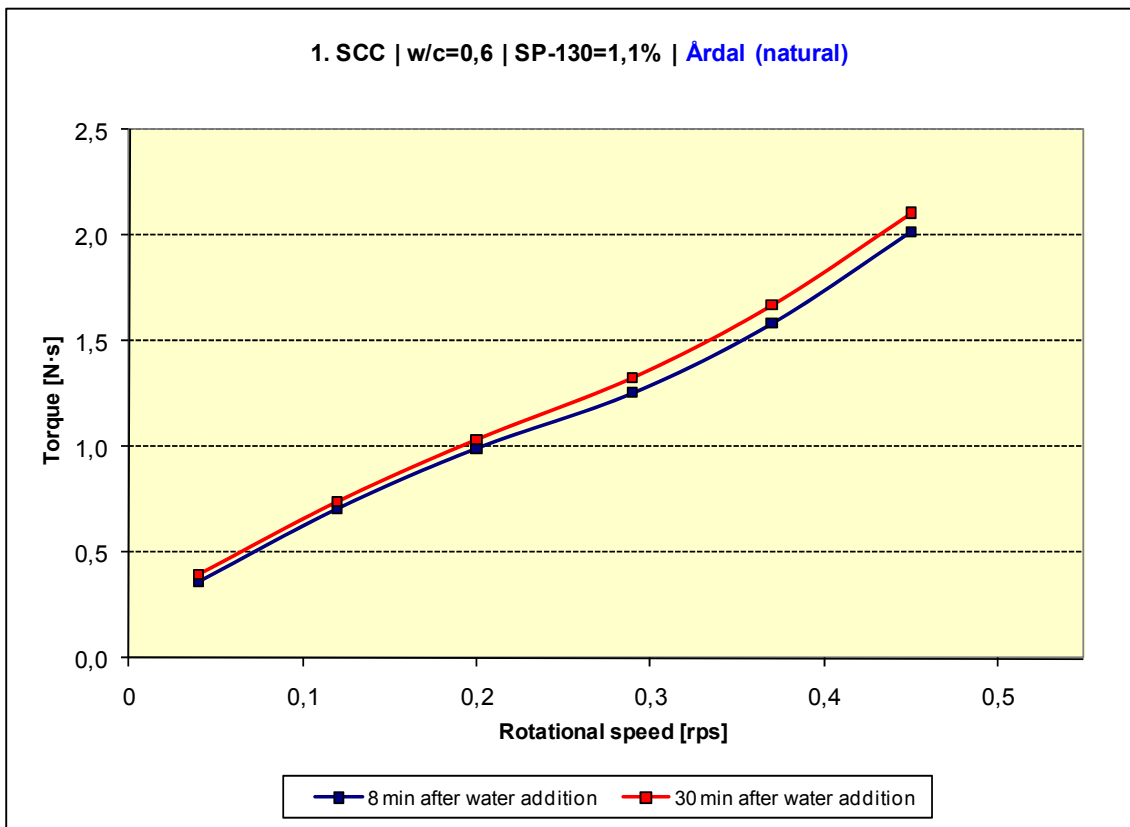


Fig. F-9: Relation torque (T) - rotational speed (N) of SCC mix No. 9

SCC mix No. 10

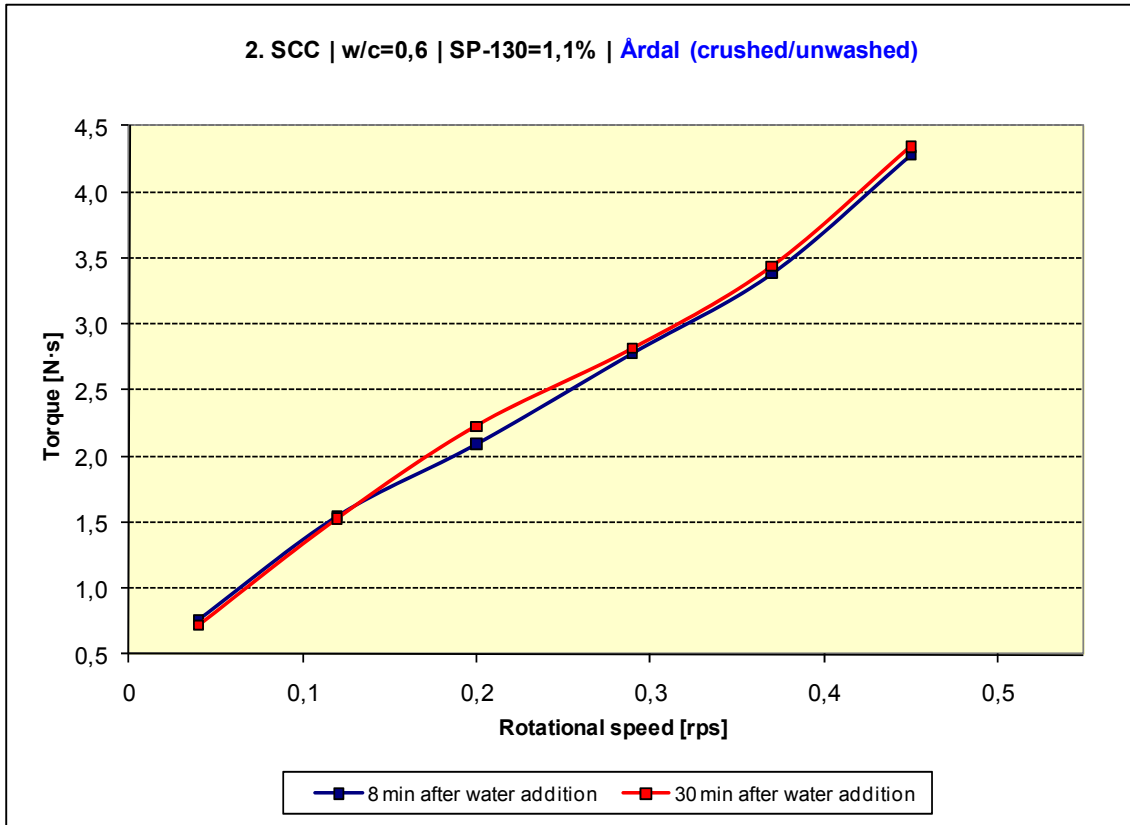


Fig. F-10: Relation torque (T) - rotational speed (N) of SCC mix No. 10

SCC mix No. 11

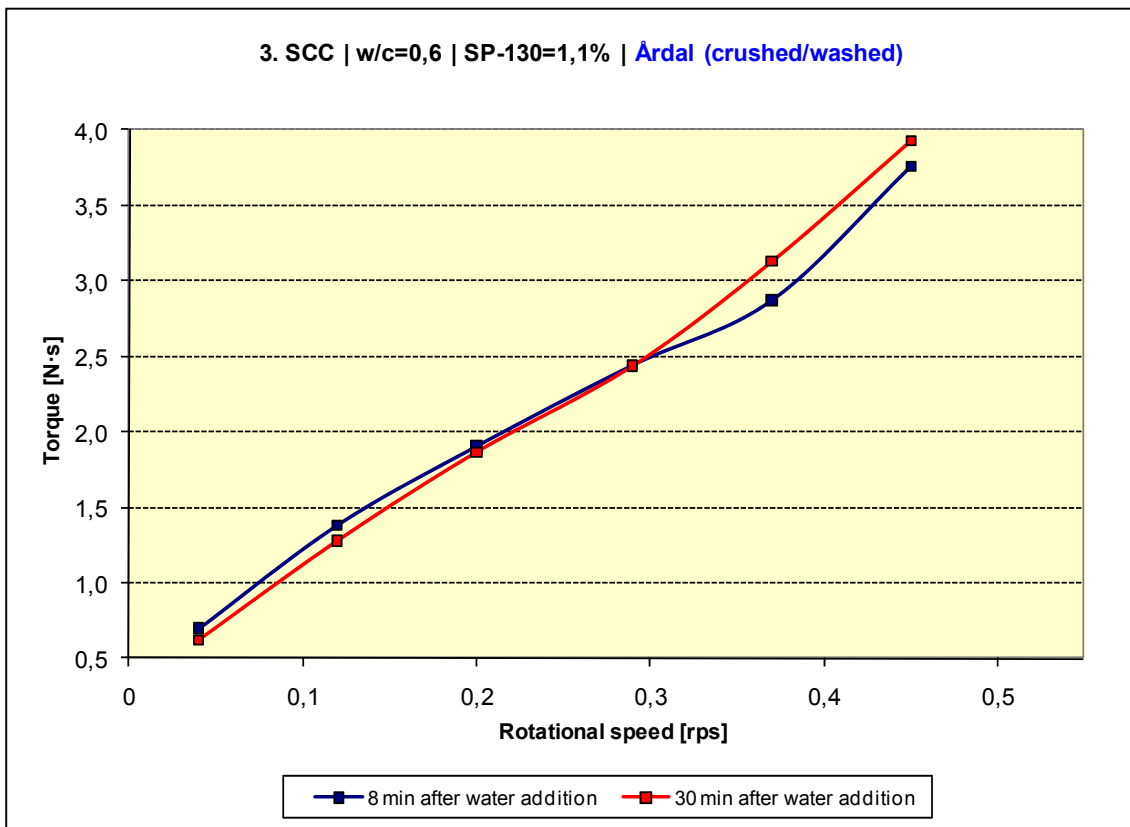


Fig. F-11: Relation torque (T) - rotational speed (N) of SCC mix No. 11

SCC mix No. 12

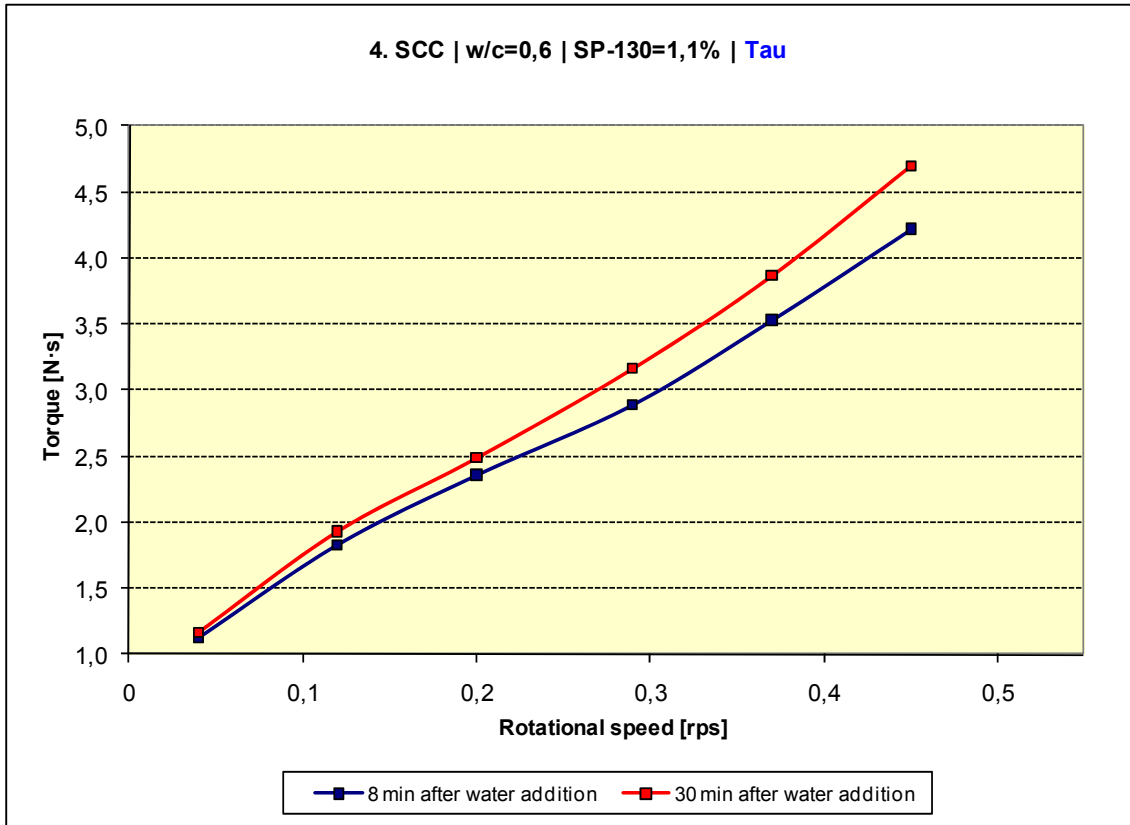


Fig. F-12: Relation torque (T) - rotational speed (N) of SCC mix No. 12

SCC mix No. 13

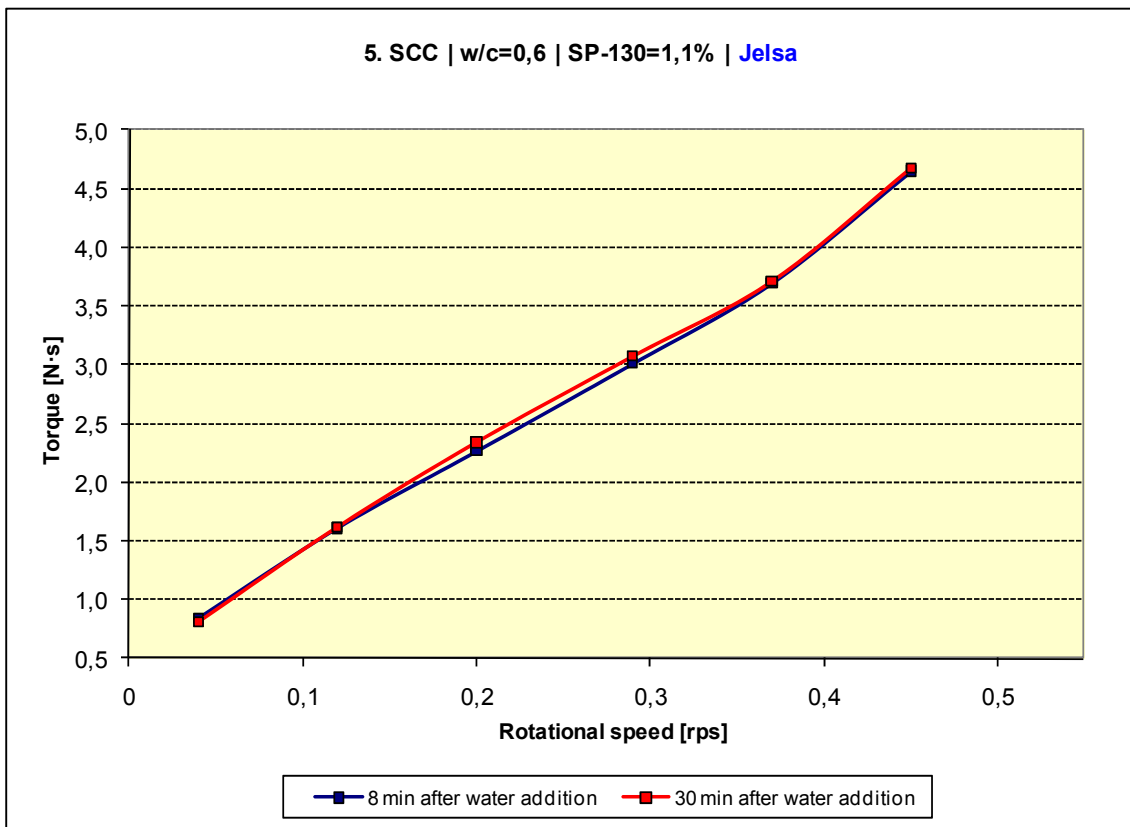


Fig. F-13: Relation torque (T) - rotational speed (N) of SCC mix No. 13

SCC mix No. 14

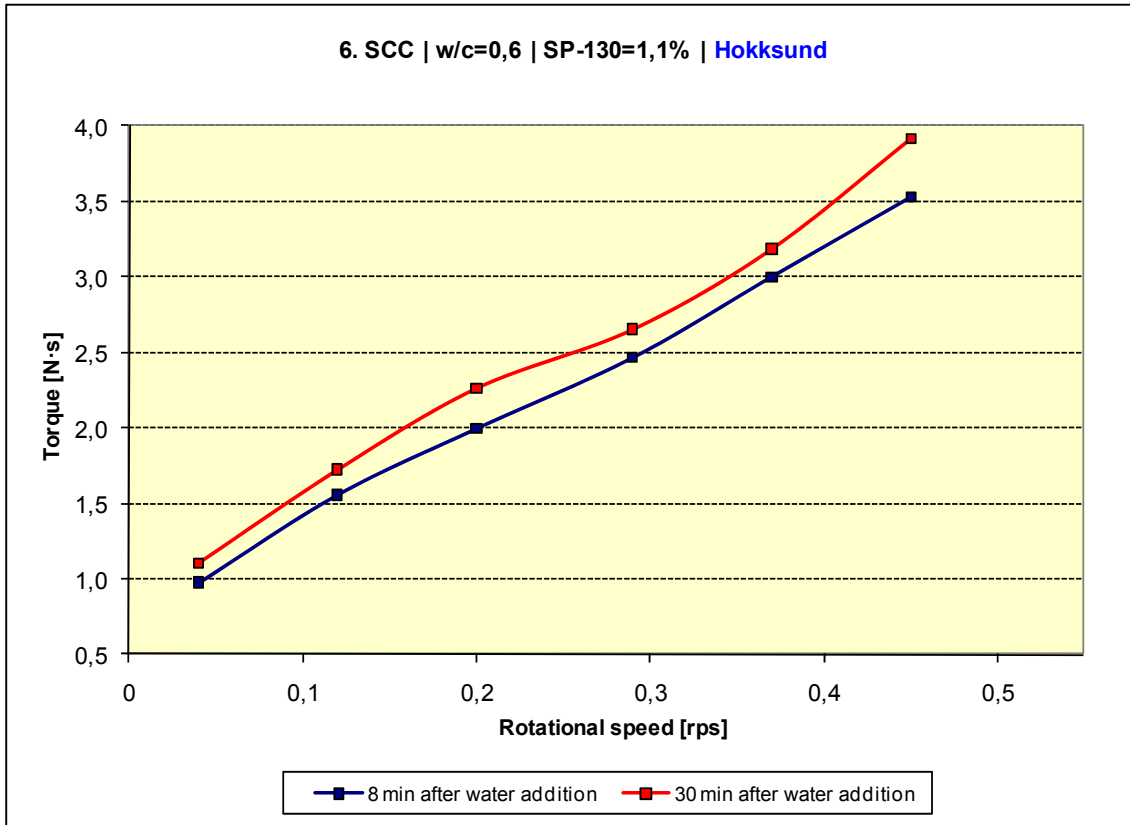


Fig. F-14: Relation torque (T) - rotational speed (N) of SCC mix No. 14

SCC mix No. 15

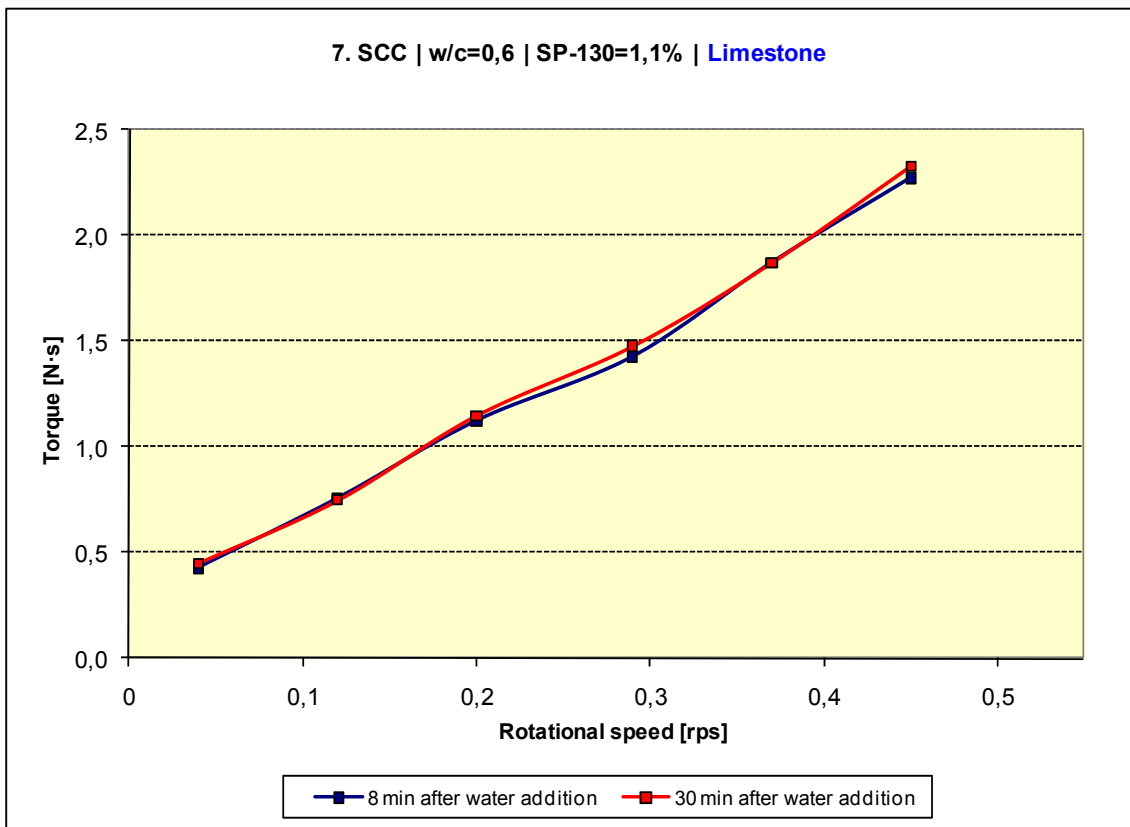


Fig. F-15: Relation torque (T) - rotational speed (N) of SCC mix No. 15

SCC mix No. 16

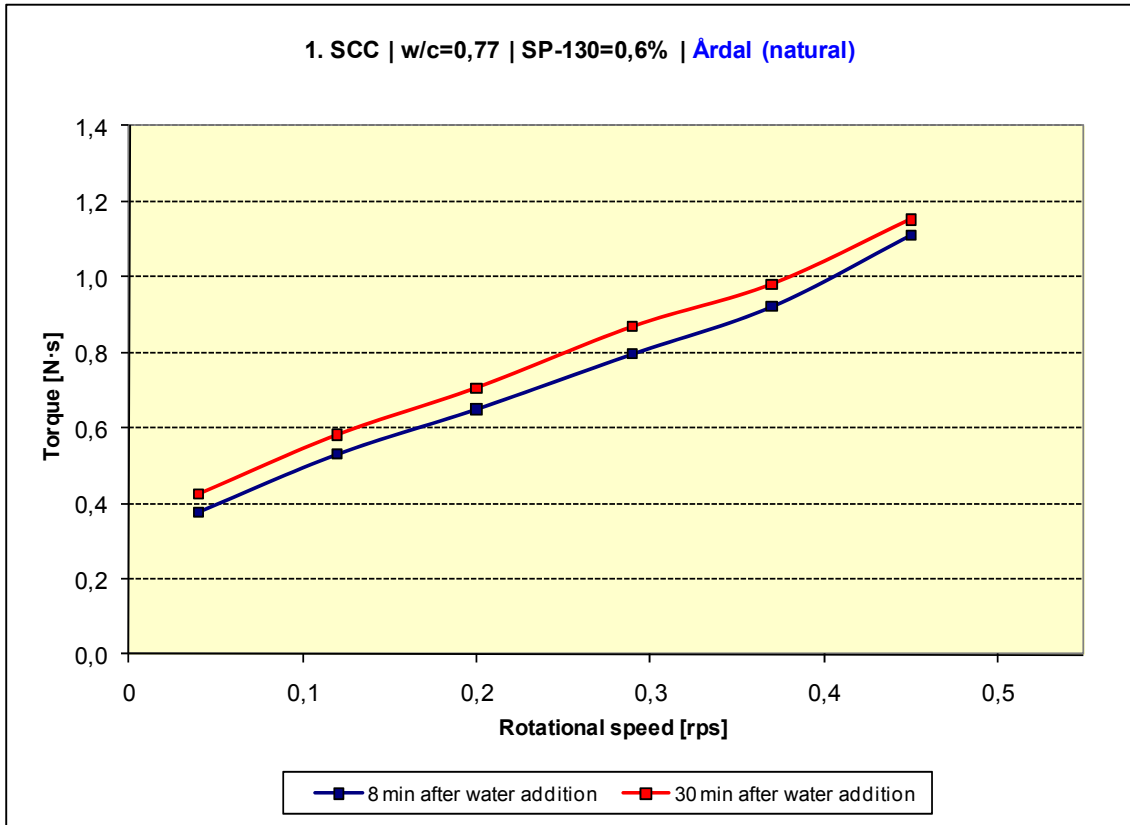


Fig. F-16: Relation torque (T) - rotational speed (N) of SCC mix No. 16

SCC mix No. 17

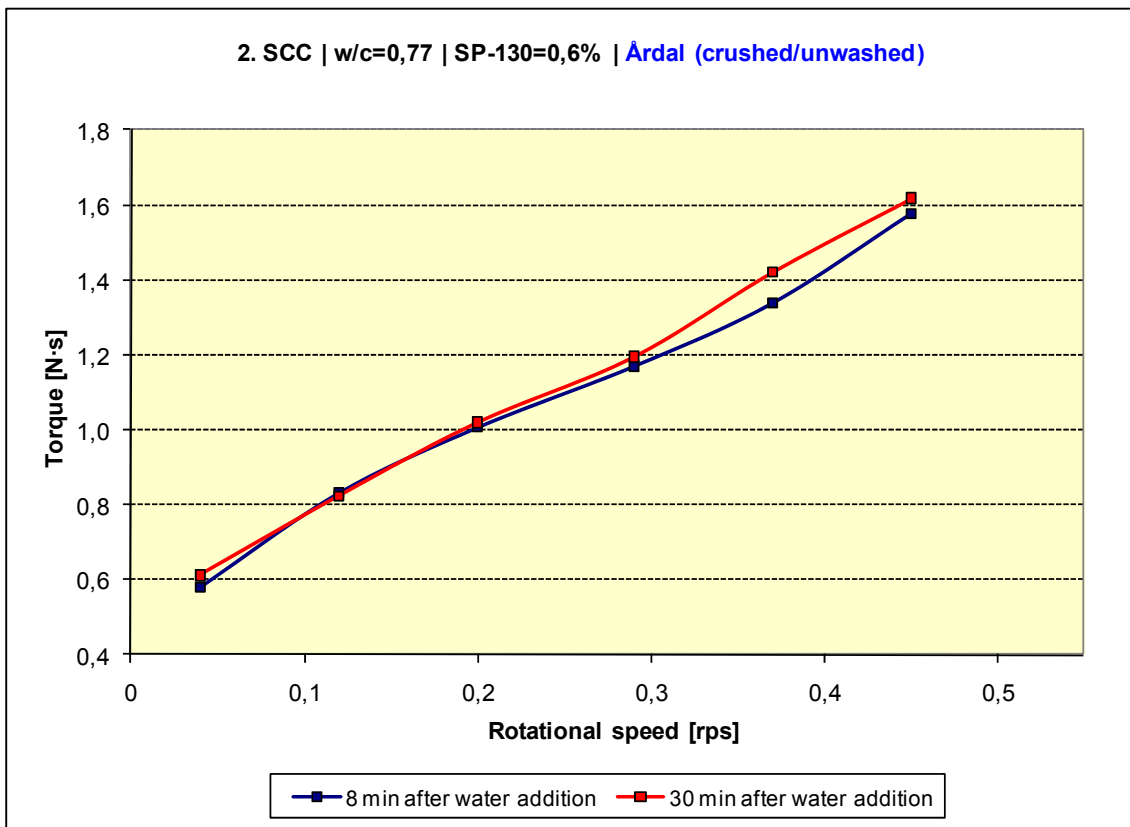


Fig. F-17: Relation torque (T) - rotational speed (N) of SCC mix No. 17

SCC mix No. 18

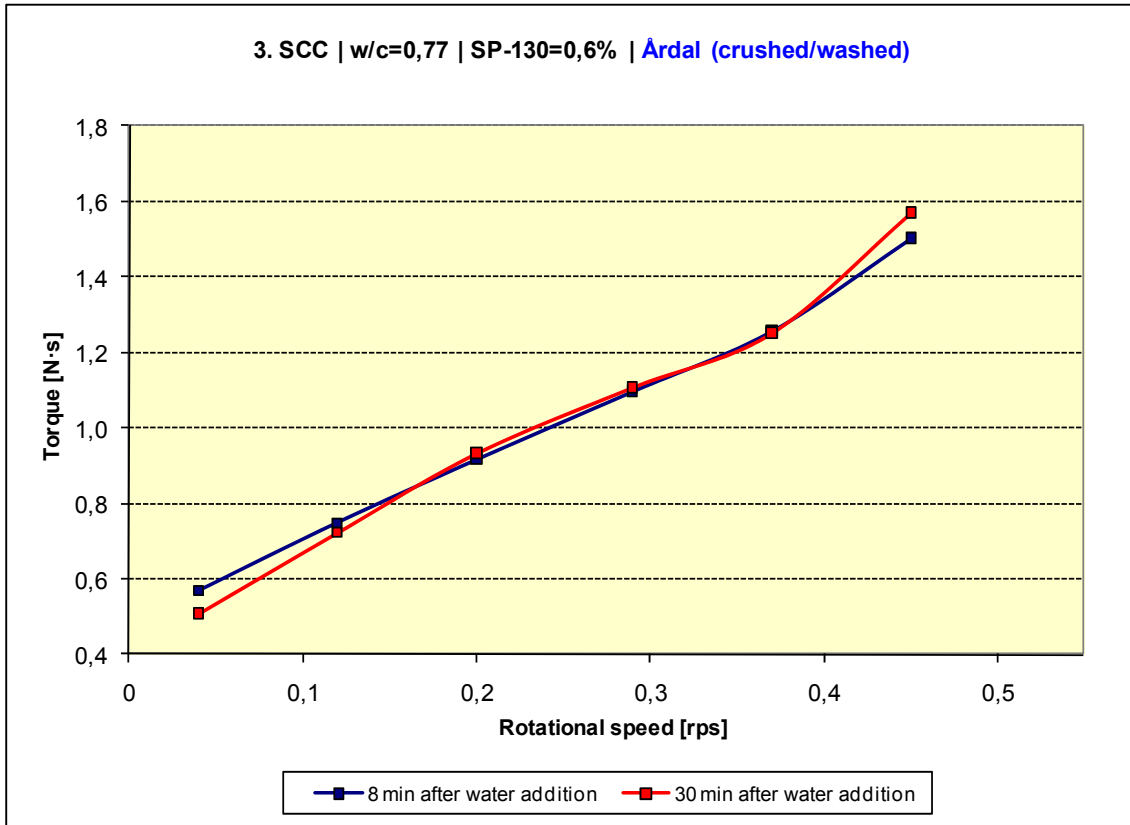


Fig. F-18: Relation torque (T) - rotational speed (N) of SCC mix No. 18

SCC mix No. 19

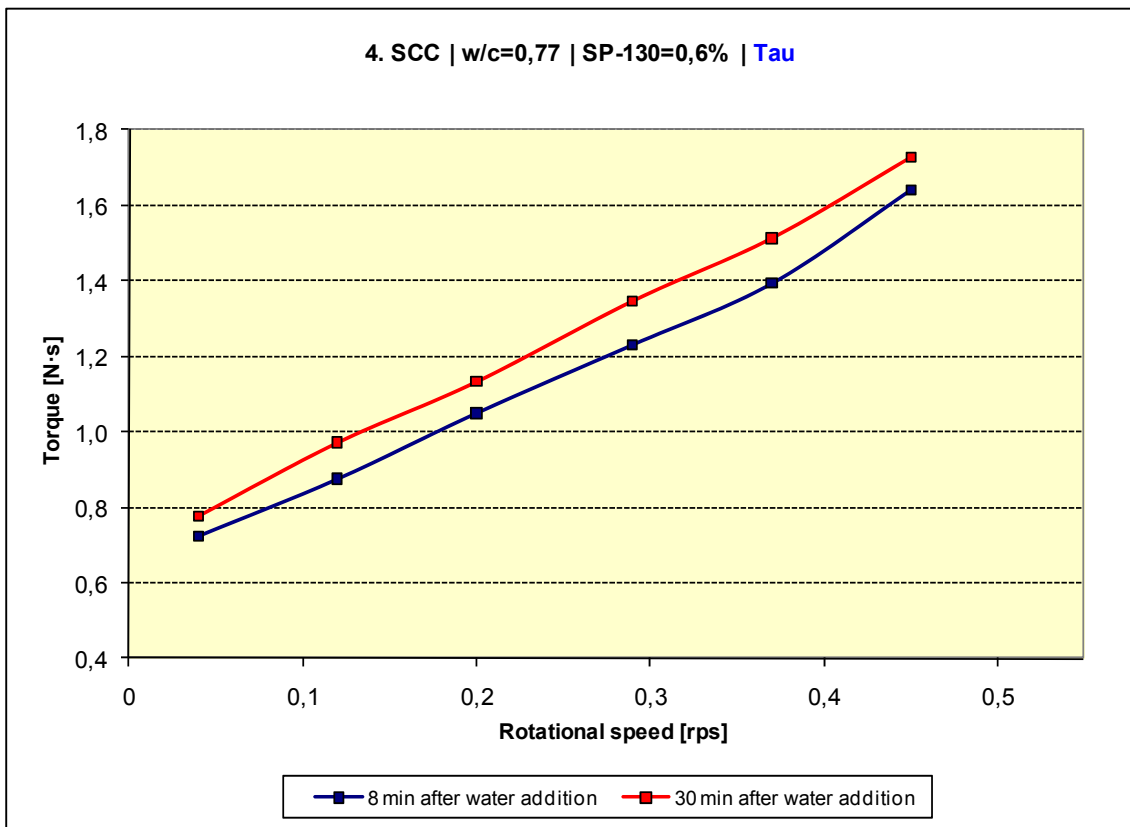


Fig. F-19: Relation torque (T) - rotational speed (N) of SCC mix No. 19

SCC mix No. 20

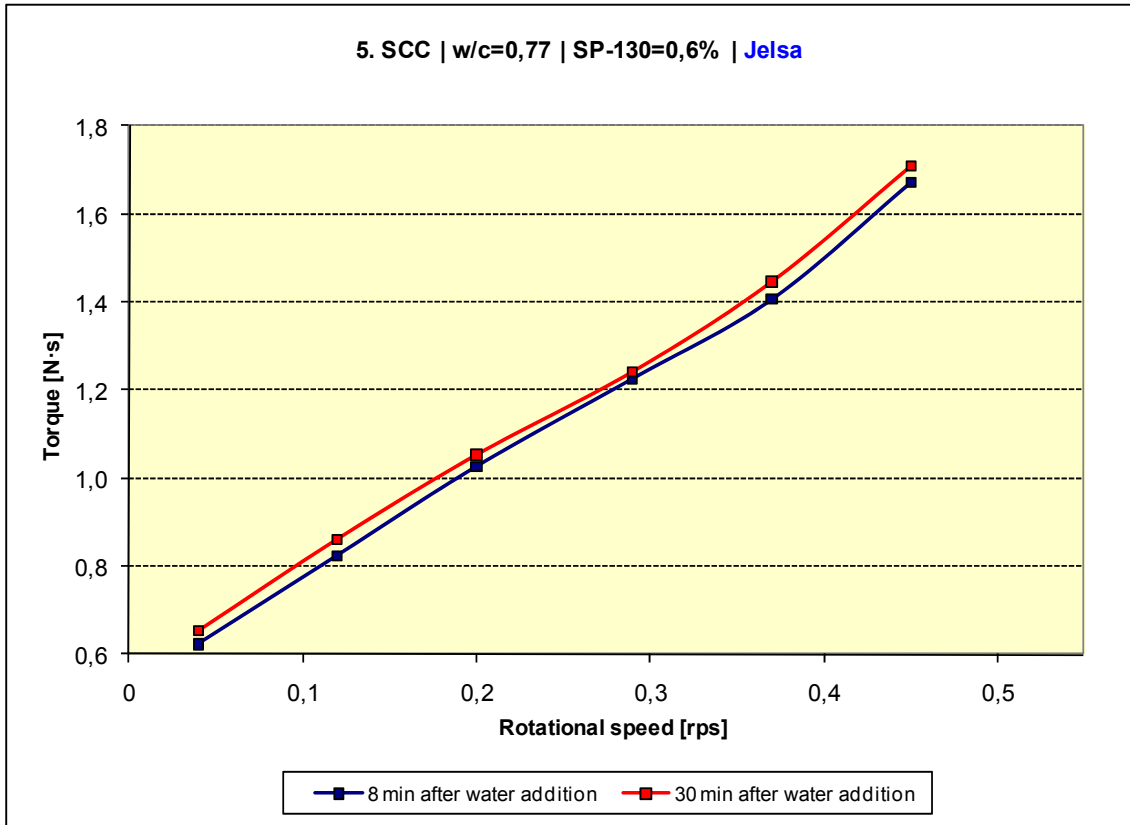


Fig. F-20: Relation torque (T) - rotational speed (N) of SCC mix No. 20

SCC mix No. 21

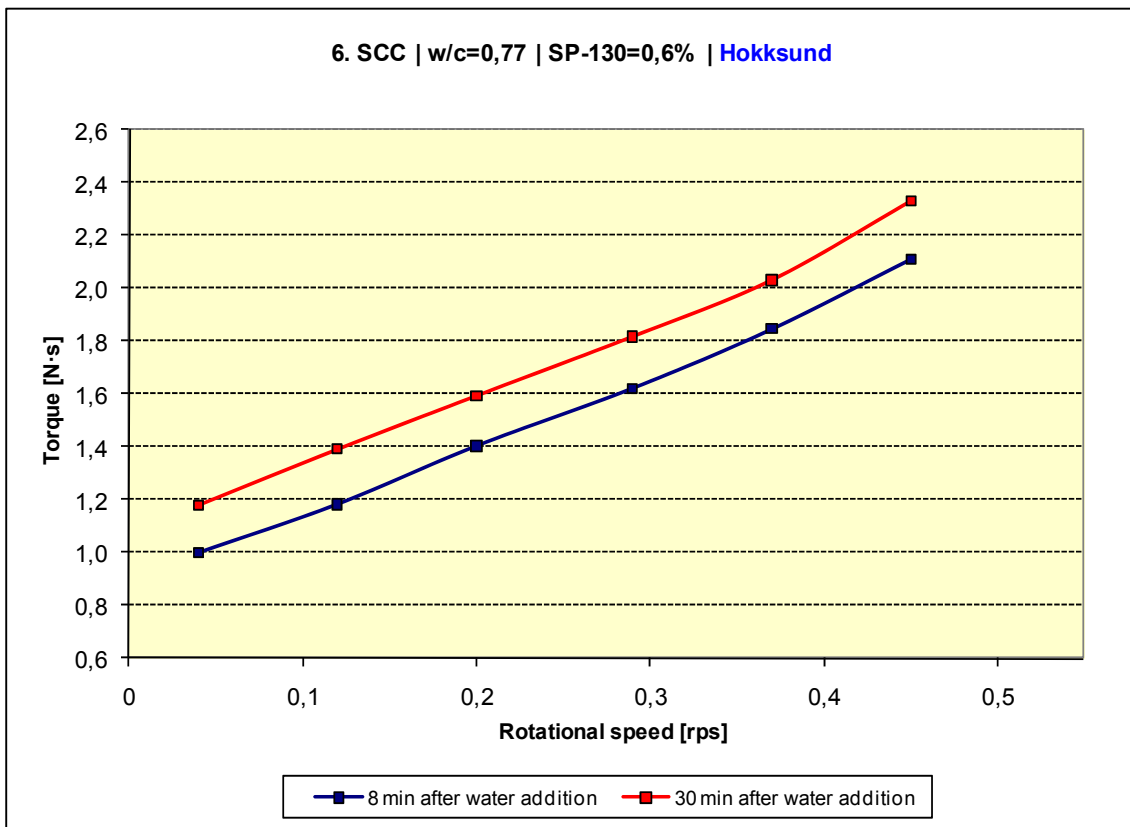


Fig. F-21: Relation torque (T) - rotational speed (N) of SCC mix No. 21

SCC mix No. 22

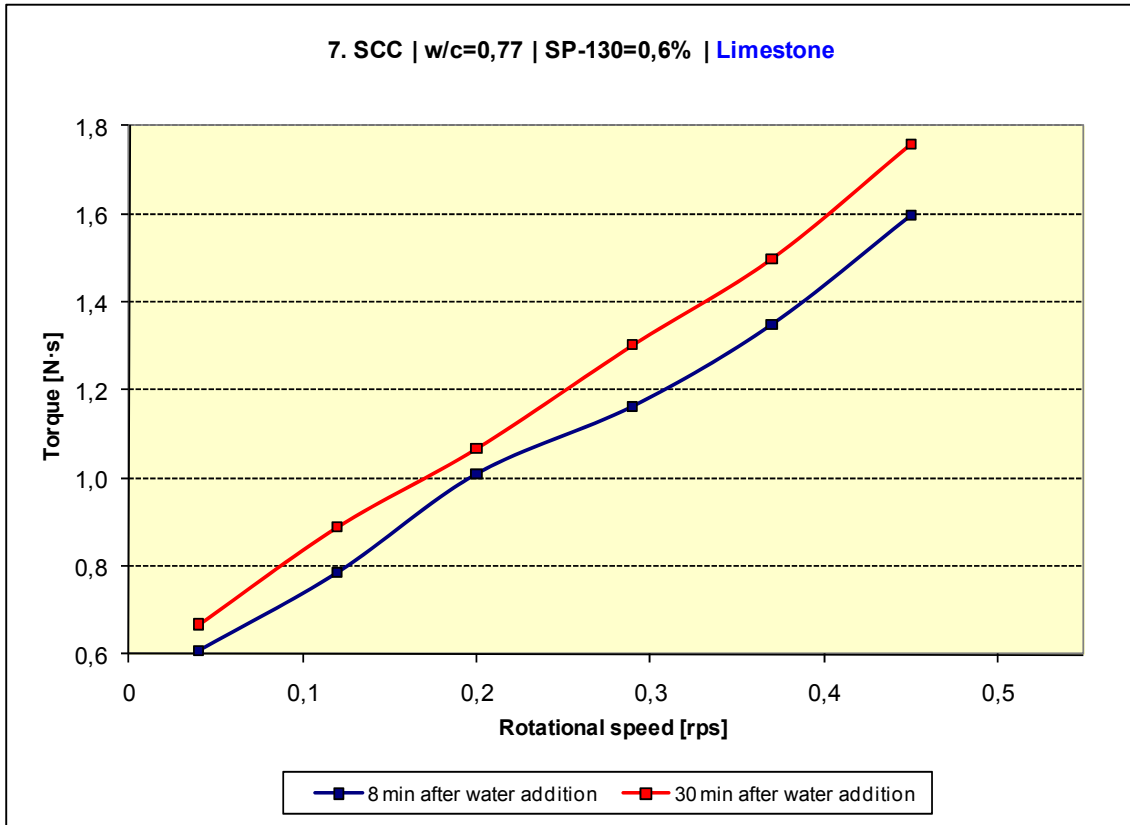


Fig. F-22: Relation torque (T) - rotational speed (N) of SCC mix No. 22

APPENDIX G – Correlation analysis between median particle size D_{50} of the fillers and rheological parameters of SCC

In the following (Tables G-1 to G-4) correlation analysis between median particle size D_{50} of the fillers and rheological parameters of SCC is presented.

Table G-1: Correlation analysis between median particle size D_{50} of the fillers and rheological parameters of matrices SCC with Dynamon SP-130 at $w/c=0.5$

Correlation analysis										
Method	Fresh concrete properties		Segregation coefficient		Bingham Parameters				Static yield stress	AVERAGE
	Air content	Slump-flow	1	2	τ_{y1}	τ_{y2}	μ_1	μ_2		
	1	2	3	4	5	6	7	8	9	
	Squared linear correlation coefficient $[R^2]$ for SCC matrices with Dynamon SP-130 at $w/c=0.5$									
LS Particle Size Analyzer	0.4308	0.5446	0.0212	0.0053	0.0720	0.2177	0.2862	0.2451	0.0200	0.2048
Micrometrics SediGraph 5100	0.4563	0.5940	0.0009	0.0067	0.1166	0.1952	0.2723	0.1322	0.0009	0.1972
MIN=	0.4308	0.5446	0.0009	0.0053	0.0720	0.1952	0.2723	0.1322	0.0009	
MAX=	0.4563	0.5940	0.0212	0.0067	0.1166	0.2177	0.2862	0.2451	0.0200	
AVERAGE=	0.4435	0.5693	0.0111	0.0060	0.0943	0.2064	0.2793	0.1887	0.0104	

Table G-2: Correlation analysis between median particle size D_{50} of the fillers and rheological parameters of matrices SCC with Dynamon SP-130 at $w/c=0.6$ and 0.77

Correlation analysis										
Method	Fresh concrete properties		Segregation coefficient		Bingham Parameters				Static yield stress	AVERAGE
	Air content	Slump-flow	1	2	τ_{y1}	τ_{y2}	μ_1	μ_2		
	1	2	3	4	5	6	7	8	9	
	Squared linear correlation coefficient $[R^2]$ for SCC matrices with Dynamon SP-130 at $w/c=0.6$									
LS Particle Size Analyzer	0.0145	0.0249	0.0910	0.0925	0.0562	0.0354	0.1643	0.2181	0.0723	0.0855
Micrometrics SediGraph 5100	0.0734	0.0752	0.1760	0.1902	0.0805	0.0600	0.1044	0.1287	0.1498	0.1154
MIN=	0.0145	0.0249	0.0910	0.0925	0.0562	0.0354	0.1044	0.1287	0.0723	
MAX=	0.0734	0.0752	0.1760	0.1902	0.0805	0.0600	0.1643	0.2181	0.1498	
AVERAGE=	0.0440	0.0501	0.1335	0.1414	0.0684	0.0477	0.1343	0.1734	0.1111	
Squared linear correlation coefficient $[R^2]$ for SCC matrices with Dynamon SP-130 at $w/c=0.77$									AVERAGE	
LS Particle Size Analyzer	0.1215	0.4441	0.2268	0.2145	0.4327	0.3221	0.0591	0.6758	0.1939	0.2989
Micrometrics SediGraph 5100	0.0702	0.5337	0.3681	0.3496	0.5296	0.3710	0.1232	0.7583	0.3334	0.3819
MIN=	0.0702	0.4441	0.2268	0.2145	0.4327	0.3221	0.0591	0.6758	0.1939	
MAX=	0.1215	0.5337	0.3681	0.3496	0.5296	0.3710	0.1232	0.7583	0.3334	
AVERAGE=	0.0958	0.4889	0.2975	0.2820	0.4812	0.3465	0.0912	0.7170	0.2637	

Table G-3: Correlation analysis between median particle size D_{50} of the fillers and rheological parameters of matrices SCC with Dynamon SP-130 at $w/c=0.5$ (excluding Hokksund and Limestone filler results)

Correlation analysis										
Method	Fresh concrete properties		Segregation coefficient		Bingham Parameters				Static yield stress	AVERAGE
	Air content	Slump-flow	1	2	τ_{y1}	τ_{y2}	μ_1	μ_2		
	1	2	3	4	5	6	7	8	9	
	Squared linear correlation coefficient [R^2] for SCC matrices with Dynamon SP-130 at $w/c=0.5$									
LS Particle Size Analyzer	0.2968	0.4845	0.0013	0.0713	0.2440	0.6079	0.1750	0.6040	0.0010	0.2762
Micrometrics SediGraph 5100	0.3134	0.4831	0.0008	0.0440	0.2567	0.5950	0.2056	0.5390	0.0006	0.2709
MIN=	0.2968	0.4831	0.0008	0.0440	0.2440	0.5950	0.1750	0.5390	0.0006	
MAX=	0.3134	0.4845	0.0013	0.0713	0.2567	0.6079	0.2056	0.6040	0.0010	
AVERAGE=	0.3051	0.4838	0.0010	0.0577	0.2503	0.6015	0.1903	0.5715	0.0008	

Table G-4: Correlation analysis between median particle size D_{50} of the fillers and rheological parameters of matrices SCC with Dynamon SP-130 at $w/c=0.6$ and 0.77 (excluding Hokksund and Limestone filler results)

Correlation analysis										
Method	Fresh concrete properties		Segregation coefficient		Bingham Parameters				Static yield stress	AVERAGE
	Air content	Slump-flow	1	2	τ_{y1}	τ_{y2}	μ_1	μ_2		
	1	2	3	4	5	6	7	8	9	
	Squared linear correlation coefficient [R^2] for SCC matrices with Dynamon SP-130 at $w/c=0.6$									
LS Particle Size Analyzer	0.1676	0.3823	0.4129	0.4420	0.4649	0.4391	0.4178	0.2319	0.3864	0.3717
Micrometrics SediGraph 5100	0.2201	0.4298	0.4540	0.4822	0.5106	0.4969	0.4145	0.1811	0.4266	0.4018
MIN=	0.1676	0.3823	0.4129	0.4420	0.4649	0.4391	0.4145	0.1811	0.3864	
MAX=	0.2201	0.4298	0.4540	0.4822	0.5106	0.4969	0.4178	0.2319	0.4266	
AVERAGE=	0.1938	0.4060	0.4335	0.4621	0.4877	0.4680	0.4162	0.2065	0.4065	
	Squared linear correlation coefficient [R^2] for SCC matrices with Dynamon SP-130 at $w/c=0.77$									AVERAGE
LS Particle Size Analyzer	0.0046	0.6777	0.5501	0.7762	0.4079	0.1947	0.4747	0.8065	0.5362	0.4921
Micrometrics SediGraph 5100	0.0026	0.6522	0.6027	0.7975	0.4576	0.2421	0.4360	0.7879	0.5975	0.5084
MIN=	0.0026	0.6522	0.5501	0.7762	0.4079	0.1947	0.4360	0.7879	0.5362	
MAX=	0.0046	0.6777	0.6027	0.7975	0.4576	0.2421	0.4747	0.8065	0.5975	
AVERAGE=	0.0036	0.6650	0.5764	0.7868	0.4327	0.2184	0.4553	0.7972	0.5668	

SINTEF Building and Infrastructure is the third largest building research institute in Europe. Our objective is to promote environmentally friendly, cost-effective products and solutions within the built environment. SINTEF Building and Infrastructure is Norway's leading provider of research-based knowledge to the construction sector. Through our activity in research and development, we have established a unique platform for disseminating knowledge throughout a large part of the construction industry.

COIN – Concrete Innovation Center is a Center for Research based Innovation (CRI) initiated by the Research Council of Norway. The vision of COIN is creation of more attractive concrete buildings and constructions. The primary goal is to fulfill this vision by bringing the development a major leap forward by long-term research in close alliances with the industry regarding advanced materials, efficient construction techniques and new design concepts combined with more environmentally friendly material production.

